ON THE SYNTHESIS OF OPTIMUM MONOPULSE ANTENNA ARRAY DISTRIBUTIONS

D.A. McNAMARA

Thesis submitted for the Degree of Doctor of Philosophy in Engineering at the University of Cape Town

Supervisor: Prof. P.N. Denbigh

September 1986

To My Parents

Whose Support And Dedication Granted Me The Privilege

Of A Formal Education And Whose Example and Love

Granted Me the Greater Priviledge Of An Informal Education

Teach me so Thy works to read
That my faith - new strength accruing -
May from world to world proceed,
Wisdom's fruitful search pursuing;
Till, Thy truth my mind imbuing,
I proclaim the Eternal Creed,
Oft the glorious them renewing
God our Lord is God indeed.

James Clerk Maxwell

ACKNOWLEDGEMENTS

The author wishes to thank his supervisor, Prof. N. Denbigh, for his patience during the protracted course of the research programme of this thesis.

A number of people contributed to the thesis through advice, support, and assistance in the use of computing facilities. Thanks are due to Prof. J.A.G. Malherbe for his constant exhortation. A word of appreciation is extended to Dr. D.E. Baker for allowing the author use of the excellent computing facilities in his laboratory at the CSIR. The advice of Mr. L. Botha and Mr. R. Anderson on the use of these facilities is gratefully acknowledged. Mr. J.L. Hutchings kindly checked all the tables of numerical data.

The author's interest in array synthesis grew principally from the work and publications of Dr. R.C. Hansen and Prof. R.S. Elliott, and to them he expresses his gratitude.

The thesis was typed by Mrs. G. Proudfoot in her usual impeccable manner.

Finally, the author wishes to thank his parents for their unfailing support, and to them this thesis is dedicated.

ABSTRACT

The stringent specifications of modern tracking systems demand antennas of high performance. For this reason arrays are finding increasing application as monopulse antennas.

A new exact procedure is introduced for the synthesis of optimum difference distributions for linear arrays of discrete elements, with a maximum sidelobe level specification. The method is based on the Zolotarev polynomial, and is precisely the difference mode equivalent of the Dolph-Chebyshev synthesis for sum patterns. When the interelement spacings are a half-wavelength or larger the element excitations are obtained in a very direct manner from the Chebyshev series expansion of the Zolotarev polynomial. For smaller spacings, a set of recursive equations is derived for finding the array excitation set. Efficient means of performing all the computations associated with the above procedure are given in full. In addition, a set of design tables is presented for a range of Zolotarev arrays of practical utility.

A novel technique, directly applicable to arrays of discrete elements, for the synthesis of high directivity difference patterns with arbitrary sidelobe envelope tapers is presented. This is done by using the Zolotarev space factor zeros and correctly relocating these in a well-defined manner to effect the taper.

A solution to the direct synthesis of discrete array sum patterns with arbitrary sidelobe envelope tapers is introduced. In this case the synthesis is also done by correct placement of the space factor zeros.

The above techniques enable high excitation efficiency, low sidelobe, sum and difference patterns to be synthesized independently. Contributions to the simultaneous synthesis of sum and difference patterns, subject to specified array feed network complexity constraints, are also given. These utilise information on the excitations and space factor zeros of the independently optimal solutions, along with constrained numerical optimisation.

The thesis is based on original research done by the author, except where explicit reference is made to the work of others.

PREFACE

The purpose of this preface is not to supplant Chapter 1 which provides a general overview of the individual chapters contained in this thesis. It is intended rather to direct the reader towards the main emphases of the thesis.

The essential points of the thesis are contained in the abstract, Chapter 1, Section 3.7, and Chapter 9. The detailed workings that support the central themes may be found in Chapters 4 to 8. Chapters 2 and 3 have been included to place the thesis as a whole in the context of other research in its relevant field, and to derive certain expressions not readily available in the literature.

CONTENTS

CONTENTS (Continued) Page

CONTENTS (Continued) Page

CHAPTER 1

INTRODUCTION

1.1 THE MONOPULSE CONCEPT

The function of a tracking radar is to select a particular target and follow its course in range and angle. An essential requirement is the measurement of the angle of arrival of the received signal using a directive antenna beam which is pointed towards the target. The characteristics of the antenna must be such that errors in pointing are measured and made available as error signals to control the positioning servos of the antenna.

Tracking radars may be divided into two general types - sequential lobing and simultaneous lobing (monopulse) [1]. The simultaneous lobing technique is referred to as "monopulse" since it permits in principle the extraction of complete error information from each received pulse.

A monopulse antenna has three ports: the sum channel (Σ), elevation difference channel (Δ_e) and azimuth difference channel (Δ_a). This is illustrated schematically in Fig. 1.1. If a plane wave is incident on the antenna and the radiation pattern of the antenna measured at the sum port, the form of the pattern $E_s(\theta)$ will be as shown in Fig. 1.2 for any spatial plane in which the measurement is performed. Here θ is the angle measured with respect to the boresight direction of the antenna. Should the pattern be measured in the elevation (azimuth) plane at the elevation difference port (azimuth difference port), the form will be that in Fig. 1.3. The essential considerations for both elevation and azimuth difference patterns are the same.

When coupled to the transmitter of the monopulse radar system, the sum mode provides illumination of the distant target; when coupled to the receiver it provides range information and a reference signal. The azimuth and elevation difference ports are coupled to receivers whose signals, when combined with (normalised with respect to) the received reference sum signal, provide azimuth and elevation angle information, respectively. Although only the sum mode actually exists in transmission, it is common practice to consider all three modes in transmission for ease of analysis; by reciprocity [2] the antenna patterns are the same whether obtained in transmission or reception.

With each difference signal (E_{da} or E_{de}), one lobe must be in-phase with the sum signal (E_s) and the other 180° out of phase with it. The beamforming network must ensure that this requirement is satisfied in order to provide the correct servo information.

Assume that a target has been illuminated and a return from the target is incident on the monopulse radar antenna. If the antenna is pointing directly at the target (that is, the antenna boresight is aimed at the target), there will be no signal at either the azimuth or elevation difference ports, since these ports have patterns which have nulls on boresight. If the antenna boresight is off target, a signal will appear at either the elevation or azimuth difference channels, or both. The phase difference between non-zero E_{de} and/or E_{da}, and the sum signal E_s (either 0° or 180° in the case of the ideal monopulse antenna) provide information on the direction of offset in the elevation and azimuth difference planes independently. This information is used to drive servos to re-align the antenna boresight on the target. Thus complete tracking capability may be achieved.

To summarise then, the amplitudes of the difference channels in comparison with that of the sum are a measure of the displacement of the target from the radar axis and the relative phase of the signals indicates the direction of this displacement.

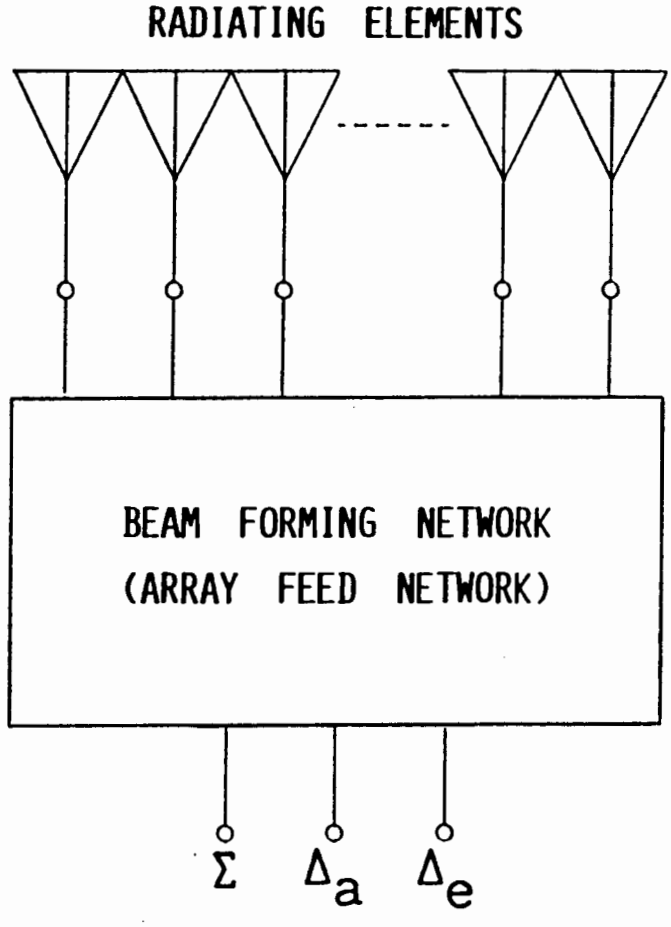

FIGURE 1.1 SCHEMATIC DIAGRAM OF A MONOPULSE ANTENNA

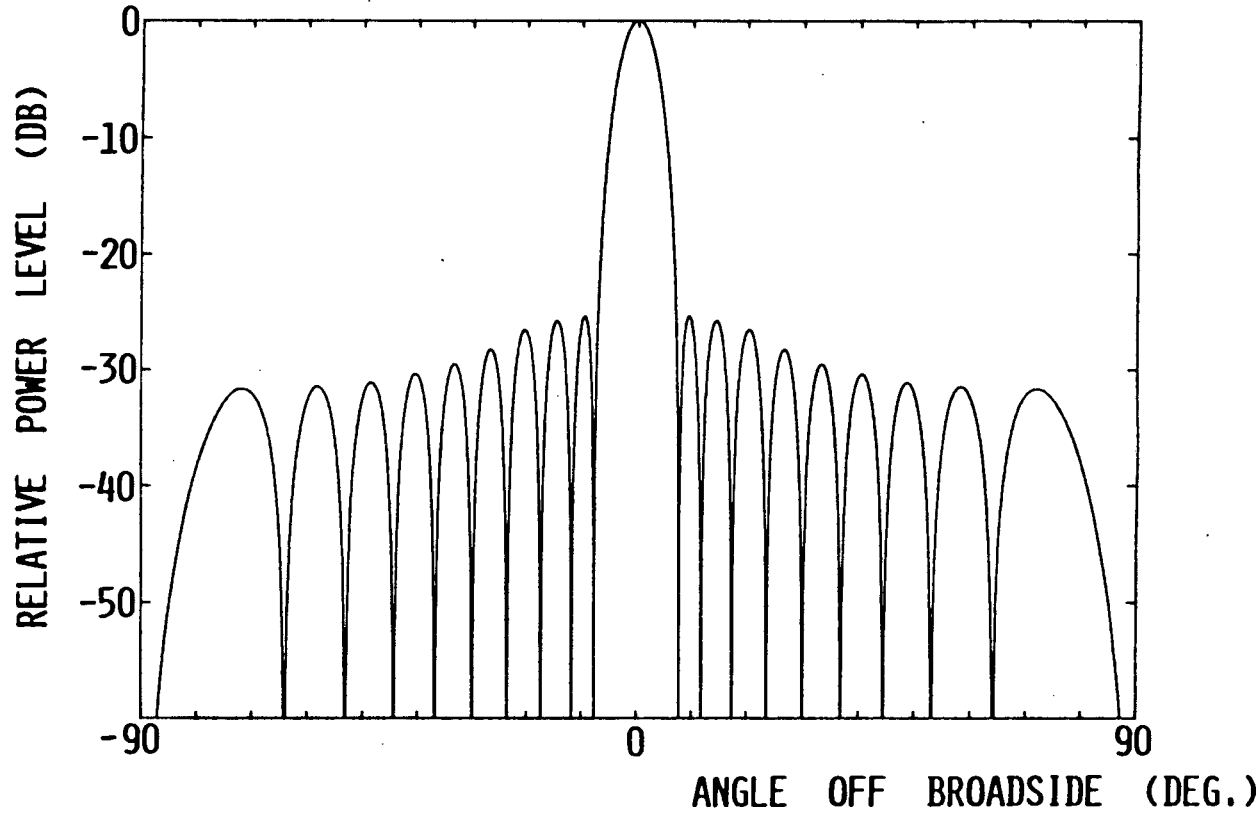

FIGURE 1.2 TYPICAL SUM PATTERN

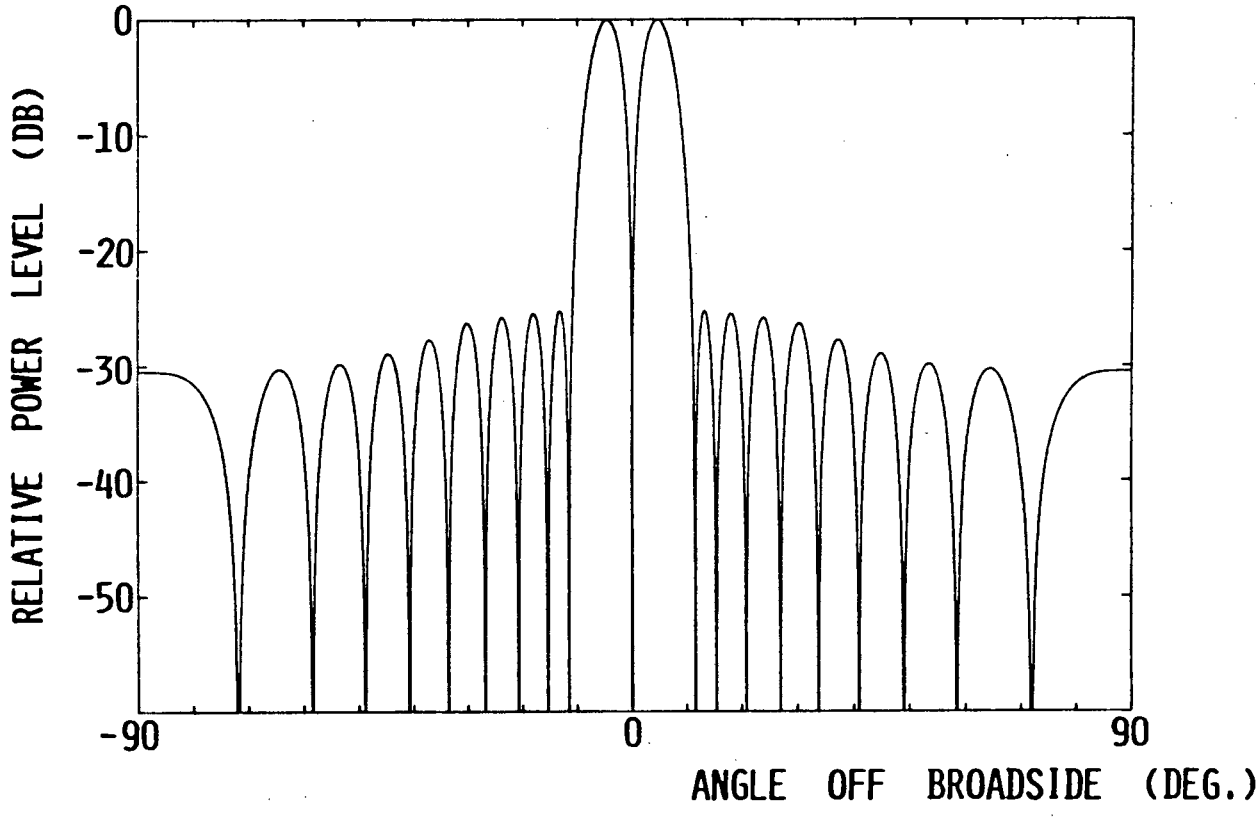

FIGURE 1.3 TYPICAL DIFFERENCE PATTERN

1.2 ARRAY ANTENNAS

A source of electromagnetic radiation may take many different forms. It could be a conducting wire, horn radiator, waveguide slot, or one of many other possibilities. The radiation pattern of a single element is fixed for a given frequency of excitation and consists, in general, of a main beam and a number of smaller sidelobes. In many applications there is a need for improving the performance above that obtainable with a single radiating element. There are, broadly speaking, two methods available for this purpose. One technique uses a properly shaped reflector or lens fed by a radiating element, and the other employs a number of radiating elements correctly arranged in space to form an antenna array. Whether the reflector or array option is to be used depends on a multitude of factors related to particular applications and environments in which the antenna is to operate.

Array antenna development can be divided into three stages: specification, synthesis and realisation. These should not be taken as clear-cut divisions, however, as there is a considerable amount of overlap between the last two stages. Means of unambiguously specifying the required performance of a monopulse antenna are discussed in the following chapter. The synthesis problem involves the determination of the excitations and spacings of the array elements required to obtain desired radiation characteristics. Synthesis is usually performed subject to a set of constraints. The latter may set bounds on certain radiation pattern characteristics (e.g. sidelobe levels), but may also include constraints on other quantities in an attempt to allow easier practical realisability. This second kind of constraint may include factors such as the sensitivity of the array performance to imperfections, or constraints on the complexity of the feed network. It is in the setting down of constraints that engineering judgement must be exercised in the midst of the mathematical techniques.

The final step in the design of an antenna array is the actual establishment of the determined excitations in the form of hardware. The realisation of the array includes the selection of the radiating elements to be used, though this would no doubt have been kept in mind during the synthesis stage. The realisation phase would further involve the determination (theoretically or experimentally) of the element radiation characteristics and the coupling between elements, both externally and internally via the feed network. This information is then used to establish the correct excitation determined from the synthesis procedure.

1.3 OVERVIEW OF THE THESIS

This thesis deals exclusively with array synthesis.

Chapter 2 first summarises the definitions of numerous factors used in the literature to specify the performance of monopulse antennas. Thereafter essential information on array analysis pertinent to this work is given. This includes expressions for the performance indices associated with symmetrically and anti-symmetrically excited linear arrays, which (as far as can be established) do not appear to be given explicitly in the literature. Hence their inclusion in some detail here.

In Chapter 3 the development of the synthesis of sum patterns is reviewed, followed by a review of the state of difference pattern synthesis. Thirdly, an overview is given of the problem of simultaneous sum and difference pattern synthesis. The chapter concludes (Section 3.7) with a summary of synthesis problems which have not been adequately dealt with in the literature, and which form the subject of this thesis.

Chapters 4, 5, 6, 7 and 8 contain the principal contributions of the present work to the theory of monopulse array synthesis. A more detailed indication of the contents of these chapters is more appropriate after the limitations of existing synthesis techniques has been gauged; this is therefore postponed until the end of the third chapter (Section 3.7).

Finally, some general conclusions are reached in Chapter 9, and the research reported herein put into perspective.

Appendix I contains a summary of concepts from the mathematical theories of approximation and optimisation referred to in the thesis, in order to make the latter more self-contained. Appendix II contains tables of design data relating to the synthesis procedure developed in Chapters 4 and 5.

1.4 REFERENCES

[1] M.I. Skolnik, Radar Handbook, (McGraw-Hill, New York, 1970).

[2] R.E. Collin and F.J. Zucker, Antenna Theory: Part I, Chap. 4, (McGraw-Hill, New York, 1969).

CHAPTER 2

MONOPULSE ARRAY SPECIFICATION AND ANALYSIS

2.1 MONOPULSE ANTENNA SPECIFICATIONS

2.1.1 Preliminary Remarks

The primary goal of an antenna design is the establishment of a radiation pattern with specified characteristics. Except for its terminal (circuit-like) properties such as impedance, impedance bandwidth, conversion efficiency, and so on, the parameters which characterize the performance of an antenna are all based on the shape of the radiation pattern. Performance optimisation is therefore the process of maximisation or minimisation of certain pattern performance indices subject to constraints on others. Before such a process can be effected, it is of course necessary that these measures of performance be precisely defined.

For monopulse antennas there is a plethora of such specifications [1]-[7], some related not only to the antenna as a separate unit and measured at the radio frequencies (RF), but to the response with the antenna already connected to intermediate frequency circuitry. Such specifications are commonly referred to as pre-comparator and post-comparator parameters, though this is somewhat of a misnomer. Here only the pre-comparator specifications will be of interest. These are those measured at the output of the essential RF stages at which sum and difference output can be observed for the first time. These are usually the outputs of the RF comparators, and will henceforth be accepted as such here.

Though all of the performance specifications considered are applicable to monopulse antennas of any physical type, the terminology here is specifically directed toward arrays. In what follows, the angle θ will be measured with respect to the direction broadside to the array. Under normal conditions, the maximum of the sum pattern will be in the $\theta = 0$ direction. Terms of the form $E_s(\theta)$ or $E_d(\theta)$ will represent "voltage" values of the radiation pattern.

2.1.2 Sum Pattern Specifications

The directivity $D_s(\theta)$ in a direction θ is defined as the ratio of the radiation intensity (radiated power per unit solid angle) in the direction θ to the average radiation intensity [2]. Let the maximum directivity of the sum pattern (in the direction of the sum pattern peak or boresight direction) of the given array be denoted by D_s^m. Furthermore, let D_s^{max} be the maximum possible directivity obtainable with the given array; this will be that obtained when the elements have identical excitations (in both amplitude and phase). Then the excitation efficiency is defined as

$$\eta_s = D_s^m / D_s^{max} \tag{1}$$

Here the conversion efficiency is assumed to be unity, so that gain and directivity $D_s(\theta)$ are identical.

Further specifications relating to the sum pattern are illustrated in Fig. 2.1. All sum pattern sidelobe levels are measured relative to the sum pattern maximum. The sidelobe ratio (SLR) is the reciprocal of the sidelobe level. In decibels therefore the sidelobe level will be a negative number and the sidelobe ratio positive. In the above discussion, the subscript "s" signifies a sum mode quantity.

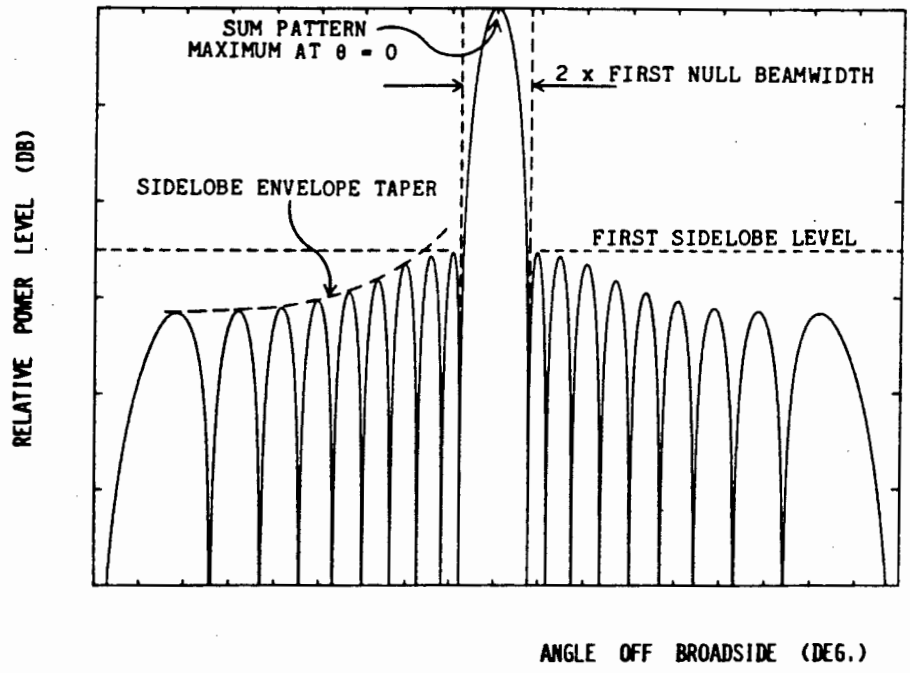

FIGURE 2.1 SUM PATTERN SPECIFICATIONS

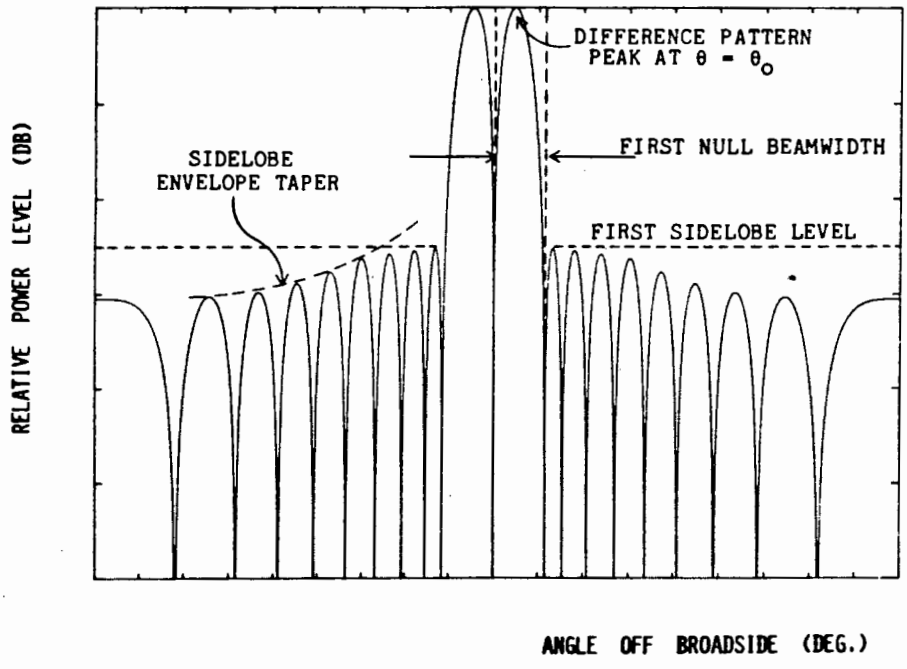

FIGURE 2.2 DIFFERENCE PATTERN SPECIFICATIONS

2.1.3 Difference Pattern Specifications

The difference pattern, illustrated in Fig. 2.2, has a null on boresight (the $\theta = 0$ direction), two maxima either side ($\theta = \pm\theta_o$) of the boresight direction and thereafter a number of sidelobes. These sidelobe levels (sidelobe ratios) will usually be measured relative to the difference pattern maxima. In some instances, however, it is preferable to measure these with respect to the maximum level of the sum pattern of the same array. Unless otherwise stated, the former convention is implied. As for the sum pattern, it is possible to define the directivity $D_d(\theta)$, excitation efficiency η_d, and quantities D_d^m and D_d^{max}.

For monopulse antennas an additional class of parameters have been introduced in order to represent some measure of the slope of the difference pattern in the boresight ($\theta = 0$) direction. Since there has not been complete standardisation in the literature, a number of different slope parameters are defined here, and their relationships shown.

Let $E_d(\theta)$ be the "voltage" pattern (space factor) of the array operating in the difference mode, and $\alpha = kL \sin\theta$ the normalised angle. In this expression k is the free space wavenumber and L the total length of the array. Furthermore, let $D_d(\theta)$ represent the directivity of the difference pattern as a function of θ. The several boresight slope parameters currently in use can then be defined as shown below.

(i) The difference slope is given by Rhodes [4] as,

$$K_d = \left. \frac{\partial E_d(\theta)}{\partial \alpha} \right|_{\alpha = 0} \qquad (2)$$

(ii) The normalised difference slope used by Kirkpatrick [5] is,

$$K = \left. \frac{\partial [D_d(\theta)]^{\frac{1}{2}}}{\partial \alpha} \right|_{\alpha = 0} \tag{3}$$

(iii) If K_o is the maximum value of K possible with a given array of co-phasal excitations and K the actual value for the array, then the difference slope ratio is,

$$K_r = \frac{K}{K_o} \tag{4}$$

(iv) Several other boresight slope quantities are also in use, but these involve sum pattern qualities as well. For instance, Ricardi and Niro [6] define angular sensitivity as,

$$K_a = \sqrt{D_s^{max}}\ K_d \tag{5}$$

with D_s^{max} as defined for the sum pattern in the previous section. As figures of merit for the difference pattern, Hannan [7] defines the relative difference slope,

$$K_g = \frac{K_d}{\sqrt{D_s^{max}}} \tag{6}$$

and a further quantity,

$$K_m = \frac{\theta_{3dB} K_d}{2\sqrt{D_s^m}}$$

where D_s^m and θ_{3dB} are the main beam directivity and half-power beamwidth of the sum pattern, respectively, of the array in question. The tracking sensitivity is often taken to be

$$K_t = \frac{K_d}{\sqrt{D_s^m}}$$

This is also called the normalised angular sensitivity by Kinsey [3]. Finally, Rhodes [4] deals with two further quantities, the slope-sum ratio $K_d/E_s(0)$ and the slope-sum product $K_d E_s(0)$.

The above slope parameters are all RF parameters, measured at the output of the beamforming network, and are of importance at the synthesis stage. While they are all clearly interrelated, for comparing the boresight slope performance of array distributions only K_d, K and K_r are required. The others are more important from an overall tracking system point of view.

When an array antenna is realised in hardware, imperfections in the practical components necessitate the introduction of parameters to measure their effect. Boresight error results, for example, because of the non-idealness of the RF comparator; the difference pattern null is raised and shifts off the boresight direction by a small amount. The array elements will also have cross-polarised field components [8], and therefore the allowable cross-polarisation levels of the array must be specified.

2.2 LINEAR ARRAY ANALYSIS

2.2.1 Introduction

If the elements of an array all lie along a common straight line, they form a linear array. This geometry is not only important in its own right, but is also an essential building block of the majority of planar arrays. The synthesis of such linear arrays is therefore fundamental to all array design.

Before a synthesis problem can be attempted, means of analysing a linear array must be available. Such analyses are treated in some detail in [9], [10] and [11], and a complete treatment is not intended here. Instead, only the most relevant material will be considered, certain new expressions presented, and some concepts written in a more concise form. In what follows, the background to any statements made without proof can be found in the above references.

In order to be clear on exactly which aspects of antenna array analysis are pertinent to the matters at hand here, it is perhaps best to state clearly what categories are not of concern. Firstly, arrays with non-uniform element spacing and those which can be classified as thinned arrays (certain elements removed for various reasons), will not form part of the discussion. Electronically scanned and general shaped-beam array synthesis will also be set aside. Of prime importance is the design of monopulse linear arrays with high directivity (narrow beamwidth) and low sidelobes, for both sum and difference patterns. In all cases the main beam of the sum pattern and null of the difference pattern coincide, and this in the direction broadside to the array. Thus endfire arrays, for example, will not be considered. Although this may seem overly restrictive, such is not really the case. While linear arrays have a long history of development and have achieved a certain level of maturity, the synthesis problem is not yet complete, as will be pointed out in Chapter 3, and there is much scope for research in this area. Furthermore, this type of array is that of greatest concern for practical monopulse tracking systems.

2.2.2 Preliminary Considerations

If the radiation patterns of the individual elements of an array are broad (as is most often the case since the elements usually have low directivity), the significant features of the array pattern are controlled by what is known as the array factor [10]. This latter factor is the pattern of an array of isotropic radiators, with spacings identical to those between the phase centres of the actual elements, and with relative complex (amplitude and phase) weighting or excitations equal to those of the actual array elements. The synthesis problem deals with the array factor. Henceforth, if the "radiation pattern" of an array is mentioned, it is the array factor that is being referred to.

Consider the linear array geometry shown in Fig. 2.3, consisting of 2N elements with uniform element spacing d. The complex excitation of the n-th element is a_n, and the discrete distribution of excitations is called the aperture distribution of the array. The array factor (also called the space factor) is a superposition of contributions from each element, and is given by [9, p. 142],

$$E(\theta) = \sum_{n=-N}^{-1} a_n \, e^{j(2n+1)\frac{kd}{2}\sin\theta} + \sum_{n=1}^{N} a_n \, e^{j(2n-1)\frac{kd}{2}\sin\theta} \qquad (7)$$

where k is the free-space wavenumber.

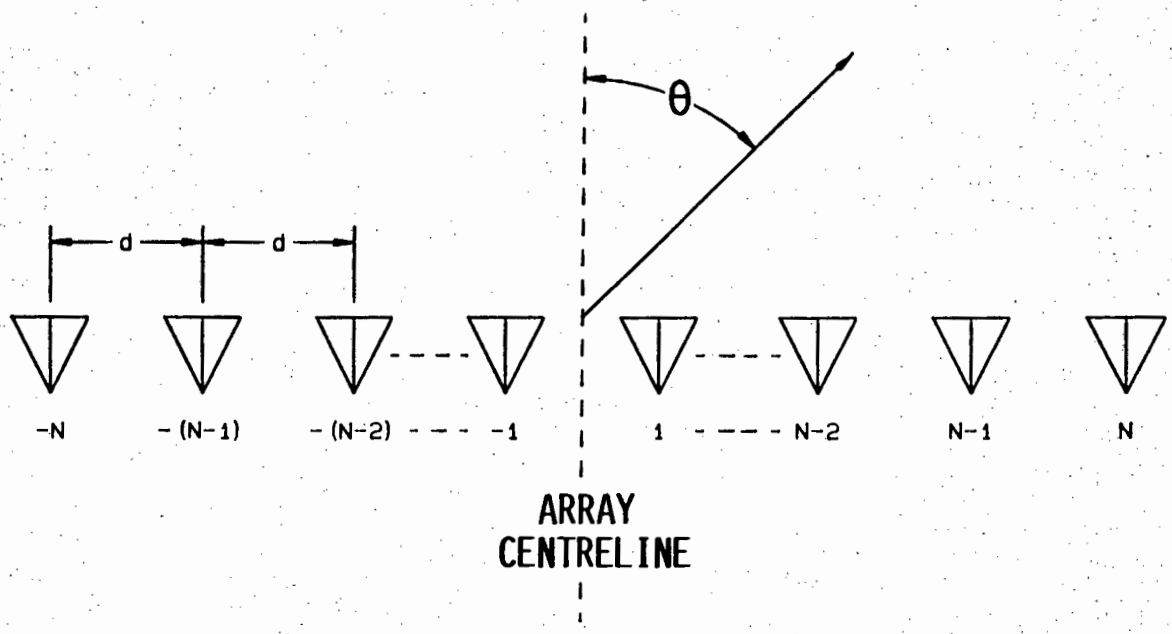

FIGURE 2.3 LINEAR ARRAY GEOMETRY

It is convenient to define an additional variable $\psi = kd \sin\theta$. The latter will be used interchangeably with θ to denote the pattern angle. If this new variable is used, an alternative expression for the array factor is

$$E(\psi) = \sum_{n=-N}^{-1} a_n e^{j(2n+1)\frac{\psi}{2}} + \sum_{n=1}^{N} a_n e^{j(2n-1)\frac{\psi}{2}} \tag{8}$$

Distributions for which $|a_{-n}| = |a_n|$ are of particular importance; reasons will be given in the next chapter.

With symmetrical excitation, $a_{-n} = a_n$, and the array factor becomes [9, p. 142],

$$E_s(\psi) = 2 \sum_{n=1}^{N} a_n \cos\left[(2n-1)\frac{\psi}{2}\right] \tag{9}$$

while for anti-symmetrical (difference) excitation, $a_{-n} = -a_n$, in which case

$$E_d(\psi) = 2j \sum_{n=1}^{N} a_n \sin\left[(2n-1)\frac{\psi}{2}\right] \tag{10}$$

Recall that the array factor expressions given apply to an array of 2N elements (an even number). An array of 2N+1 elements (an odd number) is not suited to anti-symmetric (difference pattern) operation because of the central element. Hereafter <u>all</u> arrays considered in this thesis will be assumed to have an even number of elements, and to be either symmetrically or anti-symmetrically excited.

Expressions for array performance can be concisely written through use of matrix notation. The excitation vector is therefore defined as,

$$[J] = \begin{bmatrix} a_1 \\ a_2 \\ \vdots \\ a_N \end{bmatrix} \tag{11}$$

for an array of 2N elements. The radiation vector is defined as,

$$[F_s] = \begin{bmatrix} \cos[\psi/2] \\ \cos[3\psi/2] \\ \vdots \\ \cos[(2N-1)\psi/2] \end{bmatrix} \tag{12}$$

for symmetric (sum excitation), and as

$$[F_d] = \begin{bmatrix} \sin[\psi/2] \\ \sin[3\psi/2] \\ \vdots \\ \sin[(2N-1)\psi/2] \end{bmatrix} \tag{13}$$

for anti-symmetric (difference) excitation. The corresponding array factors are then, from equations (9) and (10),

$$E_s(\psi) = 2[F_s]^T[J] \tag{14}$$

$$E_d(\psi) = 2j[F_d]^T[J] \tag{15}$$

where $[\ ]^T$ denotes the Hermitian transpose or adjoint (transpose of the conjugate). In the present case the vectors $[F_s]$ and $[F_d]$ are real, so that this simply reduces to the transpose.

The subscript or superscript "s" ("d") has been used to designate quantities associated with sum (difference) excitation. This practice will be continued throughout; when such subscripts and superscripts are omitted, a result applicable to both types of excitation is implied. The terms symmetric (anti-symmetric) and sum (difference) excitation are synonomous.

The following five subsections will define further, and give expressions for, various array performance factors.

2.2.3 Directivity

For an array of isotropic elements the directivity is governed entirely by the array factor. In the case of a linear array with array factor $E(\theta)$, the expression for the directivity in a direction θ reduces to [11],

$$D(\theta) = \frac{2\, E(\theta)\, E^{*}(\theta)}{\int_{-\pi/2}^{\pi/2} E(\theta')\, E^{*}(\theta')\, \cos\theta'\, d\theta'} \tag{16}$$

While Cheng [12] and Collin and Zucker [11] give expressions for $D(\theta)$ in terms of matrices (quadratic forms), this is only done for arrays with quite general excitation. The fact that an array is symmetrically or anti-symmetrically excited should obviously be exploited in order to lower the dimension of any analysis or synthesis work. It is surprisingly cumbersome to attempt to simplify the general results in [11] and [12] to the present special case.

A direct first principle approach applying expressions (9) and (10) to (16) yields the required results with less effort. Explicit expressions for these desired quantities do not appear to be available in the literature, and are therefore derived here.

Consider the case of symmetrical excitation. From (9), the power density term

$$E_s(\psi)E_s^*(\psi) = \{ \sum_{n=1}^{N} a_n \cos [(2n-1)\frac{\psi}{2}] \} \{ \sum_{n=1}^{N} a_n^* \cos [(2n-1)\frac{\psi}{2}] \}$$

$$= \sum_{m=1}^{N} \sum_{n=1}^{N} a_m a_n^* \cos [(2m-1)\frac{\psi}{2}] \cos [(2n-1)\frac{\psi}{2}] \quad (17)$$

If an NxN matrix $[A_s] = \{a_{mn}^s\}$ with m,n = 1,2,$\cdots$N, with elements given by $a_{mn}^s = \cos[(2m-1)\frac{\psi}{2}]\cos[(2n-1)\frac{\psi}{2}]$, is defined, then (17) can be written as

$$E_s(\psi)E_s^*(\psi) = [J]^T[A_s][J] \quad (18)$$

The result (17) can be used in the denominator of (16). Thus,

$$\int_{-\pi/2}^{\pi/2} E_s(\theta')E_s^*(\theta')\cos\theta' d\theta' = \sum_{m=1}^{N} \sum_{n=1}^{N} a_m a_n^* b_{mn}^s$$

with

$$b_{mn}^s = \int_{-\pi/2}^{\pi/2} \cos[(2m-1)\frac{kd\sin\theta'}{2}]\cos[(2n-1)\frac{kd\sin\theta'}{2}]\cos\theta' d\theta' \quad (19)$$

Expansion of the indexed cosine terms as the sums of complex exponentials enables the integral to be evaluated in closed form as,

$$b^s_{mn} = \text{sinc}[(n+m-1)kd] + \text{sinc}[(n-m)kd] \tag{20}$$

where sinc x = sin x/x.

A matrix $[B_s]$ is now defined to be $[B_s] = \{b^s_{mn}\}$, m,n = 1,2,···N. The directivity of this symmetrically excited linear array of 2N elements, in direction θ (or equivalently $\psi = kd \sin\theta$), can therefore be written as the ratio of quadratic forms,

$$D_s(\theta) = \frac{2[J]^T[A_s][J]}{[J]^T[B_s][J]} \tag{21}$$

For the case of an anti-symmetrically excited array the derivation follows the same lines as that just completed, except that the cosine functions with indexed arguments in (17) and (19) are replaced by sine functions. Hence, with

$$[A_d] = \{a^d_{mn}\}$$

$$[B_d] = \{b^d_{mn}\}$$

$$a^d_{mn} = \sin[(2m-1)\tfrac{\psi}{2}]\sin[(2n-1)\tfrac{\psi}{2}]$$

$$b^d_{mn} = \text{sinc}[(n-m)kd] - \text{sinc}[(n+m-1)kd] \tag{22}$$

$$m,n = 1,2,\cdots N$$

The directivity in direction θ for the anti-symmetrically excited array is given by,

$$D_d(\theta) = \frac{2[J]^T[A_d][J]}{[J]^T[B_d][J]} \tag{23}$$

The matrices $[A]$ in either of the above cases can be written in terms of the radiation vectors as,

$$[A] = [F][F]^T$$

2.2.4 Power Pattern and Excitation Efficiency

The symmetric excitation will always produce a pattern with a peak at $\theta = \theta_o = 0$, the anti-symmetric excitation a pattern with peaks at $\theta = \pm\theta_o$, the θ_o value depending on the particular excitations and element spacings selected. If $[A^o]$ is the matrix $[A]$ evaluated at $\theta = \theta_o$, then the normalised power pattern is,

$$P(\theta) = \frac{[J]^T[A][J]}{[J]^T[A^o][J]} \tag{24}$$

Since for the symmetric case the pattern peak occurs at $\theta = 0$, the peak directivity is found from examination of (17) and (21) to be,

$$D_s^m = \frac{2\left|\sum_{n=1}^{N} a_n\right|^2}{[J]^T[B_s][J]} \tag{25}$$

If the array is uniformly excited, the elements of the excitation vector are all unity, and the numerator of (25) becomes $2N^2$. The denominator reduces to a sum of all the elements of $[B_s]$, and (25) therefore becomes,

$$D_s^{max} = 2N^2 \Big/ \sum_{m=1}^{N} \sum_{n=1}^{N} b_{mn}^{s} \tag{26}$$

The excitation efficiency is then,

$$\eta_s = D_s^m / D_s^{max} \tag{27}$$

A similar quantity can be defined for the difference pattern. In this case the co-phasal excitation set which, for a given array size, provides the maximum possible value for the directivity of the difference pattern peak, is not a uniform distribution. But suppose that this maximum value is D_d^{max} and occurs at an angle $\theta = \theta_p$. Then if the maximum directivity of the array being evaluated is D_d^m at $\theta = \theta_o$, the excitation efficiency is

$$\eta_d = D_d^m / D_d^{max} \tag{28}$$

It is also possible to define an excitation efficiency for the difference array in terms of D_s^{max} for a uniform sum array of the same size as,

$$\eta_{ds} = D_d^m / D_s^{max} \tag{29}$$

2.2.5 Array Excitation Tolerance Sensitivity

In the engineering design problem an important question is that concerning the sensitivity of a particular array excitation synthesised. Since the practical realisation of the excitation [J] is never exact, it is important to ascertain how such imperfections will effect the array factor $E(\psi)$. If the smallest error in [J] shifts the resulting $E(\psi)$ far off the desired one, then the synthesis is not an acceptable one from an engineering point of view, even if it is exact.

The tolerance sensitivity S is defined as the ratio,

$$S = \frac{[J]^T[J]}{[J]^T[A][J]}$$

It is important to realise that, since [A] is dependent on θ, so is S. The minimum value of S possible is 1/2N [11, p. 197].

2.2.6 Array Q-Factor

The Q-Factor of an array is defined by [11, p. 200]

$$Q = \frac{[J]^T[J]}{[J]^T[B][J]} \tag{30}$$

From this definition it follows that Q = SD. Since it is proportional to S, and yet independent of pattern angle, it is widely used as a measure of array realisability. A constraint on the Q-factor to a reasonably low value is equivalent to restricting the design within a practical tolerance [12]. A very complete discussion on the concept of a Q-factor for antennas is given by Rhodes [13], who shows that the array Q is proportional to the "observable" time-average electric and magnetic stored energies. By "observable" is meant those portions of the stored energies which are not identical at all frequencies.

Thus a large Q implies excessive stored energy. For co-phasal excitations and inter-elements greater than half a wavelength, the Q-factors are all fairly close to unity. It can however increase rapidly to high values for smaller spacings.

2.2.7 Difference Slope Parameters

As with directivity, for an array of isotropic sources, the boresight slope is entirely dependent on the array factor,

$$E_d(\psi) = 2 \sum_{n=1}^{N} a_n \sin\left[(2n-1)\frac{\psi}{2}\right]$$

The total length of an array of 2N elements and interelement spacing d is L = (2N-1)d. The normalised angle α defined in Section 2.1.3 is therefore $\alpha = (2N-1)kd\sin\theta$. So the relationship between ψ and α is simply $\alpha = (2N-1)\psi$.

From equation (2), and the expression for the array factor $E_d(\psi)$, the difference slope is

$$K_d = \left.\frac{\partial E_d}{\partial \alpha}\right|_{\alpha = 0}$$

$$= \left.\frac{\partial E_d}{\partial \psi} \cdot \frac{\partial \psi}{\partial \alpha}\right|_{\psi = 0}$$

$$= \sum_{n=1}^{N} (2n-1)\, a_n \,/\, (2N-1)$$

Hence $$K_d = [K]^T[J] \qquad (31)$$

where
$$[K] = \frac{1}{(2N-1)} \begin{bmatrix} 1 \\ 3 \\ 7 \\ \vdots \\ (2N-1) \end{bmatrix} \tag{32}$$

Similarly, an expression for the normalised difference slope can be derived from equations (3) and (23). It then follows, after some mathematical manipulation that,

$$K = \frac{\sum_{n=1}^{N} (2n-1)\, a_n}{(2N-1)\sqrt{2[J]^T[B_d][J]}}$$

Therefore
$$K = \frac{[K]^T[J]}{\sqrt{2[J]^T[B_d][J]}} \tag{33}$$

Inspection of equation (31) then reveals that the two slope parameters are related as,

$$K = \frac{K_d}{\sqrt{2[J]^T[B_d][J]}} \tag{34}$$

This gives a normalised difference slope factor for discrete arrays which is consistent with the original definition given by Kirkpatrick [5] for continuous line-source distributions. The equation (33) can also be used to find, for a given element number 2N and spacing d (the effects of spacing d being represented in matrix $[B_d]$), that set of excitations which provides the maximum value of K possible. If this maximum value is K_o, the value of K_r for any prescribed set of excitations on the same array is then simply

$$K_r = K/K_o \tag{35}$$

Equations (31) to (34) prove to be extremely convenient for evaluating the difference distributions to be discussed later in this thesis. As they are not set down or derived elsewhere in the open literature, they have been described in some detail here.

2.3 REFERENCES

[1] M.I. Skolnik, Radar Handbook, (McGraw-Hill, New York, 1970).

[2] R.E. Collin and F.J. Zucker, Antenna Theory : Part I, Chap. 4 (McGraw-Hill, New York, 1969).

[3] R.R. Kinsey, "Monopulse difference slope and gain standards", IRE Trans. Antennas Prop., Vol. AP-10, pp. 343-344, May 1962.

[4] D.R. Rhodes, Introduction to Monopulse, (McGraw-Hill, 1959).

[5] G.M. Kirkpatrick, "Aperture illuminations for radar angle of arrival measurements", IRE Trans. Aeronautical and Navigational Electronics, Vol. AE-9, pp. 20-27, Sept. 1953.

[6] Ricardi and Niro, "Design of a twelve-horn monopulse feed", IRE International Convention Record, Part. I, pp. 93-102, 1961.

[7] P.W. Hannan, "Optimum feeds for all three modes of monopulse antenna", I. Theory, II. Practice, IEEE Trans. Antennas Prop., Vol. AP-9, pp. 444-460, 1961.

[8] A.C. Ludwig, "The definition of cross polarisation", IEEE Trans. Antennas Prop., Vol. AP-21, pp. 116-119, Jan. 1973.

[9] R.S. Elliott, Antenna Theory and Design, (Prentice-Hall, Inc., Englewood Cliffs, New Jersey, 1981).

[10] R.C. Hansen, Microwave Scanning Antennas, Vol. 1, (Academic Press, 1964).

[11] R.E. Collin and F.J. Zucker, Antenna Theory : Part I, Chap. 5, (McGraw-Hill, 1969).

[12] D.K. Cheng, "Optimisation techniques for antenna arrays", Proc. IEEE, Vol. 59, pp. 1664-1674, Dec. 1971.

[13] D.R. Rhodes, Synthesis of Planar Antenna Sources, (Oxford University Press, 1974).

CHAPTER 3

REVIEW OF MONOPULSE ARRAY SYNTHESIS

3.1 INTRODUCTORY REMARKS

The antenna array synthesis problem can be succintly stated as one of finding the excitation $[J]$ that will produce a radiation-pattern $E(\psi)$ with certain performance indices maximised or constrained, and subject to specified (e.g. sidelobe level) constraints on the pattern and even the excitations themselves. Such constraints cannot be completely arbitrary of course, and must be consistent with the basic physical properties of the array.

As was previously stated, the general shaped beam synthesis problem is not being considered here. Here $E(\psi)$ must for the sum pattern case have a single main lobe, while for the difference mode two adjacent beams separated by a deep broadside null are required. In both instances high directivity and low sidelobes is the objective.

As far as high efficiency, low sidelobe array distributions are concerned, a number of important general rules can be stated. Although these arise from the studies reported in literature to be reviewed in the remaining sections of this chapter, they will nevertheless be highlighted at this stage:

(i) It is the zeros of the array space factor that control both the sidelobe level and envelope.

(ii) The aperture stored energy or Q (and the accompanying sensitivity to errors) depends on the shape of the aperture distribution and not just the edge taper (pedestal height).

(iii) A low Q, low tolerance sensitivity distribution requires an array space factor with a far out sidelobe envelope taper of $1/u$, where $u = (d/\lambda)\sin\theta$. A more shallow taper gives a higher Q and tolerance sensitivity, while envelope decays faster than $1/u$ can only be obtained at the cost of increased beamwidth and lower directivity (decrease in excitation efficiency).

(iv) Aperture distributions which begin to increase in amplitude near the array edges ("edge brightening") are undesirable and difficult to implement.

Array synthesis is, from a mathematical point of view, a problem of optimisation theory, and much current work adopts this approach. It can on the other hand in certain cases also be approached from the point of view of approximation theory. The early work (before the advent of the ubiquitous computer) was based almost entirely on such considerations, and research in this area continues. Optimisation and approximation theory are disciplines which are of course inextricably linked, though this connection is not always recognised in the array antenna area. The present chapter will therefore use formulations which serve to demonstrate this connection, in addition to providing an overall review of applicable synthesis methods. In order that this thesis be somewhat self-contained, a summary of pertinent concepts from optimisation and approximation theory is given in Appendix I.

3.2 SUM PATTERN SYNTHESIS

3.2.1 Maximum Directivity for Fixed Spacing and Element Number

Consider an array with a given number of elements and a fixed spacing between elements, and assume that the element excitations $[J]$ necessary for maximisation of the directivity in the broadside direction are desired. The directivity can be written as the ratio of two quadratic forms [Chap. 2, Eqn. (21)], with matrices $[A_s]$ and $[B_s]$ Hermitian, and $[B_s]$ in addition positive-definite. Such properties enable the desired excitations to be obtained directly as the solution of,

$$[B_s][J] = [F_s] \tag{1}$$

with $[F_s]$ evaluated in the broadside direction. Results of such computations have been considered by Cheng [1], Ma [2] , Pritchard [3], Lo et.al. [4], and Hansen [5]. Hansen [5, Fig. 2] has shown that for spacings above a half-wavelength, the maximum directivity is almost identically that obtained with the elements excited with uniform amplitude and phase. For smaller spacings the maximum directivity obtainable is greater than that of a uniform array; this phenomenon is called superdirectivity. However, the excitations are extremely large, have large oscillatory variations in amplitude and phase from one element to another [2, p. 162], and are always associated with an enormously large Q [4] and hence tolerance sensitivity. For this reason fabrication difficulties are usually prohibitive, and superdirectivity avoided in most instances. Experimentally it is simply not easy to produce an array with a directivity much in excess of that produced by a uniform array.

3.2.2 Dolph-Chebyshev Synthesis

Rather than maximise the directivity of the array, consider instead the problem of minimisation of beamwidth; the two approaches are not necessarily equivalent. Beamwidth minimisation subject to a constraint on the sidelobe ratio is the classic array synthesis problem solved by C.L. Dolph in his monumental 1946 paper [6]. The underlying argument behind Dolph's approach has been put concisely by Hansen [5]:

> "A symmetrically tapered (amplitude) distribution over the array ..... is associated with a pattern having lower sidelobes than those of the uniform (amplitude) array. Lowering the sidelobes broadens the beamwidth ..... Some improvement in both beamwidth and efficiency is obtained by raising the farther out sidelobes. Intuitively one might expect equal level sidelobes to be optimum for a given sidelobe level".

In order to synthesize such a pattern for broadside arrays with interelement spacing greater than or equal to a half-wavelength, Dolph made use of the Chebyshev polynomials. The latter, denoted by $T_m(x)$, where m is the order of the polynomial, have oscillations of unit amplitude in the range $-1 \leq x \leq 1$, while outside this range they become monotonically large. Furthermore, $T_m(x)$ has m zeros, all within the range $-1 \leq x \leq 1$. In order to obtain a correspondence between the polynomial and array space factor, part of the $x > 1$ region is mapped onto one side of the main beam while the oscillatory portion of the polynomial is mapped out once onto the sidelobes on one side of the main beam. Since an array of m elements has m-1 zeros, a Chebyshev polynomial of order m-1 must be used. The transformation from $T_{m-1}(x)$ to array space factor $E_s(\psi)$ is $x = x_o \cos(\psi/2)$, where $\psi = kd \sin\theta$. If the sidelobe ratio is denoted by SLR, then

$$x_o = \cosh\left\{ \frac{1}{m-1} \ln\left[SLR + \sqrt{SLR^2 - 1} \right] \right\} \qquad (2)$$

$$= \cosh\left\{ \frac{\cosh^{-1}(SLR)}{m-1} \right\}$$

and the array space factor is,

$$E_s(\psi) = T_{m-1}\left[x_o \cos(\psi/2) \right] \qquad (3)$$

From these, expressions for computing the required excitations may be derived. Such formulas have been derived by Stegen [8,12], van der Maas [9], Barbiere [10] and Bresler [17]. With current computational capabilities those due to Stegen [8] can be used directly.

For an array of m = 2N elements, the excitations are given by [8],

$$a_n = \frac{1}{N}\left\{ SLR + 2 \sum_{p=1}^{N-1} T_{2N-1}\left[x_o \cos\left(\frac{p\pi}{2N} \right) \right] \cos\left[\frac{(2n-1)p\pi}{2N} \right] \right\} \qquad (4)$$

for n = 1,2,•••••N. Care should be taken with the computations and evaluation of the Chebyshev polynomials. For large arrays or low sidelobes multiple precision is required in performing the summation in (4).

Dolph was able to prove [6] that the array so synthesised is optimum in the sense that for the specified sidelobe ratio and element number, the beamwidth (between first nulls) is the narrowest possible. Alternatively, for a specified first-null beamwidth, the sidelobe level is the lowest obtainable from the given array geometry. This means that it is impossible to find another set of excitation coefficients yielding better performance, in both beamwidth and sidelobe ratio, for the given element number and uniform spacing d.

It represents a closed form solution to the optimisation problem of beamwidth minimisation subject to sidelobe constraints. The pattern of a 20-element Dolph-Chebyshev with a 30 dB sidelobe ratio is illustrated in Fig. 3.1.

The original work of Dolph [6] is only valid for the case

$$\lambda/2 \leq d \leq \frac{\cos^{-1}(-1/x_o)}{\pi}$$

Though this is possibly the most widely used case, it should be added that Riblet [7] showed how this restriction can be lifted, but only for an array of an odd number of elements. Dolph's transformation is such that for $d < \lambda/2$ the pattern no longer contains the maximum possible number of sidelobes (the complete oscillatory region $|x| \leq 1$ is not utilised) and hence the beamwidth will not be at its minimum. The alternative transformation between x and ψ, due to Riblet, rectifies this matter. Algorithms for determining the excitations of such arrays have been given by Brown [11,13], Drane [14,15] and Salzer [16].

The Dolph-Chebyshev theory is indispensable and serves as a firm foundation for sum pattern synthesis. It provides a means of understanding array principles and indicates upper bounds on the performance that can be achieved. However, it does have a number of drawbacks as regards its use as a practical distribution. These are discussed below.

Consider a Dolph-Chebyshev array of 2N = 20 elements. The required excitations, obtained using equation (4), are shown in Table 3.1 for sidelobe ratios of 20 dB, 30 dB and 40 dB. These indicate the tendency of equal sidelobe level distributions such as the Dolph-Chebyshev to have large peaks at the array ends (a non-monotonic distribution) for certain element number/SLR combinations. For a given

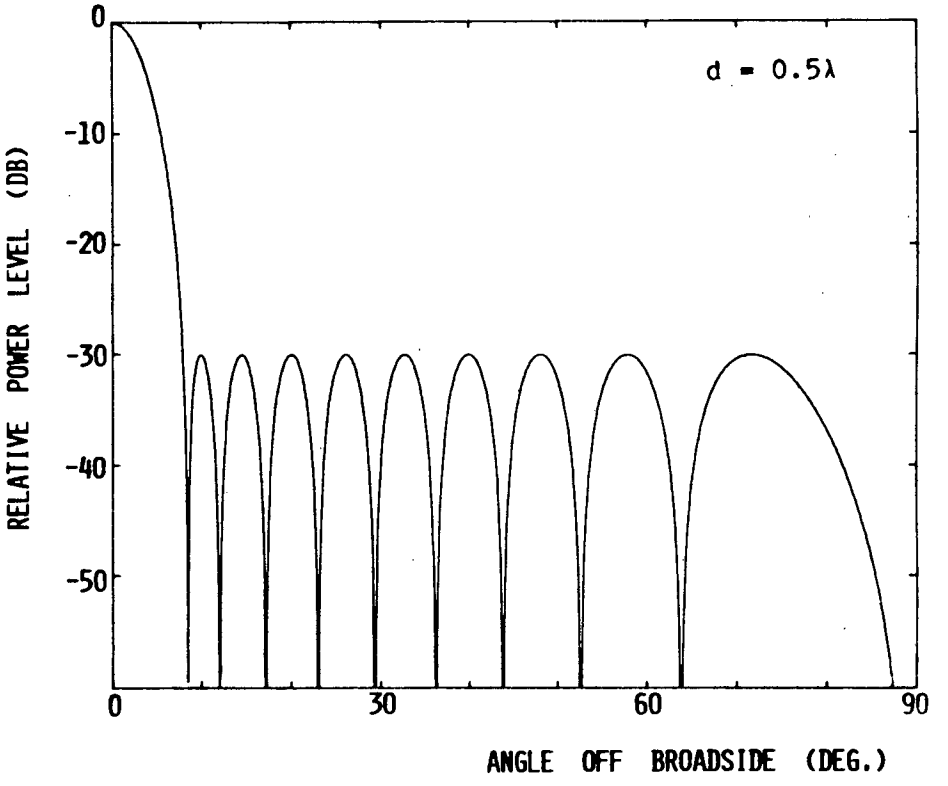

(a).

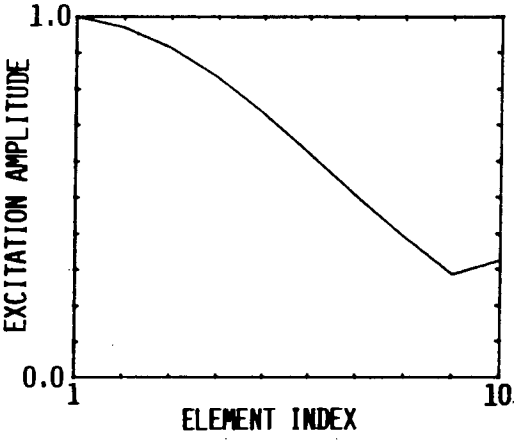

(b).

FIGURE 3.1(a) SPACE FACTOR OF A DOLPH-CHEBYSHEV ARRAY (2N=20, SLR=30 DB)

(b) ASSOCIATED APERTURE DISTRIBUTION (DISCRETE EXCITATIONS HAVE BEEN JOINED BY STRAIGHT SEGMENTS)

number of elements 2N there will be a certain SLR for which the distribution of excitations is "just" monotonic. If the number of elements is increased but this same SLR is desired, the required distribution will be non-monotonic. Increasing the SLR (lower sidelobes) will allow a monotonic distribution once more. For the example shown in Table 3.1, the distribution is already non-monotonic for a sidelobe ratio of 30 dB, while for a 20 dB sidelobe ratio the edge excitation is larger than the centre one. The peaks in the distribution at the array ends are not only disadvantageous in that they are difficult to implement and make an array which is realised more susceptible to edge effects, but they are also indicative of an increase in the Q and tolerance sensitivity [24].

Optimum beamwidth arrays do not necessarily provide optimum directivity, especially if the array is large [18, p. 91]. To see this, consider a Dolph-Chebyshev array with a fixed sidelobe ratio. Let the array size increase (increase the element number with the spacing held fixed), at each stage keeping the sidelobe ratio constant and normalising the radiation pattern. This is permissible because the directivity to be found at each stage is only dependent on the angular distribution of the radiation and not on any absolute levels. It is then observed that the denominator of the directivity expression is dominated by the power in the sidelobes after a certain array size is reached, and remains roughly constant thereafter. Thus it is found that the Dolph-Chebyshev distribution has a directivity limit [12] because of its constant sidelobe level property, and for a given array size and maximum sidelobe level, may not be optimum from a directivity point of view. To remove this limitation a taper must be incorporated into the far-out sidelobes. Array distributions which will do this are taken up in the following two sections. It should be mentioned that there may be other reasons, in addition to that given above, why low tapering sidelobes are desired, especially if the antenna is to operate in a hostile environment [19].

TABLE 3.1 : Element excitations for Dolph-Chebyshev distributions providing the sidelobe ratios indicated, for an array of 20 elements.

SLR	20 dB	30 dB	40 dB
a_1	1.00000	1.00000	1.00000
a_2	0.98146	0.97010	0.95869
a_3	0.94516	0.91243	0.88030
a_4	0.89261	0.83102	0.77266
a_5	0.82596	0.73147	0.64612
a_6	0.74789	0.62034	0.51211
a_7	0.66149	0.50461	0.38166
a_8	0.57004	0.39104	0.26408
a_9	0.47689	0.28558	0.16597
a_{10}	1.02812	0.32561	0.11820

3.2.3 Continuous Line-Source Distributions for Sum Patterns

Although arrays of discrete radiating elements are being dealt with in this work, no review of synthesis techniques would be complete without reference to similar work on the synthesis of continuous line-source distributions, especially the work of Taylor [20]. Line-source synthesis is important in the array context for several reasons. Firstly, general principles can be learned which are equally applicable to arrays (see Section 3.1). Secondly, continuous distributions can be sampled for use with arrays. Furthermore, the direct discrete array synthesis methods to be discussed in the following sub-section have developed out of the theory on continuous distributions.

Perhaps the most startling result on continuous distributions is that obtained by Bouwkamp and de Bruyn [21], who showed that with a continuous line-source of fixed length it is possible (in theory) to achieve any desired directivity. However, though this implies that there is no limit to the directivity, any directivity increase above that obtained from the aperture when it is uniformly excited is accompanied by a sharp increase in the nett reactive power required at the source to produce it [22], and thus a large Q and sensitivity. Practical considerations therefore make it unacceptable, as in the case of the unconstrained maximisation of the directivity of the discrete array (Section 3.2.1). To be realisable physically, some constraint has to be placed on the proportion of reactive to radiative power, or equivalently on the Q.

It is customary, when dealing with continuous line-source distributions, to use the variable $u = (L/\lambda)\sin\theta$, where L is the length of the source. This practice will be followed here.

The next question regarding continuous distributions is that of the distribution which provides the narrowest beamwidth for a given sidelobe level, and vice versa. This was answered by Taylor [20], who used the Dolph-Chebyshev theory as starting point. It was indicated in Section 3.2.2 that the Chebyshev polynomial $T_{m-1}(x)$ could be used to find the set of excitations which results in the optimum relationship between beamwidth and sidelobe ratio for an array of m elements. Using an asymptotic relationship for the Chebyshev polynomials given by van der Maas [9], Taylor derived the continuous equivalent of the Dolph-Chebyshev distribution. This distribution has a pattern with all sidelobes of equal level, and is optimum in the sense that it provides the narrowest beamwidth for a given sidelobe ratio of any non-superdirective distribution.

Taylor called this the "ideal" line-source distribution. "Ideal" because of the fact that it is unrealisable, having a singularity at each end; a feature indicated by the non-decaying sidelobe levels.

A solution to this problem was devised by Taylor [20], who recognised (and appears to be the first to have done so) that the synthesis problem is one of correctly positioning the zeros of the space factor (radiation pattern). Taylor observed that close-in zeros should maintain their spacings to keep the close-in sidelobes suitably low, and keep the beamwidth narrow. But at the same time further out sidelobes should decay as 1/u [18, p. 55]. Such sidelobe decay is found in the space factor $\sin \pi u/\pi u$ of a uniform line-source distribution, which has zeros at $u = \pm 1, \pm 2, \cdots\cdots$ [18, p. 48]. Suppose now that the ideal line-source has zeros at $u = \pm u_n$, $n = 1,2,3,\cdots\cdots$. What Taylor did was to stretch the u scale slightly by a dilation factor σ slightly greater than unity (so that the close-in zero locations are not shifted much) and chosen such that a some point, a shifted zero u_n is made to coincide with an integer, say $n = \bar{n}$. From this transition point, the zeros of the ideal line-source are replaced by those of the uniform line-source. That is, the zeros of the new pattern are,

$$u = \begin{cases} \pm \sigma u_n & 1 \leq n \leq \bar{n} \\ \pm n & n \geq \bar{n} \end{cases}$$

with $\sigma u_{\bar{n}} = \bar{n}$. This pattern has $\bar{n}$ roughly equal sidelobes, with a 1/u sidelobe decay beyond $u = \bar{n}$. The corresponding aperture distribution is then found as a Fourier series obtained from the above information on the zeros [18, p. 58]. The final result is a distribution (the Taylor $\bar{n}$ distribution) which for a given sidelobe ratio gives both a narrower beamwidth and higher directivity than any comparable (i.e. those with a sidelobe taper) continuous line-source distribution. Information relating the sidelobe ratio, dilation factor and $\bar{n}$ values has been given by Hansen [18, p. 57]. Also given are expressions for the aperture distribution itself [18, p. 58]. Too large a value for $\bar{n}$ (exactly how large depends on the specified sidelobe ratio) implies that the ideal line-source distribution is "being approached too closely". The aperture distribution then becomes non-monotonic with peaks at the aperture ends (though the singularities of the ideal source do not occur), with an accompanying increase in excitation tolerances. Usually the $\bar{n}$ value is selected on the basis of the aperture distribution shape and tolerances.

The Taylor $\bar{n}$ distribution was generalised by Rhodes [22, pp. 129-137] to one dependent on the parameter $\bar{n}$ and an additional one, say ν, which controls the taper rate of the sidelobe envelope for a given $\bar{n}$. A value of $\nu = -1$ corresponds to the "ideal" line-source case. If $\nu = 0$, the original Taylor $\bar{n}$ distribution results, while $\nu > 0$ provides sidelobe envelope tapers more rapid than that of the $\nu = 0$ case.

A third continuous distribution due to Taylor is his one-parameter line-source distribution [18, p. 58]. Beginning with the $\sin \pi u/\pi u$ space factor of a uniform line-source, with zeros at $u_n = \pm n$, a new set of zeros were defined as $u_n = \sqrt{n^2 + B^2}$ where the "one-parameter" B is real and greater than zero. From this altered set of zeros a low Q distribution is obtained which has a sidelobe taper of 1/u, starting at the very first sidelobe, whose level is determined by the value of B selected. The decay rate (which is expected, since $u_n \to \pm n$ for large n) is the same as that of the Taylor $\bar{n}$ line-source distribution.

Though the zeros of the Taylor one-parameter and $\bar{n}$ distributions are never identical (except for the trivial case when these both reduce to the uniform distribution, B = 0 and $\bar{n}$ = 1, respectively), the $\bar{n}$ distribution roughly speaking selects a design between the ideal and one-parameter cases. However, for the same first sidelobe ratio, the $\bar{n}$ distribution has a higher excitation efficiency (and hence directivity), and is therefore used more often. The reason for this is that the $\bar{n}$ distribution tends to flatten out at the ends of the line source while the one-parameter case does not.

The Taylor one-parameter distribution was generalised by Bickmore and Spellmire, whose work has been reported in [23] and [24], into a two-parameter continuous line-source distribution. One of the parameters (c), like the B above, selects the starting sidelobe ratio, while the other (say ν) selects the rate of decay of the sidelobes. These two parameters are completely independent and the space factor (radiation pattern) is the Lambda function

$$\Lambda_{\nu} \left(\sqrt{u^2 - c^2}\right) .$$

A value of $\nu = \frac{1}{2}$ yields the Taylor one-parameter distribution and $\nu = -\frac{1}{2}$ the Taylor "ideal" line-source, while $\nu = > \frac{1}{2}$ gives sidelobe envelope tapers more rapid than 1/u and is correspondingly less efficient.

Hansen [25] comments that for a given set of high directivity/low sidelobe requirements, the above distributions are always better than the earlier distributions such as cosine-on-a-pedestal, Hamming, and so on, and the latter should be regarded as obsolete.

3.2.4 Tapered-Sidelobe Sum Pattern Distributions for Discrete Arrays

It is clear from the previous section that the theory of continuous aperture line-source distributions for sum patterns is extensive and well-developed. If these are to be used with arrays of discrete elements, some form of discretisization process must be performed. The earliest methods simply sampled the continuous distributions at the element locations. Unless the arrays are very large, however, a badly degraded pattern may be obtained. An alternative technique was proposed by Winter [26]. The initial array element excitations are determined by sampling of the continuous distribution and then iteratively adjusting these through Newton-Raphson minimisation of an error expression comprised of the sum of the squares of the differences between calculated (discrete) and specified (continuous) levels for a selected number of sidelobes.

A more sophisticated yet direct alternative method was devised by Elliott [27]. This method matches zeros. Instead of sampling the continuous aperture distribution, one requires that the pattern zeros of the continuous case also occur in the starting pattern of the discrete case. If the resulting pattern does not meet the design goal, a perturbation procedure has to be applied to the discrete distribution in order to bring the final pattern within specification. As recently as 1982 Hansen [24] could correctly state that there were "no discrete distributions that yield a highly efficient tapered sidelobe pattern" directly and that in designing most arrays a continuous distribution had to be quantised in some manner. For the narrow beam, low sidelobe sum pattern, this is no longer the case as a result of an ingenious approach devised by Villeneuve [28]. The method utilises the important principle of synthesising aperture distributions - that of correct positioning of the space factor zeros. The Villeneuve distribution is the discrete equivalent of the highly desirable Taylor $\bar{n}$ distribution. The array element excitations can be obtained in a direct manner without the need for any form of approximation, sampling or perturbation procedures. In order to describe the Villeneuve procedure, consider an array of 2N elements

with the maximum sidelobe level specified. The first step consists of determining the space factor zeros for a Dolph-Chebyshev distribution with the same sidelobe level. Let the zeros of this Chebyshev distribution be denoted by ψ_n, $n = \pm1, \pm2, \cdots \pm(N-1), N$. Furthermore, let ψ_{on} be the zeros of a uniform array of 2N elements, given by $\psi_{on} = n\pi/N$, for the same range of n as above. Now move the zeros of the Chebyshev pattern so that for $n \geq \bar{n}$, where $\bar{n}$ is some selected zero, they coincide with those of the uniform array ψ_{on}. In addition, multiply each of the first $\bar{n}-1$ Chebyshev zeros by a dilation factor $\sigma = \bar{n}\ 2\pi/2N\ \psi_n^-$. Thus the final zeros of the array are,

$$\psi_n' = \begin{cases} \sigma\ \psi_n & n \leq \bar{n} - 1 \\ \\ \psi_{on} & n \geq \bar{n} \end{cases} \tag{5}$$

From these altered zeros, the final element excitations are obtained. Villeneuve [28] has devised efficient ways of doing this. These excitations are those of a discrete "Taylor-like" distribution, with the close-in sidelobes close to the design maximum specified, and the further out ones decreasing at the rate 1/u ($u = d/\lambda \sin\theta$ for the discrete case) in amplitude as their position becomes more remote from the main beam. As with the continuous Taylor distribution, $\bar{n}$ is a design variable. The Villeneuve distribution is of course also applicable to the case of an odd number (2N+1) of array elements. A comparison of the excitation efficiencies of the Villeneuve (discrete) and Taylor (continuous) distributions has been published by Hansen [29].

For an array of 2N elements, with a first sidelobe ratio SLR, the symmetrical element excitations a_p, $p = 1,2,\cdots N$, are determined as follows [28]:

$$x_o = \cosh \left\{ \frac{1}{2N-1} \ln \left[SLR + \sqrt{SLR^2 - 1} \right] \right\} \tag{6}$$

$$\psi_p = 2 \cos^{-1} \left\{ \frac{1}{x_o} \cdot \cos \left[\frac{(2p-1)\pi}{2(2N-1)} \right] \right\} \tag{7}$$

$$\sigma = \frac{\bar{n}\, 2\pi}{2N\, \psi_{\bar{n}}} = \frac{\bar{n}\, \pi}{2N \cos^{-1} \left\{ \frac{1}{x_o} \cos \left[\frac{(2\bar{n}-1)\pi}{2(2N-1)} \right] \right\}} \tag{8}$$

$$\psi_p' = \sigma\, \psi_p \tag{9}$$

$$a_p = \frac{1}{2N} \left\{ E_o + \sum_{m=1}^{\bar{n}-1} E_m \cos \left[\left(p - \frac{1}{2} \right) \frac{m\pi}{N} \right] \right\} \tag{10}$$

$$E_o = 2N \frac{\prod_{q=1}^{\bar{n}-1} \sin^2 \left(\frac{\psi_q'}{2} \right)}{\prod_{q=1}^{\bar{n}-1} \sin^2 \left(\frac{q\pi}{2N} \right)} \tag{11}$$

$$E_m = \frac{2N(-1)^m \prod_{q=1}^{\bar{n}-1} \sin \left(\frac{m\pi}{2N} - \frac{\psi_q'}{2} \right) \sin \left(\frac{m\pi}{2N} + \frac{\psi_q'}{2} \right)}{\sin \left(\frac{m\pi}{2N} \right) \sin \left(\frac{2m\pi}{2N} \right) \prod_{\substack{q=1 \\ q \neq m}}^{\bar{n}-1} \sin \left[\frac{(m-q)\pi}{2N} \right] \sin \left[\frac{(m+q)\pi}{2N} \right]} \tag{12}$$

The above technique is now generally referred to as the Villeneuve $\bar{n}$ distribution [29]. An example of such a distribution, along with its associated radiation pattern, is shown in Fig. 3.2 for the purposes of illustration.

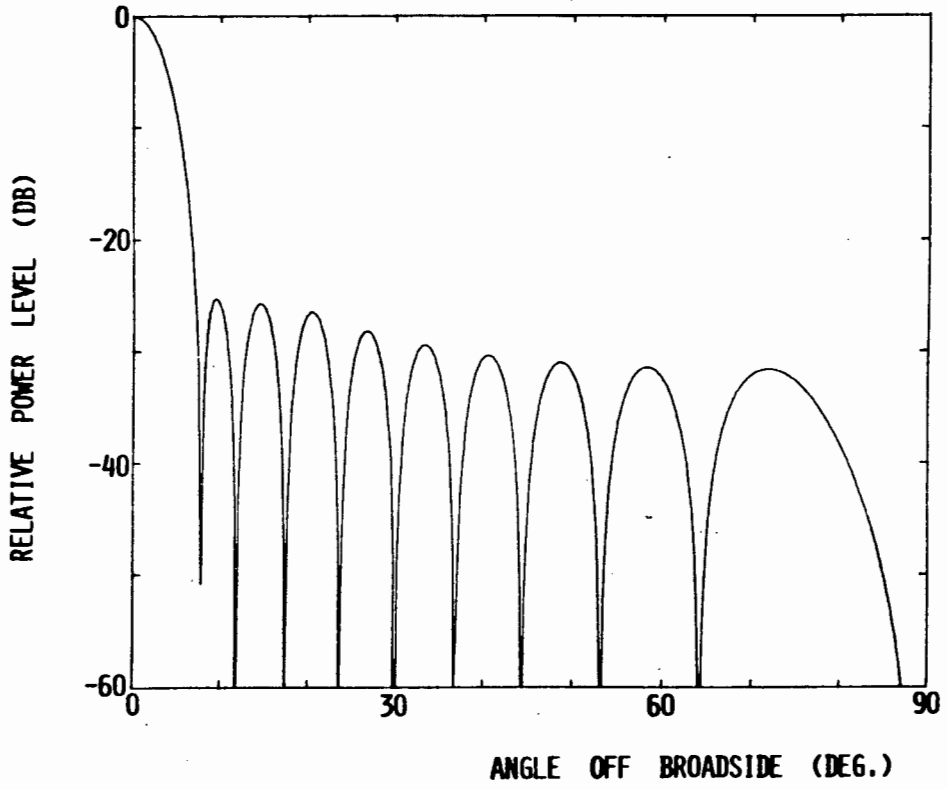

(a).

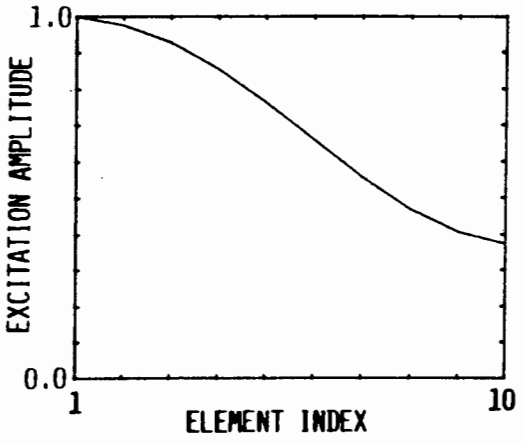

(b).

FIGURE 3.2(a) SPACE FACTOR OF A VILLENEUVE ARRAY (2N=20, SLR=25 DB)

(b) ASSOCIATED APERTURE DISTRIBUTION (DISCRETE EXCITATIONS HAVE BEEN JOINED BY STRAIGHT SEGMENTS)

3.3 DIFFERENCE PATTERN SYNTHESIS

3.3.1 Introduction

Most of the voluminous literature on the synthesis of linear arrays deals with sum patterns. Many of these principles apply equally well to the synthesis of difference patterns of course. However, additional performance indices (e.g. difference slope) are important, and alternative array distributions are required to provide high performance difference patterns. Preferably, a sequence of results paralleling that for sum patterns, analogous to Dolph-Chebyshev synthesis and the Villeneuve $\bar{n}$ distribution method, is desired. Up to the present time such has not been the case, difference pattern array synthesis not having reached the same level of completeness as that for the sum mode, especially from an antenna theory point of view. In spite of this, useful work has been reported; this will be reviewed in the following three short subsections.

3.3.2 Maximum Directivity for Fixed Spacing and Element Number

One figure of merit of a difference pattern is the directivity in the direction of the beam maxima. Such a maximisation, using a method similar to that discussed in Section (3.2.1) for sum patterns, has been briefly mentioned by Ma [2, p. 170] but no details have been published. As in that case, however, this is a case of unconstrained synthesis with its associated problems. Once more, no control over the sidelobes is possible, making it unsuitable for most applications for which monopulse arrays are needed.

3.3.3 Discrete Array Synthesis Subject to Sidelobe Constraints

A difference pattern is called optimum "in the Dolph-Chebyshev sense" if it has the largest normalised slope on boresight (i.e. in the direction of the pattern null) and narrowest beamwidth for a specified sidelobe ratio, given the fixed number of array elements and interelement spacing. Price and Hyneman [30] demonstrated that array difference patterns with equal amplitude sidelobes are optimum in this sense, in that they display both the lowest sidelobe ratio for a given difference lobe beamwidth as well as the largest slope on boresight. They then proceeded to list the properties required of a polynomial which could be used to find the element excitations for such an optimum difference pattern. Having concluded that "no known polynomial has the required characteristics" [30, p. 569], they proceeded to develop a method based on a modification (which they called a transmutation) of a Dolph-Chebyshev excitation function for sum patterns. The result is, however, a pattern with below-optimum performance.

More recently, Balakrishnan and Ramakrishna [31], in the light of appropriate polynomials not being available, devised a numerical method to obtain difference mode patterns with an equiripple sidelobe structure. They reduce the problem of obtaining the optimum excitations to a minimax problem, and solve this using a modified Remes exchange algorithm.

The above two papers appear to be the only ones available which attempt to tackle specifically the discrete array difference pattern problem directly.

3.3.4 Continuous Line-Source Distributions for Difference Patterns

Clearly work on the synthesis of discrete array distributions for difference patterns has been scarce in the open literature. Somewhat more has appeared on the subject of continuous aperture distributions. Kirkpatrick [32] in 1953, by a straightforward application of the calculus of variations, showed that the maximum normalised difference slope (K) on boresight is produced by a line-source with a linear odd distribution such as that shown in Fig. (3.3). Thereafter Hannan [33] showed that the real line-source distribution which provides maximum peak directivity of the difference beam is a truncated sine curve having an edge taper of 2.15 dB relative to its maximum value. This distribution is illustrated in Fig. 3.4. Furthermore, it was shown that the directivity of the line-source with this difference distribution is 2.15 dB below that of the same line-source operated for maximum directivity in the sum mode (uniform distribution). Nester [34] considered the maximisation of the sensitivity factor (K_s), assuming that the difference distribution was obtained from that for the sum by a simple phase reversal of one half of the sum distribution (i.e. a two-module feed network). The line-source distribution which maximises this factor is given [34] in Fig. 3.5.

Powers [35] obtained a difference space factor $L_{\nu,c}(u)$ by [26] differentiating the Bickmore-Spellmire space factor

$$\Lambda_{\nu}(\sqrt{u^2 - c^2}),$$

where $u = (L/\lambda)\sin\theta$, L being the length of the continuous line source. The rate of sidelobe decay for large u, as well as the space factor zero positions (and hence difference lobe beamwidths), can be controlled by adjusting ν and c, though these are not independent. The synthesis of the line-source distribution is carried out by taking the Fourier transform of the space factor $L_{\nu,c}(u)$ [35]. The linear odd distribution of Kirkpatrick [32] is a special case of the present distribution, though its property would not be obvious from the analysis of Powers had it not been known previously anyway.

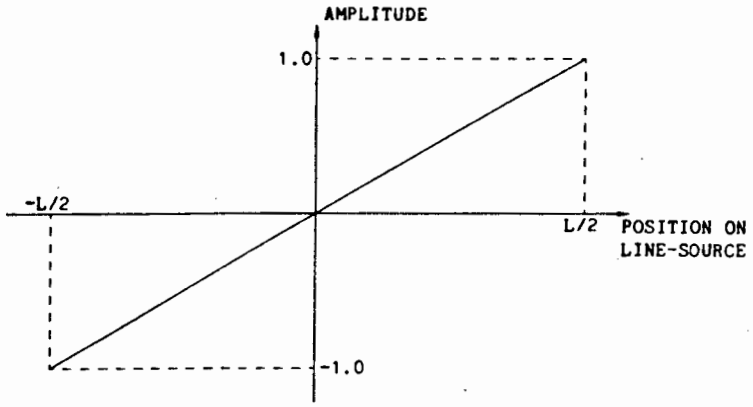

FIGURE 3.3 LINEAR ODD LINE-SOURCE DISTRIBUTION FOR MAXIMUM NORMALISED BORESIGHT SLOPE

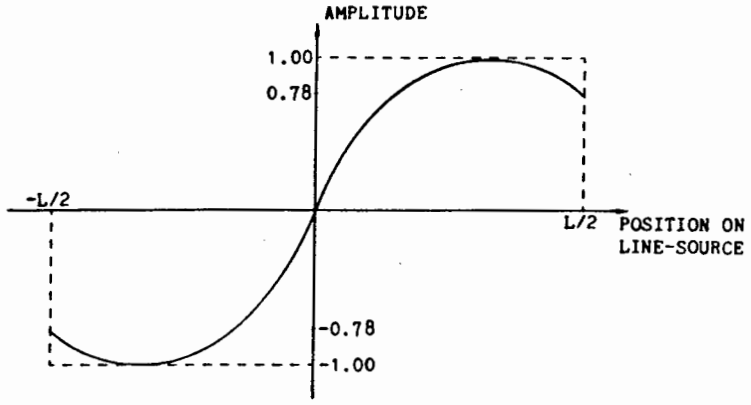

FIGURE 3.4 MAXIMUM DIFFERENCE DIRECTIVITY LINE-SOURCE DISTRIBUTION

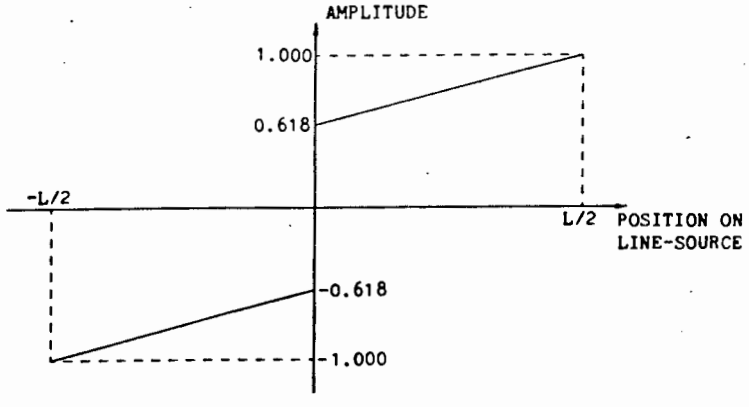

FIGURE 3.5 LINE-SOURCE DISTRIBUTION FOR MAXIMUM SLOPE-SUM RATIO

In essence the Powers distribution allows one to draw up curves of slope at boresight, and sidelobe ratio, versus the two parameters ν and c. At no stage however is one assured that, for a required sidelobe ratio, the distribution gives the maximum boresight slope or difference lobe beamwidths, or vice versa.

By far the most useful (and most used) continuous line source distributions for difference patterns are those due to Bayliss [36]. Bayliss took the derivative of Taylor's "ideal" (sum) line-source space factor, to obtain a space factor

$$u \operatorname{sinc}(\pi\sqrt{u^2 - A^2})$$

In order to obtain from this a difference space factor with the first $\bar{n}$ sidelobes close to some specified level, after which the sidelobes taper off as 1/u, Bayliss undertook a parametric study in which the zeros and A were numerically adjusted for a number of sidelobe ratio values. Fourth order fitted polynomials for A, the difference lobe peak position, and the first four zeros (the others following from these) as functions of the required sidelobe ratio were obtained from the numerical data [36]. The Bayliss distribution can be obtained from the final space factor zero positions in the form of a Fourier series, and gives near-optimum boresight difference slope for the specified sidelobe level. It is the difference pattern analogue of the Taylor distribution, though not as elegant because of the numerical root adjustment required for each new sidelobe ratio specified.

Finally, Lopez [32] has reported a method of obtaining the line-source distribution which provides maximum difference slope ratio (defined as the ratio the normalised difference slope of the line source to that of the linear odd excitation of Fig. 3.3), and this subject to a sidelobe ratio constraint. The method is entirely numerical.

Should any of the above continuous distributions be used with discrete arrays, some form of sampling, as discussed for sum distributions in Section 3.2.4, has to be used, and with the associated problems.

3.4 SOME GENERAL METHODS OF ARRAY SYNTHESIS

Numerous methods have been devised for handling the arbitrarily-shaped-beam array synthesis problem. These are all of a numerical nature, involving some form of iterative procedure. In most cases they utilise for the array problem some general mathematical constrained optimisation technique. Such methods differ principally in the following respects:

(i) The way in which the array problem is formulated as such an optimisation problem (e.g. the choice of performance indices to be minimised or maximised).

(ii) The type of constraints which are applied (e.g. limited Q, maximum sidelobe levels allowed).

(iii) The particular optimisation algorithm used (e.g. linear programming, quadratic programming, use of ratios of Hermitian quadratic forms).

A good summary of such methods has been given by Hansen [24, pp. 48-54]. Detailed overviews have also been given by Cheng [1] and Lo et. al. [4], as well as Sanzgiri and Butler [38]. In order to make this brief section yet complete, a number of further papers deserve or require special reference. Those by Elliott et. al. [39,40], though of a numerical nature, are firmly based on the important principle of correct space factor zero placement mentioned in Section 3.2. Those by Einarsson [41], Owen and Mason [42], and Ng et. al. [43] are relevant to later sections of this work.

Any of the above numerical methods could be used for the synthesis of sum and difference patterns with high directivity and low sidelobes. But more direct methods are preferred, if they are indeed available. Reasons for this are presented in Section 3.6.

3.5 SIMULTANEOUS SYNTHESIS OF SUM AND DIFFERENCE PATTERNS

3.5.1 The Problem of Simultaneous Synthesis

Assume for the moment that it is possible to synthesise separately both sum and difference array distributions with performance that can be classified as optimum. If feed networks of the type shown in Fig. 3.6(a) are available for providing independent excitations for the two modes of operation, then these separate optimum distributions should be utilised. (The network shown should be regarded as schematic. Its realisation in hardware, though providing the same desired response, is more often as shown in Fig. 3.6(b), which is called a tandem feed network [44]). The latter allows both modes to be independently optimised, but its realisation and fabrication is expensive). Such networks will henceforth be referred to here as independent feed networks. They represent the upper bounds as regards the monopulse array performance, and will be referred to as the "ideal" solutions. In many cases the performance requirements of an array are such that the complexity and expense of such feed networks are justified. But there are a large number of applications and/or array types (e.g. slotted waveguide arrays) for which a simpler (relatively speaking) feed network is desirable which cannot provide independent sum and difference excitations. In such cases there has to be a compromise between the sum and difference performance, the ideal solution not being achievable.

If the feed network of Fig. 3.6 is at one extreme, then the two-module network of Fig. 3.7 is at the other. It does not allow any independence between sum and difference excitations. Once the sum excitations are selected, the difference distribution is fixed, and vice versa. While the two-module feed arrangement is attractive because of its simplicity, the resulting antenna pattern performance may leave much to be desired, and is in many cases unacceptable.

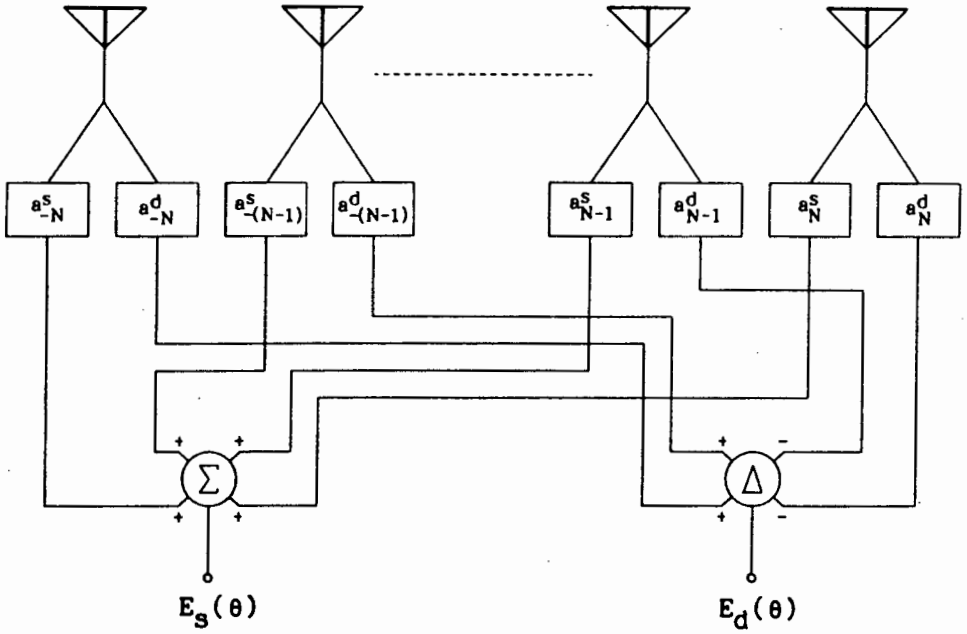

(a).

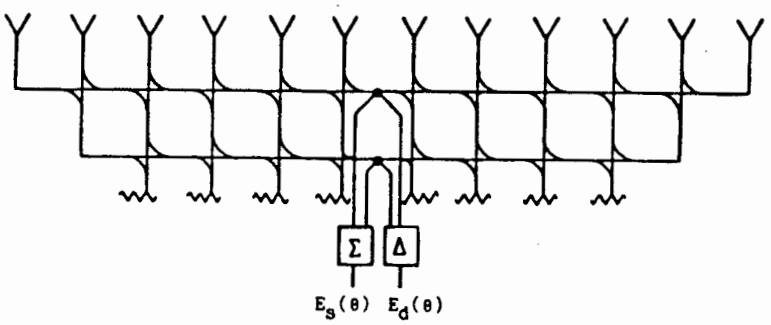

(b).

FIGURE 3.6(a) SCHEMATIC DIAGRAM OF A MONOPULSE LINEAR ARRAY WITH SEPARATE SETS OF ELEMENT EXCITATIONS FOR THE SUM AND DIFFERENCE MODES (INDEPENDENT NETWORK)

(b) POSSIBLE REALISATION OF AN INDEPENDENT NETWORK [44]

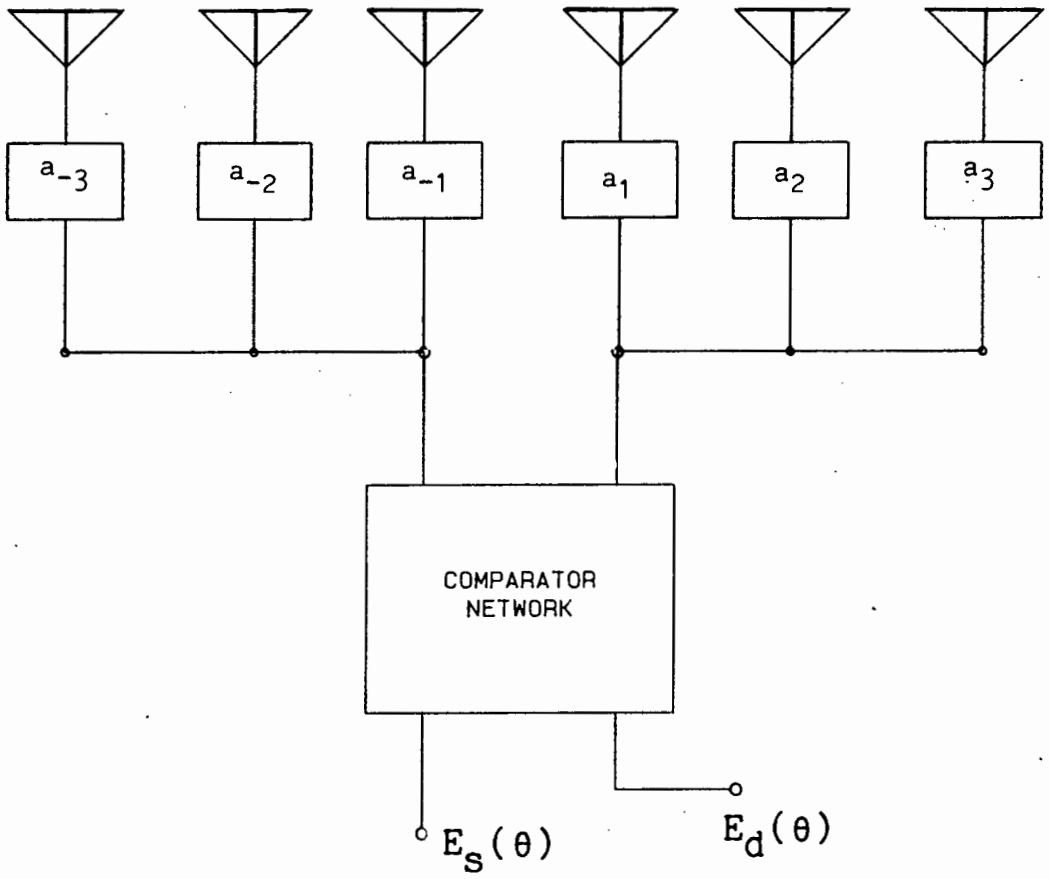

FIGURE 3.7 SERIES FED MONOPULSE LINEAR ARRAY WITH SINGLE SET OF ARRAY WEIGHTS FOR BOTH SUM AND DIFFERENCE (TWO-MODULE NETWORK) SIX ELEMENT ARRAY SHOWN FOR SIMPLICITY

In order to illustrate this, consider a linear array distribution designed for good sum pattern performance. In particular, observe the pattern of a 20 element, 30 dB sidelobe ratio, Villeneuve $\bar{n} = 4$ array with interelement spacing $d = \lambda/2$, shown in Fig. 3.8(a). The corresponding difference pattern obtained with these element excitations is shown in Fig. 3.8(b). This difference pattern has high sidelobes. Similarly, Fig. 3.9 shows the patterns of a 20 element array designed for a desired difference pattern performance, using a 30 dB sidelobe ratio, modified - Zolotarev ($\bar{n} = 4$) distribution. (These are developed in Chapter 6). The poor sum pattern performance is obvious.

Also shown in the above figures are the element excitations appropriate to each pattern. The reason for the bad difference and sum performance in the above two cases, respectively, is clear if these excitations are examined. Consider the case in Fig. 3.8(b). There is an abrupt discontinuity at the array centre for this distribution, resulting in the high difference pattern sidelobes. Likewise, for the sum distribution of Fig. 3.9(b) there are dips in the excitations at the array centre, which inevitably leads to high sum pattern sidelobes.

At this point two options are available:

(a) That a feed network of complexity intermediate between the independent and two-module types be used, in order to allow some degree of independence (though restricted) between the excitations of the two modes of operation. In this manner it may be possible to obtain a performance compromise which is sufficiently close to ideal.

(b) That the two-module feed be used and a compromise reached to obtain less than ideal but yet marginally acceptable sum and difference pattern performance.

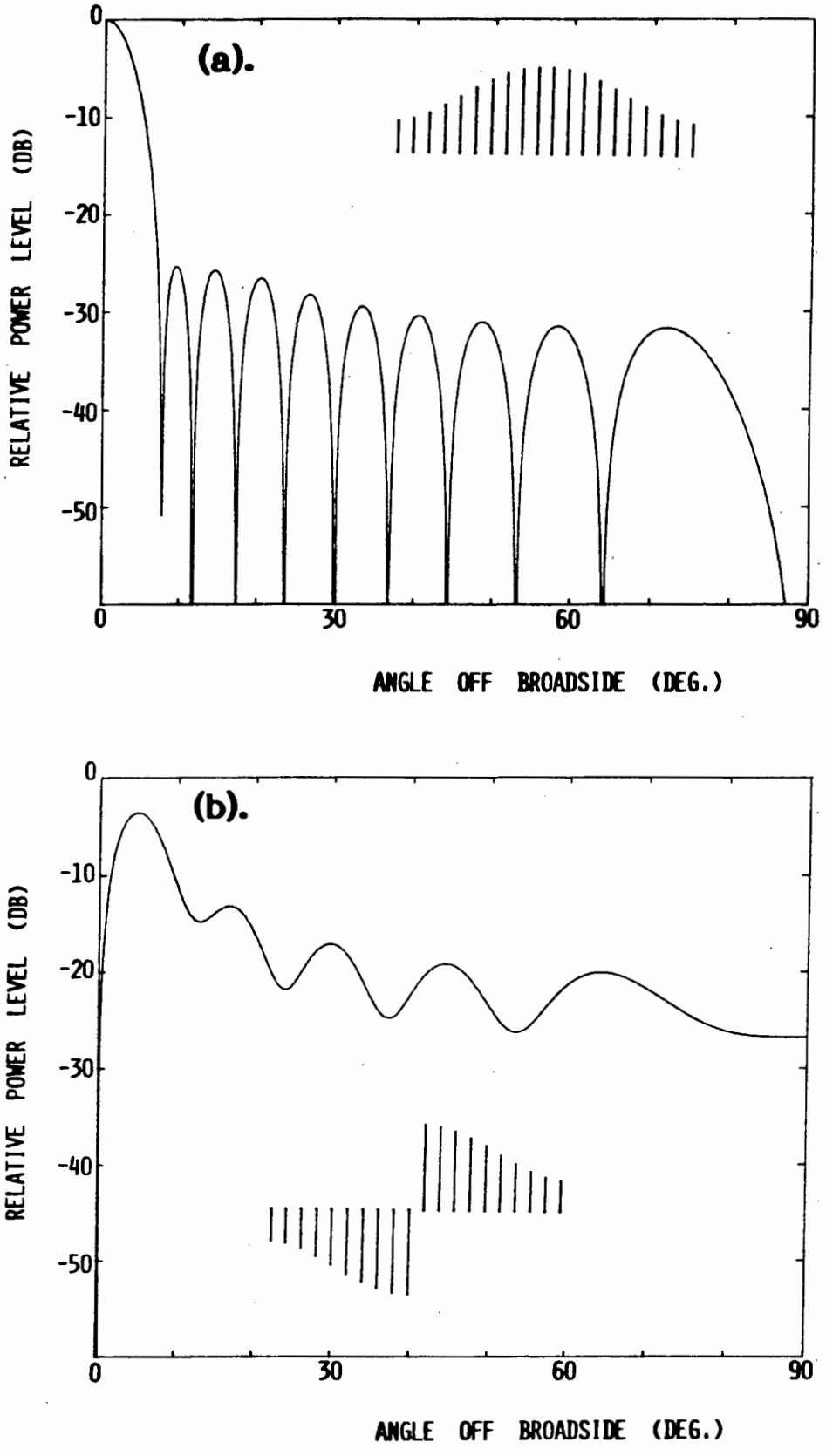

FIGURE 3.8(a) VILLENEUVE ARRAY SPACE FACTOR
(2N=20, SLR=25 DB, $\bar{n}$ =4)

(b) DIFFERENCE SPACE FACTOR OBTAINED WITH SAME EXCITATIONS AS USED IN (a)

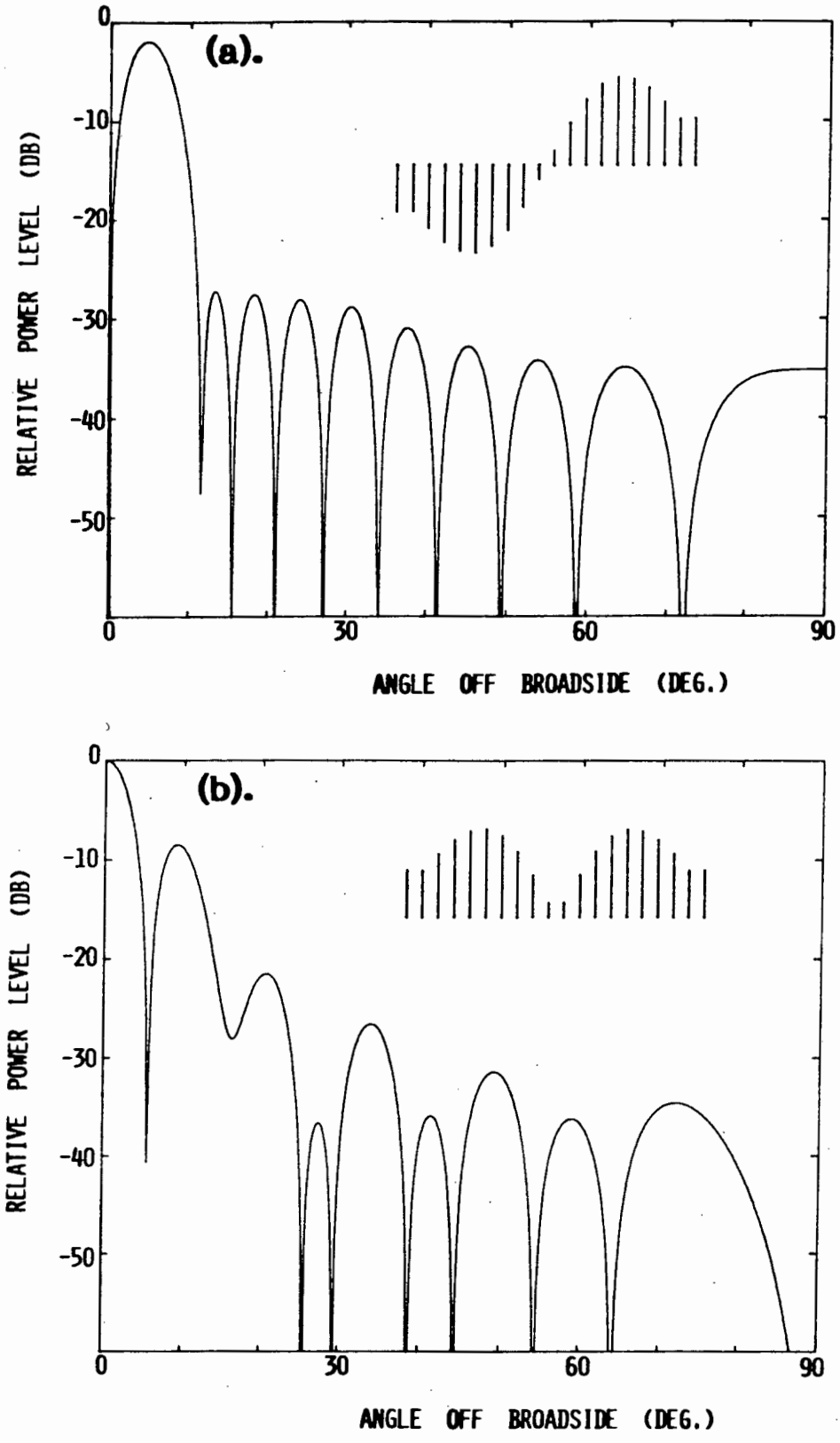

FIGURE 3.9(a) HIGH PERFORMANCE DIFFERENCE SPACE FACTOR (2N=20, SLR=25 DB) NORMALISED TO MAXIMUM OF SUM SPACE FACTOR IN (b)

(b) SUM SPACE FACTOR OBTAINED WITH SAME EXCITATIONS AS USED IN (a)

3.5.2 The Two-Module Feed Network Compromise Solution

Nester [34] considers what is equivalent to the two-module feed network case, but which applies to continuous apertures (line-sources). The angular sensitivity K_s (product of sum directivity and difference slope) is maximised using a variational technique, without constraints. Optimum performance in this instance is provided by the distributions shown in Fig. 3.5. The difference slope factor K_d is 0.3 dB below the maximum obtainable with a line source (see Section 3.3.4), and the sum pattern directivity is 0.3 dB less than its maximum value. More severe, as far as low sidelobe array synthesis is concerned, is the fact that the sum sidelobe ratio is only 8.4 dB, while the largest sidelobe of the difference pattern is only 11.3 dB below the difference peak. Furthermore, when applying these continuous distributions to discrete arrays, the same quantisation problems will arise as described in Section 3.2. This is clearly not a solution to the simultaneous synthesis problem at hand.

A compromise solution also involving a two-module feed network is that discussed by Schaffner et. al. [45]. The design of a monopulse slotted waveguide array is examined. Although the solution is specifically meant for this type of array configuration, the procedure adopted is effectively one of taking the average of the excitations which separately provide optimal sum and difference patterns.

While both [34] and [45] consider particular compromise solutions, no definite procedure for finding the best compromise when using the two-module network is given.

3.5.3 Intermediate Network Solutions

By intermediate networks is meant those of complexity lying between the completely independent and two-module types. One such is the four-module network mentioned by Lopez [44], and illustrated schematically in Fig. 3.6(b). Clearly, such a network attempts to "smooth out" the central discontinuity of the difference distribution in a stair step sense. To do this each half of the network is divided into two sub-arrays, with different sub-array weightings for the sum and difference modes. This is equivalent to saying that the increased network complexity allows a limited degree of independence. Extending this sub-arraying process by increasing the number of modules will naturally increase the degree of independence achievable. If the number of modules equals the number of elements complete independence between the sum and difference excitations is obtained; but this is then just the independent network of Fig. 3.6 anyway.

As with the two-module compromise solution, no information on a design algorithm for an n-module, or equivalent, intermediate network has appeared in the literature. This problem is taken up in Chapter 8.

3.6 EXACT (CLOSED FORM) VERSUS NUMERICAL TECHNIQUES

In engineering, just what is meant by exact or closed form as opposed to numerical techniques is seldom precisely defined. The traditional approach is to consider to be exact any technique described entirely in terms of accepted mathematical functions irrespective of how obscure the latter may be. When it comes to obtaining answers from such methods of course, some form of numerical manipulation (which may be of a reasonably complex nature) is required for evaluating, and determining the properties of the functions involved. Indeed, even if the above-defined "exact" method uses only the sine function, the evaluation of which is performed on a computer using some series expansion, it would be equally valid (albeit mundane) to claim that the method is a numerical one.

In order to strengthen the above definition of an exact method, restrictions might be placed on the subsequent numerical operations "allowed" by the definition. That is, a list of allowed elementary operations, (e.g. solution of a set of simultaneous linear equations, roots of a polynomial, and so on) can be specified as being within the domain of definition of an exact method. However, this does not make the definition less arbitrary.

Clearly, the above possibilities, while perhaps valid descriptions of exact methods prior to the advent of computers, are no longer so. This difficulty is compounded by the fact that the aim of much of modern analysis is to reach a point where computational techniques are viable, and the distinction between "exact" and "numerical" cannot perhaps be made clear-cut in general, but only for particular cases. For the present work therefore, dealing specifically with array synthesis, a definition is proposed which does not depend on the amount of numerical computation involved but rather focuses on the nature of the algorithm itself.

A synthesis method will be regarded as exact if:

(i) Only on termination of the algorithm is the complete set of excitations available, and it is the final answer.

(ii) No initial guesswork on the part of the user of the technique is required.

(iii) Any adjustment of array space factor zeros is done in a predetermined manner.

In other words, at no stage with an exact method is it necessary to take an intermediate complete set of excitations, test it to see whether the initial bounding specifications are met, and either terminate the algorithm or compute a new set of excitations in some prescribed fashion. Observe also that while exact methods may iteratively determine the excitation of a particular element from those previously computed, the full set of excitations is only available on termination of the algorithm. Finally, condition (ii) eliminates from the menu of exact methods any algorithms which require an initial estimate of sidelobe maximum positions, for example, with the latter possibly having to be altered at the next stage.

This definition can be "tested" on the synthesis techniques discussed in the preceding sections of this chapter. If this is done, the following are "found" to be exact methods for sum synthesis:

(a) Unconstrained directivity maximisation of discrete arrays.
(b) Dolph-Chebyshev synthesis of discrete arrays.
(c) Taylor synthesis of continuous line-source distributions.
(d) Synthesis of Villeneuve distributions for discrete arrays

while for difference patterns the only exact method is the near-optimum synthesis of Price and Hyneman.

All the other methods fall into the class of numerical synthesis procedures. And these are in fact what are usually considered in the antenna community to be exact and numerical synthesis algorithms, respectively, thus establishing the validity of the definitions adopted.

The ideal situation is that for which some, albeit restricted, exact synthesis techniques are available in addition to numerical approaches. For instance, though the numerical constrained optimisation methods of Section 2.2.5 are extremely powerful, it is the study of array behaviour via the exact solutions of Dolph [6], Taylor [20] and Villeneuve [28] which gives an indication of how various constraints must be specified in the first place and from which the array physics can be learned.

Furthermore, exact methods set bounds on the array performance obtainable. A numerical optimisation method applied to a particular synthesis problem may, for example, appear not to be able to bridge some performance limitation. The availability of an exact solution "close" to such a problem will indicate whether this is due to some physical limitation or whether the constraints have simply not been properly posed or have been overly restrictive.

For all numerical methods, some set of initial estimates on the optimisation variables is needed. Here the existence of "close" closed form solutions provides a "warm start" for the optimisation process.

Most important also is the fact that exact solutions facilitate the observance of trends in the performance of an array, a crucial part of any design process. General conclusions can be drawn. For example, Hansen [29] was able to make useful broad inferences regarding the effects of finite source/receiver separation distance on the measurement of low sidelobe patterns, since it could confidently be stated that "the Taylor $\bar{n}$ distribution is the only one that needs to be considered" for drawing such conclusions.

Finally, in defence of the usefulness of exact methods the present author would venture to state that, had the computer (necessity that it is) been invented before the definition of such elementary "closed form" functions as the trigonometric ones, our intuition, so essential for innovation, would have been severely limited. There is perhaps a parallel here with the comment made by Deschamps [46] with regard to the relatively simple geometrical nature of light having been recognised before its more complex wave nature:

> ".... if the (wave) nature of light and Maxwell's equations had been known earlier, optical instruments would not have been invented so readily!"

3.7 MONOPULSE ARRAY SYNTHESIS TECHNIQUES DEVELOPED IN THIS THESIS

The conventional synthesis methods have been treated in the previous sections. Those dealt with in this thesis are summarised here. A knowledge of the unconstrained maximum directivity or the maximum normalised boresight slope of a difference array of given number of discrete elements is useful for evaluating the effectiveness of distributions providing patterns with sidelobe constraints. The first part of Chapter 4 examines these topics and compares the results with those for continuous line-sources.

There has up to the present time, for difference patterns, been no equivalent of the Dolph-Chebyshev sum pattern synthesis technique. This method provides the information on space factor zeros which is crucial to sum array synthesis by correct zero positioning. In addition, it provides information on the upper bounds of array performance. Chapter 4 of this thesis develops such an exact procedure for difference patterns, which utilises the Zolotarev polynomials, and which is the difference analogue of Dolph-Chebyshev sum synthesis. For a specified sidelobe level and array size, this technique provides the set of element excitations giving maximum normalised boresight slope and minimum difference lobe beamwidths. It also provides information on space factor zero locations central to the difference synthesis problem in general. Chapter 5 considers the computational details associated with Zolotarev polynomial synthesis and discusses a number of design tables of practical use given in Appendix II.

The Zolotarev polynomial distribution proves to have a number of characteristics similar to its Dolph-Chebyshev counterpart. The space factor has sidelobes all at the same level, with the accompanying directivity limiting. Constant sidelobes may also not be the envelope desired. Furthermore, for certain element number/sidelobe level combinations the distribution has an undesirable upswing near the array edges. Now sidelobes can be raised or lowered by adjusting the relevant space factor zeros. But if some sidelobes are lowered by

moving zeros closer together, others will be raised and/or the main beam will broaden. The adjustment of zeros to taper the sidelobes (and at the same time remove the other unwanted features) cannot be done arbitrarily. Chapter 6 develops a method of correct pattern zero adjustment (using the Zolotarev space factor zeros as a starting point), enabling direct synthesis of discrete difference distributions yielding tapered sidelobe envelopes. Arbitrary sidelobe taper rates can be obtained with minimal beamwidth increase and decrease in directivity. A special case of the general method is that providing the 1/u taper, and which can be considered the discrete equivalent of Bayliss synthesis of continuous distributions.

For some applications a taper other than 1/u is desired for the sum pattern as well. Chapter 7 generalises the Villeneuve distribution for discrete arrays to a form which allows the direct synthesis of sum patterns with arbitrary sidelobe tapers. As such it is to a certain extent the discrete equivalent of the continuous line-source generalised Taylor distribution.

A further problem of importance in the design of monopulse arrays is that of simultaneous synthesis of high performance sum and difference patterns. Practical considerations related to array feed network complexity restrictions often prohibit complete independence of sum and difference excitations. In such cases some "best" compromise between the individual optimum performances is required. The inclusion of feed network constraints is essential. Some prescriptions have been offered in the literature, but the majority of them are of an ad hoc nature. A contribution towards the solution of this problem is presented in Chapter 8. A knowledge of the excitations and/or the space factor zeros of the independently optimal sum and difference distributions, synthesised using the methods of the earlier chapters, is used together with numerical optimisation.

3.8 REFERENCES

[1] D.K. Cheng, "Optimisation techniques for antenna arrays", Proc. IEEE, Vol. 59, pp. 1664-1674, Dec. 1971.

[2] M.T. Ma, Theory and Application of Antenna Arrays, (John Wiley and Sons, 1974).

[3] R.L. Pritchard, "Optimum directivity patterns for linear point arrays", J. Acoustical Soc. Amer., Vol. 25, No. 5, pp. 879-891, Sept. 1953.

[4] Y.T. Lo, S.W. Lee and Q.H. Lee, "Optimisation of directivity and signal-to-noise ratio of an arbitrary antenna array", Proc. IEEE, Vol. 54, No. 8, pp. 1033-1045, Aug. 1966.

[5] R.C. Hansen, "Fundamental limitations in antennas", Proc. IEEE, Vol. 69, No. 2, pp. 170-182, Feb. 1981.

[6] C.L. Dolph, "A current distribution for broadside arrays which optimises the relationship between beam width and side-lobe level", Proc. IRE, Vol. 34, pp. 335-348, June 1946.

[7] H.J. Riblet, "Discussion on 'A current distribution for broadside arrays which optimises the relationship between beam width and sidelobe level'.", Proc. IRE, Vol. 35, pp. 489-492, June 1947.

[8] R.J. Stegen, "Excitation coefficients and beamwidths of Tschebyscheff arrays", Proc. IRE, Vol. 41, pp. 1671-1674, Nov. 1953.

[9] G.J. van der Maas, "A simplified calculation for Dolph-Tchebycheff arrays", J. Appl. Phys., Vol. 25, No. 1, pp. 121-124, Jan. 1954.

[10] D. Barbiere, "A method of calculating the current distribution of Tschebyscheff arrays", Proc. IRE, Vol. 40, pp. 78-82, Jan. 1952.

[11] J.L. Brown, "A simplified derivation of the Fourier coefficients for Chebyshev patterns", Proc. IEE, Vol. 105C, pp. 167-168, Nov. 1957.

[12] R.J. Stegen, "Gain of Tchebycheff arrays", IRE Trans. Antennas Prop., Vol. AP-8, pp. 629-631, Nov. 1960.

[13] J.L. Brown, "On the determination of excitation coefficients for a Tchebycheff pattern", IRE Trans. Antennas Prop., Vol. AP-10, pp. 215-216, March 1962.

[14] C.J. Drane, "Derivation of excitation coefficients for Chebyshev arrays", Proc. IEE, Vol. 110, pp. 1755-1758, Oct. 1963.

[15] C.J. Drane, "Dolph-Chebyshev excitation coefficient approximation", IEEE Trans. Antennas Prop., Vol. AP-12, pp. 781-782, Nov. 1964.

[16] H.E. Salzer, "Calculating Fourier coefficients for Chebyshev patterns", Proc. IEEE, Vol. 63, pp. 195-197, Jan. 1975.

[17] A.D. Bresler, "A new algorithm for calculating the current distributions of Dolph-Chebyshev arrays", IEEE Trans. Antennas Prop., Vol. AP-28, No. 6, pp. 951-952, Nov. 1980.

[18] R.C. Hansen, Microwave Scanning Antennas, Vol. 1 (Academic Press, 1964).

[19] P.R. Dax, "Noise jamming of long range search radars", Microwaves, pp. 52-60, Sept. 1975.

[20] T.T. Taylor, "Design of line-source antennas for narrow beamwidth and low sidelobes", IRE Trans. Antennas Prop., Vol. AP-3, pp. 16-28, Jan. 1955.

[21] C.J. Bouwkamp and N.G. de Bruyn, "The problem of optimum current distribution", Philips Res. Rep., Vol. 1, pp. 135-158, 1945-1946.

[22] D.R. Rhodes, Synthesis of Planar Antenna Sources, (Oxford Univ. Press, 1974).

[23] W.D. White, "Circular aperture distribution functions", IEEE Trans. Antennas Prop., Vol. AP-25, No. 5, pp. 714-716, Sept. 1977.

[24] A.W. Rudge et. al. (Edit.), The Handbook of Antenna Design, Vol. 2, Chap. 9 (by Hansen), (Peter Peregrinus Ltd., London, 1982).

[25] R.C. Hansen, "Measurement distance effects on low sidelobe patterns", IEEE Trans. Antennas Prop., Vol. AP-32, No. 6, pp. 591-594, June 1984.

[26] C.F. Winter, "Using continuous aperture illuminations discretely", IEEE Trans. Antennas Prop., Vol. AP-25, No. 5, pp. 695-700, Sept. 1977.

[27] R.S. Elliott, "On discretizing continuous aperture distributions" IEEE Trans. Antennas Prop., Vol. AP-25, No. 5, pp. 617-621, Sept. 1977.

[28] A.T. Villeneuve, "Taylor patterns for discrete arrays", IEEE Trans. Antennas Prop., Vol. AP-32, No. 10, pp. 1089-1093, Oct. 1984.

[29] R.C. Hansen, "Aperture efficiency of Villeneuve $\bar{n}$ arrays", IEEE Trans. Antennas Prop., Vol. AP-33, No. 6, pp. 668-669, June 1985.

[30] O.R. Price and R.F. Hyneman, "Distribution functions for monopulse antenna difference patterns", IRE Trans. Antennas Prop., pp. 567-576, Nov. 1960.

[31] N. Balakrishnan and S. Ramakrishna, "Optimum difference mode excitations for monopulse arrays", IEEE Trans. Antennas Prop., Vol. AP-30, pp. 325-330, May 1982.

[32] G.M. Kirkpatrick, "Aperture illuminations for radar angle of arrival measurements", IRE Trans. Aeronautical and Navigational Electronics, Vol. AE-9, pp. 20-27, Sept. 1953.

[33] P.W. Hannan, "Maximum gain in monopulse difference mode", IRE Trans. Antennas Prop., Vol. AP-9, No. 3, pp. 314-315, May 1961.

[34] W.H. Nester, "The optimum excitation for a phase comparison array", Microwave Journal, pp. 67-73, April 1963.

[35] E.J. Powers, "Utilisation of the Lambda functions in the analysis and synthesis of monopulse antenna difference patterns", IEEE Trans. Antennas Prop., Vol. AP-15, pp. 771-777, Nov. 1967.

[36] E.T. Bayliss, "Design of monopulse antenna difference patterns with low sidelobes", Bell System Tech. J., Vol. 47, pp. 623-640, May-June 1968.

[37] A.R. Lopez, "Line-source excitation for maximum difference slope with given sidelobe level", IEEE Trans. Antennas Prop., Vol. AP-29, No. 4, pp. 671-673, July 1981.

[38] S. Sanzgiri, J.K. Butler and R.C. Voges, "Optimum aperture monopulse excitations" IEEE Trans. Antennas Prop., Vol. AP-20, pp. 275-280, May 1972.

[39] R.S. Elliott, "Improved pattern synthesis for equispaced linear arrays", Alta Frequenza, Vol. 52, p. 12-17, 1983.

[40] H.J. Orchard, R.S. Elliott and G.J. Stern, "Optimising the synthesis of shaped beam antenna patterns", IEE Proceedings, Pt. H, No. 1, pp. 63-68, 1985.

[41] O. Einarsson, "Optimisation of planar arrays", IEEE Trans. Antennas Prop., Vol. AP-27, No. 1, pp. 86-92, Jan. 1979.

[42] P. Owen and J.C. Mason, "The use of linear programming in the design of antenna patterns with prescribed nulls and other constraints", COMPEL, Vol. 3, No. 4, pp. 201-215, Dec. 1984.

[43] T.S. Ng and M.A. Magdy, "Fast algorithms for optimal weight computation in linear array pattern synthesis having null constraints", IEE Proceedings, Pt. H, No. 6, pp. 395-396, Dec. 1984.

[44] A.R. Lopez, "Monopulse networks for series feeding an array antenna", IEEE Trans. Antennas Prop., Vol. AP-16, No. 4, pp. 436-440, July 1968.

[45] J.H. Schaffner, D. Kim and R.S. Elliott, "Compromises among optimum sum and difference patterns for plannar waveguide-fed slot arrays", Alta Frequenza, Vol. L, No. 6, pp. 312-314, Nov-Dec. 1981.

[46] G.A. Deschamps, "Ray techniques in electromagnetics", Proc. IEEE, Vol. 60, No. 9, pp. 1022-1035, Sept. 1972.

CHAPTER 4

OPTIMUM DIFFERENCE PATTERN SYNTHESIS

4.1 MAXIMUM DIFFERENCE PATTERN DIRECTIVITY AND NORMALISED SLOPE

4.1.1 Motivation

The maximum possible sum directivity D_s^{max} of an array of a given number of elements is obtained when (superdirectivity excluded) the element excitations are all of equal amplitude and phase. This of course gives an array space factor with relatively high sidelobe levels. Nevertheless, a knowledge of D_s^{max} allows a meaningful evaluation of a low sidelobe distribution such as that of Villeneuve, discussed in Section 3.2.4. A set of excitations which satisfies a required sidelobe specification and yet provides a directivity D_s^m close to D_s^{max} (i.e. has a high excitation efficiency η_s) is an example of a good design. So too for the difference mode a knowledge of the excitation efficiency,

$$\eta_d = D_d^m / D_d^{max}$$

for a given set of excitations is desirable. In this case the maximum possible value of the directivity D_d^{max} of the pattern peak is unfortunately not as easily acquired as for the sum case. Although Hannan [1] has considered this problem for continuous line-source distributions, the corresponding information does not appear to be available in the literature for the discrete distributions under study here. This is therefore considered in Section 4.1.2 and some results are tabulated for later use.

In a similar manner the angular sensitivity properties of a given set of excitations should be evaluated by determining the relative difference slope K_r of its associated space factor on boresight. But since $K_r = K/K_o$, not only must the normalised difference slope K provided by the given excitation set be determined, but the maximum possible value (K_o) obtainable with the given array size must be known. Once more, while Kirkpatrick [2] has shown what this is for the continuous line-source, that for discrete distributions is unavailable. This will thus be dealt with in Section 4.1.3.

4.1.2 Determination of D_d^{max}

An expression for the directivity, as a function of pattern angle, is given by equation (23) of Chapter 2 for the difference mode as,

$$D_d = \frac{2[J]^T[A_d][J]}{[J]^T[B_d][J]} \qquad (1)$$

where the matrices $[J]$, $[A_d]$ and $[B_d]$ are defined by equations (11) and (22) of Chapter 2. Determination of the excitation vector $[J]$ which maximises D_d (without constraints) in the direction of the difference pattern peaks can be done in a manner almost identical to that described by Cheng [3] for the sum pattern case. The method uses a theorem of matrix algebra [4] which states that if a quantity is expressible as a ratio of two quadratic forms, as is D_d in (1), then the vector $[J]$ which maximises this quantity is given directly by the solution of the set of simultaneous equations

$$[B_d][J] = [F_d] \qquad (2)$$

But this is only valid if $[A_d]$ and $[B_d]$ are both Hermitian, and $[B_d]$ in addition non-singular and positive-definite [4]. An examination of the equation set (22) of Chapter 2 confirms that this is indeed the case. The elements of vector $[F_d]$ are defined by equation (13) of Chapter 2.

The elements of $[F_d]$ are functions of the angle ψ_o in which the directivity is to be maximised. For the sum case this is simply the known value $\psi_0 = 0$. On the other hand, for the difference case both the $[J]$ required to maximise the peak directivity and the resulting direction of the peak, are unknowns. Consequently (3) has to be solved iteratively. A value for ψ_o is estimated (from that obtained with the elements uniformly excited in the difference mode) and the elements of $[F_d]$ computed. The linear system of equations (3) is solved for $[J]$ and the actual value of ψ_o obtained with this excitation vector determined. This new ψ_o is used to obtain an updated $[F_d]$ and (2) solved once more for a new $[J]$. The above process is repeated until convergence (negligible difference between assumed and computed ψ_o values) is achieved. On the order of 5 or so iterations is all that is required to achieve this.

Computations performed using the above procedure are tabulated below, principally for later use in evaluating low sidelobe difference distributions.

In the cases considered only real excitations were allowed. If this is not done, the high Q factor problem will arise. Should an attempt be made to restrict this phenomenon by performing a maximisation subject to a constraint on the Q, the question arises as to what largest value of Q is to be allowed. Such arbitrariness is not acceptable as a standard. It is for this reason that excitation efficiency for continuous line-source distributons for difference patterns is also determined by comparison to the real distribution which maximises the peak directivity for the same length line source [1]. So too with the sum pattern case. Hence the use of real excitations here as well.

Although the primary purpose of this section is the devising of methods to establish a set of standards (D_d^{max}) against which to measure the effectiveness of the synthesis procedures developed in following sections, a number of interesting observations are worth noting regarding the maximum directivity discrete distributions. Unless otherwise stated, directivities are not quoted in decibels.

Consider first an array of 20 elements. Table 4.1 shows the excitations which provide maximum directivity for spacings d = 0.4 λ, d = 0.5 λ and d = 0.7 λ respectively. The associated array space factors are shown in Figs. 4.1(a), (b) and (c). It is immediately clear that the excitations are spacing dependent. Those for the smaller spacing of 0.4 λ are oscillatory, with accompanying large Q factor. Sets of excitations and D_d^{max} values for other array sizes with 0.5 λ and 0.7 λ spacings are given in Tables 4.2 and 4.3. Two typical sets of excitations for an array of 2N = 40 elements, are plotted in Figures 4.2(a) and (b), with the discrete excitations simply joined by straight line segments. Observe that for half wavelength spacing the shape of the distribution is similar to that derived by Hannan [1] for the continuous line-source, and which is illustrated in Fig. 3.4. This is also found to be the case for the other array sizes with d = 0.5 λ. Note however, that unlike the continuous case, for the discrete situation the edge taper is not a constant independent of array size. From Table 4.2 this edge taper can be seen to decrease with increasing array size. A plot of edge excitation for increasing array size, with d = 0.5 λ, is given in Fig. 4.3, and reveals that this factor tends to that of the continuous-source as 2N becomes large. At the same time the excitations of the two centre elements tend to zero.

The maximum directivity distribution for d = 0.7 λ shown in Fig. 4.2(b) is typical of that for spacings greater than a half-wavelength. While the distribution shape is similar to that of the continuous case over the initial few elements, it departs from it near the edges of the array.

TABLE 4.1 : Element excitations for maximum directivity difference space factors for an array of 2N = 20 elements.

d	0.4 λ	0.5 λ	0.7 λ
a_1	-1.00000	0.11287	0.11942
a_2	0.96311	0.33291	0.33576
a_3	-0.84491	0.53620	0.52134
a_4	0.75584	0.71249	0.70273
a_5	-0.56741	0.85290	0.85854
a_6	0.47530	0.95038	0.93574
a_7	-0.28305	1.00000	0.96343
a_8	0.23052	0.99927	1.00000
a_9	-0.08339	0.94823	0.96105
a_{10}	0.08102	0.84945	0.72557
Q	517.0495	1.00000	1.3910
D_d^{max}	10.3434	12.8450	17.8463

An examination of the tabulated data shows that the excitation efficiency factor η_{ds} (ratio of maximum difference directivity to the maximum sum directivity) is always less than 65%. Fig. 4.4 is illustrative of the behaviour of D_d^{max} as a function of the number of elements in the array. As intuitively expected, this maximum directivity increases with array size. In order to gauge the effect of element spacing on D_d^{max}, Fig. 4.5 has been included. It can be seen that D_d^{max} peaks, for a given number of array elements, somewhere between d = 0.8 λ and d = 1.0 λ, depending on the precise value of 2N. The overall behaviour is comparable to similar curves for maximum directivity sum patterns (i.e. uniform excitations).

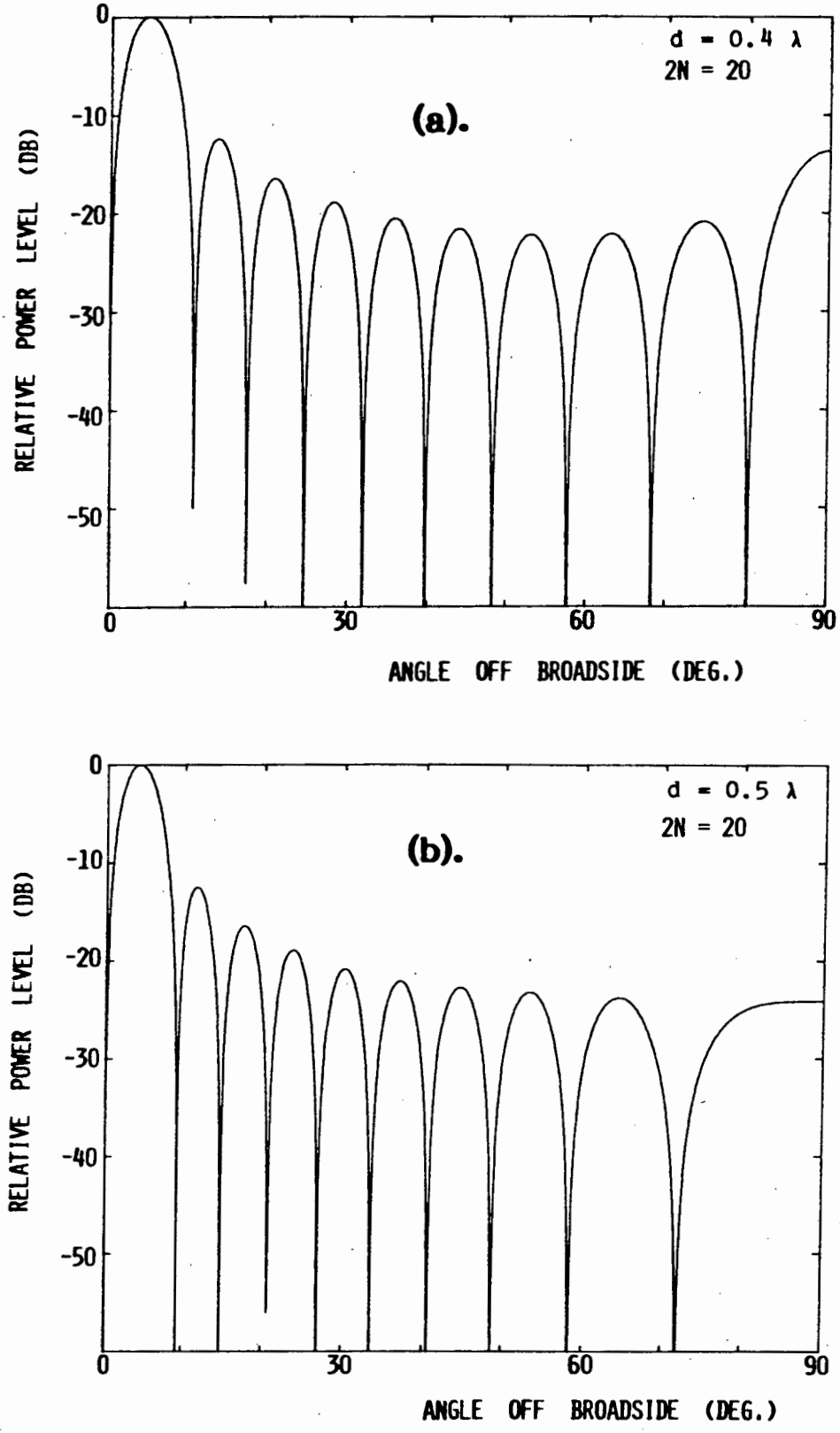

FIGURE 4.1 MAXIMUM DIFFERENCE DIRECTIVITY SPACE FACTORS FOR A 20 ELEMENT ARRAY

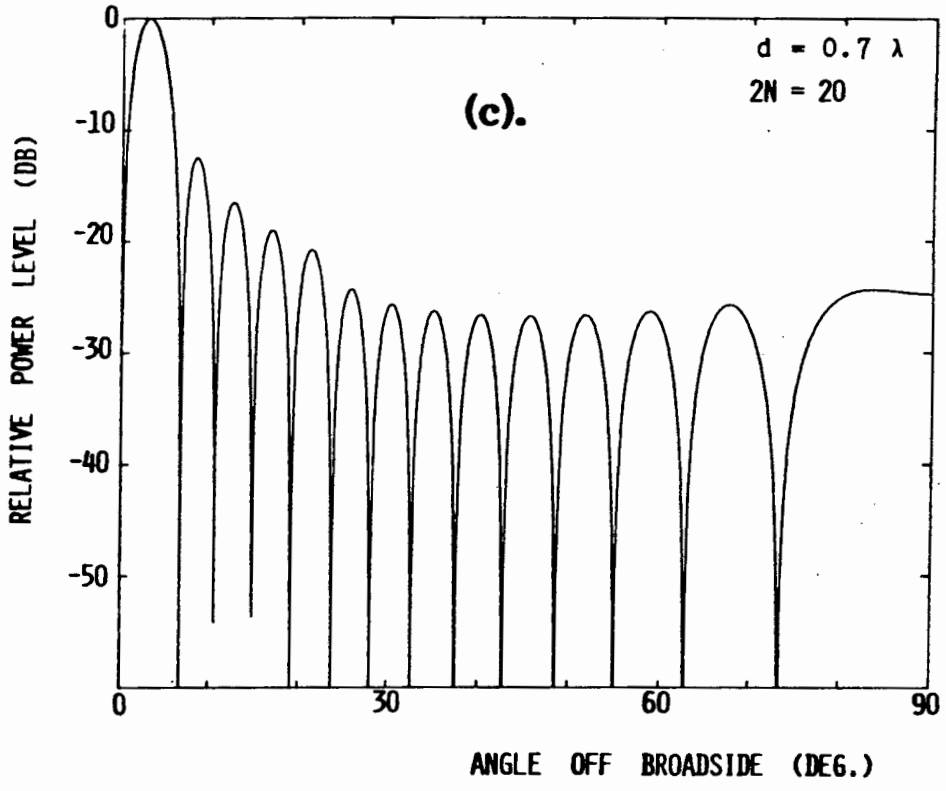

FIGURE 4.1 MAXIMUM DIFFERENCE DIRECTIVITY SPACE FACTORS FOR A 20 ELEMENT ARRAY

TABLE 4.2 : Element excitations for maximum directivity difference patterns (d = 0.5 λ).

2N	10	20	30	40	50	60
a_1	0.22354	0.11287	0.07485	0.05623	0.04493	0.03746
a_2	0.62593	0.33291	0.22287	0.16799	0.13441	0.11218
a_3	0.90323	0.53620	0.36589	0.27762	0.22281	0.18627
a_4	1.00000	0.71249	0.50072	0.38376	0.30942	0.25931
a_5	0.89691	0.85290	0.62432	0.48505	0.39352	0.33090
a_6		0.95038	0.73394	0.58023	0.47445	0.40063
a_7		1.00000	0.82711	0.66809	0.55155	0.46812
a_8		0.99927	0.90174	0.74752	0.62420	0.53298
a_9		0.94824	0.95617	0.81753	0.69180	0.59486
a_{10}		0.84946	0.98917	0.87723	0.75382	0.65340
a_{11}			1.00000	0.92586	0.80976	0.70827
a_{12}			0.98843	0.96282	0.85916	0.75918
a_{13}			0.95470	0.98764	0.90162	0.80582
a_{14}			0.89958	1.00000	0.93681	0.84795
a_{15}			0.82431	0.99975	0.96443	0.88533
a_{16}				0.98689	0.98426	0.91774
a_{17}				0.96159	0.99615	0.94500
a_{18}				0.92416	1.00000	0.96697
a_{19}				0.87507	0.99577	0.98352
a_{20}				0.81495	0.98351	0.99455
a_{21}					0.96331	1.00000
a_{22}					0.93532	0.99985
a_{23}					0.89979	0.99409
a_{24}					0.85700	0.98275
a_{25}					0.80728	0.96591
a_{26}						0.94365
a_{27}						0.91610
a_{28}						0.88342
a_{29}						0.84578
a_{30}						0.80339
η_{ds}	0.64711	0.64225	0.64135	0.64103	0.64088	0.64080
D_d^{max}	6.4711	12.8450	19.2404	25.6411	32.0440	38.4481
ψ_o	0.45087	0.22486	0.14984	0.11236	0.08988	0.07490

TABLE 4.3 : Element excitations for maximum directivity difference patterns (d = 0.7 λ).

2N	10	20	30	40	50	60
a_1	0.22686	0.11942	0.06976	0.05962	0.04155	0.03998
a_2	0.60385	0.33576	0.21981	0.16850	0.13238	0.11278
a_3	0.91625	0.52134	0.37271	0.26982	0.22634	0.18153
a_4	1.00000	0.70273	0.50122	0.38007	0.30817	0.25804
a_5	0.75936	0.85854	0.61617	0.48553	0.38823	0.33205
a_6		0.93574	0.73643	0.57145	0.47556	0.39566
a_7		0.96343	0.83402	0.65649	0.55296	0.46261
a_8		1.00000	0.89171	0.74506	0.61777	0.53295
a_9		0.96105	0.94718	0.81084	0.68837	0.59120
a_{10}		0.72557	1.00000	0.85931	0.75661	0.64458
a_{11}			0.99498	0.91643	0.80491	0.70496
a_{12}			0.95871	0.95987	0.85047	0.75722
a_{13}			0.96318	0.96776	0.90284	0.79584
a_{14}			0.92649	0.97907	0.93583	0.83977
a_{15}			0.71237	1.00000	0.95183	0.88393
a_{16}				0.97340	0.97987	0.90925
a_{17}				0.92253	1.00000	0.93171
a_{18}				0.92358	0.98727	0.96356
a_{19}				0.89626	0.98111	0.97882
a_{20}				0.69835	0.99102	0.97783
a_{21}					0.95801	0.99104
a_{22}					0.90335	1.00000
a_{23}					0.90631	0.97794
a_{24}					0.88673	0.96410
a_{25}					0.69744	0.96995
a_{26}						0.93571
a_{27}						0.88114
a_{28}						0.88693
a_{29}						0.87364
a_{30}						0.69189
η_{ds}	0.6480	0.6447	0.6425	0.6422	0.6416	0.6416
D_d^{max}	8.8687	17.8463	26.7769	35.7577	44.7082	53.6862
ψ_o	0.458806	0.226761	0.150668	0.112823	0.090175	0.075102

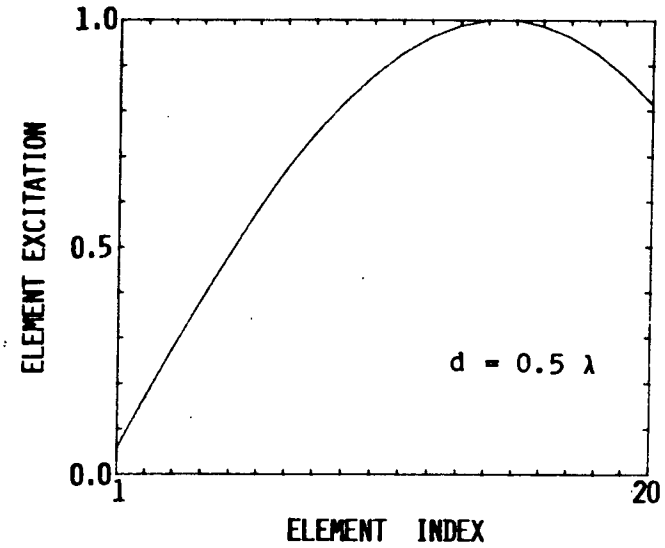

(a).

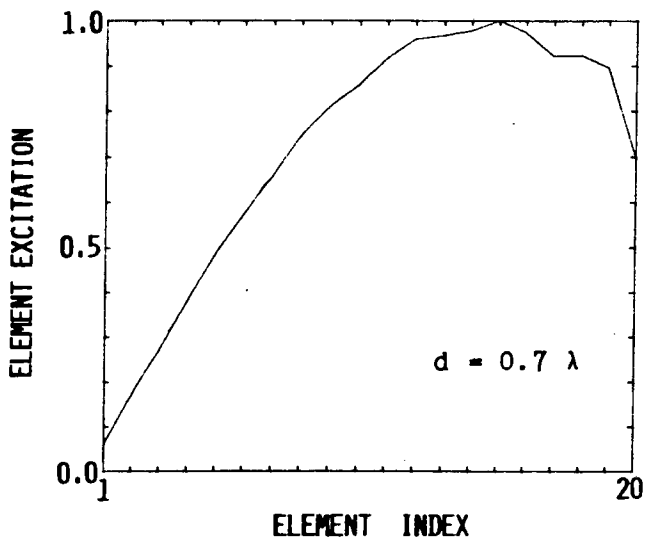

(b).

FIGURE 4.2 EXCITATIONS PROVIDING MAXIMUM DIFFERENCE DIRECTIVITY FOR TWO DIFFERENT ELEMENT SPACINGS

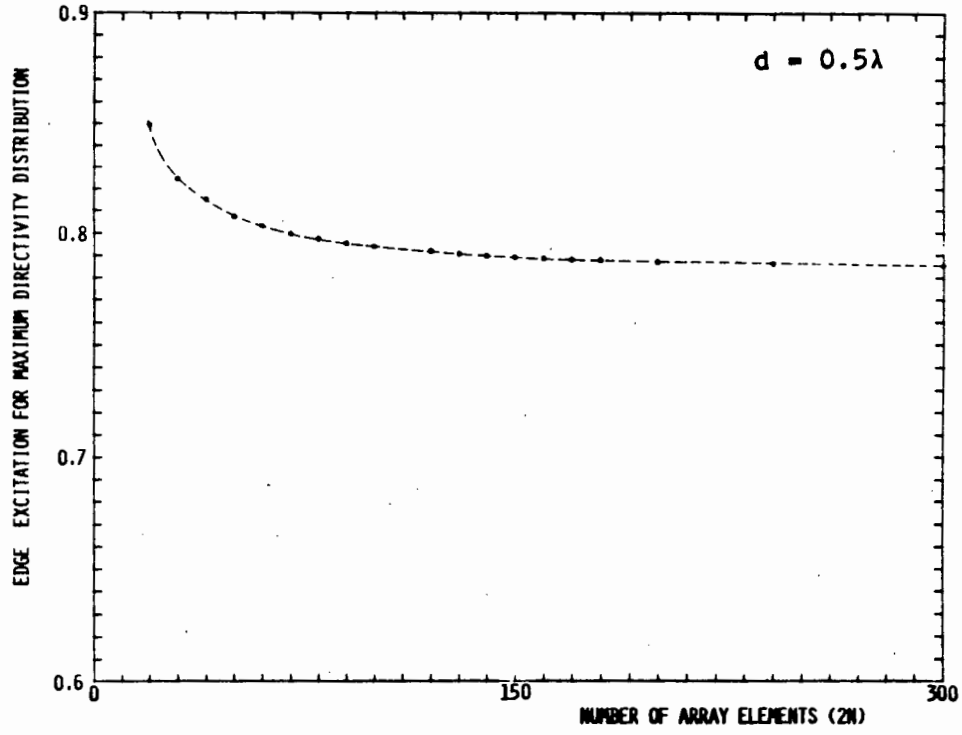

FIGURE 4.3 EDGE EXCITATION VERSUS ARRAY SIZE

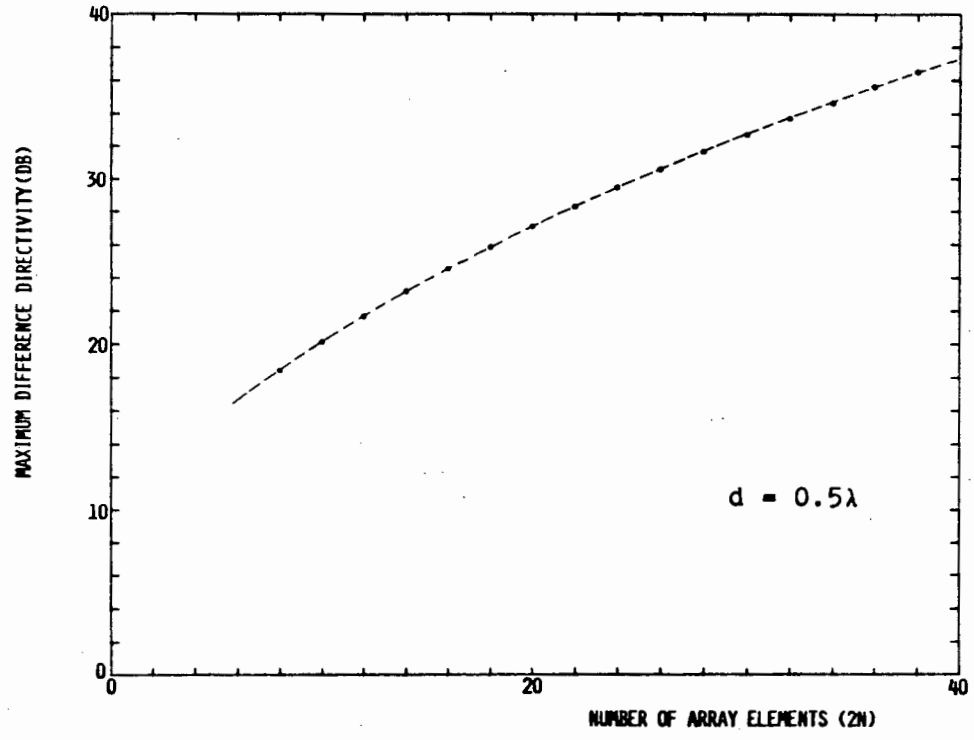

FIGURE 4.4 VARIATION OF MAXIMUM DIFFERENCE DIRECTIVITY WITH ARRAY SIZE

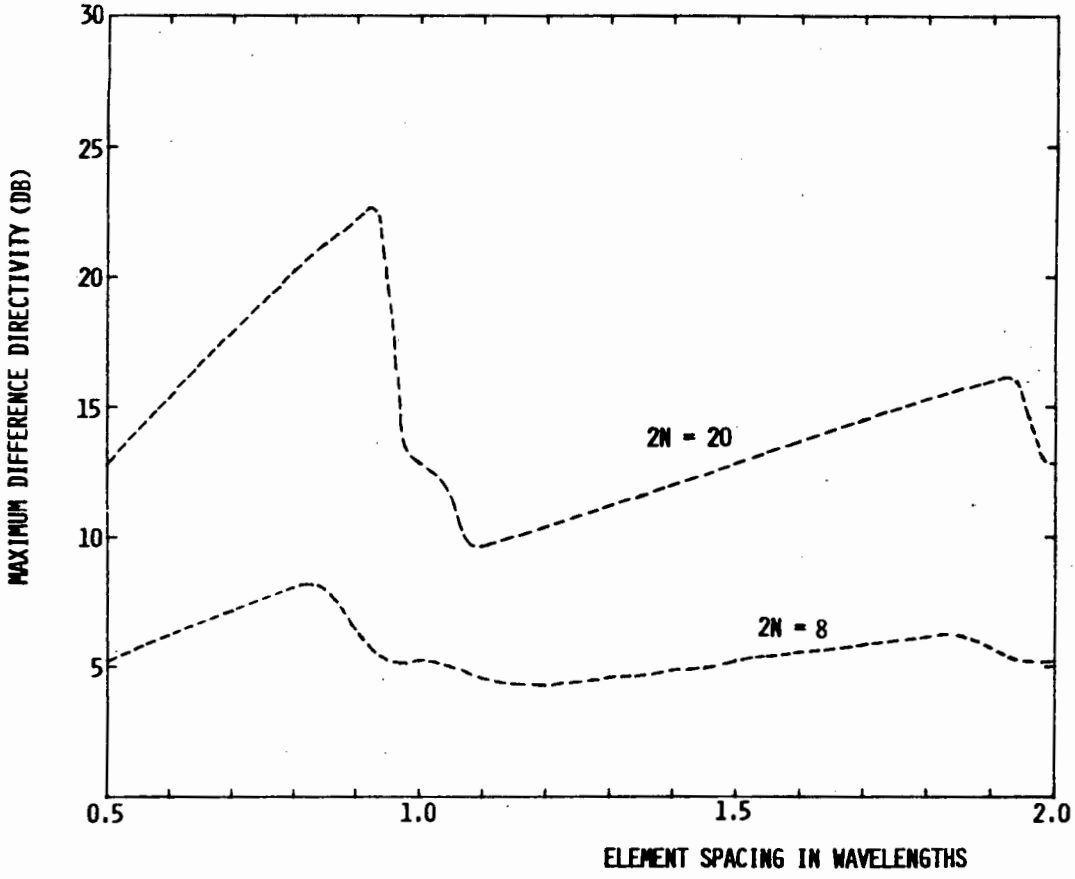

FIGURE 4.5 VARIATION OF MAXIMUM DIFFERENCE DIRECTIVITY WITH ELEMENT SPACING

4.1.3 Determination of K_o

The normalised slope of the difference pattern on boresight ($\psi = 0$) is given by equation (33) of Chapter 2 as,

$$K = \frac{[K]^T[J]}{\sqrt{2[J]^T[B_d][J]}} \tag{3}$$

with all terms as defined in Section 2.2.7. The present question is that of finding the $[J]$ which maximises K for a given number of array elements, without any constraints on the pattern or other performance indices of the array. This is a non-linear unconstrained optimisation problem and a relatively straightforward procedure like that of Section 4.1.2 is not possible. Gill et. al [5, p. 116] give a quasi-Newton algorithm for solving this type of optimisation problem. Its implementation in [18] has been used here. Once more, for the reasons given earlier, only real excitations have been permitted.

Consider first the case of half-wavelength spacing. Use of the algorithm for this spacing and a wide range of array sizes confirms that the excitation is simply a direct sampling of the continuous line-source linear odd distribution derived by Kirkpatrick [2] and shown in Fig. 3.3. The equation of the linear odd continuous distribution, when sampled at the array element positions, gives the element excitations as,

$$a_n = \frac{2n - 1}{2N - 1} \qquad n = 1,2, \cdots N \tag{4}$$

for an array of 2N elements. Furthermore, the array space factor of such an array is just the derivative (with respect to the angular variable) of the space factor of a uniformly excited array operated in the difference mode. This is easily found as,

$$E_d(\psi) = \frac{2N\cos(N\psi)\sin(\psi/2) - \sin(N\psi)\cos(\psi/2)}{\sin^2(\psi/2)}$$

The above maximum slope results hold only for d = 0.5 λ. For other spacings the discrete distributions do not follow the linear odd shape exactly. To illustrate this, consider the maximum normalised slope excitations given in Table 4.4 for the three spacings indicated. These were obtained using the numerical optimisation algorithm. The excitations for the d = 0.5 λ case are identical to those obtained via equation (4). Plots of these sets of excitations for d = 0.5 λ and d = 0.7 λ are shown in Fig. 4.6, and their associated space factors plotted in Figs. 4.7(a) and (b). The maximum slope patterns always have higher sidelobes than the maximum directivity patterns, but a narrower first null beamwidth. The distribution for the d = 0. 7 λ has a rippled shape passing just above that for d = 0.5 λ, and this is typical of cases for which d > 0.5 λ. When d < 0.5 λ, as for d = 0.4 λ, the distribution obtained has a number of definite zero excitations, resulting in a type of thinned array. An example of such a case is that shown in the first column of Table 4.4. Since the excitations for d = 0.5 λ are easily obtained from equation (4), they are not tabulated here at all. Instead, only the values of K_o are given for a selection of array sizes in Table 4.5. On the other hand, Table 4.6 gives the excitations, which provide maximum normalised boresight slope, for the case d = 0.7 λ.

In order to indicate the overall behaviour of K_o as a function of element spacing and the number of array elements, Figs. 4.8(a) and (b) have bee plotted. The variation of K_o with 2N or d/λ is seen to be similar to that of D_d^{max}.

It is noted that as for the continuous case the excitations providing maximum directivity for a discrete array is not the same as that which gives the largest normalised difference slope on boresight.

TABLE 4.4 : Element excitations for maximum normalised boresight slope for an array of 2N = 20 elements.

d	0.4 λ	0.5 λ	0.7 λ
a_1	0.21702	0.05263	0.06426
a_2	0.00000	0.15790	0.17412
a_3	0.15943	0.26316	0.26596
a_4	0.40141	0.36842	0.38376
a_5	0.00000	0.47368	0.51974
a_6	0.80177	0.57895	0.61105
a_7	0.00000	0.68421	0.69153
a_8	1.00000	0.78947	0.85588
a_9	0.14561	0.89474	1.00000
a_{10}	0.98473	1.00000	0.90964
K_o	1.2605	1.3572	1.5857
Q	1.3796	1.00000	1.3734
D_d^m	9.5310	11.4472	15.8892

TABLE 4.5 : Maximum normalised difference slope (K_o) values.

NUMBER OF ELEMENTS (2N)	K_o FOR SPACING d = 0.5 λ	K_o FOR SPACING d = 0.7 λ
8	0.9258	1.0658
10	1.0092	1.1628
12	1.0871	1.2604
14	1.1602	1.3498
16	1.2293	1.4312
18	1.2948	1.5126
20	1.3572	1.5857
22	1.4170	1.6585
24	1.4744	1.7272
26	1.5297	1.7926
28	1.5831	1.8576
30	1.6348	1.9182
32	1.6848	1.9787
34	1.7335	2.0367
36	1.7809	2.0927
38	1.8270	2.1484
40	1.8720	2.2013
50	2.0825	2.4519
60	2.2737	2.6792

TABLE 4.6 : Element excitations for maximum normalised boresight slope for spacing (d = 0.7 λ).

2N	10	20	30	40	50	60
a_1	0.11502	0.06426	0.02895	0.03038	0.01621	0.02001
a_2	0.36534	0.17412	0.10121	0.07952	0.05843	0.05156
a_3	0.68076	0.26596	0.18339	0.12183	0.10586	0.07887
a_4	0.96883	0.38376	0.24656	0.17919	0.14078	0.11692
a_5	1.00000	0.51974	0.30567	0.23713	0.17635	0.15383
a_6		0.61105	0.38886	0.27840	0.22478	0.18022
a_7		0.69153	0.46657	0.32686	0.26611	0.21326
a_8		0.85588	0.51625	0.39082	0.29711	0.25391
a_9		1.00000	0.58688	0.43869	0.34120	0.28346
a_{10}		0.90964	0.68504	0.47645	0.38994	0.31076
a_{11}			0.73834	0.53898	0.42147	0.35130
a_{12}			0.77473	0.60063	0.45699	0.38709
a_{13}			0.89598	0.63142	0.51019	0.41090
a_{14}			1.00000	0.68081	0.54891	0.44664
a_{15}			0.87834	0.76101	0.57477	0.48909
a_{16}				0.79686	0.62547	0.51430
a_{17}				0.81325	0.67760	0.54162
a_{18}				0.91446	0.69766	0.58776
a_{19}				1.00000	0.73495	0.62041
a_{20}				0.86407	0.80467	0.63868
a_{21}					0.83051	0.68169
a_{22}					0.83549	0.72755
a_{23}					0.92510	0.74070
a_{24}					1.00000	0.77016
a_{25}					0.85593	0.83302
a_{26}						0.85236
a_{27}						0.84996
a_{28}						0.93200
a_{29}						1.00000
a_{30}						0.85066
K_o	1.1628	1.5857	1.9182	2.2013	2.4519	2.6792

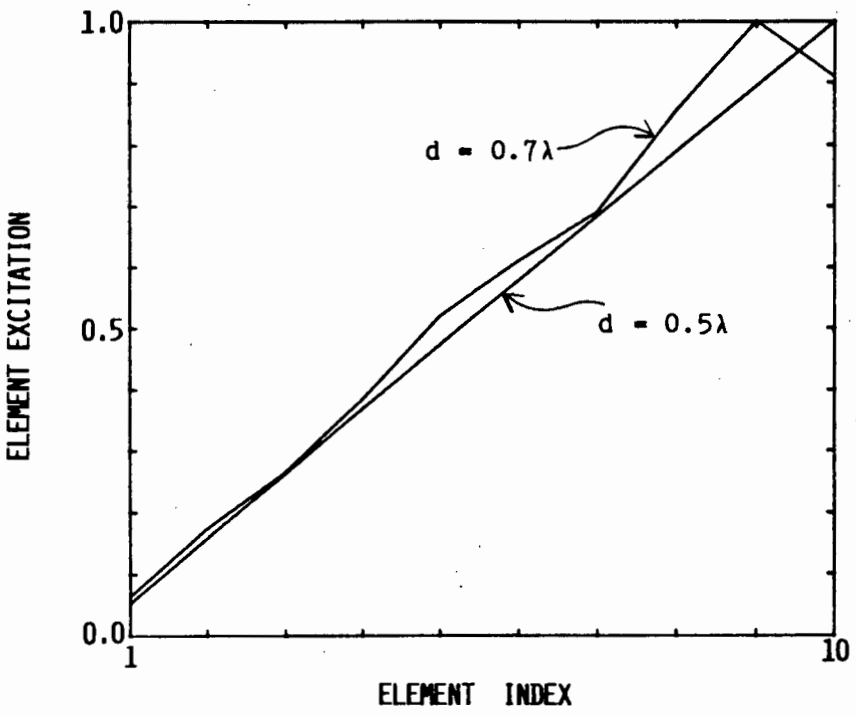

FIGURE 4.6 EXCITATIONS PROVIDING MAXIMUM NORMALISED BORESIGHT SLOPE

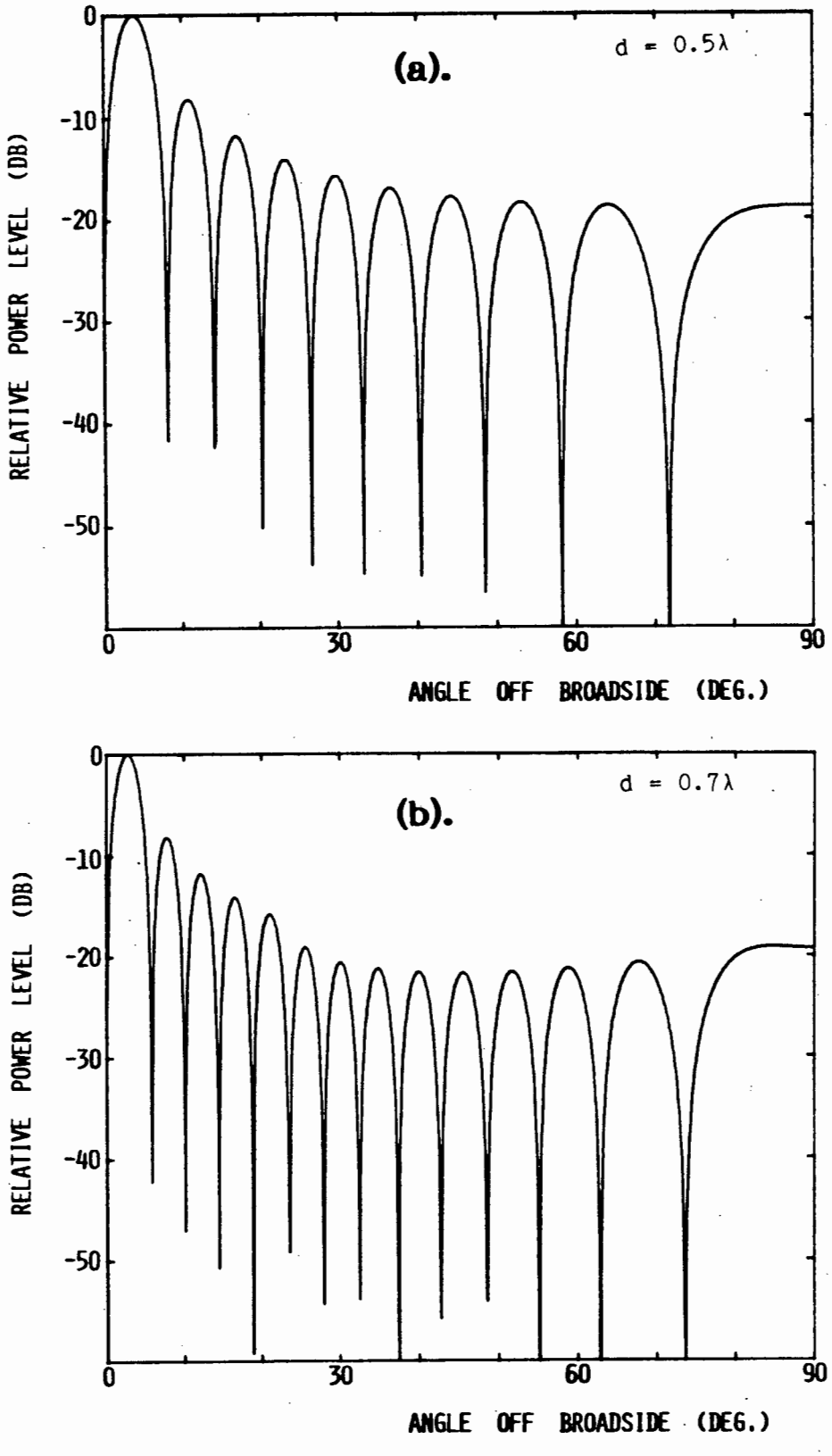

FIGURE 4.7 SPACE FACTORS WITH MAXIMUM NORMALISED BORESIGHT SLOPE

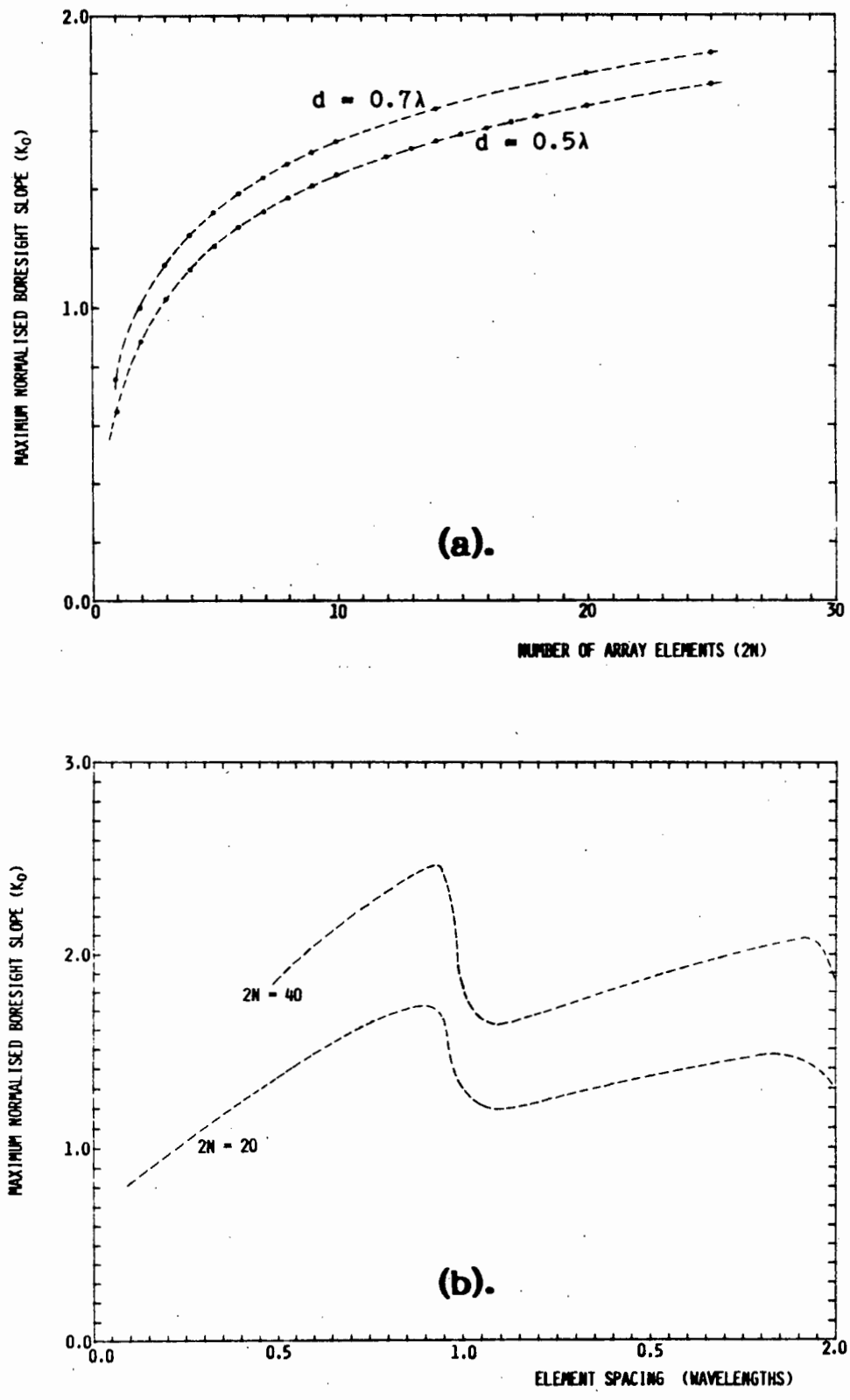

FIGURE 4.8 VARIATION OF MAXIMUM NORMALISED BORESIGHT SLOPE WITH ARRAY SIZE AND ELEMENT SPACING

4.1.4 Discussion

The previous two subsections have determined the maximum possible values of D_d and K, denoted D_d^{max} and K_o, respectively, achievable from an array of a given number of elements, without constraints placed on the sidelobe levels of the space factor obtained with the associated sets of excitations. Application of sidelobe constraints will result in an altered set of excitations for which the pattern will have a directivity and normalised difference slope somewhat less than these maximum attainable values. Once again, a good design is that which satisfies the necessary sidelobe constraints and yet achieves a directivity and slope close to these maximum values. The remainder of this chapter and the two following it will discuss a new class of distributions which can be used to accomplish this exactly.

4.2 OPTIMUM POLYNOMIALS FOR DIFFERENCE PATTERNS WITH MAXIMUM SIDELOBE LEVEL CONSTRAINTS

Consider the class C(a) of odd, real polynomials of degree n,

$$p_n(x) = a_1 x + a_3 x^3 + \cdots + a_n x^n$$

defined over $x \in (-\infty, \infty)$, and which have the following properties:

(i) The zeros of all $p_n(x)$ of C(a) are real, and all lie in the interval $(-1,1)$.

(ii) All the $p_n(x)$ of C(a) have maxima on either side of $x = 0$ which are of equal magnitude A_o, say.

(iii) All the $p_n(x)$ of C(a) have their second largest maxima in $(-1,1)$ at unity magnitude, the others all lying between zero and unity or at unity.

Then the theorem and corollary given below can be established. These were originally stated by Price and Hyneman [6], who were however not aware of the existence of a class of polynomials with the above properties. The proof of the theorem is elaborated on here and the existence of polynomials of the class C(a) demonstrated in Section 4.3.

Theorem

If $q_n(x)$ is a member of C(a) but has the additional property that <u>all</u> subsidiary maxima (i.e. all those besides the innermost maxima) in the interval $(-1,1)$ are of magnitude unity, then $q_n(x)$ has the smallest distance from the origin to the first zeros on either side of $x = 0$.

Proof

Form the difference polynomial $f_n(x) = q_n(x) - p_n(x)$ between the general member $p_n(x)$ of C(a) and the specific subclass $q_n(x)$ with the additional property.

Since $p_n(x)$ and $q_n(x)$ are of order n, $f_n(x)$ must be a polynomial of order less than or equal to n.

Assume now that the above theorem is not true. That is, if $\pm x_q$ are the first zeros of $q_n(x)$ on either side of $x = 0$, and $\pm x_p$ those for $p_n(x)$, then $x_q \geq x_p$.

Now since no subsidiary maxima of $p_n(x)$ may exceed unity, and all the subsidiary maxima of $q_n(x)$ are exactly at unity, it follows that since $x_q \geq x_p$, $p_n(x)$ and $q_n(x)$ must intersect at not less than n+2 points. This implies that $f_n(x)$ has n+2 zeros. But this is not possible since $f_n(x)$ is of, at most, degree n. Hence it follows that $f_n(x) = 0$ and hence $p_n(x) = q_n(x)$. This proves the theorem.

Corollary

The polynomial subclass $q_n(x)$ defined in the above theorem has the largest normalised slope at $x = 0$ of all those in C(a).

4.3 THE ZOLOTAREV POLYNOMIAL FUNCTION

4.3.1 Introduction

P.I. Chebyshev considered the problem of approximation to zero, in the minimax sense, over a single continuous interval. The work of Chebyshev was developed further by his student E. Zolotarev [7]. Zolotarev's work was described in detail and extended further by Achieser [8,9]. Building on the work of Zolotarev, Achieser considered the problem of best approximation to zero (in the minimax sense) in the intervals $-1 < x < -x_3$ and $x_3 < x < 1$ by means of an odd polynomial. The result was a unique class of optimum odd polynomials $Z_{2n+1}(x)$, giving equiripple approximation to zero in the above intervals. These are now known as the Zolotarev polynomials. Mathematical details of their derivation by Achieser [8,9] have been reproduced in the engineering literature by Levy [10], who used them in the microwave circuit design context. These derivations will not be given here. Instead, only the essential results derived in [8,9,10] which are necessary as the starting point for application of these mathematical ideas to the array synthesis problem, are given. The notation used here is different from that in the above references, but more suitable for the array problem.

4.3.2 Definition of the Zolotarev Polynomial

The Zolotarev polynomial of order (2n+1) is defined by

$$Z_{2n+1}(x) = \cosh\left[\left(n + \frac{1}{2}\right) \ell n \left\{\frac{H(M+\nu,k)}{H(M-\nu,k)}\right\}\right] \tag{5}$$

(i)
$$x = \frac{sn(M,k)\,cn(\nu,k)}{\sqrt{sn^2(M,k) - sn^2(\nu,k)}} \tag{6}$$

(ii)
$$x_1 = \frac{k' x_3}{dn(M,k)} \tag{7}$$

(iii) $$M = \frac{-K(k)}{2n+1} \tag{8}$$

(iv) $$x_2 = x_3 \sqrt{1 - \frac{cn(M,k)z(M,k)}{sn(M,k)dn(M,k)}} \tag{9}$$

(v) $$x_3 = sn(-M,k) \tag{10}$$

(vi) $$k' = \sqrt{1 - k^2} \tag{11}$$

(vii) K(k) is the complete elliptic integral of the first kind, to modulus k [11, p. 12].

(viii) H(ν,k) is the Jacobi eta function [12, p. 411].

(ix) sn(ν,k), cn(ν,k) and dn(ν,k) are the Jacobi elliptic functions [11, p. 1].

(x) z(ν,k) is the Jacobi zeta function [12, p. 405].

In elliptic function terminology, k is called the Jacobi modulus, and k' the complementary modulus. While the expression (5) is the correct formal expression for $Z_{2n+1}(x)$, it should not be used directly for computational purposes. Such numerical aspects are dealt with in detail in Chapter 5.

Although k is used in the array literature (and in this thesis) to denote the free space wavenumber, its use as the Jacobi modulus of the elliptic functions is too entrenched to be denoted otherwise. Its meaning at any stage will usually be clear from the context; if not, specific note will be made as to its interpretation.

Finally, just as the Chebyshev polynomial satisfies a differential equation, the Zolotarev polynomial $Z_{2n+1}(x)$ satisfies the non-linear differential equation,

$$\frac{d}{dx} Z_{2n+1}(x) = (2n+1) \left[\frac{(Z_{2n+1}^2 - 1^2)(x^2 - x_2^2)^2}{(x^2 - 1)(x^2 - x_3^2)(x^2 - x_1^2)} \right]^{\frac{1}{2}} \qquad (12)$$

4.3.3 Properties of the Zolotarev Polynomial

An example of the Zolotarev polynomial defined formally in equation (5) is shown in Fig. 4.9. The polynomials are defined throughout the region $x \in (-\infty, \infty)$, but only the region $x \in [-1,1]$ is relevant to the array synthesis application. A Zolotarev polynomial $Z_{2n+1}(x)$ of specified order is a function of both x and k. Here it will be considered to be a function of x, with k as a parameter determining the amplitudes of the maxima on either side of $x = 0$ relative to the peak value. Although it is possible to prove rigorously [10] that the definition (5) is a real polynomial, it is not possible to directly write $Z_{2n+1}(x)$ in standard polynomial form. Use of the secondary variable ν, related to x via the transformation (6), makes the form of the polynomial more manageable. This transformation is illustrated in Fig. 4.10. Although ν is complex, x and $Z_{2n+1}(x)$ are always real.

The points x_1, x_2 and x_3, given by relations (7), (9) and (10), respectively, are significant. As x increases from 0 to x_1, $Z_{2n+1}(x)$ increases from 0 to 1. In the region $x_1 < x < x_3$, the polynomial is greater than unity, with a maximum value A_o occurring at $x = x_2$, the magnitude of A_o depending on the Jacobi modulus k. At $x = x_3$, $Z_{2n+1}(x) = 1$. From x_3 to 1 it oscillates (n+1) times alternately between ± 1, and there are n zeros in this interval. This behaviour is mirrored in the region $-1 \leq x \leq 0$, so that together with the zero at $x = 0$, $Z_{2n+1}(x)$ has all (2n+1) zeros real and lying in the interval $|x| < 1$. For $|x| > 1$, the magnitude of $Z_{2n+1}(x)$ increases indefinitely, becoming infinite at $x = \pm\infty$ (which is equivalent to the point $\nu = -M$ in Fig. 4.10).

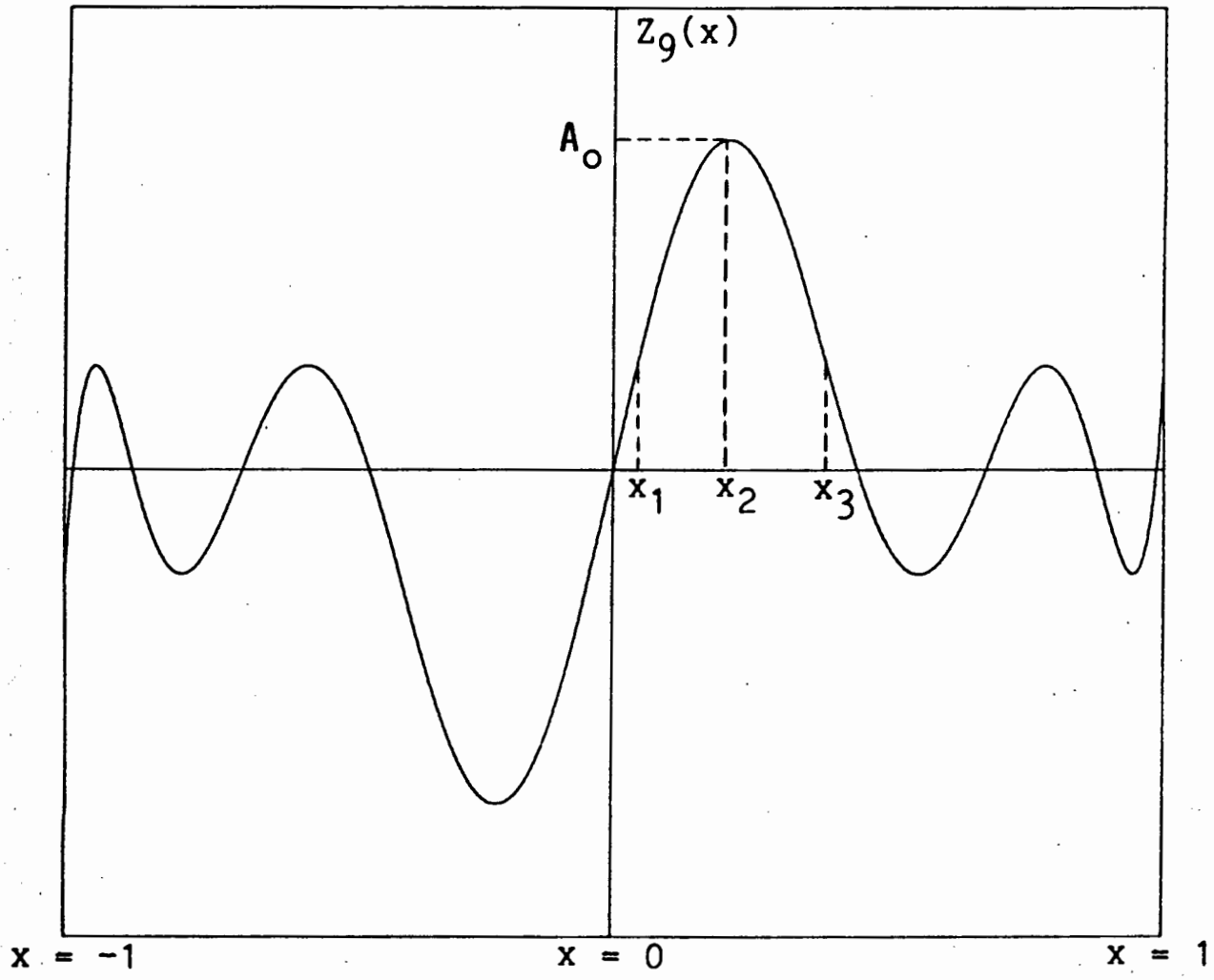

FIGURE 4.9 TYPICAL ZOLOTAREV POLYNOMIAL FUNCTION

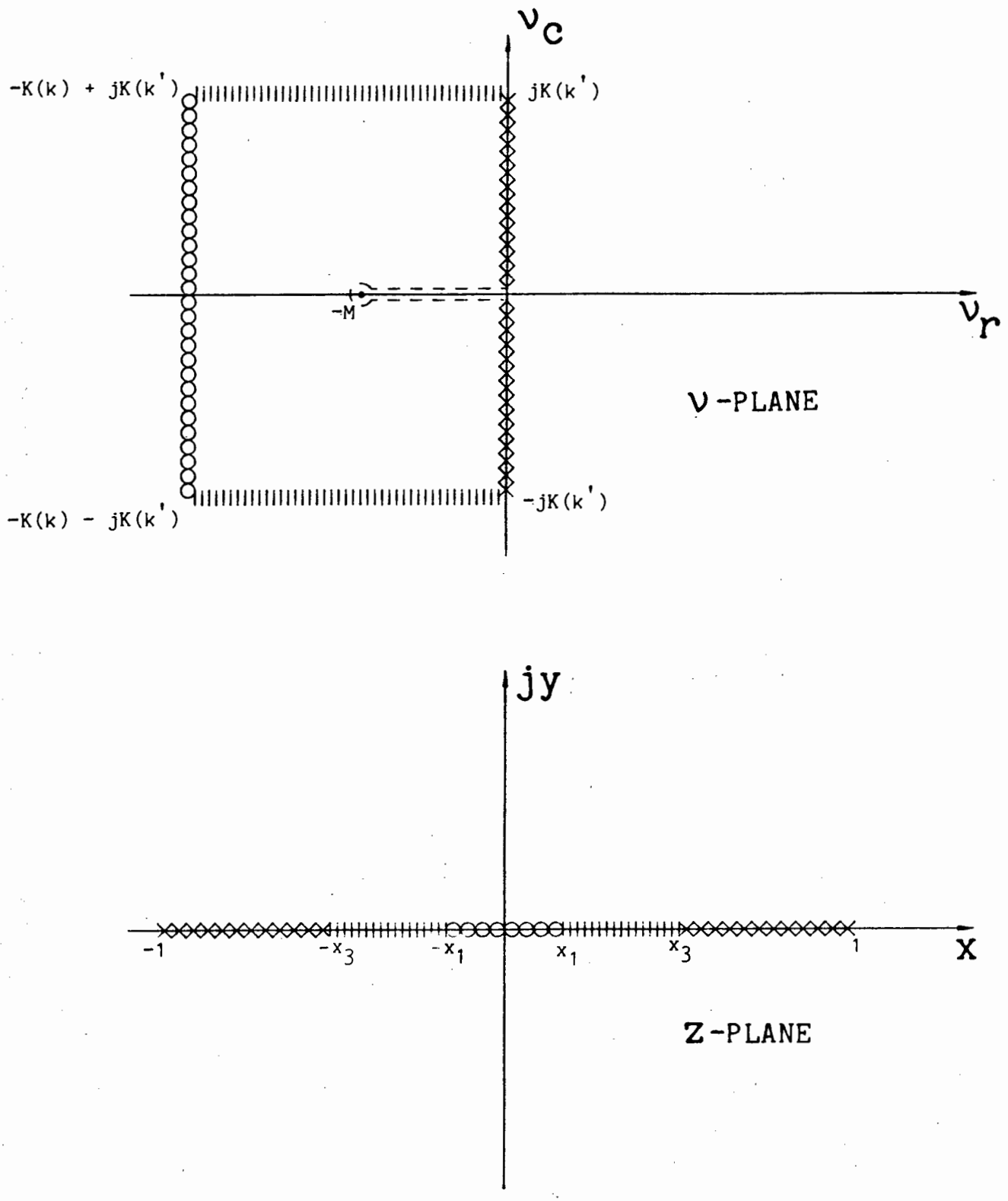

FIGURE 4.10 TRANSFORMATION FROM THE X TO ν PLANE

Consideration of the properties of $Z_{2n+1}(x)$ given above leads to the conclusion that the Zolotarev polynomials are exactly the class of odd polynomials identified in Section 4.2 as being optimum for difference pattern synthesis. The next step then is to determine how these polynomials may be used to synthesize an optimum set of array element excitations.

4.4 ARRAY ELEMENT EXCITATIONS FOR SPACINGS GREATER THAN OR EQUAL TO HALF A WAVELENGTH

4.4.1 The Difference Space Factor as a Chebyshev Series

Consider a linear array of 2N elements, excited anti-symmetrically so as to obtain a difference pattern. The space factor is given by equation (10) of Chapter 2 as (ignoring the constant factor 2j),

$$E_d(\psi) = \sum_{n=1}^{N} a_n \sin\left[(2n-1)\frac{\psi}{2}\right] \tag{13}$$

The sine function in (13) can be expanded as [13, p. 28]

$$\sin\left[(2n-1)\frac{\psi}{2}\right] = (2n-1)\left\{\sin\frac{\psi}{2} - \frac{[(2n-1)^2 - 1^2]}{3!}\sin^3\frac{\psi}{2} + \frac{[(2n-1)^2 - 1^2][(2n-1)^2 - 3^2]}{5!}\sin^5\frac{\psi}{2} - \cdots\right\} \tag{14}$$

Elliott [14, p. 566] gives a general expression for the Chebyshev polynomial of odd order 2n-1 as,

$$T_{2n-1}(x) = \sum_{m=1}^{n} (-1)^{n-m}\frac{2^{m-2}(2n-1)}{(n+m-1)}\binom{n+m-1}{2m-1}x^{2n-1} \tag{15}$$

A comparison of (13) and (14) reveals that,

$$\sin\left[(2n-1)\frac{\psi}{2}\right] = (-1)^n T_{2n-1}\left(\sin\frac{\psi}{2}\right) \tag{16}$$

It thus follows that (13) can be written as

$$E_d(\psi) = \sum_{n=1}^{N} a_n (-1)^n T_{2n-1}\left(\sin \frac{\psi}{2}\right) \tag{17}$$

a series of Chebyshev polynomials of argument sin $\psi/2$. From (17) it is also clear that for the array of 2N elements in question, $E_d(\psi)$ is a polynomial of order 2N-1 in sin $\psi/2$.

4.4.2 Zolotarev Polynomial as a Chebyshev Series

The correspondence between the space factor $E_d(\psi)$ and the Zolotarev polynomial $Z_{2n+1}(x)$ must be established to enable the desirable properties of the latter to be utilised for array synthesis. This is best done by expanding the Zolotarev polynomial as a Chebyshev series,

$$Z_{2n+1}(x) = b_1 T_1(x) + b_2 T_3(x) + \cdots + b_{n+1} T_{2n+1}(x) \tag{18}$$

The use of such a form is not only useful as an artifice here, but the use of Chebyshev series is also advantageous from a numerical analysis point of view [15]. A discussion thereof and means of computing the series coefficients in (18) will be postponed to Section 5.3.5 in order not to obscure the essence of the theory being developed here.

If such a Chebyshev series expansion is used, then for a Zolotarev polynomial of order 2N-1 it will be,

$$\begin{aligned} Z_{2N-1}(x) &= b_1 T_1(x) + b_2 T_3(x) + \cdots + b_N T_{2N-1}(x) \\ &= \sum_{n=1}^{N} b_n T_{2n-1}(x) \end{aligned} \tag{19}$$

4.4.3 Correspondence of Zolotarev and Space Factor Polynomials

For the case of half-wavelength spacing between array elements, $\psi/2 = (\pi/2)\sin\theta$. Therefore, as θ varies over the range of observation angles from $-\pi/2$ to $\pi/2$, the term $\sin(\psi/2)$ goes from -1 to 1. If the spacing d is greater than a half-wavelength, the term $\sin(\psi/2)$ also always reaches -1 and 1 in the visible range $-\pi/2 \leq \theta \leq \pi/2$. Thus a correspondence $x = \sin(\psi/2)$ can be made, so that (17) becomes

$$E_d(x) = \sum_{n=1}^{N} a_n (-1)^n T_{2n-1}(x) \qquad (20)$$

Comparison of (19) and (20) clearly shows that the required optimum array coefficients $\{a_n\}$ are simply related to the expansion coefficients $\{b_n\}$ of the Chebyshev series for $Z_{2N-1}(x)$ by,

$$a_n = (-1)^n b_n \qquad (21)$$

4.5 ARRAY ELEMENT EXCITATIONS FOR SPACINGS LESS THAN HALF A WAVELENGTH

For spacings less than a half-wavelength the determination of the array coefficients is not as straightforward. If the correspondence $x = \sin(\psi/2)$ is made for some general spacing, then for $-\pi/2 \leq \theta \leq \pi/2$, the corresponding x variation is $-\sin(kd/2) \leq x \leq \sin(kd/2)$, where k is the free space wavenumber. For example, for a spacing of 0.4 of a wavelength, the range of x values is only $-0.951 \leq x \leq 0.951$, with the result that the pattern does not have as many secondary lobes as are possible, and is therefore non-optimum.

This can be remedied by setting,

$$x = \frac{\sin\left(\frac{\psi}{2}\right)}{\sin\left(\frac{kd}{2}\right)} \tag{22}$$

but then the Chebyshev expansion (in x) of the space factor given in equation (20) is not possible. For spacing d less than a half-wavelength, then, a more direct and tedious approach must be used. In what follows, let $x_o = \sin(kd/2)$.

Assume then that the Zolotarev polynomial is available in the standard polynomial form,

$$Z_{2N}(x) = b_1 x + b_2 x^3 + \cdots + b_N x^{2N-1} \tag{23}$$

Methods of obtaining the b_i are discussed in Section 5.3.5.

The expansion given in (14) can after some manipulation be written in the form,

$$\sin[(2n-1)\psi/2] = \sum_{i=1}^{n} g_i(n)[\sin \psi/2]^{2(n-i)+1} \tag{24}$$

where $$g_i(n) = (-1)^n(-1)^{i+1}2^{2(n-i)}\left[\frac{2n-1}{2n-i}\right]\binom{2n-i}{i-1} \tag{25}$$

$$\binom{p}{n} = \frac{p(p-1) \cdots (p-n+1)}{1.2 \cdots n} \tag{26}$$

$$\binom{p}{o} = 1 \tag{27}$$

Thus, for each term in the series (13),

$$a_N \sin[(2N-1)\psi/2] = a_N g_1(N)(\sin \psi/2)^{2N-1} + a_N g_2(N)(\sin \psi/2)^{2N-3} + a_N g_3(N)(\sin \psi/2)^{2N-5} \vdots + a_N g_N(N)(\sin \psi/2)^{1}$$

$$a_{N-1} \sin\{[2(N-1)-1]\psi/2\} = a_{N-1} g_1(N-1)(\sin \psi/2)^{2N-3} + a_{N-1} g_2(N-1)(\sin \psi/2)^{2N-5} + a_{N-1} g_3(N-1)(\sin \psi/2)^{2N-7} \vdots + a_{N-1} g_{N-1}(N-1)(\sin \psi/2)^{1}$$

$$a_{N-2} \sin\{[2(N-2)-1]\psi/2\} = a_{N-2} g_1(N-2)(\sin \psi/2)^{2N-5} + a_{N-2} g_2(N-2)(\sin \psi/2)^{2N-7} + a_{N-2} g_3(N-2)(\sin \psi/2)^{2N-9} \vdots + a_{N-2} g_{N-2}(N-2)(\sin \psi/2)^{1}$$

$$\vdots$$

$$a_1 \sin \psi/2 = a_1 g_1(1)(\sin \psi/2)^{1}$$

Comparing (13) with (23), and letting $x = \frac{\sin(\psi/2)}{x_o}$ it follows that

$$b_N = a_N g_1(N)\, x_o^{2N-1}$$

$$b_{N-1} = \left[a_N g_2(N) + a_{N-1} g_1(N-1)\right] x_o^{2N-3}$$

$$b_{N-2} = \left[a_N g_3(N) + a_{N-1} g_2(N-1) + a_{N-2} g_1(N-2)\right] x_o^{2N-5}$$

$$\vdots$$

$$b_1 = \left[a_N g_N(N) + a_{N-1} g_{N-1}(N-1) + \cdots a_1 g_1(1)\right] x_o$$

Thus the array element excitations are given by,

$$a_N = b_N'/g_1(N)$$

$$a_{N-1} = \left[b_{N-1}' - a_N g_2(N)\right]/g_1(N-1)$$

$$a_{N-2} = \left[b_{N-2}' - a_N g_3(N) - a_{N-1} g_2(N-1)\right]/g_1(N-2)$$

$$\vdots$$

$$a_n = \left[b_n' - \sum_{j=n+1}^{N} a_j g_p(j)\right] / g_1(n) \qquad (28)$$

where $p = j - n + 1$

$$b_n' = b_n/x_o^{2n-1}$$

In this manner, the array excitations can be obtained for some general element spacing. For the case of half-wavelength spacing (28) and (21) give identical excitations of course.

4.6 SYNTHESIS PROCEDURE

While details of a computational procedure are left until Chapter 5, the steps in the synthesis procedure just developed are summarised here.

Suppose that the number of array elements (2N) and the required sidelobe ratio (SLR) have been specified. A Zolotarev polynomial of order 2N-1 is then required. The first step of the synthesis procedure is the solution of the equation,

$$Z_{2N-1}(x_2) = SLR \tag{29}$$

for the required Jacobi modulus k, since x_2 is the position of the maximum of the polynomial. The quantities x_2 and k are of course related through (8), (9) and (10). With the order 2N-1 and Jacobi modulus k known, the polynomial $Z_{2N-1}(x)$ is completely determined. Its expansion in the form of a Chebyshev series or conventional polynomial form, depending on whether the spacing is greater than a half-wavelength or not, is then carried out, for the set of coefficients $\{b_i\}$, i = 1,2,3, ••• N. If $d \geq 0.5\ \lambda$, the excitations follow directly from (21). For $d < 0.5\ \lambda$, specification of the spacing d serves to determine x_o, which together with the b_i coefficients is used in (28) to find the array excitations $\{a_n\}$, n = 1,2,3, ••• N. Once these have been found any other array performance indices can be evaluated using the expressions given in Chapter 2.

As an example, consider an array of 20 elements with a sidelobe ratio of 30 dB and half-wavelength spacing. Since 2N = 20 in this case, a polynomial $Z_{19}(x)$ is required. Solution of equation (29) gives the value of Jacobi modulus k = 0.999971042. The normalised array element excitations are found as given in Table 4.7. The corresponding array pattern is shown in Fig. 4.11, along with a plot of the excitations.

TABLE 4.7 : Array element excitations for a 20 element, 30 dB sidelobe ratio, Zolotarev array.

n	a_n
1	0.180205
2	0.515913
3	0.782293
4	0.947927
5	1.000000
6	0.945505
7	0.808179
8	0.622164
9	0.424087
10	0.329244

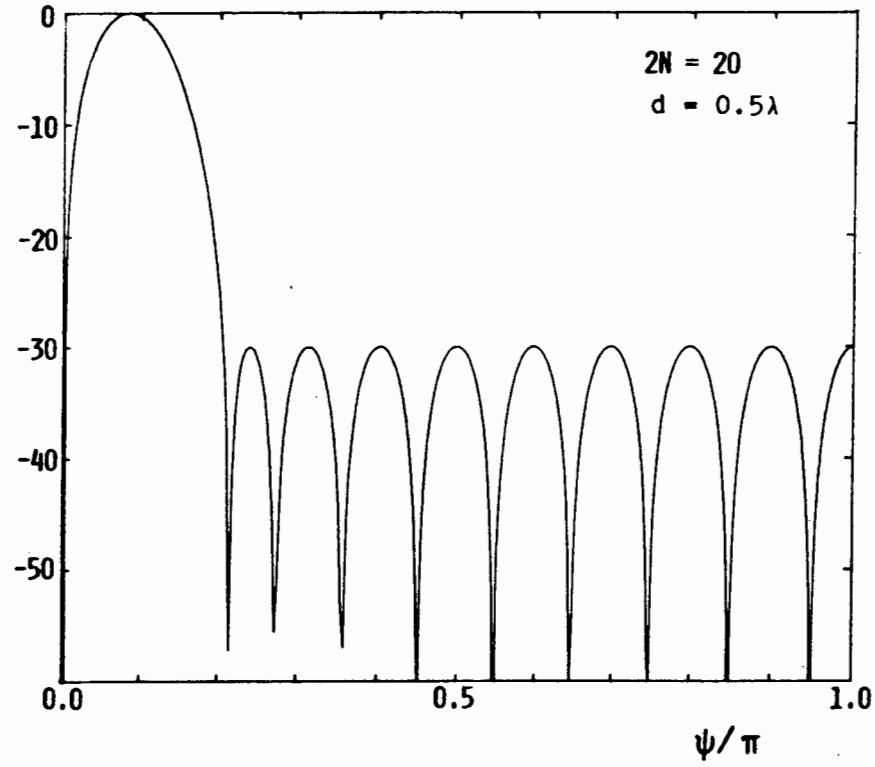

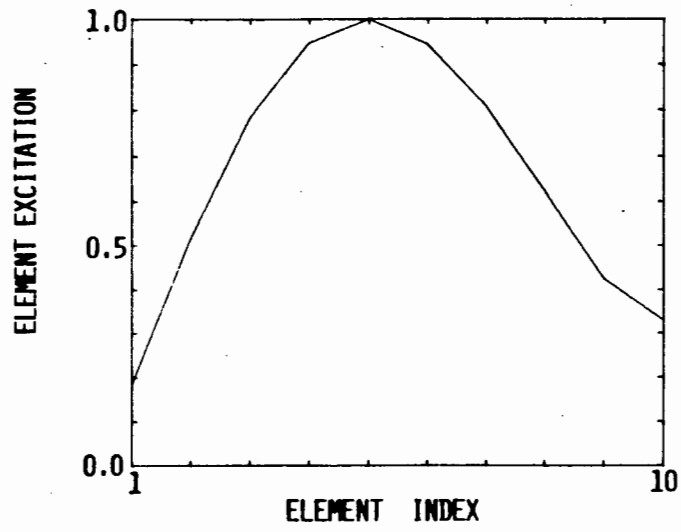

FIGURE 4.11 ZOLOTAREV POLYNOMIAL ARRAY

4.7 CONCLUSIONS

The form of the real distributions providing (without sidelobe constraints) either the maximum directivity or maximum normalised boresight slope that is possible with a given number of array elements and spacings has been established using unconstrained numerical optimisation. For half wavelength interelement spacings these are similar to those of the corresponding continuous distributions. The tables of data on K_o and D_d^{max} can be used as the standards against which to evaluate distributions providing array space factors with constrained sidelobe levels.

A difference pattern can be defined as optimum in the Dolph-Chebyshev sense if it has the narrowest first null beamwidth and largest normalised difference slope on boresight for a specified sidelobe level constraint. Such patterns will have sidelobes all at the same required level. The principal contribution made in this chapter is the development of a new exact synthesis method for determining the linear array excitations which will provide such optimum performance. The method uses Zolotarev polynomials, and is analogous to the Chebyshev polynomial synthesis of sum patterns. The identification of the appropriate polynomials here, and the subsequent development of the synthesis technique (methods of obtaining the element excitations) completes this aspect of array antenna theory in a satisfactory and satisfying manner. Preliminary work has been published by the author [16,17].

4.8 REFERENCES

[1] P.W. Hannan, "Maximum gain in monopulse difference mode", IRE Trans. Antennas Prop., Vol. AP-9, No. 3, pp. 314-315, May 1961.

[2] G.M. Kirkpatrick, "Aperture illuminations for radar angle of arrival measurements", IRE Trans. Aeronautical and Navigational Electronics, Vol. AE-9, pp. 20-27, Sept. 1953.

[3] D.K. Cheng, "Optimisation techniques for antenna arrays", Proc. IEEE, Vol. 59, pp. 1664-1674, Dec. 1971.

[4] F.R. Gantmacher, Theory of Matrices, Vol. I, (Chelsea Publ. Co., 1960).

[5] P.E. Gill, W. Murray and M. Wright, Practical Optimisation, (Academic Press, 1981).

[6] O.R. Price and R.F. Hyneman, "Distribution functions for monopulse antenna difference patterns", IRE Trans. Antennas Prop., Vol. AP-8, pp. 567-576, Nov. 1960.

[7] E.I. Zolotarev, "Application of elliptic functions to questions concerning functions more or less deviating from zero", Notes of the Russian Sci. Acad., Vol. 30, Appendix 5, pp. 1-71, 1877.

[8] N.I. Achieser, "Über einige funktionen, die in gegebenen interrvallen am wehigsten von null abweichen", Bull. de la Soc. Phys. Math. de Kazan, Vol. 3, p. 111, 1928.

[9] N.I. Achieser, Theory of Approximation, (English Translation by C.J. Hyman, Publ. by Ungar, N.Y., 1956).

[10] R. Levy, "Generalised rational function approximation in finite intervals using Zolotarev functions", IEEE Trans. Microwave Theory Techniques, Vol. MTT-18, No. 12, pp. 1052-1064, Dec. 1970.

[11] L.M. Milne-Thomson, Jacobian Elliptic Function Tables, (Dover Publications Inc., 1950).

[12] E.T. Copson, An Introduction to the Theory of Functions of a Complex Variable, (Oxford University Press, 1935).

[13] I.S. Gradshteyn and I.M. Ryzhik, Tables of Integrals, Series and Products, (Academic Press, 1980).

[14] R.S. Elliott, Antenna Theory and Design, (Prentice-Hall Inc., 1981).

[15] L. Fox and I.B. Parker, Chebyshev Polynomials in Numerical Analysis, (Oxford University Press, 1968).

[16] D.A. McNamara, "Optimum monopulse linear array excitations using Zolotarev polynomials", Electronics Letters, Vol. 21, No. 6, pp 681 -682, 1st Aug., 1985.

[17] D.A. McNamara, "Optimum difference mode excitations for discrete monopulse arrays", Accepted for publication in the IEEE Trans. Antennas Propagation.

[18] Numerical Algorithms Group (NAG), Mathematical Software Library, (FORTRAN Routine E04JAF), Oxfordshire, England.

CHAPTER 5

COMPUTATIONAL ASPECTS OF ZOLOTAREV POLYNOMIAL ARRAY SYNTHESIS

5.1 INTRODUCTION

The concept of Zolotarev polynomial synthesis is by itself important from an antenna theorist's point of view. However, the utility of the method rests on the computational tasks involved. The present chapter will consider in detail such computational aspects as the algorithms for elliptic function generation, series evaluation, and root finding.

On the basis of these considerations a highly efficient interactive computer code has been developed. Given the number of array elements, required sidelobe ratio, and element spacing, the code finds the array element excitations and space factor zeros. In the second portion of this chapter some tables of such information generated by the code and presented in Appendix II, are discussed. These have, of necessity, been restricted to those cases considered either particularly illustrative or most common in practice.

After presentation of the tables, a number of properties of the Zolotarev distribution are highlighted. This leads logically to the subject of Chapter 6 - that of direct synthesis of difference patterns with tapered sidelobe heights.

5.2 DERIVATION OF EXPRESSIONS SUITABLE FOR COMPUTATION

5.2.1 **Introduction**

A comment was made in Chapter 4 that the formal definition (5) given there should not be used for computational purposes. The aim of the present section therefore is to arrange the formulations of the previous chapter into a form suitable for numerical computation.

In order to do this, the domain $0 \leq x \leq 1$ is divided into three regions:

(a) Region I for which $0 \leq x \leq x_1$

(b) Region II for which $x_1 \leq x \leq x_3$

(c) Region III for which $x_3 \leq x \leq 1$

which can easily be identified in Fig. 4.10. The region for which $|x| > 1$ is of no interest as far as the array synthesis problem is concerned, and will not be considered. It is because of the symmetry of the polynomial that only the positive portion of the domain $|x| \leq 1$.

For convenience, the expression defining the Zolotarev polynomial of order 2n+1 is repeated here,

$$Z_{2n+1}(x) = \cosh\left[\left(n + \frac{1}{2}\right)\ell n\left\{\frac{H(M + \nu,k)}{H(M - \nu,k)}\right\}\right] \qquad (1)$$

In addition to the special functions K(k), sn(ν,k), cn(ν,k), dn(ν,k), z(ν,k), and H(ν,k) defined and referenced in Section 4.3.2, two further ones will be used in this chapter. These are the second Jacobi eta function $H_1(\nu,k)$ and the Jacobi theta function $\Theta(\nu,k)$, whose relationships to H(ν,k) are given in references [2] and [4].

Only the first five of the above functions need eventually to be numerically evaluated individually. The advantage of the introduction of the eta and theta functions is the considerable simplification effected in the mathematical manipulation of the Zolotarev polynomials. When working with these functions use is made of a quantity q called the nome [1], and defined by

$$q = e^{-\pi K'(k)/K(k)}$$

The complementary nome q' is defined as,

$$q' = e^{-\pi K(k)/K'(k)}$$

5.2.2 Region I ($0 \leq x \leq x_1$)

It is observed in Fig. 4.10 that for this range of x, the variable ν is a complex quantity given by,

$$\nu = -K(k) + j\phi \tag{2}$$

where ϕ is real, $0 \leq \phi \leq K'(k)$, k being the Jacobi modulus. Therefore,

$$\frac{H(M + \nu,k)}{H(M - \nu,k)} = \frac{H(M - K + j\phi,k)}{H(M + K - j\phi,k)} \tag{3}$$

Gibbs [4, p. 188] gives the relationships between the first Jacobi eta function H(u,k) and the second Jacobi eta function $H_1(u,k)$ as,

$$H_1(u,k) = H(u + K,k)$$

$$H_1(u,k) = -H(u - K,k)$$

It therefore follows that the right hand side of (3) becomes,

$$e^{-j\pi} \frac{H_1(M + j\phi,k)}{H_1(M - j\phi,k)} \tag{4}$$

since $e^{-j\pi} = -1$.

From Abramowitz and Stegun [2, p. 577] the natural logarithm of the ratio of two such second Jacobi eta functions is conveniently given by the series expansion,

$$\ln\left\{ \frac{H_1(b + u,k)}{H_1(b - u,k)} \right\} = \ln \frac{\cos \frac{(b + u)\pi}{2K}}{\cos \frac{(b - u)\pi}{2K}}$$

$$+ 4 \sum_{r=1}^{\infty} \frac{(-1)^r}{r} \frac{q^{2r}}{1 - q^{2r}} \sin \frac{r\pi b}{K} \sin \frac{r\pi u}{K} \tag{5}$$

where q is the nome.

For the case of equation (4), b = M and u = $j\phi$.

Consequently,

$$\frac{(b \pm u)\pi}{2K} = \frac{(M \pm j\phi)\pi}{2K} \tag{6}$$

Use of (6) and the identity,

$$\frac{\cos(\alpha + j\beta)}{\cos(\alpha - j\beta)} = e^{-j\ 2\tan^{-1}(\tan\alpha \tanh\beta)}$$

reduces the logarithm term in (5) to,

$$- j\ 2\tan^{-1}\left(\frac{\pi M}{2K} \right)\tanh\left(\frac{\pi \phi}{2K} \right) \tag{7}$$

In the series terms of (5), substitution of $u = j\phi$ leaves

$$\sin\left(\frac{r\pi u}{K} \right) = j \sinh\left(\frac{r\pi \phi}{K} \right) \tag{8}$$

Therefore, from (3), (4), (5), (7) and (8) it follows that,

$$\ln\left\{ \frac{H(M + \nu,k)}{H(M - \nu,k)} \right\} = - j\pi - j\ 2\tan^{-1}\left[\tan\left(\frac{\pi M}{2K} \right)\tanh\left(\frac{\pi \phi}{2K} \right)\right]$$

$$+ j4 \sum_{r=1}^{\infty} \frac{(-1)^r}{r} \frac{q^{2r}}{1-q^{2r}} \sin\left(\frac{r\pi M}{K} \right)\sinh\left(\frac{r\pi \phi}{K} \right) \tag{9}$$

$$= 2j\ h(M,\phi,k) \tag{10}$$

where for convenience,

$$h(a,b,k) = - \frac{\pi}{2} - \tan^{-1}\left[\tan\left[\frac{\pi a}{2K(k)} \right]\tanh\left[\frac{\pi b}{2K(k)} \right]\right]$$

$$+ 2 \sum_{r=1}^{\infty} \frac{(-1)^r}{r} \left[\frac{q^{2r}}{1-q^{2r}} \right]\sin\left[\frac{r\pi a}{K(k)} \right]\sinh\left[\frac{r\pi b}{K(k)} \right] \tag{11}$$

and which is real for real a and b.

From (1) then,

$$Z_{2n+1}(x) = \cosh[j\,2(n + \tfrac{1}{2})h(M,\phi,k)]$$

$$= \cos[(2n + 1)h(M,\phi,k)] \qquad (12)$$

for this region. With $\nu = -K + j\phi$, use of the properties of the Jacobian elliptic function [6, p. 914] reduces expression (6) of Chapter 4, the transformation between x and ν, to the form,

$$x = sn(M,k)\left[\frac{1 - dn^2(\phi,k')}{1 - sn^2(M,k)dn^2(\phi,k')}\right]^{\frac{1}{2}} \qquad (13)$$

This gives x once ϕ is specified. In order to find the inverse transformation, $sn(\phi,k')$ is made the subject of expression (13), utilising the elliptic function identities [6, p. 916], to give

$$sn(\phi,k') = \frac{x\ cn(M,k)}{\sqrt{1 - x^2}\ k'\ sn(M,k)}$$

Now the incomplete elliptic integral of the first kind [2, p. 589] is defined as,

$$F(a,b) = \int_0^a [(1 - v^2)(1 - b^2v^2)]^{-\frac{1}{2}}\,dv \qquad (14)$$

It then follows that since [1, p. 392],

$$sn^{-1}(a,b) = F(a,b)$$

the desired inverse transformation is,

$$\phi = F(t,k') \tag{15}$$

where $$t = \frac{x\ cn(M,k)}{\sqrt{1 - x^2}\ k'\ sn(M,k)}$$

If x is given, the corresponding ϕ can be found from (15).

5.2.3 Region II ($x_1 \leq x \leq x_3$)

From Fig. 4.10, for $x_1 \leq x \leq x_3$, the variable ν is a complex quantity $\nu = s + jK'(k)$, where s is real and $-K(k) < s < 0$. Thus,

$$\frac{H(M + \nu,k)}{H(M - \nu,k)} = \frac{H(M + s + jK',k)}{H(M - s - jK',k)} \tag{16}$$

Copson [1, p. 411] gives an expression relating the eta and theta functions,

$$H[u + jK',k] = j\ q^{-\frac{1}{4}}\ e^{-j\frac{\pi}{2}u/K}\ \Theta(u,k)$$

It therefore follows that (16) can be written as,

$$e^{-j\pi(1 + M/K)}\ \frac{\Theta(M + s,k)}{\Theta(M - s,k)} \tag{17}$$

and therefore, in this region,

$$\ln\left[\frac{H(M+\nu,k)}{H(M-\nu,k)}\right] = -j\pi\left(1+\frac{M}{K}\right) + \ln\frac{\theta(M+s,k)}{\theta(M-s,k)} \tag{18}$$

But from equation (8) of Chapter 4,

$$M = -\frac{K(k)}{2n+1}$$

For this reason then,

$$-j\pi\left(1+\frac{M}{K}\right) = -j\pi\left[\frac{2n}{2n+1}\right]$$

Thus, from (1)

$$Z_{2n+1}(x) = \cosh\left[-j\,n\pi + \left(n+\frac{1}{2}\right)\ln\left\{\frac{\theta(M+s,k)}{\theta(M-s,k)}\right\}\right]$$

$$= \cos[n\pi]\cosh\left[\left(n+\frac{1}{2}\right)\ln\left\{\frac{\theta(M+s,k)}{\theta(M-s,k)}\right\}\right] \tag{19}$$

Let $$f(a,b,k) = \ln\left\{\frac{\theta(a+b,k)}{\theta(a-b,k)}\right\} \tag{20}$$

Instead of first computing the theta functions, direct series expansions are available [2,3,5] for f(a,b,k) in terms of either q or its complement q'. For most of the antenna synthesis problems k is near to 1, so that K(k) is very large, and q close to unity, while q' is small. Series in terms of q' are then more rapidly convergent and are preferred if many computations are required. For this reason use is made of the expansion

$$f(a,b,k) = -\frac{\pi ab}{KK'} + \ell n \frac{\cosh \frac{(a+b)\pi}{2K}}{\cosh \frac{(a-b)\pi}{2K}}$$

$$- 4 \sum_{r=1}^{\infty} \frac{(-1)^r}{r} \frac{q'^{2r}}{1 - q'^{2r}} \sinh \left(\frac{r\pi a}{K'} \right) \sinh \left(\frac{r\pi b}{K'} \right) \quad (21)$$

Therefore (19) can be written in compact form as,

$$Z_{2n+1}(x) = \cos(n\pi)\cosh \left[\left(n + \frac{1}{2}\right) f(M,s,k) \right] \quad (22)$$

The transformations between x and s for this region are found using a procedure similar to that applied for region I. Starting with expressions (6) of Chapter 4, substitution of $\nu = s + jK'$ leads to the result,

$$x = \frac{sn(M,k)dn(s,k)}{\sqrt{cn^2(M,k) + sn^2(M,k)dn^2(M,k)}} \quad (23)$$

The inverse transformation is similarly found in terms of the incomplete elliptic integral as,

$$s = F(p,k) \quad (24)$$

$$p = \frac{1}{k} \left[\frac{sn^2(M,k) - x^2}{sn^2(M,k)(1 - x^2)} \right]^{\frac{1}{2}}$$

5.2.4 Region III ($x_3 \leq x \leq 1$)

For this range of x values, ν is entirely imaginary, being given by $\nu = j\phi$, where ϕ is real, and $0 \leq \phi \leq K'(k)$. In this case, then,

$$\frac{H(M + \nu,k)}{H(M - \nu,k)} = \frac{H(M + j\phi,k)}{H(M - j\phi,k)} \tag{25}$$

An expansion in terms of q' is given in [5, Eq. 72] as,

$$\ln\left\{ \frac{H(b + u,k)}{H(b - u,k)} \right\} = -\frac{\pi b u}{KK'} + \ln \frac{\sinh \frac{(b + u)\pi}{2K'}}{\sinh \frac{(b - u)\pi}{2K'}}$$

$$= 4 \sum_{r=1}^{\infty} \left(\frac{1}{r} \right) \frac{q'^{2r}}{1-q'^{2r}} \sinh\left(\frac{r\pi b}{K'} \right) \sinh\left(\frac{r\pi u}{K'} \right) \tag{26}$$

In the case of (25), $b = M$ and $u = j\phi$.

Thus $(b \pm u)\pi/2K' = (M \pm j\phi)\pi/2K'$

$$= j(\phi \mp jM)\pi/2K'$$

Using the fact that $\sinh[j(\alpha + j\beta)] = j \sin(\alpha + j\beta)$, and the identity,

$$\frac{\sin(\alpha - j\beta)}{\sin(\alpha + j\beta)} = e^{j2\tan^{-1}(\tan\alpha/\tanh\beta)}$$

the logarithm term in (26) reduces to

$$j2\tan^{-1}\left[\tan\left(\frac{\pi\phi}{2K'} \right) / \tanh\left(\frac{\pi M}{2K'} \right)\right] \tag{27}$$

In the series term in (26), with $u = j\phi$,

$$\sinh\left(\frac{r\pi u}{K'}\right) = j \sin\left(\frac{r\pi\phi}{K'}\right) \tag{28}$$

So, if the function g(a,b,k) is defined for notational convenience as,

$$g(a,b,k) = -\frac{\pi ab}{KK'} + 2\tan^{-1}\left[\frac{\tan\left[\frac{\pi b}{2K'}\right]}{\tanh\left[\frac{\pi a}{2K'}\right]}\right] - 4\sum_{r=1}^{\infty}\frac{1}{r}\left[\frac{q'^{2r}}{1-q'^{2r}}\right]\sinh\left[\frac{r\pi a}{K'}\right]\sin\left[\frac{r\pi b}{K'}\right] \tag{29}$$

which is real for real a and b, then from (25), (26), (27) and (28)

$$\ln\left\{\frac{H(M+\nu,k)}{H(M-\nu,k)}\right\} = j\, g(M,\phi,k) \tag{30}$$

Substitution of (30) into (1) gives,

$$-Z_{2n+1}(x) = \cosh\left[j\left(n+\frac{1}{2}\right) g(M,\phi,k)\right]$$

$$= \cos\left[\left(n+\frac{1}{2}\right) g(M,\phi,k)\right] \tag{31}$$

All that remains is to relate x to ϕ in the region. Once again, as for regions I and II, the derivation is relatively straightforward but tedious. Use of the transformation (6) of Chapter 4 and the elliptic function identities, with $\nu = j\phi$, leads finally to the following relationships,

$$x = \frac{sn(M,k)}{\sqrt{sn^2(M,k)cn^2(\phi,k') + sn^2(\phi,k')}} \tag{32}$$

and its inverse,

$$\phi = F(r,k') \tag{33}$$

$$r = \frac{sn\ (M,k)}{cn(M,k)} \cdot \frac{\sqrt{1 - x^2}}{x}$$

5.2.5 **Relating Jacobi Modulus k to the Sidelobe Ratio**

The maximum value of the Zolotarev polynomial (position of the difference peak) occurs at $x = x_2$, with

$$Z_{2N-1}(x_2) = SLR \tag{34}$$

since the Zolotarev polynomial as defined in (1) gives sidelobe levels of unity. This maximum occurs in region II, so that with

$$x_2 = x_3 \sqrt{1 - \frac{cn(M,k)\ z(M,k)}{sn(M,k)dn(M,k)}}$$

$$s_2 = F(p_2,k)$$

$$p_2 = \frac{1}{k}\left[\frac{sn^2(M,k) - x_2^2}{sn^2(M,k)(1 - x_2^2)}\right]^{\frac{1}{2}}$$

equation (34) can be written as,

$$\cos[n\pi]\cosh\left[\left(n + \frac{1}{2}\right)f(M,s_2,k)\right] = SLR$$

Given the order (2n+1) of the polynomial, and the sidelobe ratio SLR, this equation can be solved for the value of the modulus k required to give such a sidelobe ratio.

5.2.6 **Finding the Zeros of the Zolotarev Polynomial**

A knowledge of the zeros of the Zolotarev polynomial will be required in Chapters 6 and 8.

The zeros of the Zolotarev polynomial all lie in Region III in which,

$$Z_{2n+1}(x) = \cos\left[\left(n + \frac{1}{2}\right)g(M,\phi,k)\right] \qquad (36)$$

This is the "equiripple" region, and the zeros of $Z_{2n+1}(x)$ can be found from

$$\left(n + \frac{1}{2}\right)g(M,\phi,k) = \left(m + \frac{1}{2}\right)\pi \qquad (37)$$

for $m = 0,1,2,\cdots$

Solution of this equation gives the zeros in terms of ϕ, from which the x values are found from equation (32).

5.3 COMPUTATIONAL ASPECTS

5.3.1 Introductory Remarks

Central to the numerical problem is the accurate computation of the special functions used. Three further numerical topics are the summation of the series and finding the zeros of a function. Each of the above aspects is considered separately in the sections that follow. Routines available in high quality mathematical software libraries have been used wherever possible.

5.3.2 The Elliptic Integrals of the First Kind

For the usual range of sidelobe ratios of interest the Jacobi modulus k lies between 0.9 and 1.0, being closer to 1.0 in most cases. An array of 20 elements, for example, requires k = 0.999895316 for a sidelobe ratio of 25 dB and k = 0.999971042 for a sidelobe ratio of 30 dB. Accurate computation of the elliptic integrals for this range of modulus k values is consequently of the utmost importance.

Fortunately, a very accurate routine S21BBF for doing just this is available in the NAG library [8]. This routine calculates an approximation to the integral,

$$R_F(x,y,z) = \frac{1}{2} \int_0^\infty [(t + x)(t + y)(t + z)]^{-\frac{1}{2}} dt$$

where x, y, z $\geq$ 0 and at most one is zero, and which is referred to as the symmetrised elliptic integral of the first kind [9,10]. The result is accurate to within a small multiple of machine precision [8], and uses the algorithm of Carlson [9,10].

If the following terms are defined,

$$w = 1 - a^2$$

$$v = 1 - b^2a^2$$

then the incomplete elliptic integral of the first kind, defined in equation (14), is simply given by [8],

$$F(a,b) = a\, R_F(w,v,1.0)$$

and the complete elliptic integral of the first kind by,

$$K(k) = R_F(0.0,1-k^2,1.0)$$

Computation of the elliptic integrals in this manner has been found to be very satisfactory.

5.3.3 Computation of the Jacobian Elliptic Functions sn, cn and dn

The functions sn, cn and dn were computed using routines based on the algorithms given by Bulirsch [7]. These are available as FORTRAN subroutines JELF and DJELF (single- and double-precision versions, respectively) in the IBM Scientific Subroutine Package [11]. All three Jacobian elliptic functions are computed simultaneously by the above routines.

5.3.4 Convergence of Series

The series used for evaluation of the functions in expressions (11), (21) and (29) are all three very rapidly convergent. No special methods are required for their evaluation and a simple term-by-term convergence test is suitable.

5.3.5 Generation of the Polynomial Forms of $Z_{2n+1}(x)$

The coefficients of either the Chebyshev series in equation (18) of Chapter 4, or of the conventional polynomial form in equation (23) of Chapter 4, are necessary for the determination of the array excitations, depending on whether the element spacing $d \geq 0.5\ \lambda$ or $d < 0.5\ \lambda$.

Consider first the Chebyshev series expansion,

$$Z_{2N-1}(x) = b_1 T_1(x) + b_2 T_3(x) + \cdots + b_N\ T_{2N-1}(x) \tag{38}$$

In order to find the set of coefficients $\{b_i\}$, a set of N values of x are selected in the interval $0 < x < 1$. Enforcement of equation (38) at each of these points $x_1, x_2, \cdots x_N$ results in a set of linear simulataneous equations,

$$\begin{bmatrix} T_1(x_1) & T_3(x_1) & \cdots\cdots & T_{2N-1}(x_1) \\ T_1(x_2) & T_3(x_2) & \cdots\cdots & T_{2N-1}(x_2) \\ \vdots & & \ddots & \vdots \\ T_1(x_N) & \cdots\cdots\cdots\cdots & & T_{2N-1}(x_N) \end{bmatrix} \begin{bmatrix} b_1 \\ b_2 \\ \vdots \\ b_N \end{bmatrix} = \begin{bmatrix} Z_{2N-1}(x_1) \\ Z_{2N-1}(x_2) \\ \vdots \\ Z_{2N-1}(x_N) \end{bmatrix} \tag{39}$$

which can be solved for the expansion coefficients. The sample points x_i selected must be chosen such that the matrix is well-conditioned. This will be so if the x_i are evenly spaced throughout the region, with one of them at the position of the maximum.

The advantage of representing a polynomial as a Chebyshev series has been pointed out by Fox and Parker [12]. They also warn that straightforward use of the above method in finding the coefficients of the conventional polynomial form directly in powers of x,

$$Z_{2N-1}(x) = b_1 x + b_2 x^3 + \cdots + b_{N-1} x^{2N-1} \tag{40}$$

leads to a seriously ill-conditioned matrix if the coefficients b_i have large numerical values. Since this is the case with the Zolotarev polynomials, the following alternative least squares procedure has been found to work well:

(a) Select a set of points

$$\{x_1, x_2, \cdots x_M\} , \quad M > N$$

fairly evenly spaced over the interval.

(b) Set up a system of equations as was done in (39). Here, however, there will be M equations in the N unknowns coefficients, with M > N. The system of equations is then solved in a least squares sense.

5.3.6 Root Finding

Determination of the zeros of a function is required for relating the Jacobi modulus k to the sidelobe ratio, and for determining the zeros of the Zolotarev array space factor. The mathematics for these tasks has been given in Sections (5.2.5) and (5.2.6), respectively. For the present case in which the functions have complicated forms, root finding procedures which do not require derivatives are desirable. Routines for doing this are available in most mathematical subroutine libraries. In the computations used to draw up the tables presented in Appendix II, the IMSL [13] routine ZFALSE was used. ZFALSE uses the "regula falsi" technique to find the solution of an equation $f(x) = 0$ and requires as input values of x known to be to the left and right of the root. For the computations required in Section 5.2.6 the routine is called successively until all the zeros have been found. The left and right bounds are found in all cases by simply incrementing the independent variable in sufficiently small steps and detecting a sign change in the particular function $f(x)$.

5.3.7 Computer Code

Based on the above considerations, an interactive computer code has been developed. The code has been found to be very flexible and easy to use, and has been used to assemble the design tables given in Appendix II. It has been used with single-precision arithmetic on a CDC Cyber 174 computer, which is a 64-bit machine. The code consists of three modules. The first determines the value of the Jacobi modules k required for a given element number and sidelobe ratio. Representative results are given in Table II.1 and II.2 of Appendix II.

The second module computes the required array element excitations. A range of array distributions can be found in Tables II.3 to II.10. The third module is optional, and finds the roots of the associated polynomial. Some results are presented in Tables II.19 to II.34. It is possible to use the third module without having executed the second if the roots are required for the synthesis procedures to be discussed in Chapter 6.

5.4 DESIGN TABLES FOR ZOLOTAREV DISTRIBUTIONS

5.4.1 Selection of Range of Parameters

Most modern radar and satellite communications antennas have sidelobe specifications requiring levels at least 25 dB down from the main beam(s). Such levels are considered to be "moderate" [14]. On the other hand an array with a sidelobe ratio of 50 dB is considered to be a very low sidelobe antenna, even by present standards [14,15]. In order that the tables presented adequately cover this range of levels, the "standard" sidelobe ratios between 15 dB and 60 dB are considered.

A survey of the commercial literature soon reveals that the number of elements used per linear array (or per linear "stick" of a planar array) varies too widely to make it possible to identify "standard" element numbers. The tables have therefore simply been restricted to arrays of between 10 and 60 elements to limit the data presented to a manageable size. These are given in Appendix II.

If the Zolotarev distributions are to be used directly, all that is needed is the set of element excitations. Any of the array performance parameters can then be found as outlined in Chapter 2. However, if the tapered sidelobe modified Zolotarev $\bar{n}$ distributions of Chapter 6 must be synthesized, then the array space factor zeros are required quantities. Hence their inclusion in the tables in Appendix II.

The notation of the tables is consistent with that used thus far in the thesis. The number of array elements is always denoted by 2N, while SLR stands for the sidelobe ratio. The symbol a_n denotes the excitation of the n-th element of the array, numbered from the central element out towards the edge. Since the distribution is symmetric, only one half of the excitations is tabulated. All directivities quoted are <u>not</u> in decibels.

5.4.2 Contents of the Tables

Table II.1 gives the modulus k required for a specified SLR and number of array elements 2N. Due to the fact that the values of k are all clustered close to unity, a "sidelobe parameter"

$$\zeta = \log_{10}(1 - k)^{-1}$$

has been introduced and the information of Table II.1 repeated in Table II.2, but with ζ displayed instead of k.

Tables II.3 to II.10 provide the element excitations for the case $d \geq 0.5\ \lambda$, for a range of array sizes and sidelobe ratios. The performance parameters (i.e. relative slope ratio K_r and excitation efficiencies η_d and η_{ds}) for these same arrays are given in Tables II.11 to II.18, for the specific spacing $d = 0.5\ \lambda$. From these the essential characteristics of the Zolotarev polynomial distributions can be gleaned, and these are discussed in the next section.

In Tables II.19 to II.26 the roots (on the x-axis) of the polynomials associated with the above tabulated cases are presented, along with the values of x_1, x_2 and x_3. These can be used to find, from the appropriate transformation equations,

$$x = \begin{cases} \sin(\psi/2) & d \geq 0.5\ \lambda \\ \sin(\psi/2)/\sin(2\pi d/\lambda) & d < 0.5\ \lambda \end{cases}$$

the space factor zeros ψ_n for any spacing. This is particularly useful when using the synthesis methods developed in Chapter 6.

Finally, for the case $d \geq 0.5\ \lambda$, these space factor zeros ψ_n are given in Tables II.27 to II.34. Only values up to $\psi_n = \pi$ are given, these applying exactly to the case of spacing $d = 0.5\ \lambda$. For larger spacings, these ψ_n values simply repeat themselves.

5.5 THE PERFORMANCE OF ZOLOTAREV DISTRIBUTIONS

The Zolotarev polynomial distribution, like its Dolph-Chebyshev sum mode counterpart, tends towards large peaks at the array ends for certain ranges of array sizes and sidelobe ratios. For instance, consider the case of an array of 2N = 20 elements, for spacings $d \geq 0.5\ \lambda$. The excitations, obtained from Tables II.3 to II.8 are plotted in Fig. 5.1 for various sidelobe ratios. For a 15 dB sidelobe ratio the largest excitation is seen to be at the array edge. That this is required to provide the desired space factor is clear from the plot of the latter in Fig. 5.2.

As the sidelobes are lowered (i.e. sidelobe ratio increased) edge excitation decreases, with the peak excitation occurring elsewhere. The distribution may still increase at the edge though. However, if the sidelobes are lowered further, a point is reached at which the peaking at the edge disappears. For the 20 element array this "edge brightening" disappears for a sidelobe ratio of approximately 25 dB. A summary of such information for other arrays sizes (for $d \geq 0.5\ \lambda$) is presented in Table 5.1. The sidelobe ratios quoted are approximate and merely intended to give a rough idea of the array sizes/sidelobe ratios at which the various phenomena occur.

TABLE 5.1 : Sidelobe ratios associated with particular excitation characteristics.

NUMBER OF ARRAY ELEMENTS (2N)	SIDELOBE RATIO GREATER THAN WHICH DISTRIBUTION DOES NOT INCREASE AT THE ARRAY EDGE	SIDELOBE RATIO AT WHICH, AND LESS THAN WHICH, THE EDGE EXCITATION IS THE LARGEST
10	16 dB	15 dB
20	25 dB	19 dB
30	33 dB	21.5 dB
40	40 dB	23.5 dB
50	45 dB	25 dB
60	50 dB	26 dB

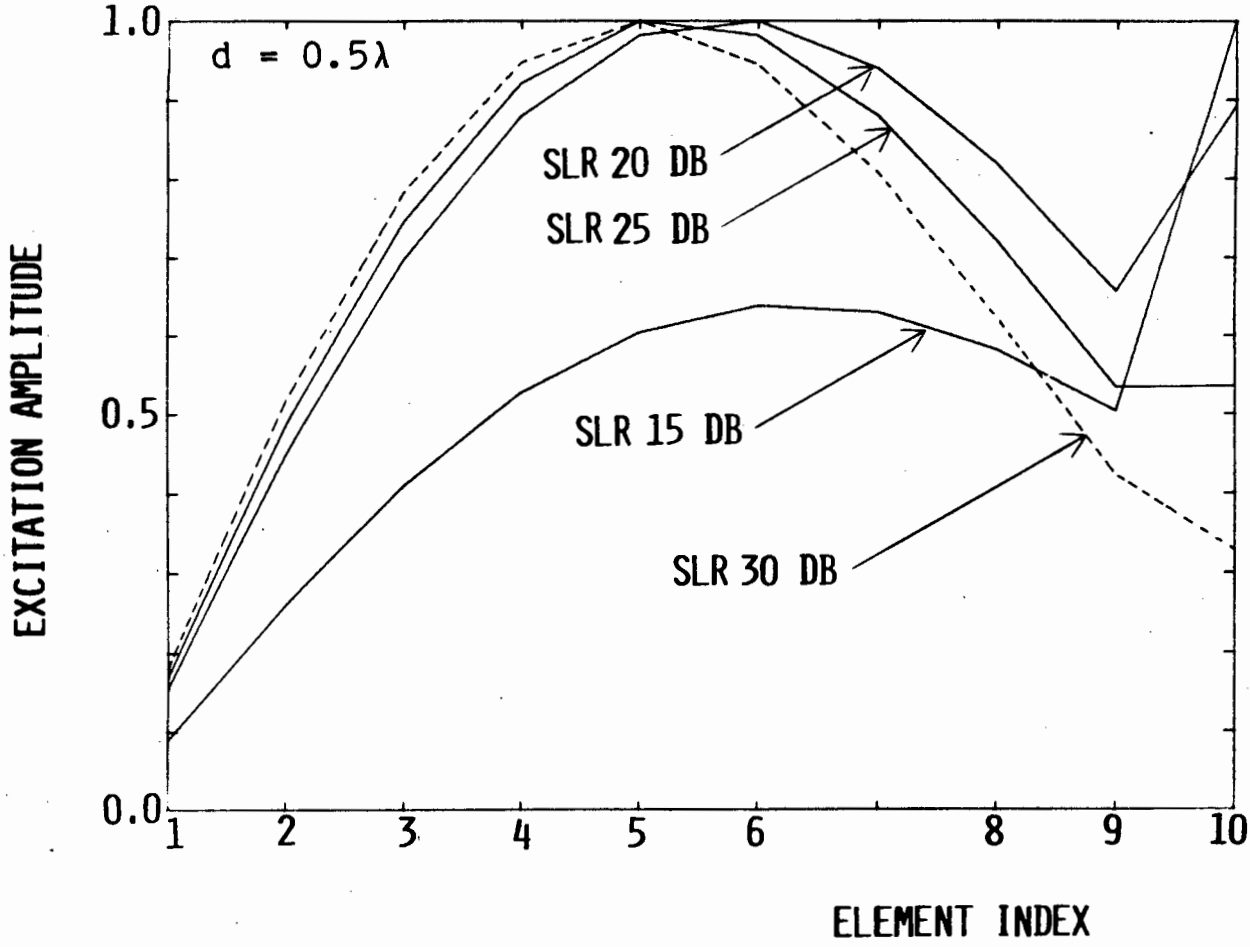

FIGURE 5.1 ZOLOTAREV POLYNOMIAL ARRAY APERTURE DISTRIBUTIONS

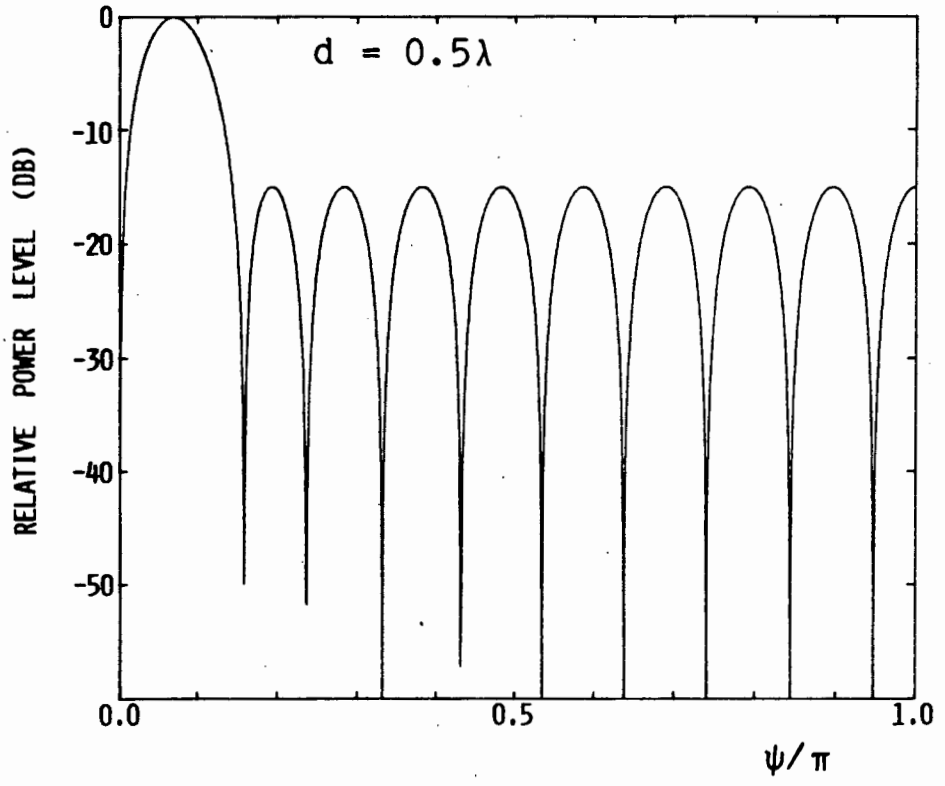

FIGURE 5.2 SPACE FACTOR OF A 20-ELEMENT ZOLOTAREV POLYNOMIAL ARRAY WITH A 15 dB SIDELOBE RATIO

Observe also that, for an array of fixed size, the maximum point on the "hump" of the distribution shifts toward the centre of the array as the sidelobe ratio is lowered until the point is reached at which the distribution does not begin to increase at the array edges. Thereafter the element with maximum excitation is fixed regardless of sidelobe ratio.

It is interesting to examine the directivity and slope information contained in Tables II.11 to II.18. This information is summarised in Figs. 5.3. Though the numerical results apply only to the case $d = 0.5\ \lambda$, the overall behaviour is applicable to other spacings as well. Observe from Fig. 5.3 that for each array size (2N value) there is a sidelobe ratio giving maximum directivity. The reason is that smaller sidelobe ratios (i.e. higher sidelobe levels) result in significant power in the equal-level sidelobes, while larger sidelobe ratios give a lower excitation efficiency due to the larger beamwidths (of the difference lobes) associated with the lower sidelobes. This behaviour parallels that of the Dolph-Chebyshev sum distribution discussed in Section 3.2.2.

A similar plot, but of the relative slope ratio K_r is shown in Fig. 5.4. It shows maximum points similar to those of the directivity, but these are shifted down to lower sidelobe ratios. The relatively high K_r values for the prescribed sidelobe levels is indicative of the optimum property of the Zolotarev polynomial distribution.

A further graph is shown in Fig. 5.5. Here the beam broadening factor is plotted versus sidelobe ratio for various element numbers. This factor has been defined here as the ratio of the first null beamwidth of the difference lobe (see Fig. 2.2) to the corresponding quantity of the maximum slope array of the same number of elements (since the latter always has a narrower beamwidth than that of the maximum directivity array). The price paid for sidelobe reduction is clear from this figure, and is as expected. The decrease in excitation efficiency with sidelobe reduction is also clear from the tables.

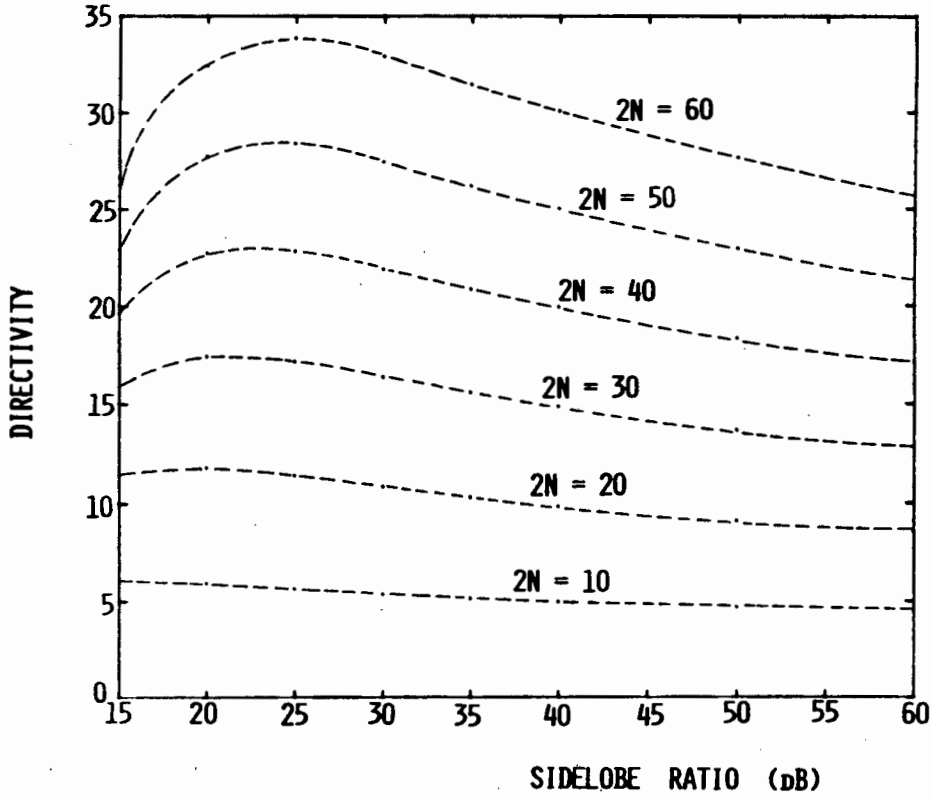

FIGURE 5.3 DIRECTIVITY OF ZOLOTAREV DISTRIBUTIONS VERSUS SIDELOBE RATIO $d = 0.5\lambda$

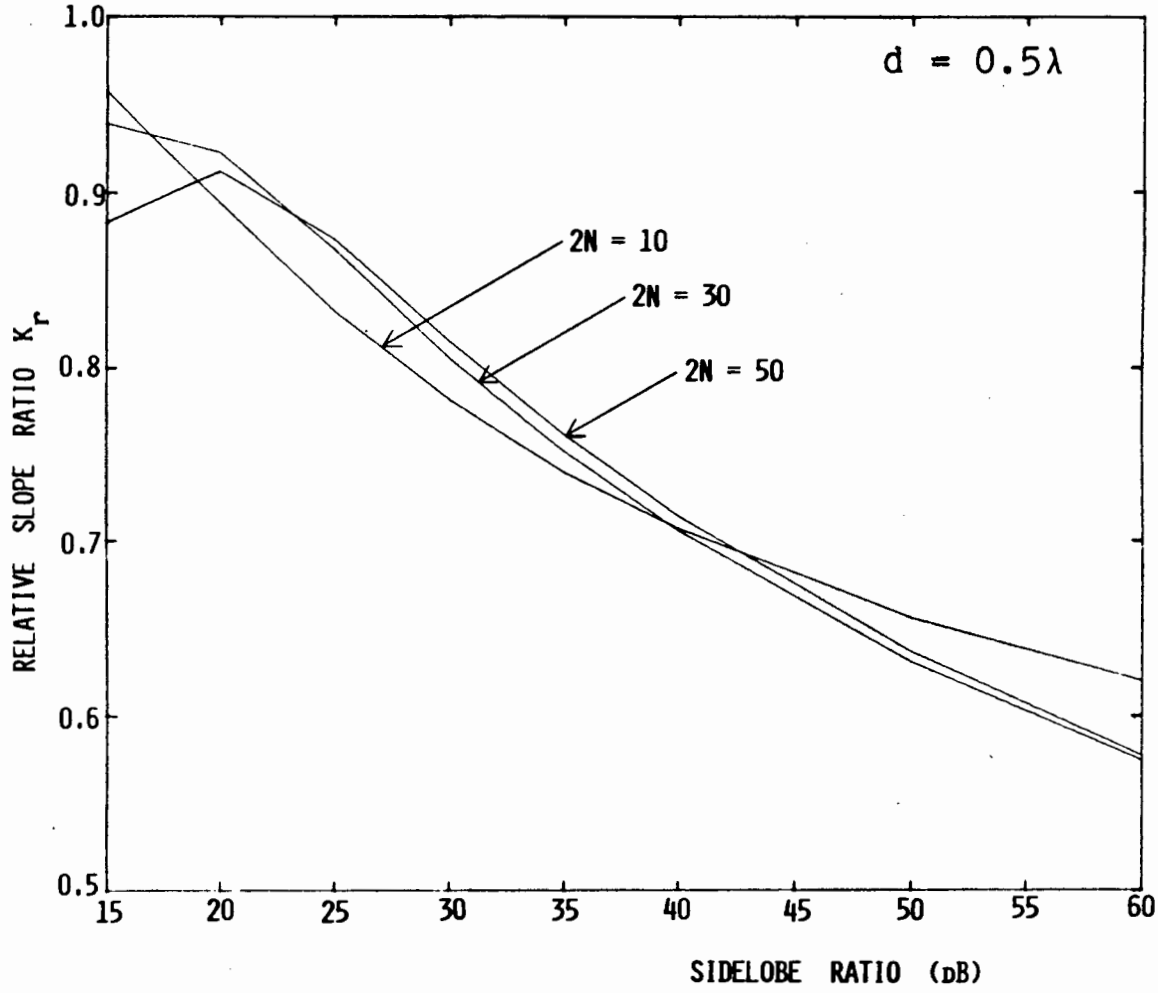

FIGURE 5.4 RELATIVE SLOPE RATIO OF ZOLOTAREV DISTRIBUTIONS VERSUS SIDELOBE RATIO

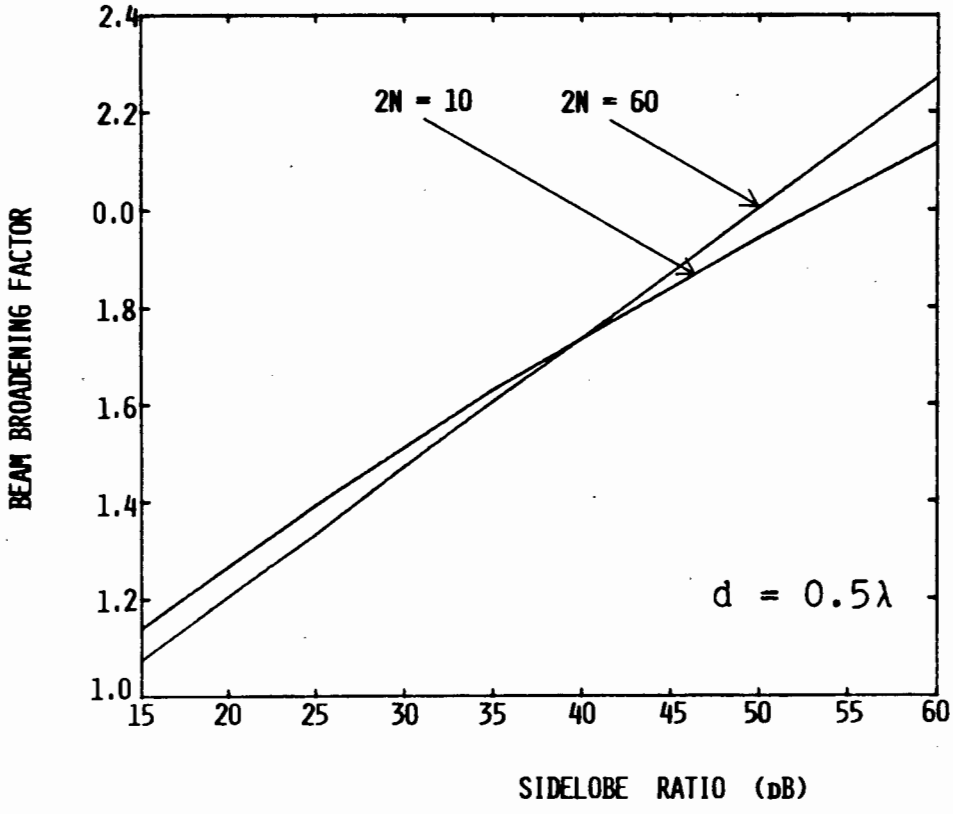

FIGURE 5.5 BEAM BROADENING FACTOR OF ZOLOTAREV DISTRIBUTIONS VERSUS SIDELOBE RATIO

The directivity information is plotted in another form in Fig. 5.6. Here D_d^m is plotted as a function of array element number 2N, with sidelobe ratio as a parameter. This form exhibits the "gain compression" of the Zolotarev polynomial distribution with increasing array size, for a given sidelobe ratio. Once more, this is precisely the behaviour observed with the Dolph-Chebyshev distribution. In that case this undesirable performance was alleviated by altering the excitations in order to provide some sidelobe taper. For the difference pattern case this is done in the next chapter.

Before proceeding, two final examples are considered simply for the purposes of illustration. The space factor of an array of 2N = 50 elements and sidelobe ratio 40 dB is shown in Fig. 5.7. This was plotted from the excitations in Table II.8, and is for a spacing $d = 0.5\ \lambda$. As an example of an array with spacing less than a half-wavelength, consider $d = 0.4\ \lambda$ and a sidelobe ratio of 30 dB for a 20 element array. The methods of Section 4.5 give the required excitations as shown in Table 5.2. Observe by comparison with the information in Table II.6 that the excitations are different from those for $d \geq 0.5\ \lambda$. The excitations for $d = 0.4\ \lambda$ have alternating signs, resulting in a characteristically high Q-factor. The space factor of the array is drawn in Fig. 5.8.

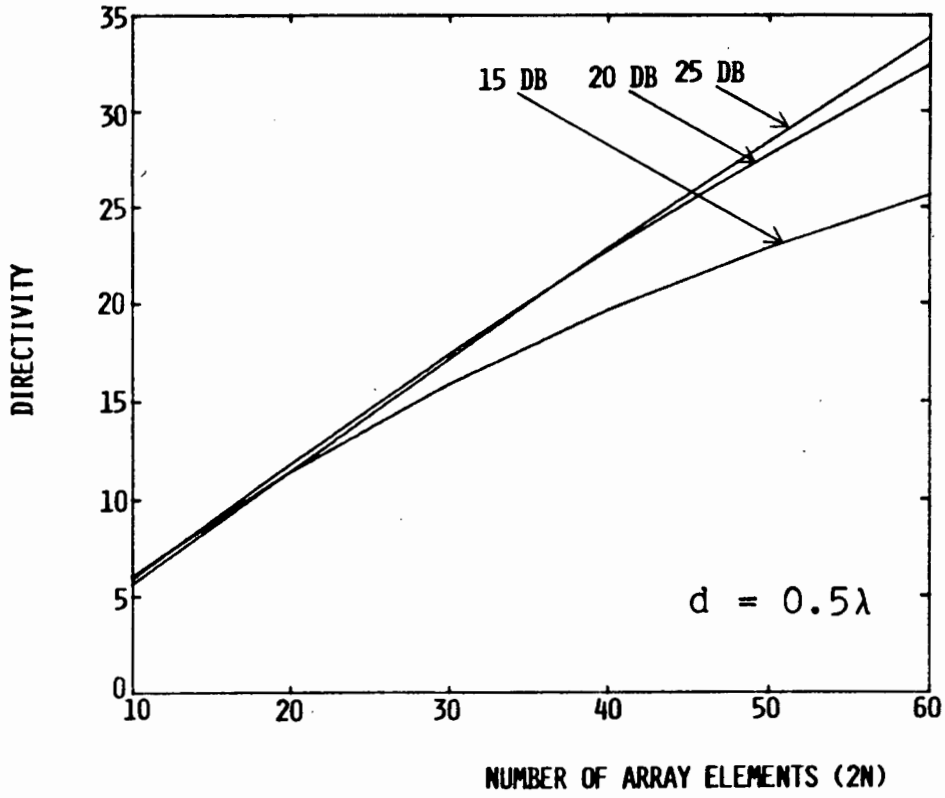

FIGURE 5.6 DIRECTIVITY OF ZOLOTAREV DISTRIBUTIONS AS A FUNCTION OF ARRAY SIZE

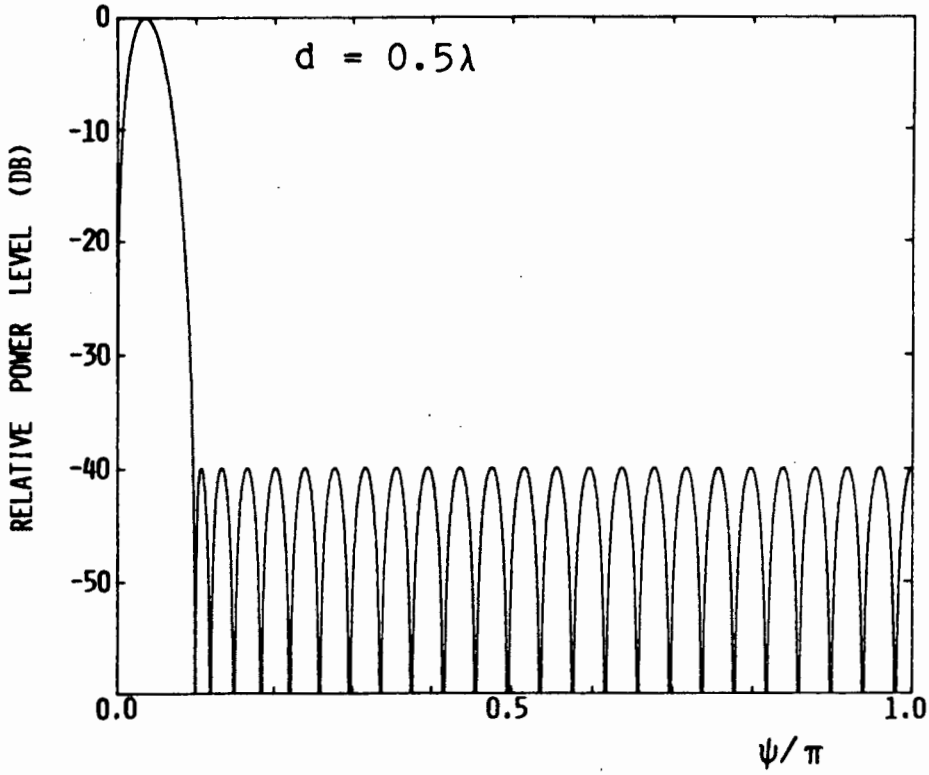

FIGURE 5.7 SPACE FACTOR OF A ZOLOTAREV ARRAY OF 50 ELEMENTS AND SIDELOBE RATIO 40 dB

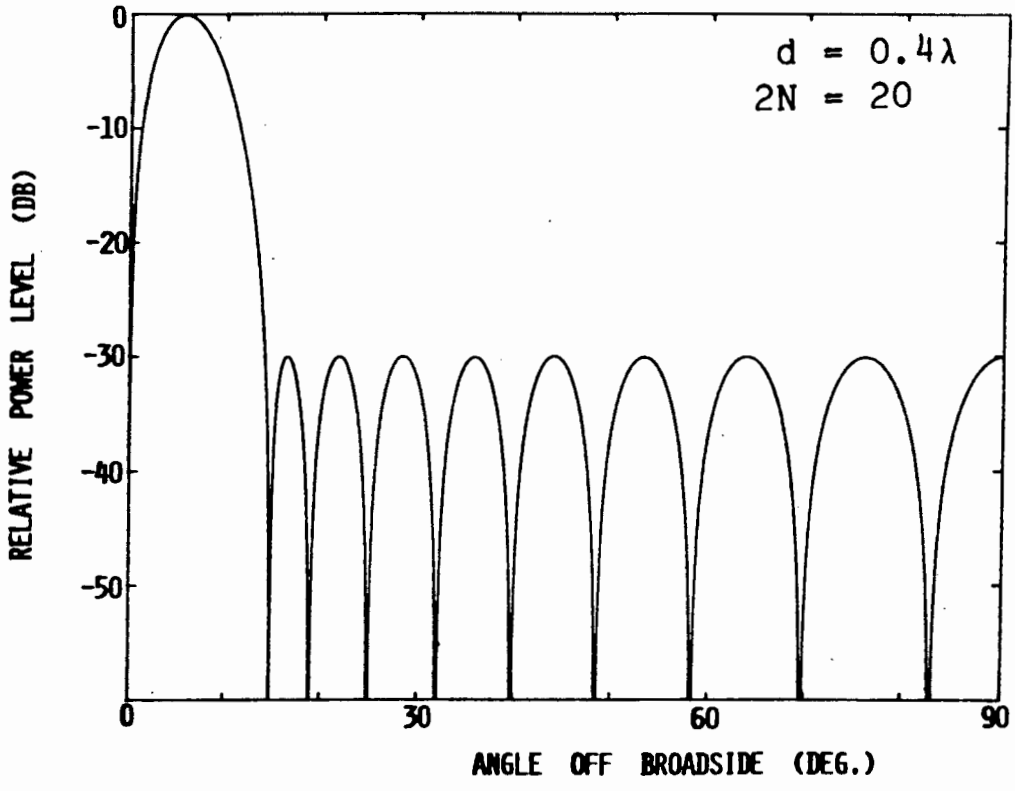

FIGURE 5.8 SPACE FACTOR OF A ZOLOTAREV ARRAY OF 20 ELEMENTS AND SIDELOBE RATIO 30 DB

TABLE 5.2 : Element excitations for the Zolotarev polynomial array with 2N = 20, d = 0.4 λ and SLR = 30 dB.

n	a_n
1	-0.97203
2	1.00000
3	-0.77005
4	0.84061
5	-0.48498
6	0.56680
7	-0.22760
8	0.29080
9	-0.06613
10	0.10185
D_d^m	9.1419
K	1.0407
Q	46.57

5.6 CONCLUSIONS

Expressions have been given for the computations required in the application of the Zolotarev array synthesis technique. The procedures used in a computer code developed to perform such computations have been explained and the code used to draw up a set of tables of design data for a number of cases of practical importance. These tables are given in Appendix II. For a wide range of applications these tables eliminate the need for a suite of computer codes to perform the array synthesis. On the other hand, the computer software developed executes extremely rapidly and has the advantage that arbitrary array sizes and sidelobe ratios can be specified.

5.7 REFERENCES

[1] E.T. Copson, Theory of Functions of a Complex Variable, (Oxford Univ. Press, 1935).

[2] M. Abramowitz and I. Stegun, Handbook of Mathematical Functions, (Dover Publ. Inc., 1972).

[3] E.T. Whittaker and G.N. Watson, A Course of Modern Analysis, (Cambridge Univ. Press, 1940).

[4] W. Gibbs, Conformal Transformations in Electrical Engineering, (Chapman and Hall Ltd., London, 1958).

[5] R. Levy, "Generalised rational function approximation in finite intervals using Zolotarev functions", IEEE Trans. Microwave Theory Tech., Vol. MTT-18, No. 12, pp. 1052-1064, Dec. 1970.

[6] I.S. Gradshteyn and I.M. Ryzhik, Tables of Integrals, Series and Products, (Academic Press, 1980).

[7] R. Bulirsch, "Numerical calculation of elliptic integrals and elliptic functions", Numerische Mathematik, Vol. 7, pp. 78-90, 1965.

[8] Numerical Algorithms Group (NAG), Mathematical Software Library, Oxfordshire, England.

[9] B.C. Carlson, "On computing elliptic integrals and functions", J. Maths. and Phys., Vol. 44, pp. 36-51, 1965.

[10] B.C. Carlson, "Elliptic integrals of the first kind", SIAM J. Math. Anal., Vol. 8, pp. 231-242, 1977.

[11] IBM Scientific Subroutine Package, Programmer's Manual, IBM Inc., 1968.

[12] L. Fox and I.B. Parker, Chebyshev Polynomials in Numerical Analysis, (Oxford Univ. Press, 1968).

[13] IMSL Library of Mathematical Software, IMSL Inc., Houston, Texas.

[14] R.C. Hansen, "Measurement distance effects on low sidelobe patterns", IEEE Trans. Antennas Prop., Vol. AP-32, No. 6, pp. 591-594, June 1984.

[15] E. Brookner, Radar Technology, (Artech House Inc., 1977).

CHAPTER 6

MODIFIED ZOLOTAREV POLYNOMIAL DISTRIBUTIONS

6.1 INTRODUCTION

The Zolotarev polynomial distribution of Chapters 4 and 5 is optimum for difference synthesis in the same sense as the Dolph-Chebyshev distribution is for sum synthesis. Examination in Section 5.5 of the characteristics of the Zolotarev polynomial distribution revealed that it, like its sum counterpart, has a number of features which for practical applications may be improved upon. Firstly there is the constant sidelobe level which results in "directivity compression" with increasing array size. Secondly there is the increase in the magnitude of the excitations at the array edges for certain element number/sidelobe ratio combinations, and the associated disadvantages. These undesirable features can be removed to some extent by incorporating a sidelobe taper. Space factors with tapered sidelobe envelopes are important not only for this reason. In many applications a prescribed tapered sidelobe envelope is a definite performance specification which has to be met. If only far-out sidelobes must be depressed below very low levels, forcing all sidelobes below these limits will result in unnecessary beam broadening and excitation efficiency decreases. Use of a tapered envelope will give a better design.

In Chapter 3 the course of further developments on the Dolph-Chebyshev sum distributions was outlined. First the work of Taylor on continuous distributions, resulting in an understanding of the physics of aperture distributions (space factor zero placement), and then the use of this knowledge by Villeneuve [1] and his subsequent invention of a method for the direct synthesis of efficient, tapered sidelobe,

sum patterns for discrete arrays which has as its point of departure the Dolph-Chebyshev space factor zero positions. In the present chapter the Zolotarev distribution is used as the starting point of a technique for the direct synthesis of the excitations of a discrete array with efficient, tapered sidelobe, difference space factors.

The discussion will use as examples arrays with spacings $d = 0.5\ \lambda$. The method applies equally well for other spacings though. A comment to this effect will be made at the end of the chapter.

6.2 FUNDAMENTAL PRINCIPLES

The Zolotarev distribution is known to provide optimum beamwidth and slope characteristics for a given array size and maximum sidelobe ratio specification. It is an "ideal" difference distribution. Any synthesis procedure for tapered sidelobe difference patterns should therefore use this ideal distribution as the starting point, and then attempt to provide the required sidelobe envelope taper with as little departure from the ideal case as is possible. The close-in space factor zeros especially should maintain their spacings as far as is possible in order to keep the close-in sidelobes at the required levels, and the beamwidth and slope factors close to optimum. The farther-out zeros must however approach those of a space factor which has the required envelope taper. As pointed out in Section 3.7, this zero shifting must be done in some ordered fashion lest a depression of sidelobes at one point be accompanied by an unacceptable increase at another.

A Zolotarev array of 2N elements and specified sidelobe ratio has a set of symmetrically positioned space factor zeros $\{\psi_n\}$, $n = \pm1, \pm2, \cdots \pm(N-1)$. These have been tabulated for a number of cases in Appendix II. Because of the symmetry of the space factor, only one half of the zeros need be considered. An additional zero is located at $\psi = 0$, as is always the case with difference patterns. This will be kept apart from the other zeros, since it is fixed under all circumstances. In order to emulate here what Villeneuve [1] did for sum patterns, the Zolotarev zeros ψ_n are retained (almost) for $n = 1,2, \cdots (\bar{n}-1)$, with $\bar{n}$ some chosen index. However, for $n \geq \bar{n}$, the Zolotarev zeros ψ_n are replaced by those of some space factor with a sidelobe envelope taper, and which will be referred to in what follows as the generic space factor zeros [2] and denoted by ψ_{on}, $n = \bar{n}, \bar{n}+1, \cdots (N-1)$. The resulting new set $\{\psi'_n\}$ of space factor zeros, with

$$\psi'_n = \begin{cases} \sigma\, \psi_n & n \leq \bar{n} \\ \psi_{on} & n \geq \bar{n} \end{cases} \qquad (1)$$

for $n = 1,2 \cdots (N-1)$, together with the zero at $\psi = 0$, completely characterises a new set of excitations. The dilation factor $\sigma = \psi_{on}/\psi_{\bar{n}}$, which must be slightly greater than unity, prevents the transition sidelobe from being raised above the maximum permissible level by providing a smooth transition between the two zero-type regions. Thus the Zolotarev zeros are not retained exactly for $n \leq \bar{n}-1$, and a slight beam broadening therefore results.

6.3 THE CHOICE OF A GENERIC DISTRIBUTION

6.3.1 The Suitability of Three Possible Generic Distributions

If it is to be utilised as a generic distribution, a distribution must at least have a space factor which itself has the sidelobe taper that the final distribution is to provide. Furthermore, it must be possible to place the generic space factor zeros ψ_{on} in an unambiguous correspondence with those of the starting Zolotarev space factor, ψ_n. For a sum array of 2N elements, Villeneuve [1] used as generic space factor that of a uniformly excited array of the same number of elements. The logical choice for the difference array case would seem to be the adoption of the uniform (magnitude) anti-symmetrically excited array as the generic distribution. (Note that by "difference distribution" of 2N elements it will be implied in what follows that the two halves of the array, each having N elements, are excited in anti-phase. This is consistent with the terminology of earlier chapters). The space factor of a uniform difference distribution of 2N elements is easily found from expression (10) of Chapter 2 with each $a_n = 1$, and the resulting series of sine terms summed [3, p. 30] to obtain

$$E_d(\psi) = \frac{\sin^2(N\psi/2)}{\sin(\psi/2)} \qquad (2)$$

with zeros at $\psi_{on} = 2n\pi/N$, $n = 1,2, \cdots N/2$, in addition to that at $\psi = 0$. Inspection of (2) reveals that as a result of the squared term in the numerator it has second order zeros, and this prohibits a correct $\psi_n \rightarrow \psi_{on}$ correspondence with the starting Zolotarev space factor. This is best seen by considering an example of an array of $2N = 20$ elements and $d = 0.5\ \lambda$. The Zolotarev space factor of a 25 dB sidelobe ratio array of this size is shown in Fig. 6.1. (The space factor zeros and element excitations for this Zolotarev array are given in Table 6.1). Superimposed is that of a uniform difference distribution for an array of the same number of elements. Clearly the uniform distribution has only half the number of <u>separate</u> zero locations necessary to be a valid generic space factor.

TABLE 6.1 : Space factor zeros and element excitations for a Zolotarev array of 20 elements and 25 dB sidelobe ratio (d = 0.5 λ). (Extracted from Tables II.29 and II.5).

n	ψ_n
1	0.61603219
2	0.81725124
3	1.09280090
4	1.39318558
5	1.70403091
6	2.02008672
7	2.33899023
8	2.65948818
9	2.98080654

n	a_n
1	0.168346
2	0.485100
3	0.745324
4	0.921637
5	1.000000
6	0.981285
7	0.880081
8	0.721111
9	0.534100
10	0.536199
η_d	0.8883
K_r	0.8551

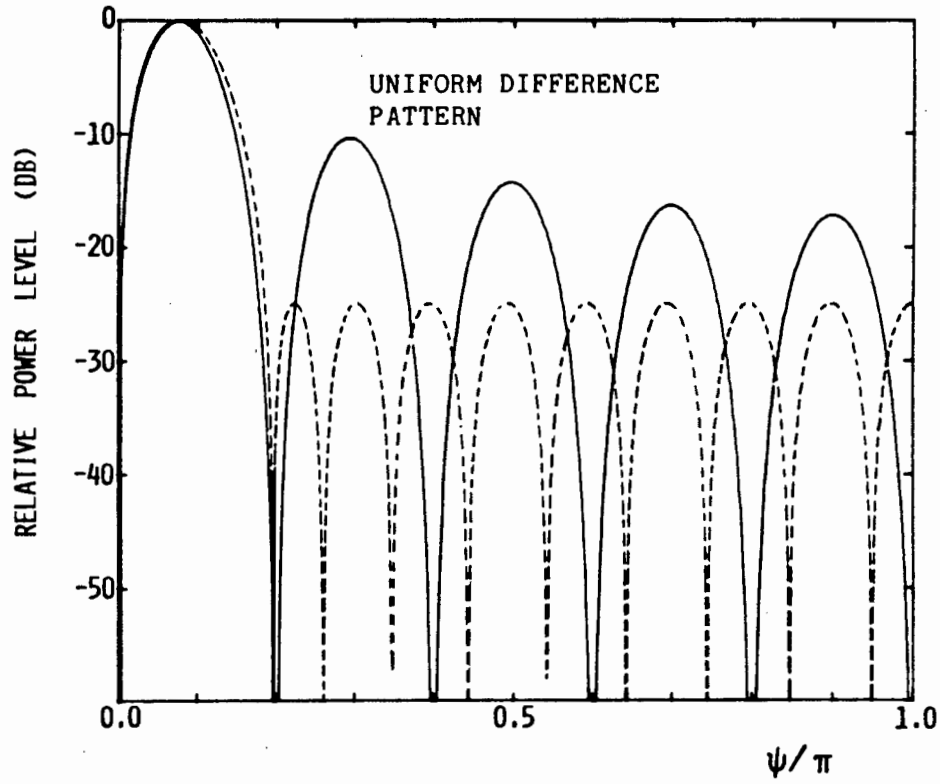

FIGURE 6.1 COMPARISON OF UNIFORM DIFFERENCE, AND ZOLOTAREV POLYNOMIAL, SPACE FACTORS

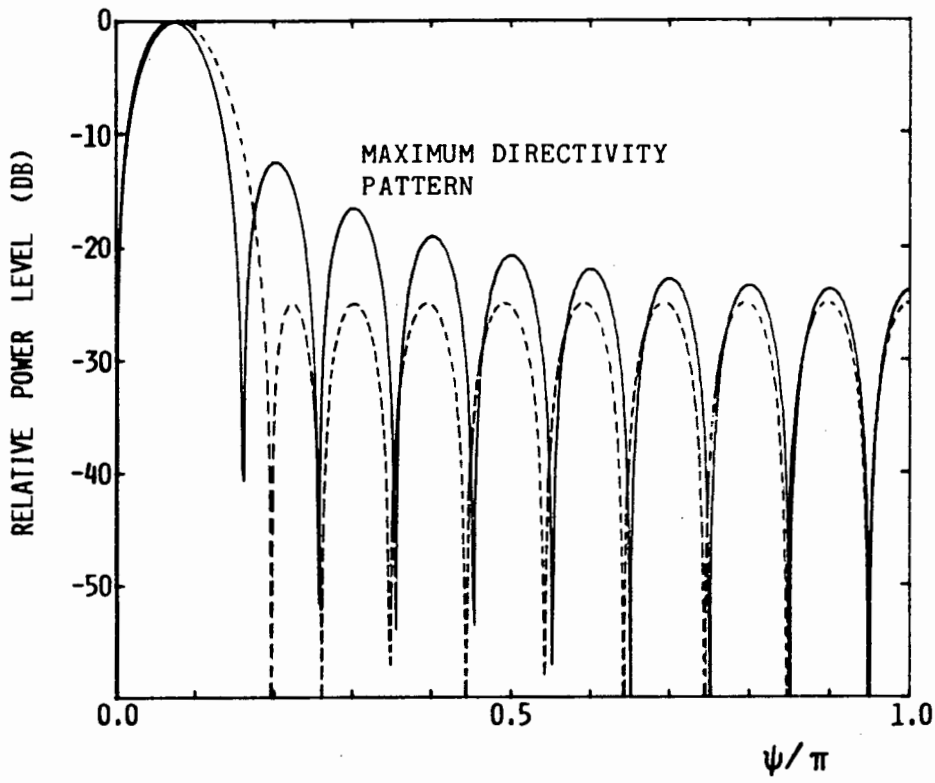

FIGURE 6.2 COMPARISON OF MAXIMUM DIFFERENCE DIRECTIVITY, AND ZOLOTAREV POLYNOMIAL, SPACE FACTORS

There are fortunately two further known difference distributions which have a 1/u sidelobe envelope taper; the unconstrained (sidelobe-wise) maximum difference peak directivity and maximum normalised slope distributions. These have been considered in Sections 4.1.2 and 4.1.3, respectively. Figures 6.2 and 6.3 compare these space factors to that of the 25 dB sidelobe ratio Zolotarev distribution, for a 20 element array. Clearly a one-to-one zero correspondence is possible. Either of the above space factors could therefore be used as the generic ones.

Now the element excitations for maximum normalised slope and maximum difference directivity distributions can be determined using the methods of Section 4.1. Once these excitations are known the zeros of the associated space factors can be found by numerically determining the roots of the expression (10) of Chapter 2.

For convenience a number of cases for $d = 0.5\ \lambda$ are presented in Tables 6.2 and 6.3.

These were found for a given array size 2N by bounding each zero through detection of a function sign change and then applying a combination of the methods of linear interpolation, extrapolation and bisection [4] in each interval to determine the precise zero location.

With this information at hand, the root shifting proposed in Section 6.2 can be examined. For conciseness, the maximum directivity and maximum normalised slope space factors will be referred to as the D_d^{max} and K_o space factors, respectively.

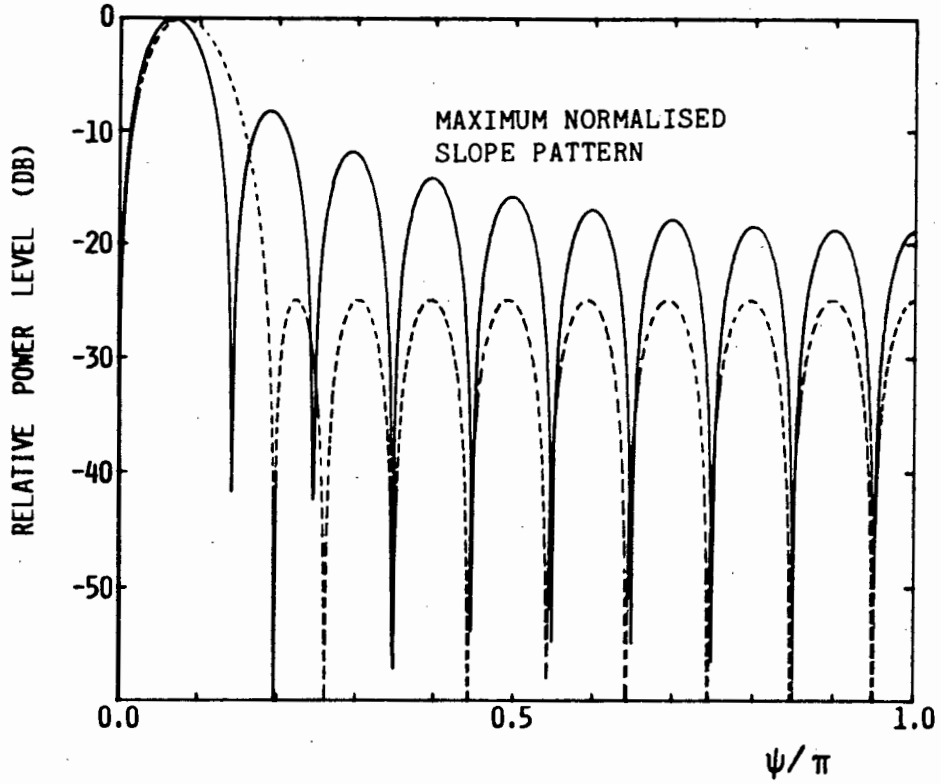

FIGURE 6.3 COMPARISON OF MAXIMUM NORMALISED BORESIGHT SLOPE, AND ZOLOTAREV POLYNOMIAL, SPACE FACTORS

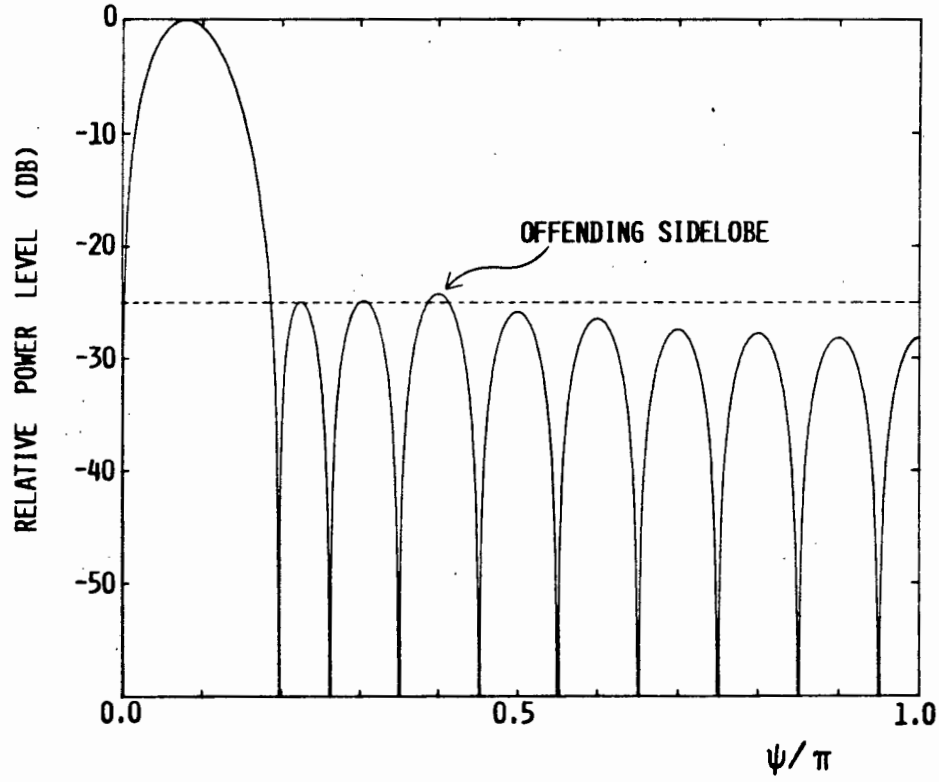

FIGURE 6.4 SPACE FACTOR OF MODIFIED ZOLOTAREV DISTRIBUTION WITH INCORRECT TRANSITION SIDELOBE BEHAVIOUR

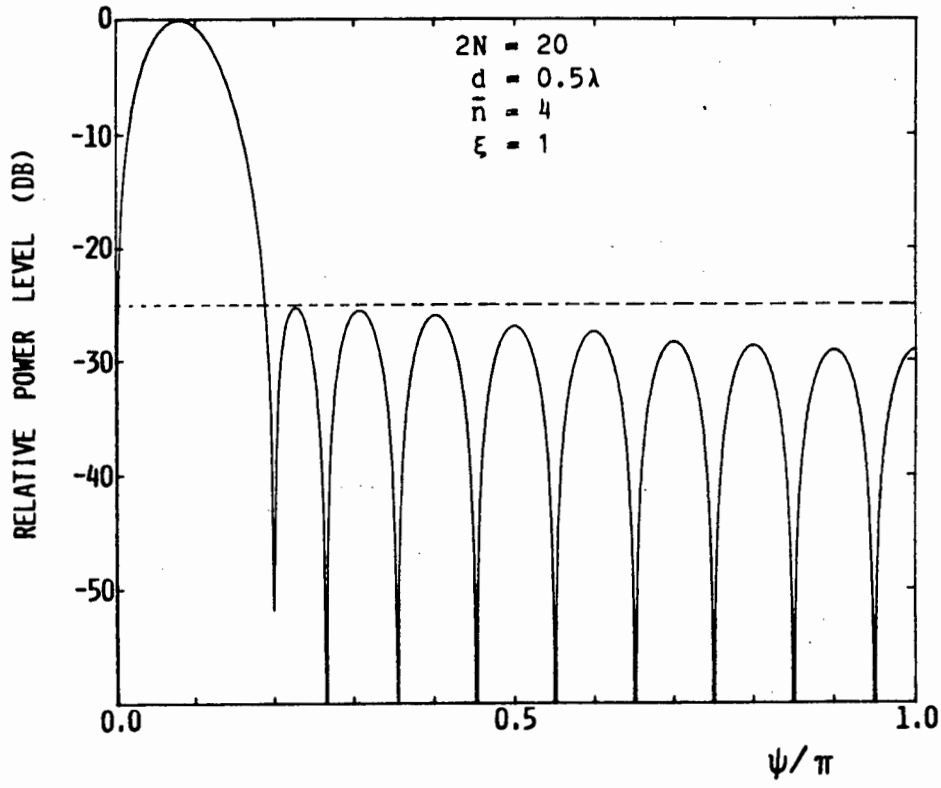

FIGURE 6.5 SPACE FACTOR OF MODIFIED ZOLOTAREV DISTRIBUTION (MAXIMUM DIRECTIVITY GENERIC DISTRIBUTION)

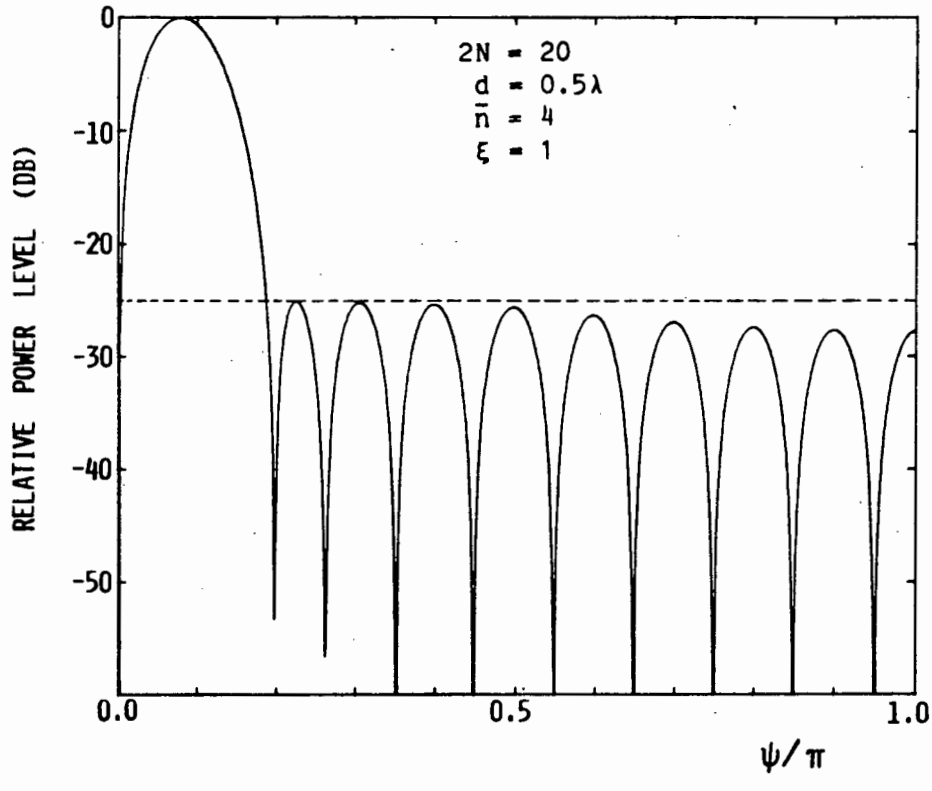

FIGURE 6.6 SPACE FACTOR OF MODIFIED ZOLOTAREV DISTRIBUTION (MAXIMUM NORMALISED SLOPE GENERIC DISTRIBUTION)

TABLE 6.2 : Zeros of maximum normalised boresight slope space factor ($d = 0.5\ \lambda$).

2N	10	20	30	40	50	60
ψ_{01}	0.901739348	0.449717293	0.299671828	0.224717338	0.179760362	0.149794192
ψ_{02}	1.550455743	0.773176549	0.515208527	0.386343298	0.309051352	0.257532269
ψ_{03}	2.188803265	1.091340961	0.727213287	0.545320282	0.436223223	0.363504457
ψ_{04}	2.824233159	1.407834254	0.938099040	0.703457503	0.562723195	0.468916713
ψ_{05}		1.723589616	1.148485530	0.861219480	0.688922814	0.574078630
ψ_{06}		2.038961610	1.358606433	1.018781203	0.814962017	0.679106807
ψ_{07}		2.354117635	1.568569980	1.176223566	0.940905462	0.784055109
ψ_{08}		2.669150237	1.778433438	1.333589203	1.066787201	0.888951898
ψ_{09}		2.984118522	1.988230162	1.490902761	1.192626892	0.993813539
ψ_{010}			2.197981101	1.648179520	1.318436690	1.098650145
ψ_{011}			2.407700294	1.805429483	1.444224524	1.203468304
ψ_{012}			2.617397741	1.962659507	1.569995793	1.308272496
ψ_{013}			2.827081025	2.119874478	1.695754309	1.413065876
ψ_{014}			3.036756307	2.277078004	1.821502847	1.517850733
ψ_{015}				2.434272843	1.947243481	1.622628767
ψ_{016}				2.591461171	2.072977799	1.727401274
ψ_{017}				2.748644772	2.198707046	1.832169257
ψ_{018}				2.905825164	2.324432217	1.936933507
ψ_{019}				3.063003694	2.450154127	2.041694662
ψ_{020}					2.575873456	2.146453238
ψ_{021}					2.701590787	2.251209664
ψ_{022}					2.827306629	2.355964300
ψ_{023}					2.953021442	2.460717454
ψ_{024}					3.078735649	2.565469389
ψ_{025}						2.670220340
ψ_{026}						2.774970515
ψ_{027}						2.879720105
ψ_{028}						2.984469286
ψ_{029}						3.089218224

TABLE 6.3 : Zeros of maximum directivity space factor (d = 0.5 λ).

2N	10	20	30	40	50	60
ψ_{01}	0.881875823	0.440507754	0.293612802	0.220193749	0.176149074	0.146788234
ψ_{02}	1.600041359	0.801466094	0.534491786	0.400916340	0.320750646	0.267300203
ψ_{03}	2.197446750	1.100642132	0.733919123	0.550476914	0.440394918	0.367001736
ψ_{04}	2.835823827	1.420733659	0.947536219	0.710752267	0.568638878	0.473882534
ψ_{05}		1.729354281	1.153288149	0.865055247	0.692075636	0.576743610
ψ_{06}		2.045667797	1.364337645	1.023399961	0.818774170	0.682336325
ψ_{07}		2.356844978	1.571888924	1.179060907	0.943298610	0.786104034
ψ_{08}		2.672099246	1.782141761	1.336799582	1.069510657	0.891290884
ψ_{09}		2.984093633	1.990420096	1.493021298	1.194486520	0.995435507
ψ_{010}			2.200334894	1.650493509	1.320483003	1.100442061
ψ_{011}			2.408954485	1.806994980	1.445686864	1.204777794
ψ_{012}			2.618710708	1.964329101	1.571569598	1.309688684
ψ_{013}			2.827489081	2.120985316	1.696903056	1.414133917
ψ_{014}			3.037179999	2.278241758	1.822719232	1.518988215
ψ_{015}				2.434987267	1.948131990	1.623501481
ψ_{016}				2.592199354	2.073906737	1.728319819
ψ_{017}				2.748994784	2.199370088	1.832877740
ψ_{018}				2.906183766	2.325118271	1.937672118
ψ_{019}				3.063001747	2.450614259	2.042260413
ψ_{020}					2.576345510	2.147038360
ψ_{021}					2.701861884	2.251647706
ψ_{022}					2.827583041	2.356414264
ψ_{023}					2.953110628	2.461038192
ψ_{024}					3.078827058	2.565796950
ψ_{025}						2.670430693
ψ_{026}						2.775184371
ψ_{027}						2.879824184
ψ_{028}						2.984574988
ψ_{029}						3.089217705

6.3.2 Comparison of Modified Zolotarev Space Factors

The problem of finding the set of element excitations resulting from the zero shifting operations indicated in expressions (1) will be dealt with in Section 6.5. Of immediate concern in this section is the behaviour of the space factors which are the outcome of such alterations to the zeros. This is best observed through use of a particular example. Suppose once more that an array of $2N = 20$ elements with a specified maximum sidelobe ratio of 25 dB is desired.

Tables 6.1, 6.2 and 6.3 can be used to obtain the information on the zeros ψ_n and ψ_{on} required for the zero shifting procedure. Since the factor σ must be greater than unity (it is not possible, for the given first sidelobe level, to have a beamwidth narrower than that of the Zolotarev array), any $\bar{n}$ that may be selected must at least satisfy the conditon,

$$\psi_{o\bar{n}} \geq \psi_{\bar{n}} \tag{3}$$

This is equivalent to saying that the Zolotarev zeros may only be shifted outward. Therefore, for the present example, when the D_d^{max} pattern is used as the generic space factor, the smallest $\bar{n}$ that may be selected according to condition (3) is $\bar{n} = 3$. For the K_o pattern as the generic one, the minimum $\bar{n}$ allowed by (3) is $\bar{n} = 4$. Thus, not only is the D_d^{max} space factor analogous to the maximum sum directivity (uniform array) space factor used as the generic pattern by Villeneuve [1] for sum pattern synthesis, but it appears at first sight to offer more flexibility than the K_o pattern. However, this will be seen not to be the case. Fig. 6.4 shows the modified Zolotarev pattern which results after using as the generic space factor zeros those provided by the D_d^{max} distribution, for the case $\bar{n} = 3$. The sidelobes are seen to increase above the design sidelobe level of 25 dB, indicative of incorrect behaviour of the transition zeros. If this same generic distirbution is used with $\bar{n} = 4$, such irregular behaviour does not occur, as illustrated in Fig. 6.5.

Now consider the space factor which results when the K_o distribution is used as the generic one. In this instance, for its lower bound $\bar{n} = 4$, the modified Zolotarev pattern resulting from the zero perturbation procedure defined by (1) is shown in Fig. 6.6. Thus, for its minimum allowable $\bar{n}$, no unwanted sidelobe behaviour is obtruded. Furthermore, the first sidelobe in Fig. 6.6 is closer to the design level than it is in Fig. 6.5. In addition, further computations show that this is so for any given $\bar{n}$, and that utilisation of the K_o rather than D_d^{max} pattern always results in a slightly larger excitation efficiency and normalised slope. This has also been found to be the case for other array sizes and design sidelobe ratios. (For very large $\bar{n}$ values, the modified distributions obtained with either generic space factors are very close to that of the starting Zolotarev distribution. Their performance indices are then not very different). Since the D_d^{max} has therefore nothing extra to offer in its favour, the K_o pattern will be utilised throughout the remainder of this thesis, and will simply be referred to as <u>the</u> generic space factor for difference pattern synthesis.

Observe from the set of excitations shown with Fig. 6.6 that while the starting Zolotarev excitations (obtained from Table 6.1) are just beginning to increase again at the edge element, such is not the case with the new set. Incorporating the sidelobe taper has removed this. The price paid is a beamwidth broadening by a factor $\sigma = 1.01051$ from the starting Zolotarev array, though this is small. The difference between the levels of the first and last sidelobes is only 2.67 dB. For many applications this may not be satisfactory. If it is not possible to increase the number of array elements, the only alternative is the incorporate into the distribution a factor which allows control over the sidelobe envelope taper rate. This is done in the next section.

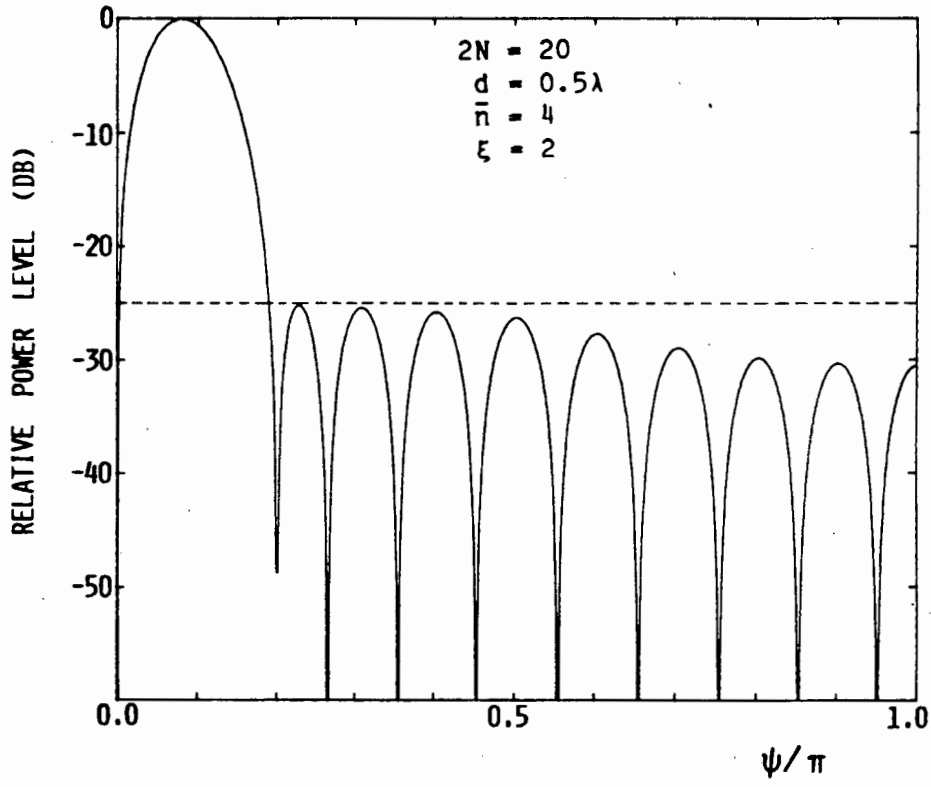

FIGURE 6.7 PATTERN OF MODIFIED ZOLOTAREV ARRAY

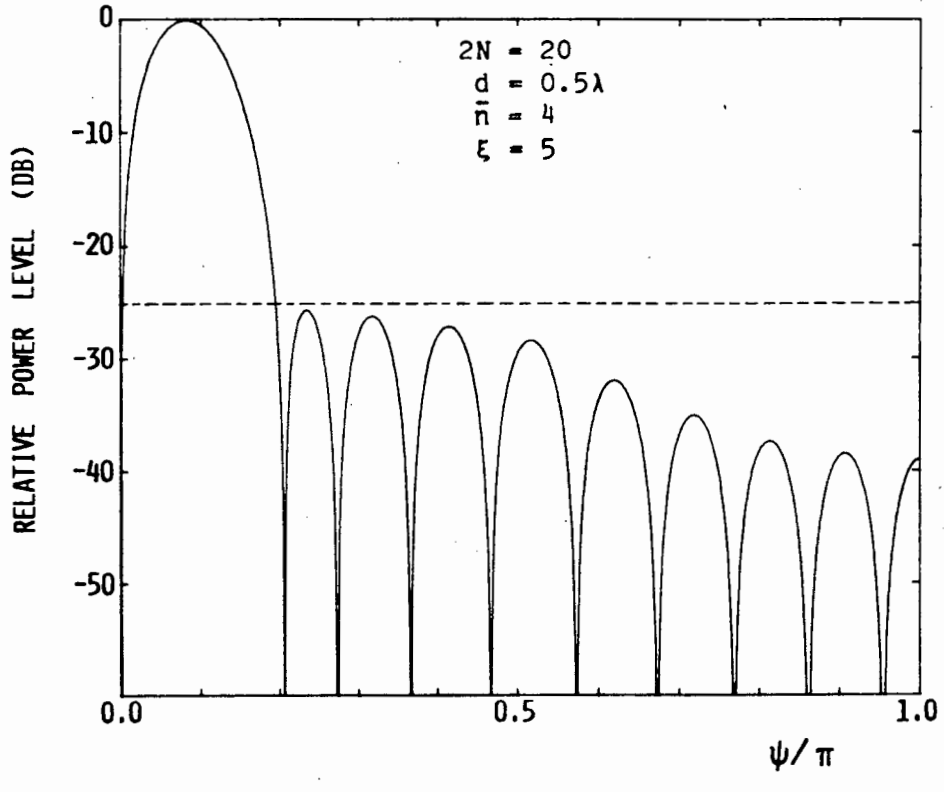

FIGURE 6.8 PATTERN OF MODIFIED ZOLOTAREV ARRAY

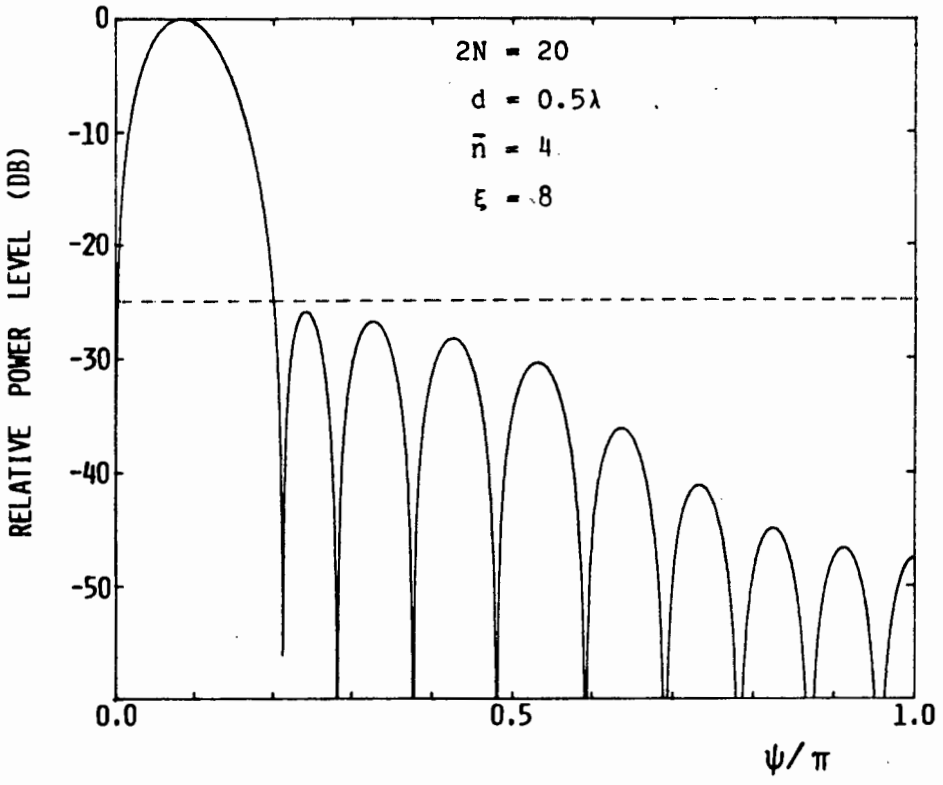

FIGURE 6.9 PATTERN OF MODIFIED ZOLOTAREV ARRAY

6.4 GENERALISATION TO ARBITRARY SIDELOBE ENVELOPE TAPERS

Determination of the best pattern for a given application requires careful consideration of the relative importance of the peak sidelobe specification and the level of the more remote sidelobes. For this, and some additional reasons mentioned in Section 6.1, a distribution which allows some control over the sidelobe envelope taper rate and not just the point at which taper begins, is highly desirable. In order to effect such a distribution which applies directly to discrete arrays, the zero shifting procedure defined by equation (1) must be modified. This will be done in such a way that (1) is a special case. The general zero shifting procedure is given here in complete form, even at the risk of repetition of part of Section 6.2. Once again, symmetry permits only one half of the zeros to be considered.

For an array of 2N elements and a given sidelobe ratio specification there will be associated an optimum Zolotarev distribution (which will be referred to as the starting distribution) with space factor zeros $\{\psi_n\}$, n = 1,2, $\cdots$ (N-1), with the additional mandatory zero at $\psi = 0$. Similarly, the generic space factor will have a set of zeros $\{\psi_{on}\}$ for the same range of n, and the zero at $\psi = 0$. The altered set of space factor zeros $\{\psi_n'\}$ is now given by,

$$\psi_n' = \begin{cases} \sigma\,\psi_n & n \leq \bar{n} \\ \psi_n + \xi(\psi_{on} - \psi_n) & n \geq \bar{n} \end{cases} \tag{4}$$

with the dilation factor σ given by,

$$\sigma = [\psi_{\bar{n}} + \xi(\psi_{o\bar{n}} - \psi_{\bar{n}})]/\psi_{\bar{n}} \tag{5}$$

When $\xi = 0$, the zero shifting operation is nullified and the starting Zolotarev zeros (and associated distribution) are unchanged, giving a space factor which has uniform sidelobes (zero taper).

A value of $\xi = 1$ reduces the zero shifting algorithm of (4) to that of (1), which gives a 1/u sidelobe envelope taper.

A value of $\xi > 1$ gives a more rapid sidelobe envelope taper. There is with increasing ξ an increase in the dilation factor σ and hence in the amount of beam broadening.

Since it is not possible, for a given maximum sidelobe level, to obtain a difference lobe beamwidth less than that of the appropriate Zolotarev array it is necessary that $\sigma \geq 1$. From equation (5) this implies that,

$$\psi_{o\bar{n}} \geq \psi_{\bar{n}} \tag{6}$$

is a requirement, and any $\bar{n}$ selected in a specific situation is only valid if (6) is satisfied. There will in all cases be a minimum allowable value for $\bar{n}$ for a given number of array elements 2N and prescribed sidelobe ratio SLR. With the chosen generic space factor (i.e. the K_o space factor), condition (6) has been found in all cases considered to be a sufficient condition for determining this minimum $\bar{n}$, and ensures that an increase in the transition sidelobes above the design sidelobe level will not occur.

The use of the general procedure just described is illustrated in Figs. 6.7, 6.8 and 6.9 for the same array and specifications of Fig. 6.6, but for increasing value of the taper parameter. Its effect is clear. While $\bar{n}$ determines the point of onset of the taper proper, the ξfactor controls its rapidity. The pattern of Fig. 6.6 is of course just that for which $\xi = 1$, and has a first sidelobe at precisely the same level as that of the starting Zolotarev distribution, then three sidelobes of the kind conventionally referred to as the "almost equal level sidelobes", and thereafter a sidelobe envelope with a 1/u taper. For the larger ξ values in Figs. 6.7 to 6.9 the first sidelobe has decreased from that of the starting distribution, but the essential pattern structure is the same, except for the increased outer sidelobe taper rates.

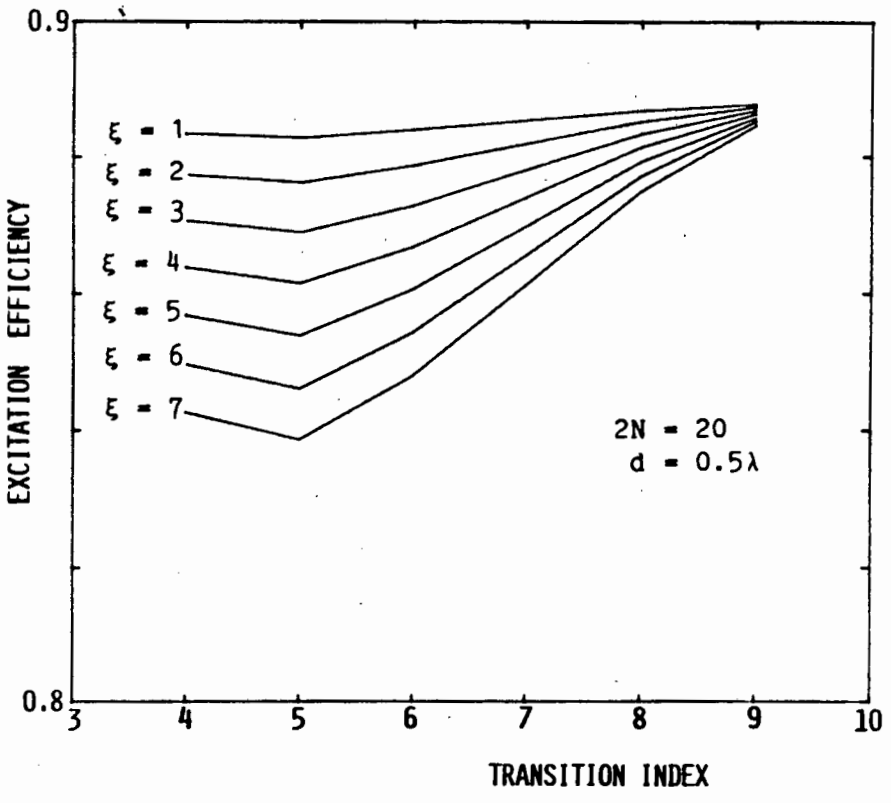

FIGURE 6.10 EXCITATION EFFICIENCY AS A FUNCTION OF THE TRANSITION INDEX (2N = 20, SLR = 25 dB)

The number of elements 2N in a monopulse array will in most cases be determined by the sum directivity (D_s^m) requirements. This quantity is the determining factor as regards the range capability of a tracking radar. It is reasonable therefore to discuss the behaviour of the present modified Zolotarev distributions for given fixed element numbers.

A comprehensive discussion of the results of a parametric study of the influence of $\bar{n}$ and ξ on the array performance is given in Section 6.6.

In order to have a complete synthesis procedure, a method is required for obtaining the element excitations once the altered zero locations $\{\psi_n'\}$ are known. This is dealt with in the next section.

6.5 DETERMINATION OF MODIFIED ZOLOTAREV DISTRIBUTION EXCITATIONS

Consider again the expression for the space factor of the anti-symmetrically excited (difference) array of 2N elements, given by equation (10) of Chapter 2 as (ignoring the constant factor 2j),

$$- \quad E_d(\psi) = \sum_{n=1}^{N} a_n \sin[(2n-1)\psi/2] \tag{7}$$

The methods of the previous section provide the set of zeros $\{\psi_i'\}$, $i = 1,2, \cdots (N-1)$, of the desired space factor. An additional zero occurs on boresight at $\psi = 0$. For reasons of symmetry, only one half of the excitations and zeros need be considered. While there are (N-1) zeros ψ_i', there are N unknown excitations. However, it is the relative excitations that are significant. One of the excitations can be assumed equal to unity and all the others found relative to it. This is valid even if complex excitations are being considered. Let $a_N = 1$ in this case, so that (7) becomes,

$$E_d(\psi) = \sin[(2N-1)\psi/2] + \sum_{n=1}^{N-1} a_n \sin[(2n-1)\psi/2] \tag{8}$$

If equation (9) is enforced at the (N-1) zeros, a set of (N-1) linear simultaneous equations, in the (N-1) unknowns $a_1, a_2, \cdots a_{N-1}$ is obtained, with $E_d(\psi_i') = 0$ for each i.

The full set of equations is of the form,

$$\sum_{n=1}^{N-1} a_n \sin[(2n-1)\psi_1'/2] + \sin[(2N-1)\psi_1'/2] = 0$$

$$\sum_{n=1}^{N-1} a_n \sin[(2n-1)\psi_2'/2] + \sin[(2N-1)\psi_2'/2] = 0$$

$$\vdots$$

$$\sum_{n=1}^{N-1} a_n \sin[(2n-1)\psi_{N-1}'/2] + \sin[(2N-1)\psi_{N-1}'/2] = 0$$

The process can be represented in matrix notation as,

$$\begin{bmatrix} S_{11} & S_{12} & \cdots\cdots & S_{1,N-1} \\ S_{21} & S_{22} & \cdots\cdots & S_{2,N-1} \\ \vdots & & & \\ S_{N-1,1} & S_{N-1,2} & \cdots\cdots & S_{N-1,N-1} \end{bmatrix} \begin{bmatrix} a_1 \\ a_2 \\ \vdots \\ a_{N-1} \end{bmatrix} = \begin{bmatrix} b_1 \\ b_2 \\ \vdots \\ b_{N-1} \end{bmatrix} \qquad (9)$$

where

$$S_{ni} = \sin[(2n-1)\psi_i'/2] \quad \text{and} \quad b_i = -\sin[(2N-1)\psi_i'/2].$$

Once the (N-1) unknowns have been found, the complete set of excitations $a_1, a_2, \cdots a_N$ can be renormalised to the excitation of largest magnitude of the set.

The reason for selecting the above appraoch is the fact that there exist very efficient routines for linear simultaneous equation solution. This allows rapid and accurate determination of array excitations.

6.6 THE PERFORMANCE OF MODIFIED ZOLOTAREV POLYNOMIAL DISTRIBUTIONS

For discrete arrays, results are not as easily presented in the general form possible with continuous line-sources. Instead the results of the parametric study of the performance of modified Zolotarev polynomial distributions will be illustrated by two examples (both with $d = 0.5\ \lambda$) which exhibit all the principal characteristics of the distribution.

The first is that which has been considered earlier in this chapter ($2N = 20$, SLR = 25 dB), and the second a 30 element, 15 dB sidelobe ratio array. The former case has a starting Zolotarev distribution (see Table 6.1) which is not peaked at the edge. The latter example can be seen from Table II.3 to have a starting distribution with maximum excitation at the edge. This array suffers from the "directivity compression" problem discussed in Section 5.5, while the first array does not. Shown in Fig. 6.10 is a plot of the excitation efficiency of the 20 element array as a function of $\bar{\bar{n}}$, with ξ as a parameter. For a fixed $\bar{n}$, increasing ξ causes a decrease in η_d, as expected, since the distribution of excitations is becoming increasingly tapered at the edges of the array. The vertical scale in Fig. 6.10 is much expanded and the change in directivity is really very small in spite of the fact that an increased sidelobe taper is obtained. As $\bar{n}$ gets larger, the excitation efficiency becomes less dependent on the parameter ξ, since the modified distributions are tending to the starting Zolotarev distribution. The excitation efficiencies of the modified distributions are all seen to be lower than that of the starting distribution. This is only true because of the fact that the starting Zolotarev distribution does not suffer from "diretivity compression", and will not be so for the second example. The behaviour of K_r and beamwidth broadening above for the 20 element array parallels that of the excitation efficiency. Recalling that σ gives directly the amount of first null broadening above that of the starting pattern, it is noted that over the range $4 \leq \bar{n} \leq 9$ and $0 \leq \xi \leq 8$, the variation in σ for this example is $1 \leq \sigma \leq 1.09182$.

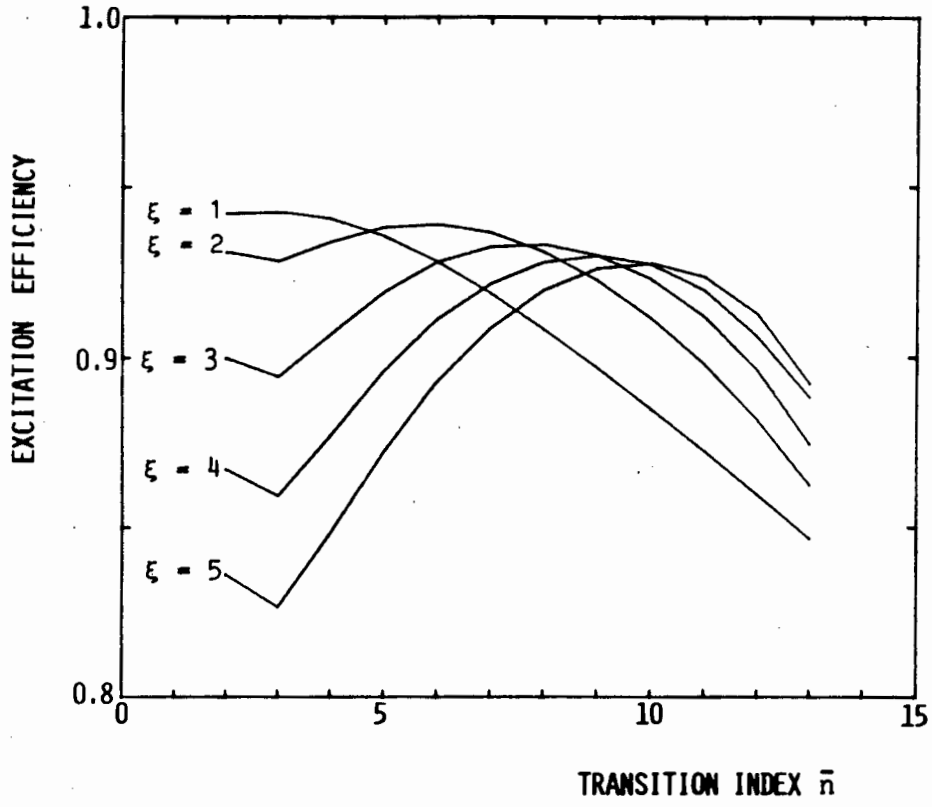

FIGURE 6.11 EXCITATION EFFICIENCY AS A FUNCTION OF THE TRANSITION INDEX (2N = 30, SLR = 15 dB)

The largest value occurs for the somewhat extreme case of $\bar{n} = 4$, $\xi = 8$, which has a pattern which falls very rapidly below the -60 dB point after only the first few sidelobes. Even then the beamwidth broadening of 8.4% is relatively small considering the greatly increased sidelobe taper obtained.

Now consider the 30 element array with a sidelobe ratio of 15 dB. A plot of its excitation efficiency as a function of $\bar{n}$ is given in Fig. 6.11. For a given ξ there is a particular $\bar{n}$ which gives maximum directivity. Smaller and larger values than this result in lower directivities. Such behaviour is a characteristic of distributions whose starting Zolotarev distributions have "directivity compression". Incorporating a sidelobe taper can be used to improve the directivity above that of the starting distribution. The relative difference slope (K_r) of this array is seen from Fig. 6.12 to show a similar behaviour, but the maxima occur for different $\bar{n}$ values.

Examination of the excitation sets also reveals that for each ξ, there is a value of $\bar{n}$ greater than which there is "edge brightening". For the 30 element array, the distributions of element excitations are presented in Fig. 6.13, for $\xi = 0$, 1, 2 and 3, for the case of $\bar{n}$ equal to its minimum allowable value of 2. With $\xi = 1$, the distribution has a maximum at the edge. Increasing $\bar{n}$ will only serve to make the distribution more like that of the starting Zolotarev case ($\xi = 0$). The only way to remove this "edge brightening" for the given number of elements and design sidelobe ratio is by increasing the parameter ξ. This confirms both the necessity and utility of introducing the additional parameter ξ in the zero alteration procedure of expression (4).

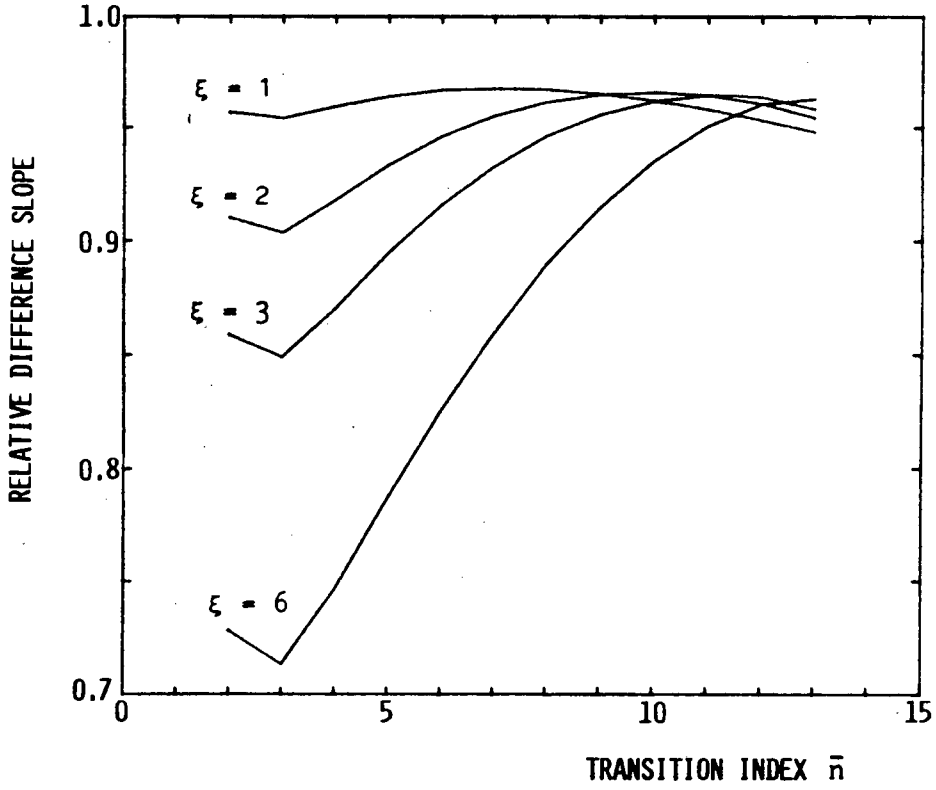

FIGURE 6.12 RELATIVE DIFFERENCE SLOPE AS A FUNCTION OF THE TRANSITION INDEX (2N = 30, SLR = 15 dB)

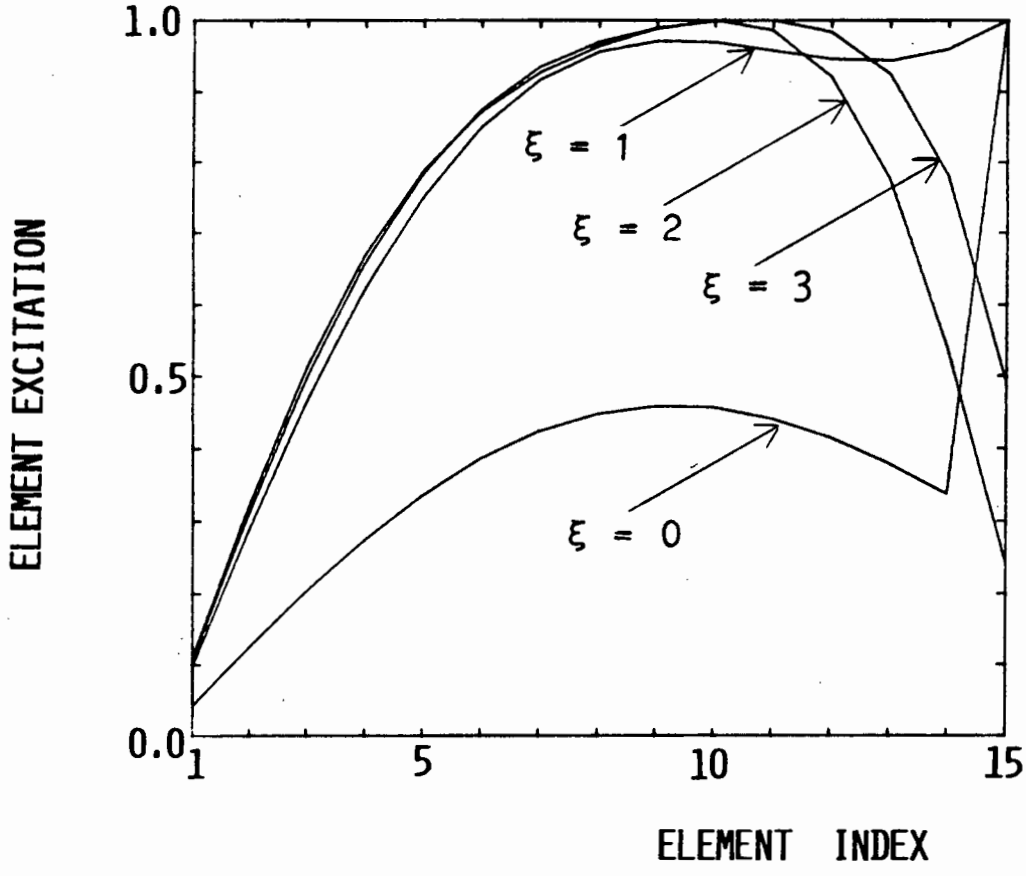

FIGURE 6.13 MODIFIED ZOLOTAREV ARRAY APERTURE DISTRIBUTIONS

6.7 ARRAYS WITH SPACINGS OTHER THAN HALF A WAVELENGTH

The examples discussed in this chapter have all assumed $d = 0.5\ \lambda$. This has simply been for convenience, however, and is not a necessity. For general spacings the zeros ψ_n of the starting Zolotarev space factor are simply determined from the synthesis procedures of Chapter 4, as is done for $d = 0.5\ \lambda$. When $d > 0.5\ \lambda$, only the unique (non-repeating) zeros are used, and these are the same as those for $d = 0.5\ \lambda$. Similarly, the zeros ψ_{on} of the generic space factor (K_o distribution) are found by using the method of Section 4.1.3 to determine the required excitations for the given spacing, and then finding the space factor zeros numerically, as indicated in Section 6.3.

6.8 CONCLUSIONS

Chapter 4 added to the theory of antenna arrays by developing, for the synthesis of discrete difference distributions, the analogue of the fundamental Dolph-Chebyshev synthesis of sum patterns through use of the Zolotarev polynomials. In the present chapter a tapered sidelobe difference pattern synthesis method has been outlined, which technique parallels the Villeneuve $\bar{n}$ distribution approach of sum patterns. Just as the Villeneuve procedure provides the array excitations for a discrete "Taylor-like" distribution directly, so does the present one allow direct synthesis of high performance discrete "Bayliss-like" distributions. In addition the approach has been extended to incorporate a parameter which controls the sidelobe envelope taper rate. As such this chapter completes a further aspect of array antenna theory.

The synthesis procedure begins with the set of zeros of the Zolotarev space factor associated with the given problem. These are then altered according to a well-defined procedure given by expression (4), making use also of the known zero locations of the maximum normalised slope space factor for an array of the same number of elements. The altered set of zeros is then used in (9) to obtain the required set of excitations.

Use of this method alleviates the need to sample the continuous Bayliss line-source distribution (which itself is determined by a numerical search procedure) and then iteratively adjust the excitations to obtain the final desired pattern. Direct synthesis methods for discrete arrays are particularly useful when the number of array elements is too small for sampling of continuous distributions to be satisfactory. Preliminary work on the topic of this chapter has been published by the author [5,6].

6.9 REFERENCES

[1] A.T. Villeneuve, "Taylor patterns for discrete arrays", IEEE Trans. Antennas Prop., Vol. AP-32, No. 10, pp. 1089-1093, Oct. 1984.

[2] R.S. Elliott, Antenna Theory and Design, (Prentice-Hall Inc., 1981).

[3] I.S. Gradshteyn and I.M. Ryzhik, Table of Integrals, Series and Products, (Academic Press, 1980).

[4] Numerical Algorithms Group (NAG), Mathematical Software Library, (FORTRAN routine C05ADF),Oxfordshire, England.

[5] D.A. McNamara, "Discrete $\bar{n}$ distribution for difference patterns", Electronics Letters, Vol. 22, No. 6, pp.303-304, 13th March, 1986.

[6] D.A. McNamara, "The exact synthesis of optimum difference patterns for discrete arrays", IEEE Intl. Antennas and Prop. Symp. Digest, pp.391-394, Philadelphia, USA, June 1986.

CHAPTER 7

GENERALISED VILLENEUVE DISTRIBUTIONS FOR SUM SYNTHESIS

7.1 INTRODUCTION

The synthesis of sum patterns was reviewed in Section 3.2. To design high-performance low-sidelobe space factors the emphasis is on the pattern zeros. The optimum constant sidelobe ratio Dolph-Chebyshev distribution [1] provides the crucial initial space factor zero locations. With this as basis, and the appropriate controlled zero shifting, the tapered sidelobe Villeneuve distributions [2] are derived. The close-in zeros are correctly placed from a knowledge of the Dolph-Chebyshev zeros to obtain a few nearly equal sidelobes at the design level, while the farther-out zeros are made to match those of the uniformly excited array in order to give a 1/u sidelobe envelope.

Also reviewed were the corresponding continuous line-source distributions - the constant sidelobe level "ideal" Taylor distribution and the Taylor $\bar{\bar{n}}$ distribution, respectively. In addition, sidelobe envelope taper as well as close-in sidelobe levels can be controlled in the family of distributions known as the generalised Taylor distributions [3]. Taylor's $\bar{n}$ distribution is a special case of these.

In the present chapter the work of Villeneuve [2] is generalised to a class of distributions, directly applicable to discrete arrays, which allows the sidelobe envelope taper to be controlled. The arguments are similar to those of Section 6.4 and the motivation given there is applicable here as well.

7.2 DETAILED FORMULATION

7.2.1 Array With An Even Number of Elements

The case of an array of an even number of elements is considered first.

Consider an array of 2N elements with uniform spacing d. For a design sidelobe ratio SLR, the 2N-1 unique space factor zeros of the Dolph-Chebyshev distribution are given for $d \geq 0.5\ \lambda$ by [2],

$$\psi_n = \pm 2 \cos^{-1}\left\{ \frac{1}{u_o} \cos\left[\frac{(2n-1)\pi}{2(2N-1)} \right] \right\} \qquad (1)$$

$$n = 1,2, \cdots N$$

where $$u_o = \cosh\left\{ \frac{1}{2N-1} \ln\left[SLR + \sqrt{SLR^2 - 1}\ \right] \right\} \qquad (2)$$

These are the zeros of the starting space factor.

The generic space factor is that of a uniform array of 2N elements, with its 2N-1 zeros at,

$$\psi_{on} = \pm n\pi/N \qquad n = 1,2, \cdots N \qquad (3)$$

Let the space factor zeros now be altered to the set ψ_n', with

$$\psi_n' = \begin{cases} \sigma\ \psi_n & n \leq \bar{\bar{n}} \\ \psi_n + (\nu + 1)(\psi_{on} - \psi_n) & n \geq \bar{n} \end{cases} \qquad (4)$$

with the dilation factor given by,

$$\sigma = [\psi_{\bar{n}} + (\nu + 1)(\psi_{o\bar{n}} - \psi_{\bar{n}})] / \psi_{\bar{n}} \qquad (5)$$

In other words, the new set of space factor zeros is obtained by shifting outward the outer zeros to new positions dependent on those of the generic space factor in order that the desired remote sidelobe behaviour be obtained. At the same time the central zeros are dilated to obtain nearly equal sidelobes in the central region of the pattern.

As before, the quantity $\bar{n}$ is a design parameter. Here the ν is the additional parameter to be selected. If $\nu = -1$, then $\sigma = 1$, and the space factor zeros ψ'_n are just the Dolph-Chebyshev zeros ψ_n.

On the other hand, a value $\nu = 0$ gives,

$$\sigma = \psi_{o\bar{n}} / \psi_{\bar{n}}$$

$$= \frac{\bar{n}\,\pi}{N\,\psi_{\bar{n}}}$$

and the altered space factor zeros ψ'_n are identical to those of the Villeneuve distribution [2], with the 1/u sidelobe envelope taper.

If $\nu > 0$ the sidelobe envelope tapers are more rapid than 1/u, but the physics of the array problem then demands a decrease in the excitation efficiency. A $\nu < 0$ gives envelope tapers more shallow than 1/u. The parameter ν has been used in its present form so that it parallels the effect of the taper parameter in earlier work on continuous line-source distributions by Rhodes [3,4], on the generalised Taylor $\bar{n}$ distributions.

7.2.2 Array With An Odd Number of Elements

Although odd numbers of elements are seldom used with monopulse arrays, a brief note on the generalised Villeneuve distribution as applied to an array of 2N+1 elements is in order. The synthesis procedure is almost identical to that for the even array case except that the generic space factor is now that of a uniform sum array of 2N+1 elements with space factor zeros,

$$\psi_{on} = \pm \frac{2\pi\, n}{2N+1} \tag{6}$$

$$n = 1,2,3, \cdots N.$$

For the case of an odd number of elements, if spacings $d < 0.5\ \lambda$ are required, the Dolph-Chebyshev zeros can be obtained from references given in Section 3.2.2.

7.2.3 Computation of the Element Excitations

For the generalised case just developed, finite product expressions for the excitations similar to those given by Villeneuve [2] do not appear to be possible. Instead a matrix method is used for reasons similar to that given in Section 6.5. The space factor for a symmetrical sum pattern of 2N elements is, according to equation (9) of Chapter 2,

$$E_s(\psi) = \sum_{n=1}^{N} a_n \cos\left[(2n-1)\psi/2\right] \tag{7}$$

where the multiplicative constant factor of 2 has been ignored.

Array symmetry permits consideration of only one half of the space factor zeros in finding the excitation set $\{a_n\}$, n = 1,2, ••• N. The zero perturbation procedure of Section 7.2.1 provides a set of desired space factor zeros $\{\psi_i'\}$, i = 1,2, •• N. Using the same arguments as in Section 6.5, if (7) is enforced at the first N-1 space factor zeros, a set of N-1 linear simultaneous equations in the first N-1 excitations a_1, a_2, ••• a_{N-1} results, as in equation (10) of Chapter 6. For the present case the matrix elements are,

$$S_{ni} = \cos[(2n-1)\psi_i'/2] \tag{8}$$

and the right hand side vector elements

$$b_i = -\cos[(2N-1)\psi_i'/2] \tag{9}$$

Once the $\{a_n\}$ for n = 1,2, ••• N-1 have been found, with $a_N = 1$ as assumed without loss of generality, the complete set of N excitations can be normalised to the maximum value of the set, and the distribution is determined.

7.3 GENERAL OBSERVATIONS

For given maximum sidelobe level and number of elements, it is known that it is not possible to obtain a first null beamwidth less than that of the Dolph-Chebyshev distribution. Therefore, if the sidelobe constraints are not to be violated, it is required that,

$$\psi_1' \geq \psi_1 \tag{10}$$

and it therefore follows from (4) that the dilation factor σ must be greater than or equal to unity. Equation (5) can then be invoked to obtain the condition,

$$\psi_{o\bar{n}} \geq \psi_{\bar{n}} \tag{11}$$

But since the generic zeros are given by,

$$\psi_{on} = \frac{n\pi}{N} \tag{12}$$

it follows that condition (11) reduces to,

$$\bar{n} \geq \left(\frac{N}{\pi}\right) \psi_{\bar{n}} \tag{13}$$

There is consequently a minimum allowable $\bar{n}$ for each array size/sidelobe ratio combination. The condition (13) is a necessary but not a sufficient condition, however. This can be shown by example. Consider an array of 20 elements and $d = 0.5\ \lambda$ with a sum sidelobe ratio of 25 dB. Application of condition (13) reveals that $\bar{n} \geq 2$. Fig. 7.1 depicts the resulting space factor for the case $\nu = 0$ (Villeneuve distribution), and exhibits the "incorrect" sidelobe behaviour obtained, with the second sidelobe rising above the prescribed design level. While the particular case illustrated is for

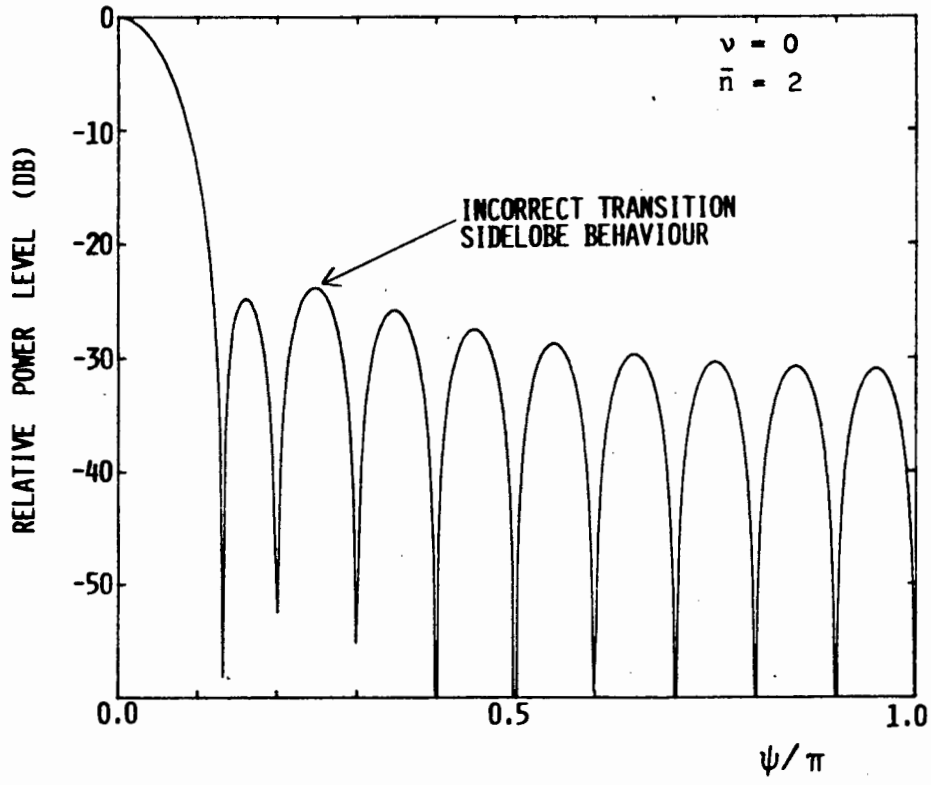

FIGURE 7.1 ARRAY FACTOR ILLUSTRATING INCORRECT TRANSITION SIDELOBE BEHAVIOUR

$\nu = 0$, examination of the pattern for $\nu > 0$ shows that the irregular transition sidelobe increases in height with increasing ν. Similar observations to the above can be made for other array sizes and sidelobe ratios. Thus, besides checking the condition (13), it is necessary also to check the resulting array factor itself in order to be certain that the $\bar{n}$ used is large enough to allow the transition zeros to behave correctly. It has been found for all the cases considered that an $\bar{n}$ equal to the next integer higher than that obtained from (13) will always ensure this.

The effect of changing the parameter ν can best be seen by keeping $\bar{n}$ fixed for a specific array size and sidelobe ratio specification, and plotting the array space factor as ν is varied. This is done in Figs. 7.2(a) to (d) for the 20 element array with a 25 dB sidelobe ratio specification. Clearly, for fixed $\bar{n}$, the effect of increasing ν is to increase the sidelobe envelope taper rate, as expected. The level of the first sidelobe changes little for the range of ν considered, and is thus virtually independent of ν. For a given $\bar{n}$, as the envelope taper rate is increased so does σ, and as a result the first null beamwidth as well. Also indicated in the above figures is the excitation efficiency η_s for each case. As expected, an increasing ν is associated with a decreasing η_s. This is still more clearly illustrated in Fig. 7.3, where η_s is plotted versus ν, with $\bar{n}$ as a parameter. The amount of beamwidth broadening (measured relative to a uniform array of 20 elements) is shown in Fig. 7.4. That the curve for $\bar{n} = 2$ is "out of place" is indicative of the fact that this is too small a value. Besides this, the form of the curve is predictable. So too is the curve shown in Fig. 7.5. Except for those points associated with $\bar{n} = 2$, there is for fixed ν a steady increase in excitation efficiency as $\bar{n}$ gets larger. The reason is that as $\bar{n}$ increases, the distribution approaches that of the starting Dolph-Chebyshev distribution. Irrespective of the values of the parameters $\bar{n}$ and ν, the generalised Villeneuve distribution has, for this specific example, a lower directivity than its parent Dolph-Chebyshev distributions, albeit with taper sidelobes. But this is not always the case. As with the modified-Zolotarev distributions discussed in the previous chapter, if the parent distribution

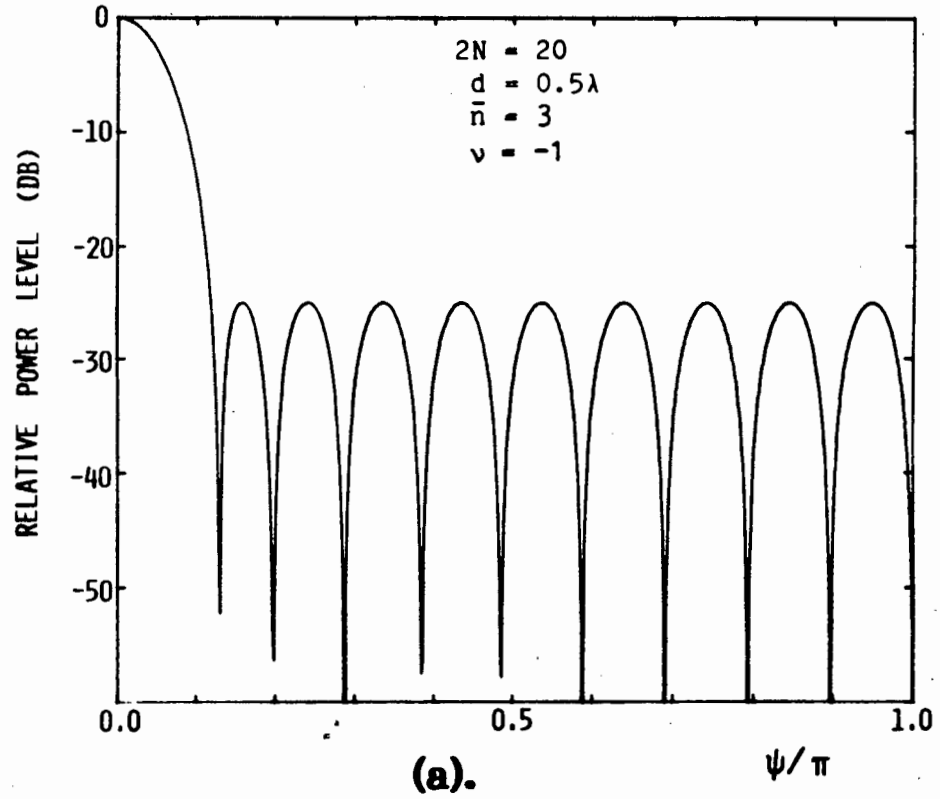

(a).

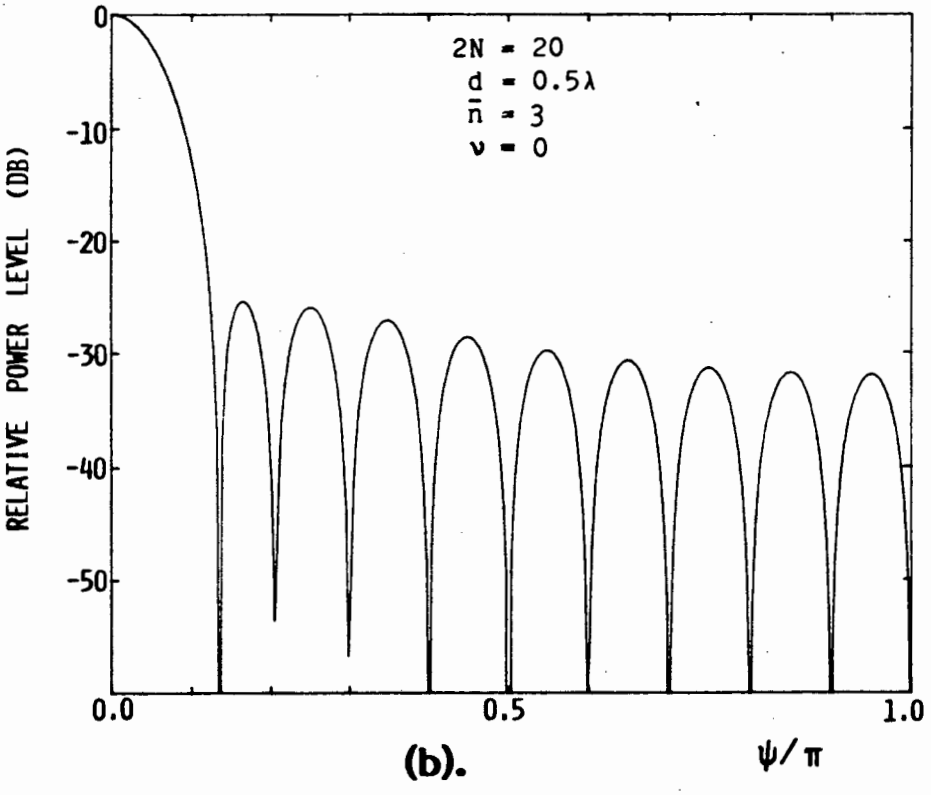

(b).

FIGURE 7.2 GENERALISED VILLENEUVE ARRAY FACTOR (2N = 20, SLR = 25 dB)

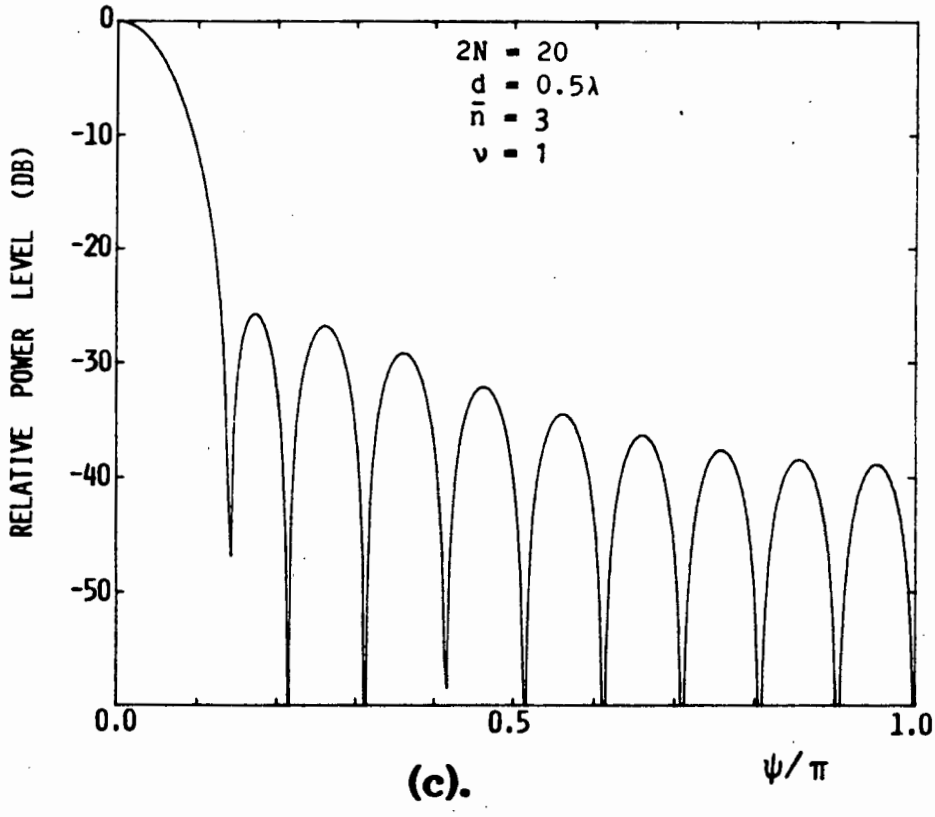

(c).

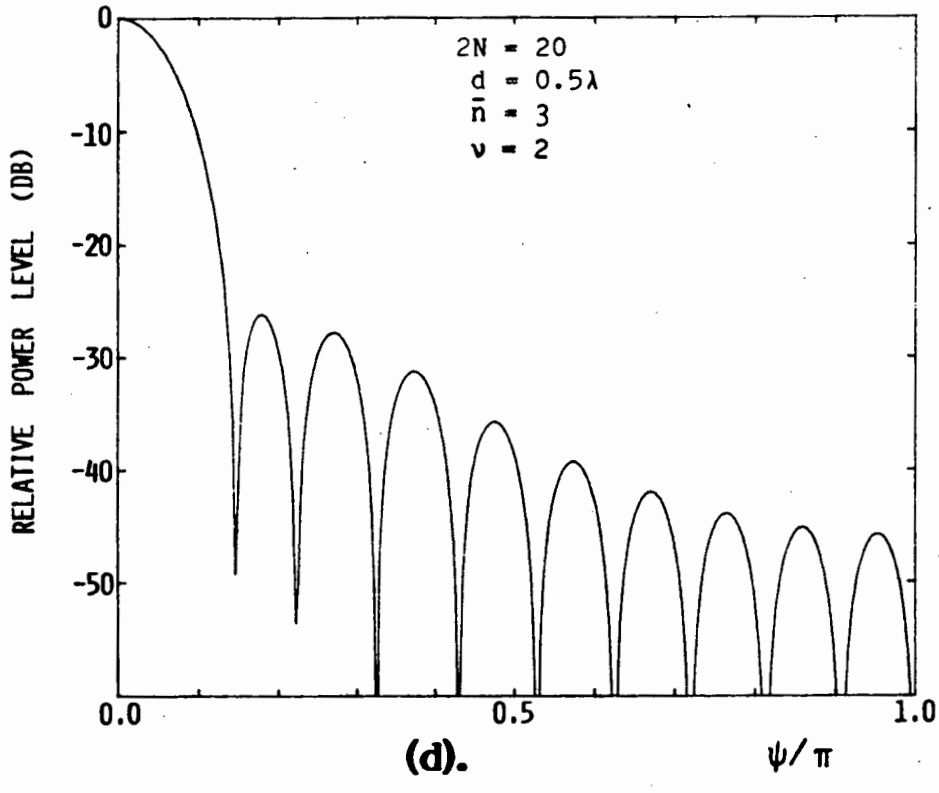

(d).

FIGURE 7.2 GENERALISED VILLENEUVE ARRAY FACTOR (2N = 20, SLR = 25 dB)

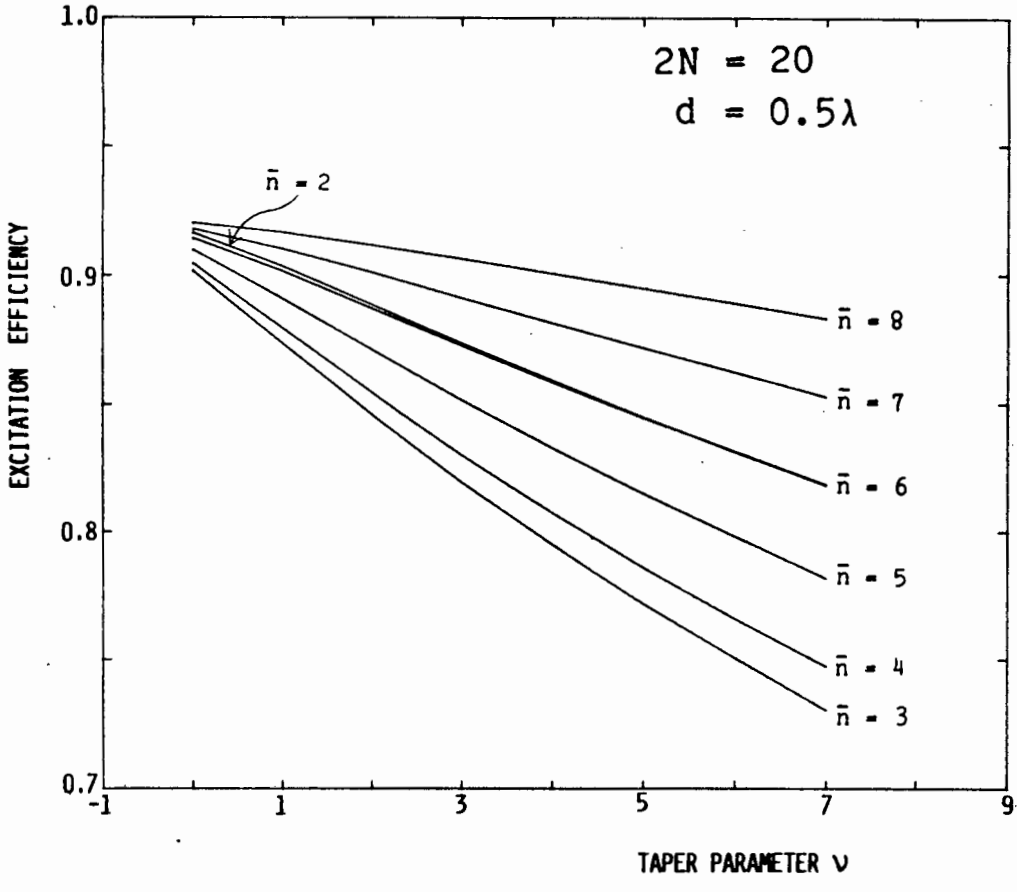

FIGURE 7.3 EXCITATION EFFICIENCY AS A FUNCTION OF THE TAPER PARAMETER

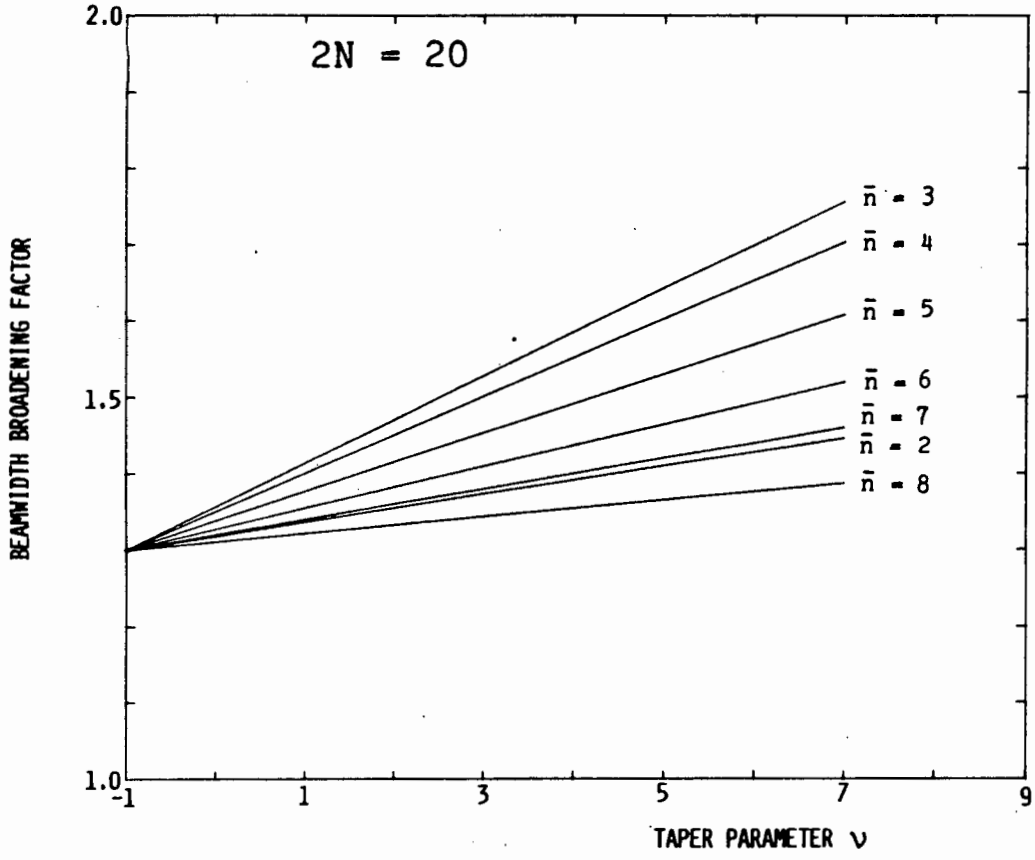

FIGURE 7.4 BEAM BROADENING FACTOR AS A FUNCTION OF THE TAPER PARAMETER

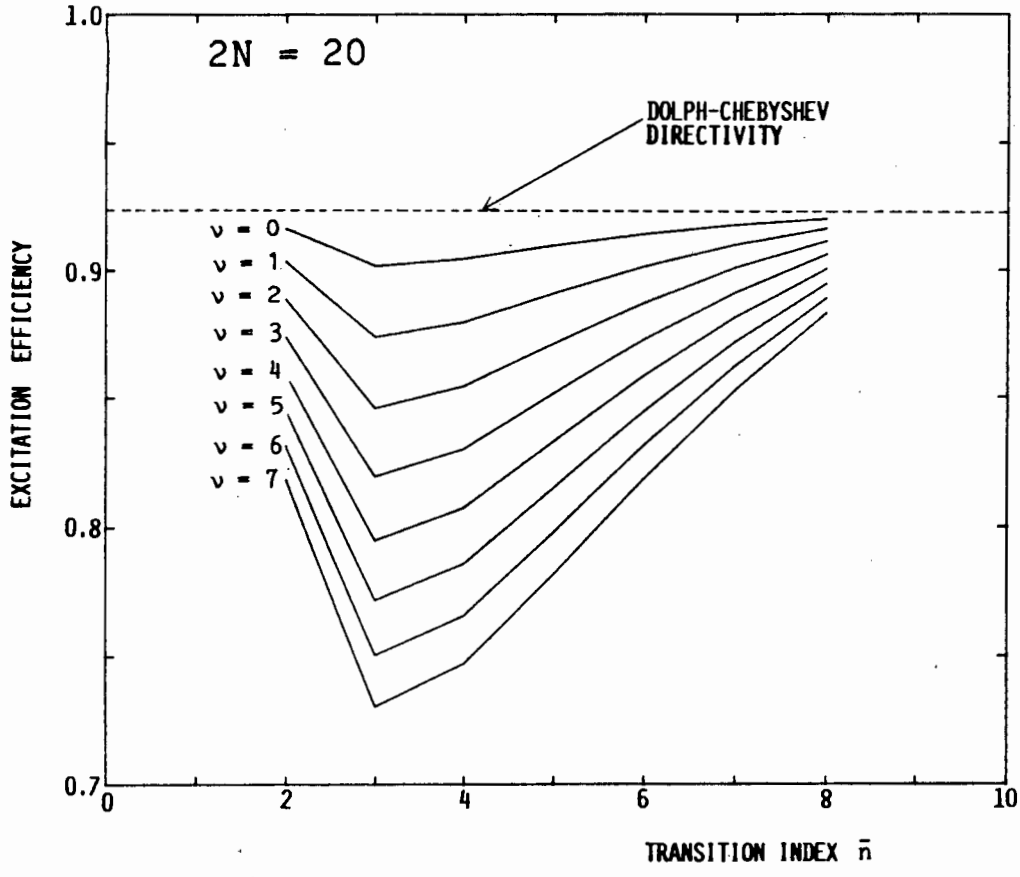

FIGURE 7.5 EXCITATION EFFICIENCY AS A FUNCTION OF THE TRANSITION INDEX

suffers from "directivity compression" (see Section 3.2.2), then the form of the curves like those of Fig. 7.5 will be different. An array of 30 elements, with a sidelobe ratio of 20 dB will serve to illustrate this point.

The graph in Fig. 7.6 is now applicable. It is immediately clear that, for a fixed ν, there is a certain value of $\bar{\bar{n}}$ which provides maximum directivity. Furthermore, for a wide range of ν and $\bar{\bar{n}}$ combinations, the generalised Villeneuve distribution has a higher directivity than the parent Dolph-Chebyshev one has. The reason is the same as that given for the modified Zolotarev difference distribution in Section 6.6.

As with the Zolotarev distribution there will be array sizes which, for a specified sidelobe ratio, will possess "edge brightening" (i.e. a non-monotonic distribution) even with $\bar{\bar{n}}$ equal to its minimum allowable value and $\nu = 0$ (i.e. Villeneuve distribution). Increasing $\bar{\bar{n}}$ will simply worsen the situation and the only solution is to increase the value of ν. Consider for instance an array with $2N = 40$ and SLR = 15 dB. The aperture distributions (with the excitations simply connected by straight lines) for the smallest permitted $\bar{\bar{n}}$ value of 2 are shown in Fig. 7.7 for the three cases $\nu = -1$, $\nu = 0$ and $\nu = 1$. The parent Dolph-Chebyshev ($\nu = -1$) case has a highly non-monotonic distribution. The Villeneuve distribution ($\nu = 0$) is just monotonic. The generalised Villeneuve distribution with $\nu = 1$ is strictly monotonic. For a still larger array with the same sidelobe level, a $\nu > 0$ will be required to obtain even a distribution which is just monotonic; this confirms the usefulness of the generalised Villeneuve distribution for reasons other than increased sidelobe envelope taper rate.

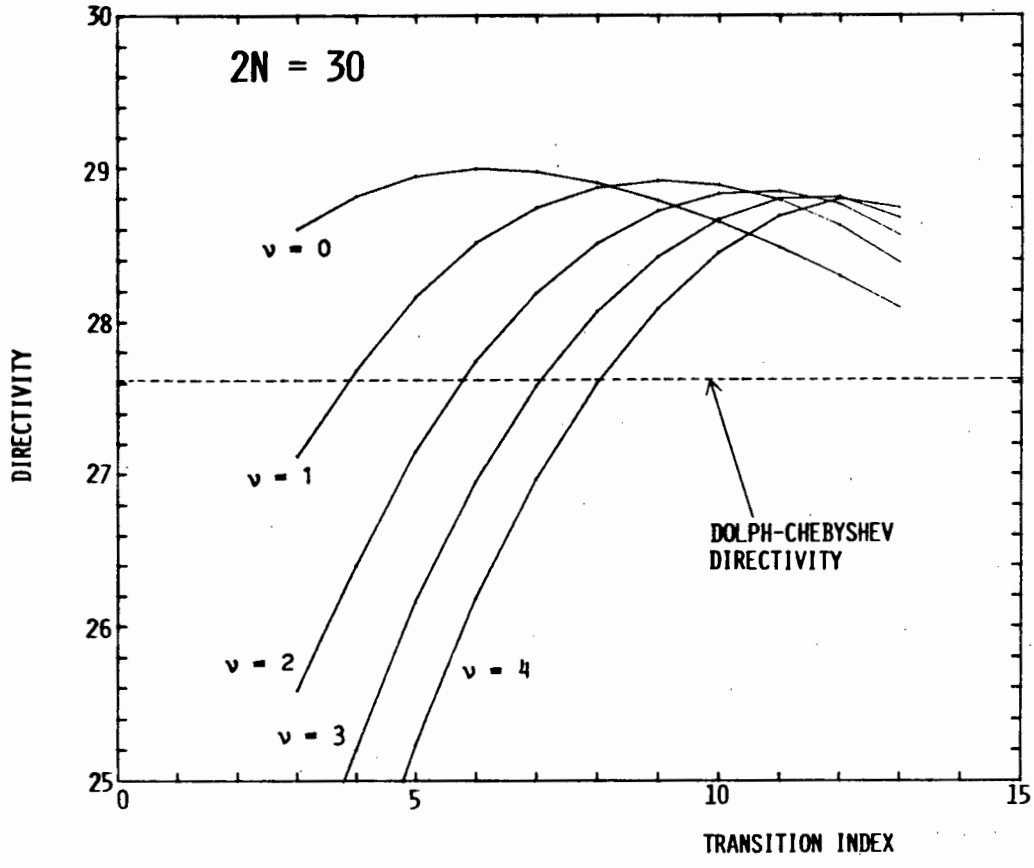

FIGURE 7.6 DIRECTIVITY AS A FUNCTION OF THE TRANSITION INDEX (FOR AN ARRAY WITH "DIRECTIVITY COMPRESSION")

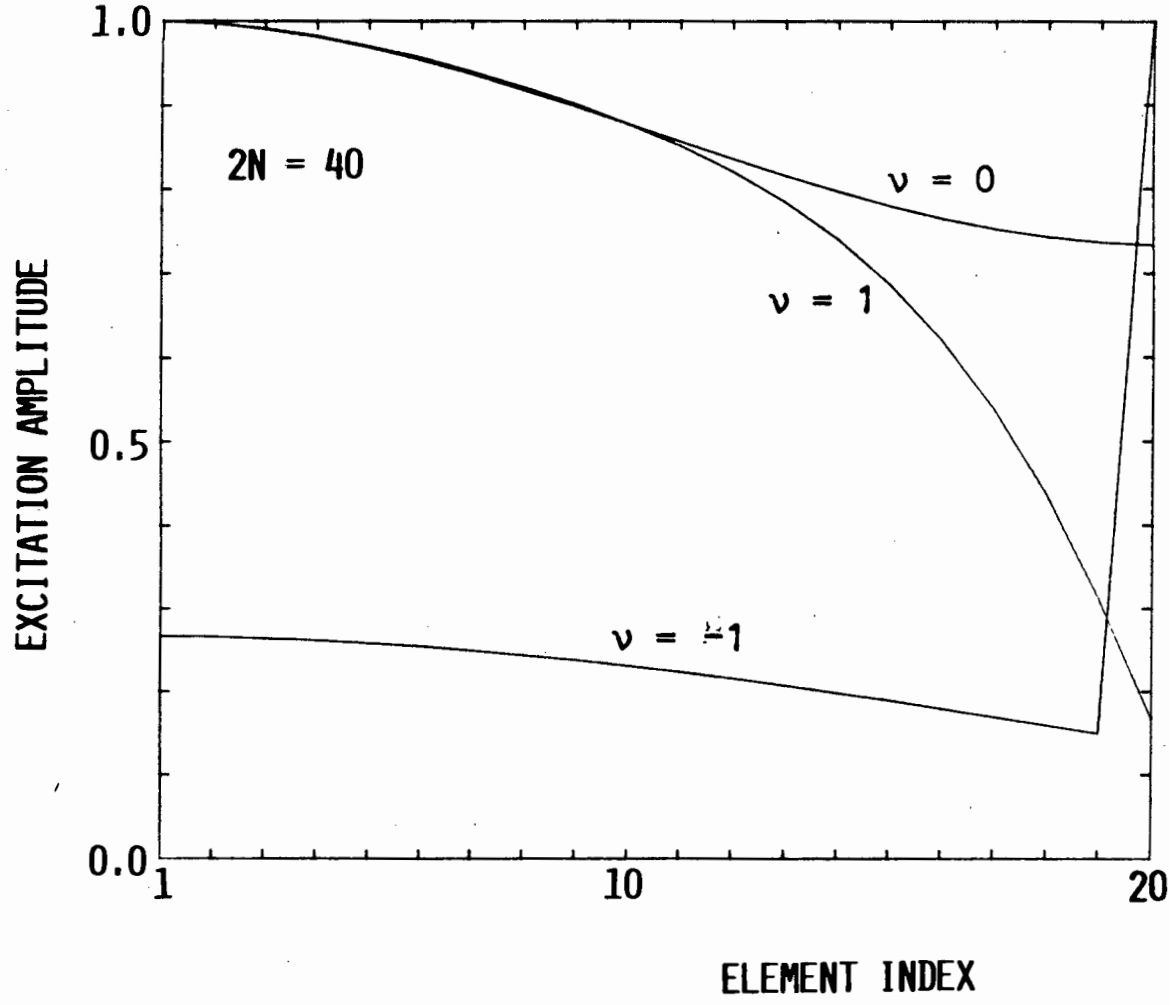

FIGURE 7.7 COMPARISON OF GENERALISED VILLENEUVE APERTURE DISTRIBUTIONS

7.4 CONCLUSIONS

The generalised Villeneuve distribution developed in this chapter permits the direct synthesis of discrete array distributions for high efficiency sum patterns of arbitrary sidelobe level and envelope taper. With the Dolph-Chebyshev distribution as the parent space factor, and the correct perturbation of space factor zeros, the excitation efficiency and beamwidths are kept as close to their optimum values as is possible under the specified sidelobe ratio and envelope taper. The level of the first sidelobe is set by the starting Dolph-Chebyshev distribution, the taper rate controlled by the parameter ν and the point at which the required taper proper begins determined by $\bar{n}$. The excitations are obtained from the perturbed space factor zeros through solution of a set of linear simultaneous equations. The synthesis procedure is extremely rapid. A computer code developed for performing the complete synthesis (with the values of $\bar{n}$, ν, SLR, 2N and d as input), and which computes the resulting space factor and directivity, takes approximately 4 CPU seconds on a CDC Cyber 174 computer for an array of 20 elements. Consequently, design trade-off studies are feasible; the proper choice of the values of $\bar{n}$ and ν for a particular application will depend on the relative importance of the peak sidelobe level compared to that of the farther-out sidelobes, and their effect on the excitation efficiency.

The method is similar to (and might perhaps be considered the discrete equivalent of) the generalised Taylor $\bar{n}$ continuous distributions [3].

7.5 REFERENCES

[1] C.L. Dolph, "A current distribution for broadside arrays which optimises the relationship between beam width and side-lobe level", Proc. IRE, Vol. 34, pp. 335-348, June 1946.

[2] A.T. Villeneuve, "Taylor patterns for discrete arrays", IEEE Trans. Antennas Prop., Vol. AP-32, No. 10, pp. 1089-1093, Oct. 1984.

[3] D.R. Rhodes, "On the Taylor distribution", IEEE Trans. Antennas Prop., Vol. AP-20, No. 2, pp. 143-145, March 1972.

[4] D.R. Rhodes, Synthesis of Planar Antenna Sources, (Oxford Univ. Press, 1974), pp. 129-137.

CHAPTER 8

SIMULTANEOUS SYNTHESIS OF SUM AND DIFFERENCE DISTRIBUTIONS

8.1 INTRODUCTION

The problem of optimum sum pattern synthesis for a discrete array was shown in Chapter 3 to have been relatively well understood, and some generalisations were presented in Chapter 7. The corresponding difference pattern synthesis has been brought to a similar level of completion by the work reported in Chapters 4, 5 and 6. Consequently high directivity, low sidelobe, sum or difference distributions can, independently, be determined directly with a certain level of confidence. On the other hand, the topic of simultaneous synthesis has not yet been dealt with. When this topic was reviewed in Section 3.5, it was indicated that no definite procedures of any form have been published to perform such syntheis.

As was pointed out in Section 3.5, any discussion of simultaneous synthesis without reference to feed network constraints is not meaningful. Since the number of conceivable array feed network architectures is essentially unlimited, an all-encompassing theory of simultaneous optimum synthesis is not possible. (There is perhaps an analogy here with the subject of systems theory. While a general theory for linear systems is possible, one such is not possible for non-linear systems, since each is non-linear in its own particular way). Instead, methods of simultaneous synthesis are considered here for the important and widely used class of feed network which employs sub-arraying. The two-module and independent types of network are the extreme cases of such a class of network.

In array antenna design (as in most other areas of engineering) two approaches are possible. On the one hand the performance of a number of different "likely" sets of excitations may be examined and the most desirable one selected. Alternatively, the inverse problem may be attempted - finding that set of excitations which produces the desired performance as closely as possible. The independent sum and difference synthesis methods described earlier are examples of the latter approach. The contributions to simultaneous synthesis methods presented here fall somewhere between these two approaches. Some choice on the part of the designer is required. One reason for a choice having to be made lies in the fact that, since some compromise has to be made, certain criteria may be more important to meet than others. For instance, it may in some cases be more important that the sum mode be closer to its independently optimum performance at the expense of the difference pattern, or vice versa. Selection of what is simultaneously optimum therefore depends on the intended application. Such a choice is not really a drawback since engineering design is always dependent to some extent on the experience and intuition of the designer. It is with this in mind that Bandler [2] stresses the "necessity of some (numerical) experimentation, in general, before accepting an apparently optimal solution (obtained) by any numerical optimisation procedure". The methods presented in this chapter are intended to provide means of performing such numerical experimentation.

8.2 ARRAY GEOMETRY AND NOTATION

In the interests of clarity, the sub-array geometry and associated notation used in the sections that follow will be outlined.

The general sub-arrayed configuration is shown schematically in Fig. 8.1 for one half of the array. The total number of array elements is 2N. Two sets of excitations are considered - local excitations and sub-array weights.

The set of local excitations,

$$\{a_n\} \qquad n = \pm 1, \pm 2, \cdots \pm N$$

are individually associated with each element. These will be the excitations responsible for the sum pattern obtained.

There are 2Q sub-arrays and the sub-arraying is symmetric about the array centre. The q-th sub-array has K_q array elements associated with it; thus

$$\sum_{q=1}^{Q} K_q = N \tag{1}$$

It then follows that the local excitations of the elements of the first sub-array are,

$$a_1, a_2 \cdots a_{K_1}$$

Those for the q-th sub-array are,

$$a_{K_1+K_2+\cdots+K_{q-1}+1},\ a_{K_1+K_2\cdots+K_{q-1}+2},\ \cdots\ a_{K_1+K_2+\cdots+K_q}$$

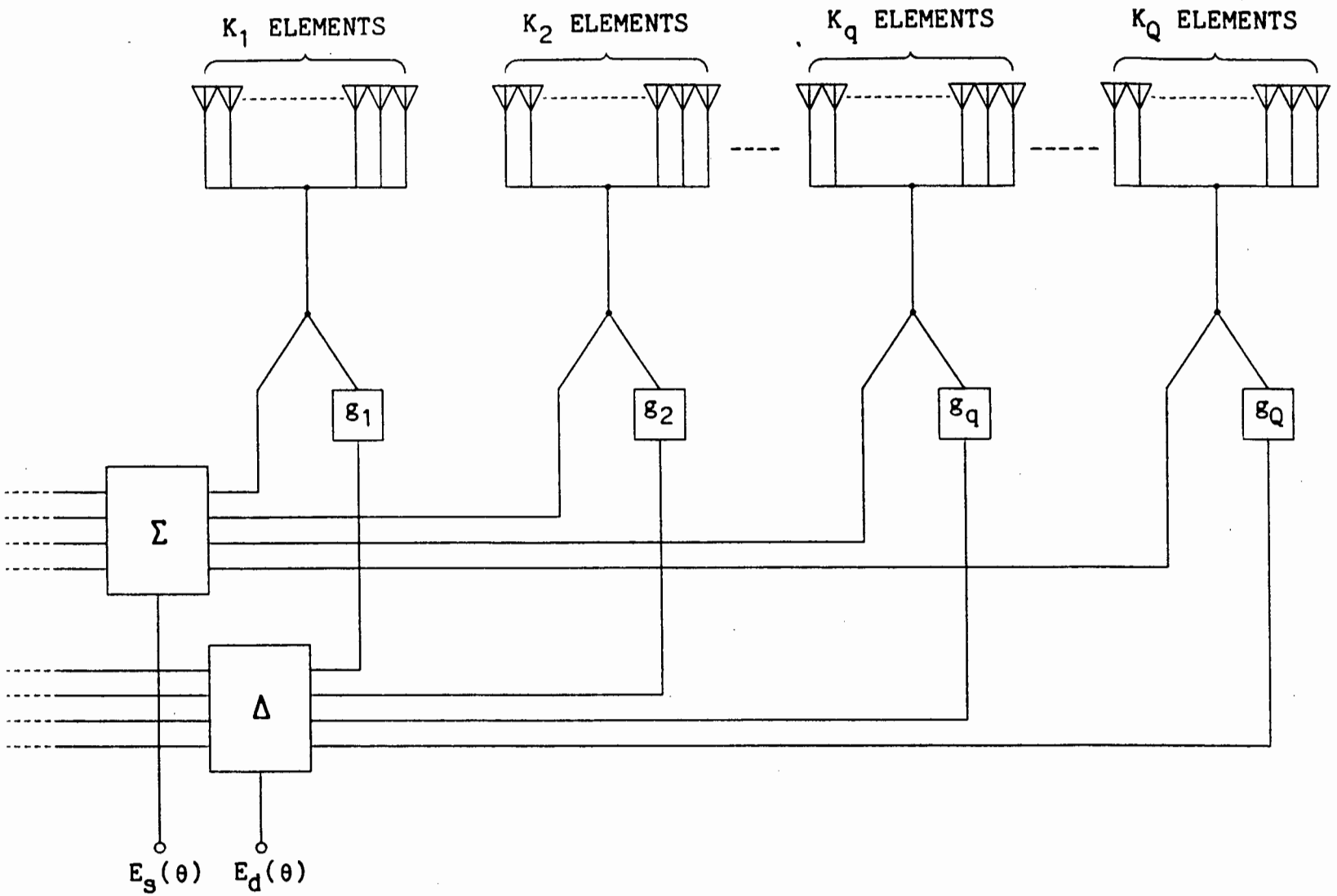

FIGURE 8.1 SCHEMATIC DIAGRAM OF SUB-ARRAY FEED NETWORK

while for the final Q-th sub-array they are,

$$a_{K_1+K_2+\cdots+K_{Q-1}+1},\ a_{K_1+K_2\cdots+K_{Q-1}+2},\ \cdots\ a_N$$

The excitation weighting of the q-th sub-array is denoted by $g_q(n)$, indicating that the particular n-th element is a member of the q-th sub-array. While for the sum pattern the n-th element has an excitation which is simply the local excitation a_n, for the difference pattern its excitation is effectively $a_n g_q(n)$.

The two-module and independent array feed networks are special cases of the above geometry. If Q = N, then the independent network results, while Q = 1 implies the two-module network.

Excitation sets $\{a_n^s\}$ and $\{a_n^d\}$ will always be used here to denote those sets of excitations which are <u>independently</u> optimal for the sum and difference cases, respectively. The corresponding space factor zeros are,

$$\{\psi_i^s\} \qquad i = \pm1, \pm2, \cdots \pm(N-1)$$

$$\{\psi_i^d\} \qquad i = \pm1, \pm2, \cdots \pm(N-1)$$

For the difference pattern there is an additional zero at $\psi = 0$, and for the sum a zero at $\psi = \pi$. However, with the symmetric arrays dealt with here these are always satisfied and need never be considered. Also, for reasons of symmetry, only one half of the array excitations and pattern zeros need be considered.

Because of the enormous number of design parameters, and the possibility of differing opinions as to what can be considered the "best" compromise in any given situation, the simultaneous synthesis technique discussions will generally be along the lines of a description of the particular method, an illustrative example, and a number of applicable comments.

The methods developed in this chapter will all be illustrated via a common example in order to facilitate comparisons. The details of independently optimum solutions, for the 20 element array with a minimum sidelobe ratio of 25 dB, are given in Table 8.1.

TABLE 8.1 : 20 element, 25 dB sidelobe ratio arrays with d = 0.5 λ.

(a) Sum mode (Villeneuve, $\bar{n} = 4$)

n	a_n^s
1	1.00000
2	0.97591
3	0.92707
4	0.85415
5	0.76156
6	0.65833
7	0.55670
8	0.46916
9	0.40570
10	0.37258

i	ψ_i^s
1	0.42406948
2	0.64273132
3	0.93785914
4	1.25663704
5	1.57079630
6	1.88495556
7	2.19911482
8	2.51327408
9	2.82743334
10	3.14159265

(b) Difference mode (Modified Zolotarev, $\bar{n} = 4$, $\xi = 3$)

n	a_n^d
1	0.17385
2	0.49612
3	0.75500
4	0.92719
5	1.00000
6	0.96589
7	0.84010
8	0.68326
9	0.54640
10	0.36091

i	ψ_i^d
1	0.63546394
2	0.84303008
3	1.12727154
4	1.43713140
5	1.76270700
6	2.07671140
7	2.38435488
8	2.68746840
9	2.99074250

8.3 A SIMPLE APPROACH FOR THE TWO-MODULE NETWORK

A simple attempt at obtaining a set of excitations which represents a compromise between sum and difference performance, when a two-module feed network is used, will first be described. Consider the sets of independently optimum excitations $\{a_n^s\}$ and $\{a_n^d\}$, n = 1,2, ••• N. These are obtained using the methods given in the earlier chapters. Suppose that the compromise excitation for the n-th element is computed as,

$$a_n = \delta\, a_n^s + (1 - \delta)\, a_n^d \qquad (2)$$

where δ is a weight factor with $0 \leq \delta \leq 1$. A value of $\delta = 0$ corresponds to the optimum difference excitations, while $\delta = 1$ gives the optimum sum excitations. The history of the resulting sum and difference patterns as δ varies from 0 to 1 is shown in Figs. 8.2 and 8.3 for a 20 element, 25 dB sidelobe ratio array. The results do not appear to be satisfactory, with sidelobes unacceptably high for one or other of the patterns. The problem with this approach is that there is no way of determining with any certainty what the best sidelobe-constrained compromise solution is for the two-module feed network, or how to improve the sidelobe performance by accepting some beamwidth increase perhaps. This is taken up in the next section.

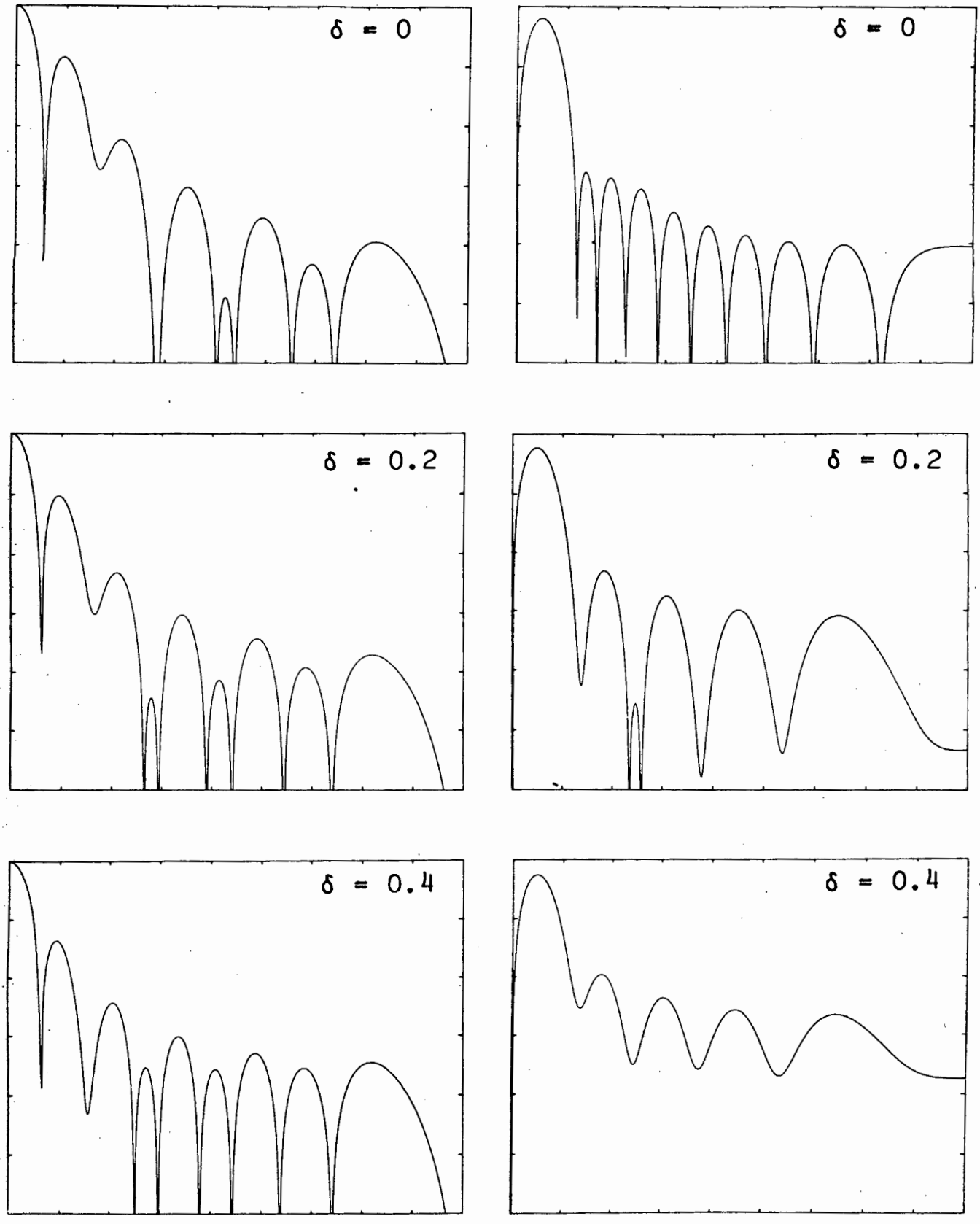

FIGURE 8.2 COMPROMISE PATTERNS OBTAINED USING SIMPLE EXCITATION WEIGHTING PROCEDURE

(Horizontal Axis Is Angle Off Broadside From 0 to 90 Degrees. Vertical Axis Is Relative Level In Decibels From -60 to 0).

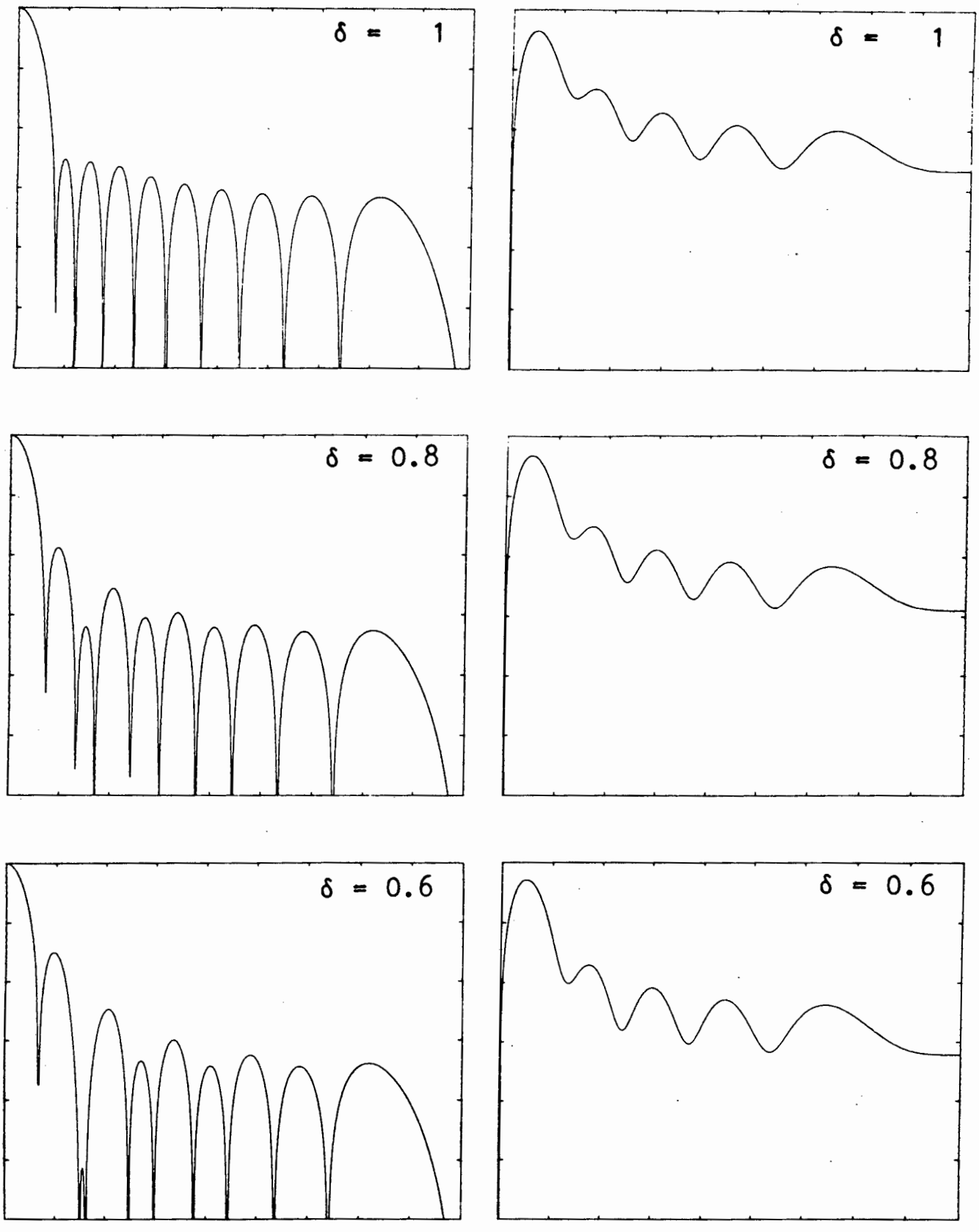

FIGURE 8.3 COMPROMISE PATTERNS OBTAINED USING SIMPLE EXCITATION WEIGHTING PROCEDURE

(Horizontal Axis Is Angle Off Broadside From 0 to 90 Degrees. Vertical Axis Is Relative Level In Decibels From -60 to 0).

8.4 SIMULTANEOUS SYNTHESIS WITH A TWO-MODULE NETWORK USING NUMERICAL OPTIMISATION

8.4.1 The Approach of Einarsson [1] for Sum Synthesis

The simultaneous synthesis method presented in this section is an extension of the numerical optimisation method used by Einarsson [1] for sum synthesis.

The notation used differs from that of Einarsson [1], but is more convenient for the simultaneous problem. Furthermore, the formulation used throughout exploits the symmetry of the linear array, making use of expressions derived in Chapter 2. Though Einarsson was concerned with symmetric excitation, the planar array geometry with which he was concerned does not allow this symmetry to be exploited to the same extent possible with linear arrays.

Recall from equation (21) of Section 2.2.3 that the sum directivity of a linear array is expressible as the ratio of two Hermitian quadratic forms,

$$D_s(\psi) = \frac{2[J]^T[A_s][J]}{[J]^T[B_s][J]} \tag{3}$$

with matrices $[A_s]$ and $[B_s]$, and excitation vector $[J]$, defined in Sections 2.2.2 and 2.2.3. The matrix $[A_s]$ can furthermore be written as,

$$[A_s] = [F_s][F_s]^T \tag{4}$$

with vector $[F_s]$ as defined in equation (12) of Chapter 2.

The expression for $D_s(\psi)$ in equation (3) is dependent on angle ψ (or equivalently θ). When evaluated in the $\psi = \phi_h$ direction, say, $[A_s]$ and $[F_s]$ will be denoted by $[A_s^h]$ and $[F_s^h]$ respectively. Matrix $[B_s]$ is always independent of ψ. As before, $D_s(\psi)$ in the direction of its maximum is simply denoted by D_s^m. For the broadside array this is in the direction $\psi = \phi_o = 0$, and therefore,

$$D_s^m = \frac{2[J][A_s^o][J]}{[J][B_s][J]} \tag{5}$$

The array factor is given, in terms of the above quantities, in the direction $\psi = \phi_h$ as,

$$E_s(\phi_h) = 2[F_s^h]^T[J] \tag{6}$$

from equation (14) of Chapter 2. In the broadside direction this is therefore,

$$E_s(0) = 2[F_s^o]^T[J] \tag{7}$$

Note that $[F_s^o]$ will simply be a vector with components all unity.

Einarsson has shown [1] that maximisation of D_s^m in (5) can be formulated as the problem of minimisation of the quantity,

$$P_s(\bar{J}) = [J]^T[B_s][J] - [F_s^o]^T[J] \tag{8}$$

where $\bar{J}$ is equivalent to $[J]$.

This is a quadratic programming problem [3]. The minimisation is done subject to a set of constraints on the sidelobe levels. If the prescribed maximum sidelobe level relative to the pattern maximum is denoted by c, then application of the sidelobe constraints at a set of angles $\psi = \phi_1, \phi_2, \cdots \phi_h, \cdots \phi_H$ can be written as,

$$\begin{aligned} E_s(\phi_h) - c\, E_s(0) &\leq 0 \\ -E_s(\phi_h) - c\, E_s(0) &\leq 0 \end{aligned} \tag{9}$$

for h = 1,2, ••• H. The fact that no assumption about the sign of the sidelobes is made explains the appearance of two terms in (9). This has the advantage that the constraint set remains linear. Use of the modulus function would convert (9) to a non-linear set of constraints in general, and prohibit the use of quadratic programming algorithms.

The set of constraints (9) can of course be re-written as,

$$\begin{aligned} [F_s^h]^T[J] - c\,[F_s^o]^T[J] &\leq 0 \\ -[F_s^h]^T[J] - c\,[F_s^o]^T[J] &\leq 0 \end{aligned} \tag{10}$$

or equivalently as,

$$\begin{aligned} ([F_s^h] - c\,[F_s^o])^T[J] &\leq 0 \\ (-[F_s^h] - c\,[F_s^o])^T[J] &\leq 0 \end{aligned} \tag{11}$$

The above method has been applied using the quadratic programming procedure described by Gill et. al. [3] and implemented in [4] as routine E04NAF. After the initial run of the optimisation it is in most cases necessary to check the space factor obtained for any sidelobe level violations at angles other than those $\{\phi_h\}$ initially selected for the constraint set, and then re-run the optimisation with the altered set of constraint angles, as suggested in [5, p. 53]. This does not cause any unforeseen problems though.

The present approach is easily extended to cases requiring a sidelobe taper, though this was not done by Einarsson. To do this a set of quantities c_h is defined, one associated with each constraint angle $\psi = \phi_h$, instead of having the same c for each such angle. This can be considered to be a sidelobe envelope taper vector,

$$\bar{C} = [c_1 \; c_2 \; \cdots \; c_H]^T \tag{12}$$

The components of $\bar{C}$ are determined from an equation for the envelope in terms of angle ψ.

Furthermore, the quadratic programming technique used allows requirements for a monotonic distribution of excitations to be incorporated as a linear constraint set, if indeed so desired.

The method has been found to work extremely well, but no results will be given here, since the aim in this section is primarily one of enlarging the scope of the method to include simultaneous synthesis. For sum synthesis alone the methods of Chapter 3 and 7 should be used.

8.4.2 Extension to Difference Synthesis

With the quantities $[F_d]$, $[A_d]$ and $[B_d]$ derived in Chapter 2 the extension of the method of Einarsson [1] to difference synthesis is relatively straightforward. Suppose that the maximum of the difference pattern is at angle $\psi = \gamma_o$; then from equation (23) of Chapter 2 it follows that,

$$D_d^m = \frac{2[J]^T[A_d^o][J]}{[J]^T[B_d][J]} \tag{13}$$

where $[A_d^o]$ is just $[A_d]$ evaluated at $\psi = \gamma_o$. Similarly, $[F_d^o]$ denotes $[F_d]$ evaluated at this same angle. Maximisation of (13) is then equivalent to minimising the function,

$$P_d(\vec{J}) = [J]^T[B_d][J] - [F_d^o]^T[J] \tag{14}$$

which is again a quadratic programming problem. In this case the precise position γ_o of the maximum is not known a priori. An iterative procedure is therefore followed, as was done in Section 4.1. The optimisation is performed with γ_o equal to that of a uniform array of the same number of elements as that under consideration, operated in the difference mode. At the end of the first run, the actual value of γ_o obtained with the resulting excitation set $[J]$ is found, and the optimisation re-run with this value. This process is repeated until convergence is obtained; this is achieved rapidly.

The sidelobe constraints are applied in much the same way as for sum synthesis. However, the set of constraint angles will be different from those for the sum case and will be denoted by $\psi = \gamma_1, \gamma_2, \cdots \gamma_r, \cdots \gamma_R$. Thus $[F_d^r]$ implies $[F_d]$ evaluated at $\psi = \gamma_r$. The set of constraint conditions corresponding to those in (9) and (10) are then,

$$\begin{aligned} E_d(\gamma_r) - c\, E_d(\gamma_o) &\leq 0 \\ -E_d(\gamma_r) - c\, E_d(\gamma_r) &\leq 0 \end{aligned} \tag{15}$$

or equivalently,

$$\begin{aligned} ([F_d^r] - c\,[F_d^o])^T[J] &\leq 0 \\ (-[F_d^r] - c\,[F_d^o])^T[J] &\leq 0 \end{aligned} \tag{16}$$

As mentioned previously, a sidelobe taper requirement can be incorporated by defining a taper vector like that in (12). The monotonicity constraint should be applied more carefully. For difference distributions it must be remembered that by "monotonic" is meant that the excitations must not increase near the array ends. The distribution as a whole is inherently non-monotonic. This requirement can still be implemented as a set of additional linear constraints however.

The quadratic programming routine E04NAF [4] has been used to implement the above procedure for difference synthesis. Once more no special problems requiring further discussion were encountered, and the final step of simultaneous synthesis can therefore be considered.

8.4.3 Simultaneous Synthesis with a Two-Module Array Feed Network

Following the work of Zionts and Wallenius [6] on multi-objective optimisation, the simultaneous synthesis problem can be formulated as one of minimising the quantity,

$$P(\bar{\bar{J}}) = \delta\, P_s(\bar{J}) + (1 - \delta) P_d(\bar{J}) \tag{17}$$

subject to some set of constraints. The quantity in (17) is a weighted addition of the functions $P_s(\bar{J})$ and $P_d(\bar{J})$ applying individually to the sum and difference cases, respectively. The quantity δ expresses a preference for one or other mode of operation. A $\delta = 0$ reduces the problem to that of difference synthesis, while if $\delta = 1$ it becomes the sum synthesis problem. Equal weighting is obtained when $\delta = 0.5$.

The next question concerns the set of constraint conditions. A single set of angles at which to apply sidelobe constraints is not acceptable. The reason is that the angular regions over which the sidelobes occur are different for the two cases, the first minimum of the sum pattern occurring earlier than that of the difference pattern. An angle at which it is appropriate to apply a sum sidelobe constraint may fall within the principal lobe of the difference pattern. Furthermore, it is usually desirable to specify difference sidelobe levels relative to the difference pattern maximum and not to the sum maximum. To do this not only different sets of constraint angles must be used but in fact two completely different sets of constraints. The procedure then is to maximise the quantity $P(\bar{J})$ in (17) subject to a constraint set consisting of those in both equations (11) and (16). In (11) let the maximum sidelobe level specification be denoted by c_s (instead of simply c) in order to distinguish it from the difference sidelobe level quantitied c_d to be used in (16). As discussed above, the sets $\{\phi_h\}$ and $\{\gamma_r\}$ of constraint angles will generally not be identical, at least not for the first few values close to the broadside direction. A conflicting constraint set is hereby avoided. This is crucial in the application of the method to simultaneous synthesis.

Since $P_s(\bar{J})$ and $P_d(\bar{J})$ are quadratic, so is their linear combination used to form $P(\bar{J})$. Therefore the quadratic programming algorithm E04NAF [4] can be applied to this problem as well.

This approach has been exercised for a number of different problems. The procedure developed from this experience will first be outlined, and then the numerical results presented for a particular example.

As the first step, the exact procedures for independent sum and difference pattern synthesis presented earlier in this thesis are used to synthesise an optimum set of sum excitations and an optimum set of difference excitations. This will give an idea of the performance achievable independently. From the space factor zeros of these independently optimum patterns, the region over which to apply sidelobe constraints in each case is clearly discernible. In this way a selection of constraint angles which are overly restrictive (require beamwidths that are too narrow) even for the independent patterns is prevented. This is important since any infeasibility of solution indicated by the numerical optimisation routine must then be solely due to the fact that simultaneous synthesis is being attempted. Thus information from the independent exact synthesis methods is used to draw up the initial constraint angle sets $\{\phi_h\}$ and $\{\gamma_r\}$, such that $\phi_1 = \psi_1^s$ and $\gamma_1 = \psi_1^d$ initially.

The next step is to set $c_s = c_d$ (i.e. identical sum and difference sidelobe specifications) and repeatedly execute the optimisation routine, each time decreasing the common sidelobe level factor until a solution subject to the given constraints is no longer feasible. That this stage has been reached is indicated by the optimisation algorithm putting all the excitations to zero and setting a flag that a feasible solution is not possible. At this point, because of the fact that the constraint angles have been selected using information from the independently optimum solutions, the beamwidths obtained with the solution $[J]$ of the optimisation routine will be close to those of the independent solutions. (This can easily be strictly enforced by requiring a very low "sidelobe" at the first constraint angles ϕ_1 and γ_1 for the sum and difference cases, respectively, if so desired).

Furthermore, the last feasible sidelobe level is at this stage also known to be the lowest achievable for the given beamwidths and the two-module feed.

If the beamwidths of both the sum and difference patterns are to remain as specified above, the maximum sidelobe level c_s of the sum pattern can only be decreased by increasing that of the difference pattern (c_d), or vice versa. Alternatively, sidelobe levels can be lowered over some sectors of the patterns and allowed to increase over others. Such sidelobe structures have been considered in [5, p. 36]. In order to determine to what extent this is possible, the optimisation routine must again be executed a number of times.

An alternative approach to the one outlined above is one which also begins with the independently optimum solutions, sets the factors c_s and c_d can be set to some desired sidelobe levels, and "allows" the beamwidths of either the sum or difference patterns, or both, to increase by shifting the first constraint angles (ϕ_1 and/or γ_1) further out, re-distributing the constraint set, and each time executing the optimisation routine until a feasible solution is obtained for the given c_s and c_d values. It is important to realise that an acceptable solution may not in fact exist for the given array size and prescribed sidelobe levels. There is a limit to the amount of beamwidth increase which can be permitted. Firstly, if the suppression of sidelobes is desired for rejection of clutter and other sources of interference, for example, there is little sense in accepting too much beam broadening for either sum or difference patterns just to lower the sidelobes over a sidelobe region with a now greatly reduced angular extent and the interference now entering via the broader main lobes. Also, associated with beam broadening is decreased directivity and boresight slope performance. A further reason for limiting the amount of beamwidth increase is that the difference lobe becomes severely deformed; what happens is that the first null of the "starting pattern" begins to fill in and merge with this difference lobe. It is advisable at each stage to check the patterns for undesirable deformities, and for "spurious" sidelobes at angles other than those of the constraint set selected before accepting any set of excitations as the final solution. The former is

easily done via modern computer graphics. "Spurious" sidelobes are easily detected numerically, their angular location included in the constraint set, inactive constraints of the previous run eliminated (this information may be requested from the optimisation routine), and the optimisation process repeated.

After some experience, using the structured approach given above, it is found that the method is flexible and becomes relatively easy to use. The formulation of the problem as a quadratic programming one offers considerable advantages as regards execution times involved, so that repeated use is feasible. The solutions have been found in all cases using a starting set of excitations of unity for each element. There appears to be no advantage in using δ values other than 0.5. The sum characteristics are rather played off against those of the difference by altering their respective sidelobe levels or beamwidths as indicated in the above guidelines.

8.4.4 Illustrative Example

Consider as an example the case of an array of 20 elements, and suppose that for both sum and difference patterns a sidelobe ratio of 25 dB is desired, though known to be over-ambitions for a two-module network. The independently optimum solutions are then just those given in Table 8.1. Using this information the optimisation problem was set up and executed. The sidelobes for both sum and difference patterns were decreased until a feasible solution with the given set of constraint angles was no longer possible and the last feasible solution examined. At this point the difference sidelobe constraint was increased slightly to the 15 dB level, and that for the sum lowered in small steps until a feasible solution was once more no longer possible. At this stage the compromise solution (with beamwidths comparable with those of the above independently optimum designs) had a sidelobe ratio of 17 dB for the sum mode and 15 dB for the difference mode. This is illustrated in Fig. 8.4.

As a next step the first constraint angle of the difference pattern was shifted outward by a factor of 1.1, with that for the sum unchanged. A sum sidelobe ratio of 18 dB was then obtainable, with that for the difference pattern unchanged. As a third step, the sum beamwidth was allowed to increase by a factor of 1.1 and that of the difference pattern by a factor 1.3. For this case the sum sidelobe ratio achievable is 20 dB, if the level of the difference sidelobe constraints is once more unaltered. This is shown in Fig. 8.5, and clearly shows the beam broadening of the difference pattern.

By altering the constraints in a systematic manner then, meaningful design trade-off studies can be performed using the quadratic programming method. The performance that can be obtained with a two-module feed network is severely restricted, however, and the constraints cannot be too tight.

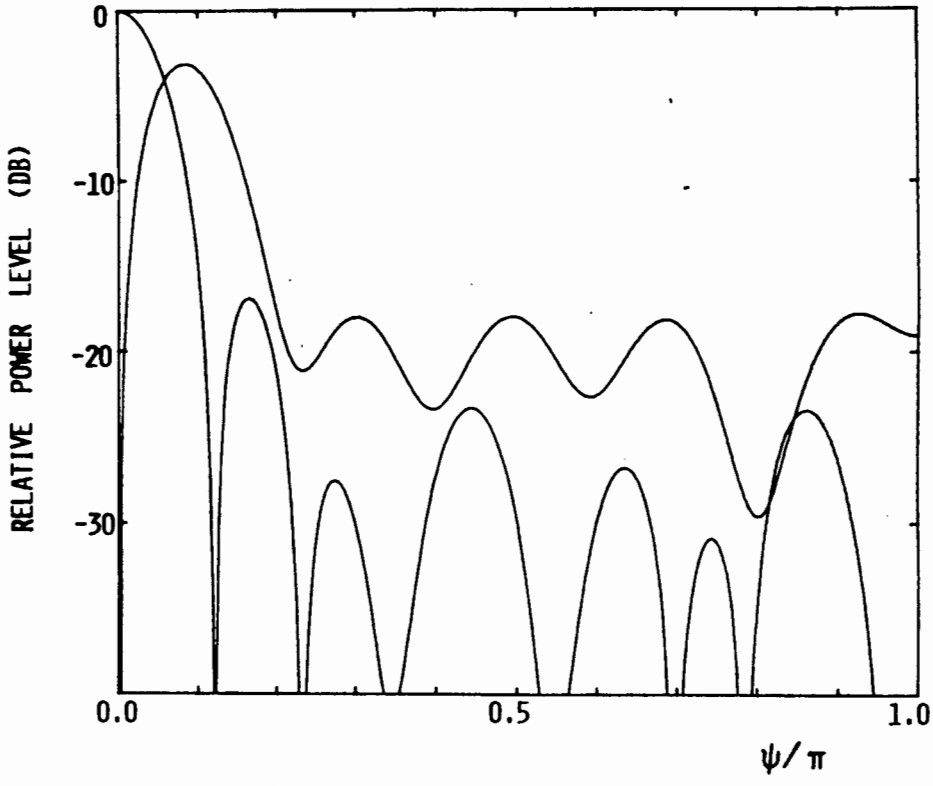

FIGURE 8.4 SUM AND DIFFERENCE PATTERNS WITH TWO-MODULE FEED NETWORK (NO BEAM BROADENING)

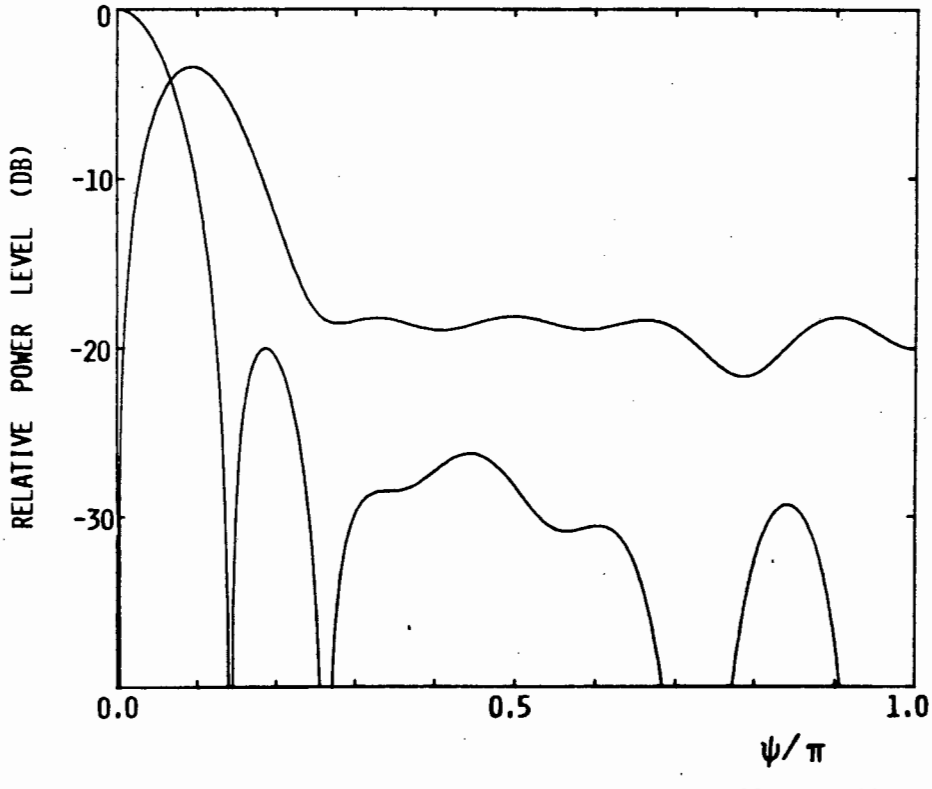

FIGURE 8.5 SUM AND DIFFERENCE PATTERNS WITH TWO-MODULE FEED NETWORK (BEAM BROADENING PERMITTED)

8.5 EXCITATION MATCHING VIA SUB-ARRAY WEIGHT ADJUSTMENT

8.5.1 Introduction

The technique dealt with in the previous section enables the best compromise simultaneous synthesis to be performed under the limitations of the two-module network. The remainder of the chapter is concerned with simultaneous synthesis of an array which utilises sub-arraying to increase the number of degrees of freedom above that available with the two-module network. The particular approach in this section is one which attempts to obtain a good compromise by dealing directly with the independently optimal excitations $\{a_i^s\}$ and $\{a_i^d\}$, and will be referred to as excitation matching.

8.5.2 The Excitation Matching Concept

Assume that the excitation sets $\{a_n^s\}$ and $\{a_n^d\}$ have been determined, and let $\{a_n^s\}$ be the local set of excitations. In other words, the sum mode will have its optimum set of excitations. With the sub-array configuration selected, the sub-array weights must be determined according to some criterion. The difference excitations will be the set $\{e_n\}$, with $e_n = g_q(n)a_n^s$, the $g_q(n)$ being the weight of the sub-array associated with the n-th element. For a given configuration of sub-arrays the g_q must be chosen so that the set $\{e_n\}$ is as close as possible to the independently optimum difference set $\{a_n^d\}$. To effect this, a set of N residuals $\{r_n\}$ is formed, with

$$r_n = a_n^d - g_q(n)\, a_n^s$$

This can be re-written as,

$$r_i = a_i^d - \sum_{j=1}^{Q} c_{ij} g_j(i) \qquad (18)$$

for each i = 1,2, ••• N. For each i value only one of the c_{ij} are non-zero, depending on the particular sub-array geometry used. More specifically,

$$c_{ij} = \begin{cases} a_i^s & \text{if element i is in sub-array j} \\ 0 & \text{otherwise} \end{cases}$$

In the case of an independent feed network (N = Q) it is possible to adjust the "sub-array" weights so that each residual r_i is exactly zero. Thus, with each $r_i = 0$, equations (18) form a system of linear simultaneous equations for the sub-array weights. In this case, with N = Q, each "sub-array" weight g_i is simply the ratio a_i^d/a_i^s.

For the case of a feed network of intermediate complexity (N > Q) it is not possible to make each of the N residuals r_i identically zero by adjusting the Q sub-array weights. Nevertheless, the system of equations,

$$\sum_{j=1}^{Q} c_{ij}\, g_j(i) = a_i^d \qquad (19)$$

can still be considered as that which will provide the solution for the sub-array weights.

But since N > Q, it is an over-determined set, with more equations than unknowns. However, such a system of equations can be "solved" by finding the set of unknowns, $\{g_q\}$, q = 1,2, ••• Q which minimises some norm of the vector of residuals,

$$\vec{R} = [r_1, r_2, \cdots r_N]^T \qquad (20)$$

Three possible norms, which have been defined in Appendix I, are

$$\|\bar{R}\|_1 = \sum_{n=1}^{N} |r_n| \tag{21}$$

$$\|\bar{R}\|_2 = \left[\sum_{n=1}^{N} r_n^2 \right]^{\frac{1}{2}} \tag{22}$$

$$\|\bar{R}\|_\infty = \max_{1 \leq n \leq N} |r_n| \tag{23}$$

The advantage of formulating the problem in the above manner is that efficient algorithms have been reported in the mathematical literature for solving the system (19) subject to any of the above ℓ_1, ℓ_2 or ℓ_∞ norms. The details of such algorithms will not be reproduced here as they are available in the references given below. The method associated with the ℓ_1 norm is described in [7] and [8] and implemented in [9], while that for the ℓ_2 norm is available in [10]. Finally, [11] gives the details for the ℓ_∞ case, and is implemented in [12].

8.5.3 Observations, Examples and Further Discussion

The excitation matching approach has been exercised for a large, though limited, number of different cases. Detailed examination of these results reveals that the ℓ_∞ norm always results in both the poorest sidelobe performance and broadest beamwidth. The sidelobes obtained through use of the ℓ_1 norm are consistently higher than those for the ℓ_2 norm. The reason for the superior performance observed for the ℓ_2 norm appears to be that it never attempts to force the compromise difference beamwidth to be narrower than that of the independently optimum difference pattern, and allows a natural

increase in this beamwidth when sub-arraying is used. On the other hand, the beamwidths of the ℓ_1 norm solution are in many cases narrower than those of the independent pattern; hence the poorer sidelobe behaviour.

When sub-arraying is used, the selection of a particular configuration is an additional design variable. There is a considerble advantage therefore in the fact that for the excitation matching approach a known sum pattern is kept fixed and only the difference pattern performance adjusted. This corresponds closely to what is usually done in practice.

The array of Table 8.1 will be used to illustrate the application of the excitation matching procedure. In all cases the independently optimum sum excitation set will be kept fixed and the sub-array weights used to adjust those for the difference mode. Three different sub-array configurations have been selected, as specified in Table 8.2.

TABLE 8.2 : Sub-array configurations.

CONFIGURATION	Q	K_1	K_2	K_3	K_4	K_5
# 1	5	2	2	2	2	2
# 2	5	1	1	2	5	1
# 3	3	3	4	3	-	-

The first configuration represents the case of paired sub-arraying over the antenna. Configuration # 2 has the same number of sub-arrays as that of the first, but a different number of elements per sub-array. For this configuration the number of elements per sub-array was chosen by observing the difference $|a_i^s - a_i^d|$ between each of the excitations of the independently optimum arrays of Table 8.1, and including in the same sub-array those elements with $|a_i^s - a_i^d|$ falling within certain intervals. The third configuration is an example of the

limited number of sub-arrays that might be used with a typical small monopulse antenna, and corresponds to a six-module feed network. It is not suggested here that the above sub-array configurations are particularly desirable. They have been selected, rather, in order that all the characteristics of the much larger number of cases actually considered be exhibited.

Only the results obtained using the ℓ_2 norm are presented, because of the superior performance obtained. These results are shown, in order, for the three configurations, in Figs. 8.6, 8.7 and 8.8. Configuration # 2, which has the same number of sub-arrays as configuration # 1, has the better overall performance. However, it should be remembered that if the element patterns of the array elements are taken into consideration, it may be possible to suppress the sub-array grating lobe effect in the end-fire direction in Fig. 8.6. If this is possible, configuration # 1 gives a very good result if it is remembered that only the five sub-array weights are adjusted instead of all ten elements.

The results shown in Fig. 8.8 for configuration # 3 appear to be open to improvement if the excitation matching were done with a sidelobe constraint imposed. Gill et. al. [3, p. 180] show that the least squares (ℓ_2) solution of a system of over-determined linear simultaneous equations subject to a set of constraints can indeed be formulated as a constrained quadratic programming problem. In particular, the least squares solution of any over-determined system of the form,

$$[S][X] = [P] \tag{24}$$

say, subject to a set of general linear constraints

$$[E][X] \leq [V] \tag{25}$$

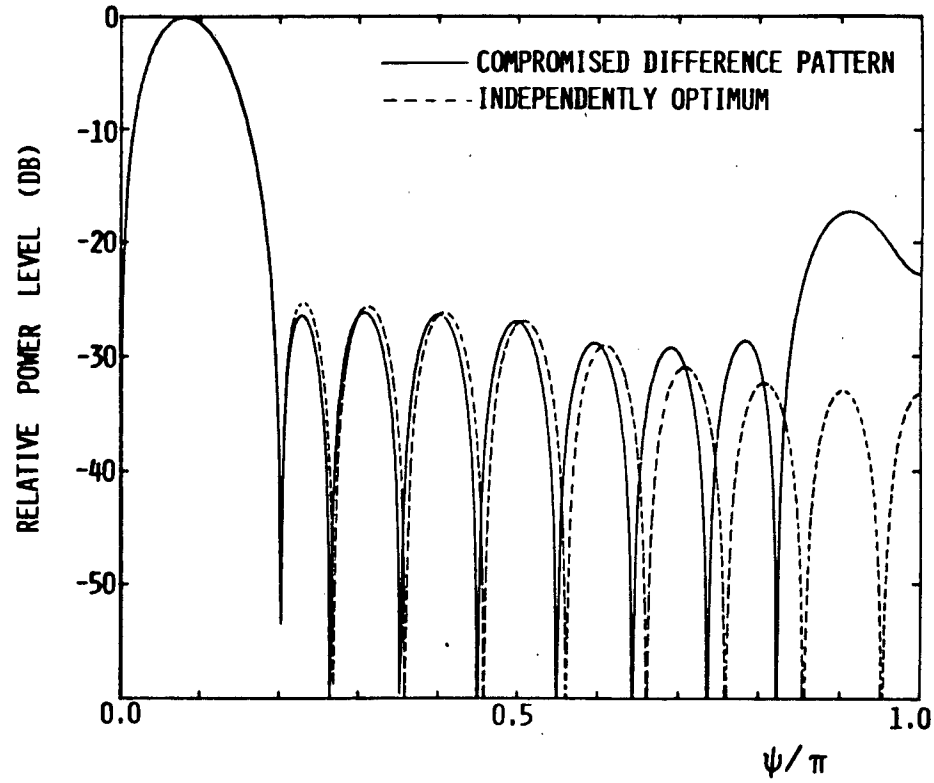

FIGURE 8.6 EXCITATION MATCHED DIFFERENCE PATTERN (SUB-ARRAY CONFIGURATION 1)

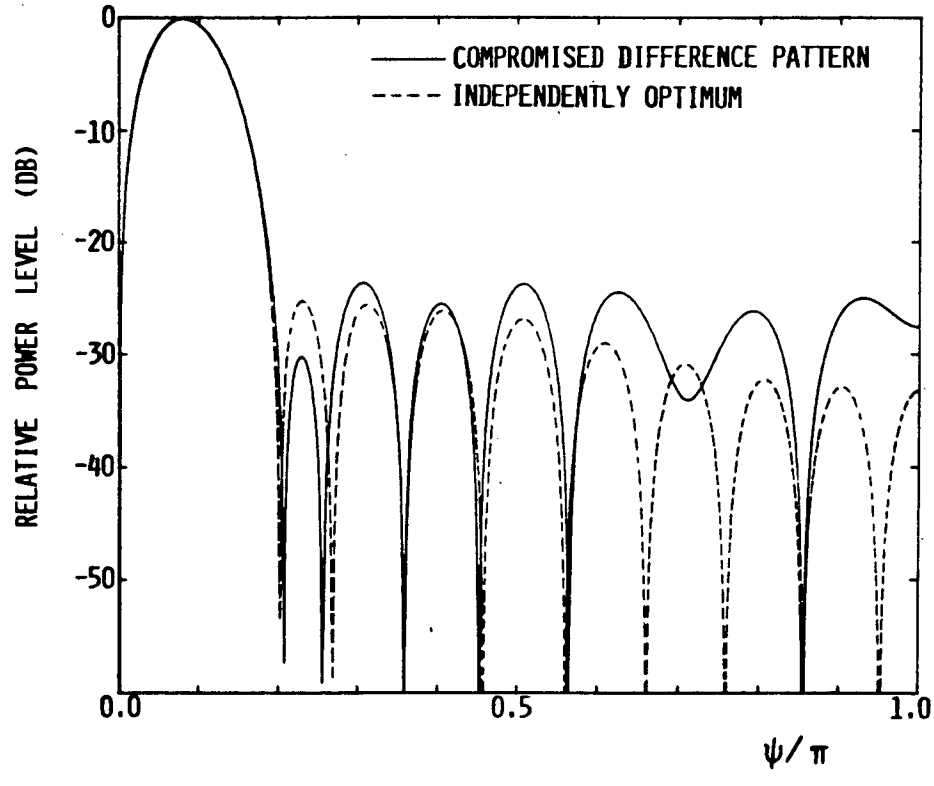

FIGURE 8.7 EXCITATION MATCHED DIFFERENCE PATTERN (SUB-ARRAY CONFIGURATION 2)

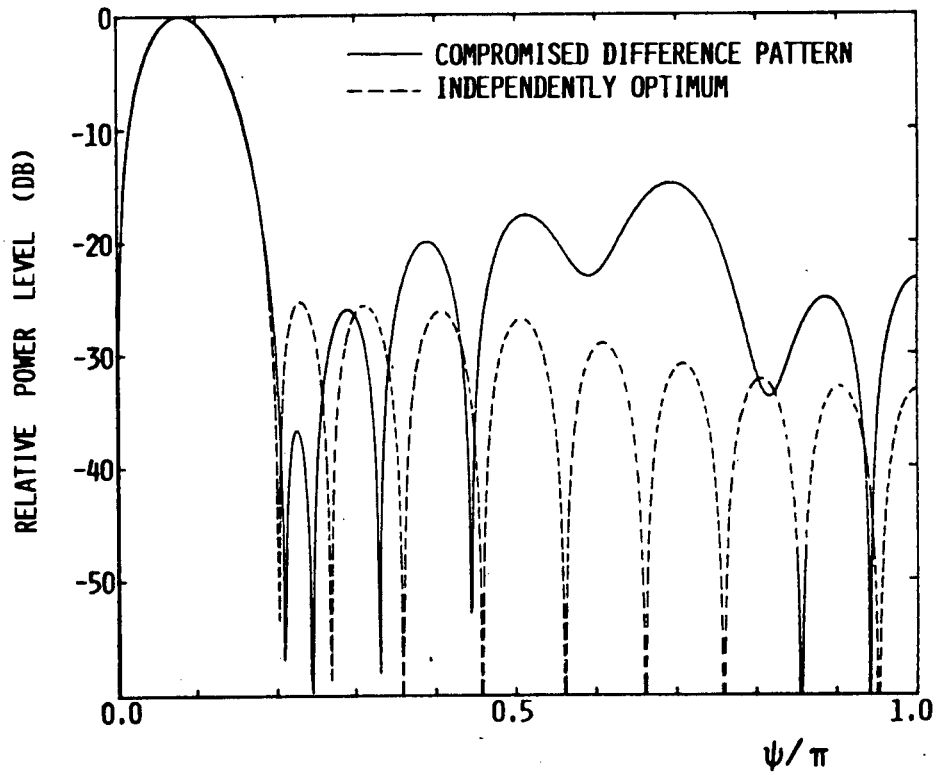

FIGURE 8.8 EXCITATION MATCHED DIFFERENCE PATTERN (SUB-ARRAY CONFIGURATION 3)

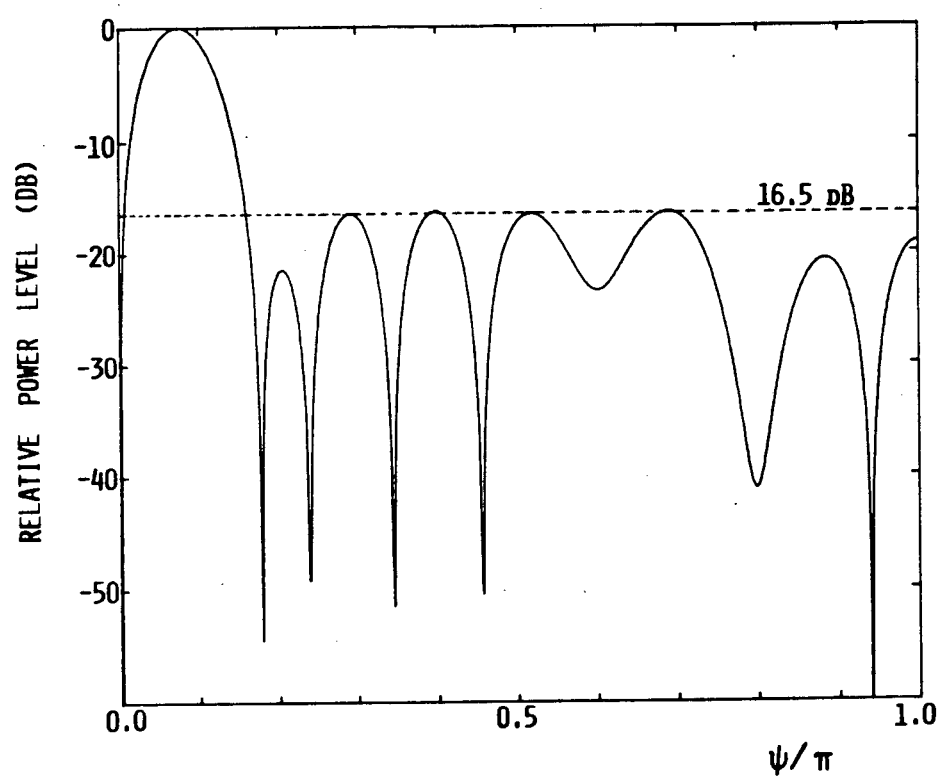

FIGURE 8.9 CONSTRAINED EXCITATION MATCHED DIFFERENCE PATTERN (SUB-ARRAY CONFIGURATION 3)

is equivalent to the quadratic programming problem,

$$\text{minimise} \qquad \{[H]^T[X] + [X]^T[G]\{X]\}$$

$$\text{subject to} \qquad [E][X] \leq [V] \tag{26}$$

$$\text{where} \qquad [G] = \frac{1}{2}[S]^T[S]$$

$$\text{and} \qquad [H] = [S]^T[P]$$

If this is applied to the problem at hand, with $[X]$ the vector of unknown sub-array weights, the system of excitation matching equations (19) can be solved in the ℓ_2 sense, subject to the set of sidelobe constraints given in equation (16). Only the difference pattern constraints are utilised of course, since the independently optimum sum mode excitations are unaltered. The initial constraint angles $\{\gamma_r\}$ are chosen using the information on the space factor zeros of the independently optimum difference pattern as suggested in Section 8.4.3. The above constrained least squares approach has been implemented using the routine E04NAF [4]. When applied to the configurations # 1 and # 2, little improvement in the sidelobe level performance could be obtained, implying that these were near to the best compromise in the first place. For configuration # 3 enforcement of sidelobe constraints showed that for a feasible solution these could be reduced only slightly to the 16.5 dB level but no further. The resulting pattern is shown in Fig. 8.9. The peak sidelobe of Fig. 8.8 has been lowered and the central sidelobes raised by a small amount. In other words, the unconstrained solution is itself close to the final answer for the sub-array weights which provide the best compromise difference pattern. Application of the constraints does some "fine-tuning".

The conclusions reached from the above observations are that the application of excitation matching with the ℓ_2 norm provides near-optimum compromised difference mode solutions for a specified sub-array geometry, array size and independently optimum set of sum excitations. Such solutions should be obtained with the set of sidelobe constraints applied, and the algorithm executed reapeatedly, each time lowering the sidelobe level factor until a feasible solution is no longer possible. The last feasible solution (set of sub-array weights) is then the best solution of the simultaneous synthesis problem.

With the first constraint angle set equal to the first null of the independently optimum difference pattern (i.e. $\gamma_1 = \psi_1^d$), the beamwidth of the compromise pattern is approximately that of the independently optimum one. The above process then indicates what the lowest sidelobe level can be under these beamwidth conditions. Alternatively, the set of constraint angles can be shifted outward (if some beamwidth increase in the compromise pattern is permitted) and the process repeated to see whether lower sidelobes can be obtained. The same care must be taken as was noted in Section 8.4.3. The constraint shifting process was not applied to the examples given in this section.

There is no reason why the excitation matching may not be performed with the independently optimum set of difference excitations $\{a_i^d\}$ kept fixed and a compromised set of sum excitations obtained by adjustment of the sub-array weights. This has not been considered, however, since it is unlikely that the difference performance will take preference over that of the sum in practice.

8.6 MINIMUM NORM SPACE FACTOR ZERO PLACEMENT

8.6.1 Motivation

This approach to simultaneous synthesis tries to take heed of the advice that "in modern antenna work easy mathematics has yielded to good physics ..... distributions should be designed by proper placement of pattern-function zeros ..... which means highly efficient" distributions [5].

Consider again the case of the monopulse array which has optimum sum mode performance (zeros), but a two-module feed network which results in the poor difference pattern performance shown in Fig. 3.8. This difference space factor has minima but no visible zeros. What has happened is that the zeros of the space factor (which is a polynomial and must therefore have a pre-determined number of zeros) have become complex and occur in invisible space. In order to have an optimum difference pattern as well, the excitations for the difference mode of operation would have to be adjusted in order to restore its optimum space factor zero positions. As has been noted repeatedly, this can only be done through use of independent feed networks. If intermediate complexity feed networks are to be used, the fact that the complete sets of optimum zero positions cannot be exactly attained for both sum and difference modes simultaneously (due to the limited number of degrees of freedom), must be accepted. The question then is, for a specified feed network constraint, how can the optimum layout of zero positions be approached "as closely as possible" under the restircted circumstances. This question is taken up below and the concept of minimum norm space factor zero placement introduced.

8.6.2 Formulation

The starting point of the technique to be discussed here is the knowledge of the zeros of the independently optimum sum and difference space factors. This information can be obtained from the techniques presented in the previous chapters. For an array of 2N elements, let the desired sum space factor zeros be the set $\{\psi_i^s\}$, $i = 1,2,3, \cdots N-1$, and those for the difference space factor be $\{\psi_i^d\}$, $i = 1,2, \cdots (N-1)$. Let the set of known local element excitations again be $\{a_1, a_2, \cdots a_N\}$, and the sub-array weights $\{g_1, g_2, \cdots g_Q\}$, Q being the total number of sub-arrays used.

From equations (9) and (10) of Chapter 2, the space factors are,

$$E_s(\psi) = 2 \sum_{n=1}^{N} a_n \cos[(2n-1)\psi/2] \tag{27}$$

$$E_d(\psi) = 2j \sum_{n=1}^{N} g_q(n)\, a_n \sin[(2n-1)\psi/2] \tag{28}$$

The synthesis problem can now be stated as one of determining the set of sub-array weights $\{g_q\}$ such that the system of equations,

$$E_s(\psi_i^s) = 0 \qquad i = 1,2, \cdots (N-1) \tag{29}$$

$$E_d(\psi_i^d) = 0 \qquad i = 1,2, \cdots (N-1) \tag{30}$$

is satisfied in some sense. Note that the zeros $\psi = \pi$ for the sum pattern, and $\psi = 0$ for the difference pattern, need not be explicitly considered since they always satisfy (29) and (30), respectively.

8.6.3 Optimum Sum and Compromised Difference Pattern

Consider the situation for which the set of local excitations is set equal to the set of independently optimal sum excitations. That is,

$$\{a_n\} = \{a_n^s\} \tag{31}$$

$$n = 1,2, \cdots N$$

For this case equations (29) are satisfied exactly. The synthesis problem then becomes one of determining the set of sub-array weights $\{g_q\}$ such that the system of equations (30) is satisfied in some sense. Since only the relative weights are of interest, the Q-th weight may be set equal to unity. The system of equations to be solved then becomes,

$$\sum_{n=1}^{N-K_Q} g_q(n)\, a_n^s \sin[(2n-1)\psi_i^d/2] = -\sum_{n=N-K_Q}^{N} a_n^s \sin[(2n-1)\psi_i^d/2] \tag{32}$$

$$\text{for each } i = 1,2, \cdots (N-1)$$

This is a set of (N-1) equations for the (Q-1) unknowns $\{g_q\}$, $q = 1,2, \cdots (Q-1)$, since g_Q has been assumed to be unity.

8.6.4 Optimum Difference and Compromised Sum Pattern

If the set of independently optimal difference excitations is taken as the set of local excitations, that is

$$\{a_n\} = \{a_n^d\} \tag{33}$$

$$n = 1,2, \cdots N$$

then equations (30) are satisfied exactly, and only the system (29) need be enforced in some sense. Thus, with $g_Q = 1$ as before, the system of equations,

$$\sum_{n=1}^{N-K_Q} g_q(n)\, a_n^d \cos[(2n-1)\psi_i^s/2] = -\sum_{n=N-K_Q}^{N} a_n^d \cos[(2n-1)\psi_i^s/2]$$

$$i = 1,2, \cdots (N-1)$$

must be solved for the sub-array weights $\{g_q\}$, $q = 1,2, \cdots (Q-1)$.

8.6.5 Application of Minimum Norm Space Factor Zero Placement

Only the case of optimum sum and compromised differene pattern performance has been considered, as formulated in Section 8.6.3. The algorithms and routines used for "solving" the system of equations (32) through minimisation of one or other norm, without constraints, are identical to those identified in the section on excitation matching. Use of the ℓ_2 norm, with constraints applied, was effected via the quadratic programming procedure also used with the excitation matching method. For the present case of minimum norm space factor

zero placement the ℓ_1 norm was also used with constraints. Though not utilised in Section 8.5, the method of Conn et. al. [7,8,9] does permit inclusion of constraints, and this has been used here.

For the present method, if sidelobe constraints are applied, an additional constraint is needed. It is necessary to keep the difference pattern primary lobe maximum fixed, lest the sub-array weights be adjusted in a manner which depresses this lobe along with the sidelobes. The condition used here to accomplish this is,

$$E_d(\psi = \psi_o) = 1$$

where ψ_o is the position of the difference lobe maximum. Since this is not known a priori, some iteration like that used in Section 4.1 is required. The solutions obtained have been found to be insensitive to small errors in the value of ψ_o used. The above condition is a linear constraint,

$$\sum_{q=1}^{Q} \sum_{n=K_{q-1}}^{K_q} a_n^s \, g_q(n) \, f_n^d(\psi_o) = 1$$

and is equivalent to normalising the pattern to its maximum value. A number of statements consistent with the results obtained for a large number of problems to which the method has been applied can be made:

(a) Application of the ℓ_∞ norm results in difference patterns with higher sidelobes than is obtained with the other two norms.

(b) For the unconstrained solutions, whether the ℓ_1 or ℓ_2 norm provides the most satisfying compromised difference pattern is dependent on the sub-array configuration under consideration.

(c) For the constrained solutions (finding the lowest sidelobe level which permits a feasible solution for a prescribed set of constraint angles) the solutions obtained using the ℓ_1 and ℓ_2 norms are almost identical. These are furthermore little different from the constrained excitation matching results. This consistency is indicative of the fact that the solutions found by the two methods are indeed the "best compromises".

For the constrained minimum norm space factor zero placement method, the constraints are applied in the same manner as in Section 8.4 and 8.5, with the sidelobe constraints of the form of equation (16) enforced at the zero positions $\{\psi_i^d\}$ of the independently optimum difference pattern, and at intermediate angles. Keeping $\gamma_1 = \psi_1^d$ fixed ensures that a compromise difference pattern is obtained with a beamwidth close to that of the independently optimum case. If beamwidth broadening is acceptable, the constraint angles can be shifted outward.

In order to facilitate comparison, an example identical to the third one described in Section 8.5.3 is used, with $\{a_i^s\}$ and $\{\psi_i^d\}$ obtained from Table 8.1. Fig. 8.10 depicts the resultant pattern when the ℓ_2 norm is used, without constraints, for the sub-array configuration # 3. On the other hand, the unconstrained ℓ_1 solution is that shown in Fig. 8.11. With the first constraint angle equal to ψ_1^d, and the constrained ℓ_1 solution sought, the pattern in Fig. 8.12 is obtained. This is of the same form as that of Fig. 8.10, except for a very slight decrease in the level of the highest sidelobes. Application of a constrained ℓ_2 norm solution alters Fig. 8.10 to a pattern that is for all practical purposes identical to that in Fig. 8.11. Finally, comparison of Fig. 8.11 and 8.9 completes the illustration of statement (c) given above.

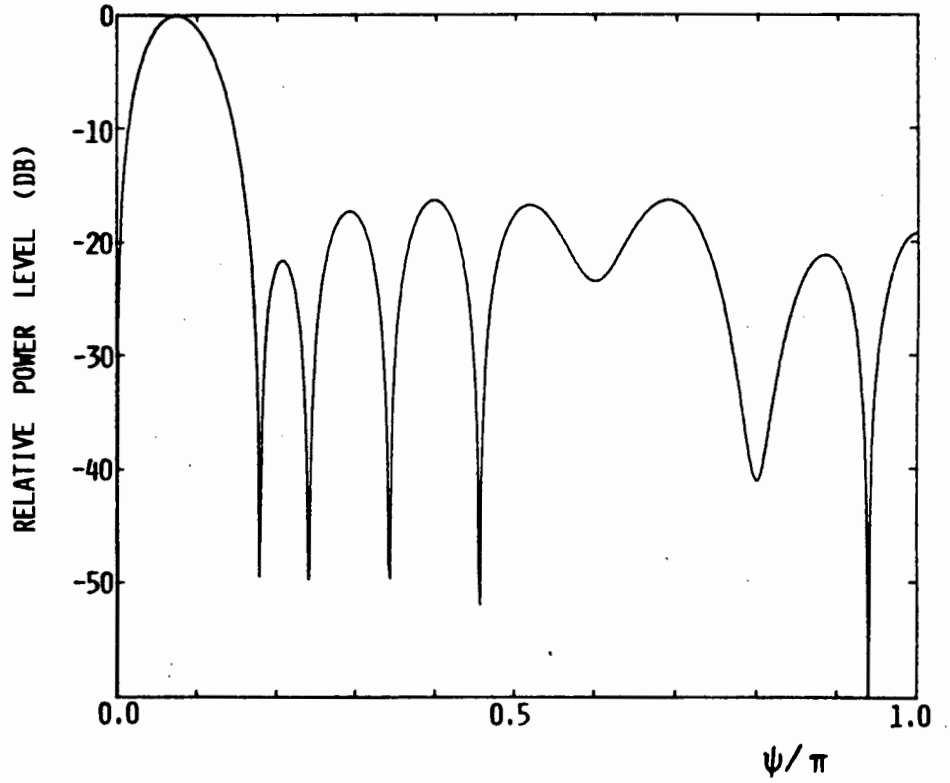

FIGURE 8.10 DIFFERENCE PATTERN SYNTHESISED USING L2 NORM ZERO PLACEMENT FOR CONFIGURATION 3 (UNCONSTRAINED)

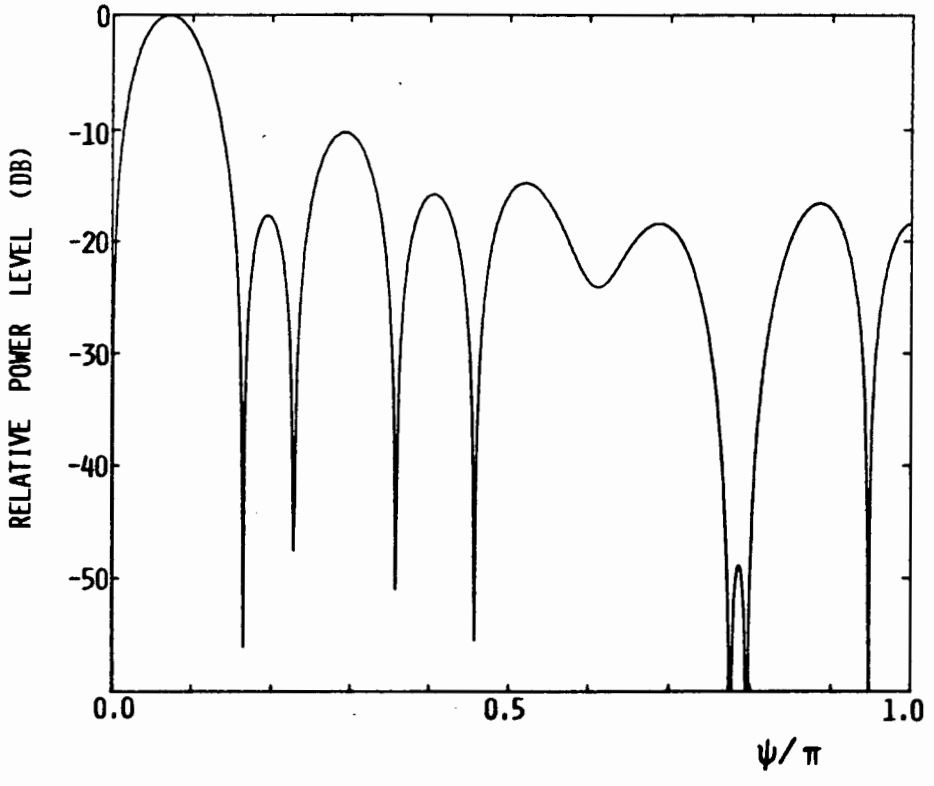

FIGURE 8.11 DIFFERENCE PATTERN SYNTHESISED USING L1 NORM ZERO PLACEMENT FOR CONFIGURATION 3 (UNCONSTRAINED)

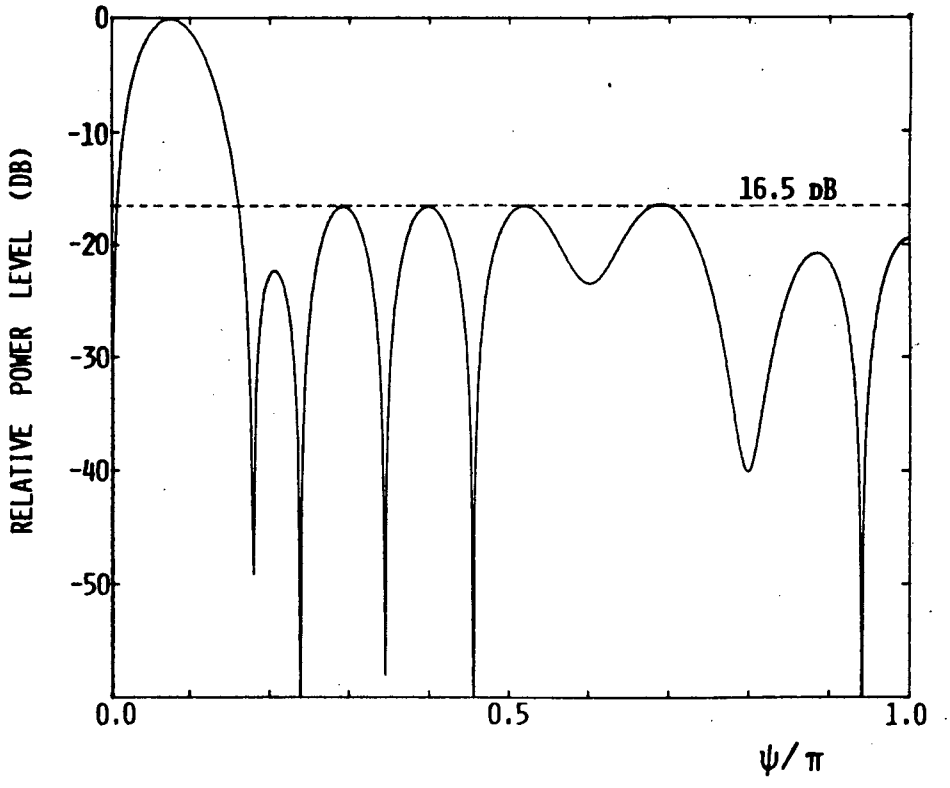

FIGURE 8.12 DIFFERENCE PATTERN SYNTHESISED USING L1 NORM ZERO PLACEMENT FOR CONFIGURATION 3 (CONSTRAINED)

8.7 CONCLUSIONS

The increased complexity and generality of the simultaneous synthesis of sum and difference patterns does not facilitate development of "deterministic" procedures like those presented for independent synthesis in Chapters 4 to 7. Instead interactive numerical procedures must be used; this appears to be a characteristic of all multi-criteria optimisation methods reported in the mathematical literature [6]. Some form of man-machine interaction is essential.

Under the restrictions of a two-module feed network the quadratic programming formualtion of Section 8.4 can be used interactively for studying simultaneous synthesis compromises and establishing bounds. Essential to the method is the introduction in this work of a composite objective function and separate subsets of sidelobe constraints for the sum and difference cases, in order to avoid a confliciting constraint set.

Improved simultaneous performance can be achieved through use of sub-arraying. Two different methods for simultaneous synthesis under such conditions have been presented. These have been termed excitation matching and minimum norm space factor zero placement, and make maximum use of information provided by the independent synthesis techniques. The advantage of these approaches is that the independently optimum sum characteristics are kept fixed and the sub-array weights adjusted, subject to a set of sidelobe constraints, to find the "best compromise" difference performance. The fact that both techniques, one working with the excitations and the other with the space factor zeros, give virtually identical results, lends support to the conclusion that these are the best compromises for a given sub-array configuration.

Since no methods which address the simultaneous synthesis problem in a systematic manner have appeared in the literature the above procedures satisfy a much needed requirement in this area.

8.8 REFERENCES

[1] O. Einarsson, "Optimisation of planar arrays", IEEE Trans. Antennas Prop., Vol. AP-27, No. 1, pp. 86-92, Jan. 1979.

[2] J.W. Bandler, "Optimisation methods for computer-aided design", IEEE Trans. Microwave Theory Tech., Vol. MTT-17, No. 8, pp. 533-552, Aug. 1969.

[3] P.E. Gill, W. Murray and M.H. Wright, Practical Optimisation, (Academic Press, 1981).

[4] Numerical Algorithms Group (NAG), Mathematical Software Library, Oxfordshire, England.

[5] A.W. Rudge et. al. (Edit.), The Handbook of Antenna Design, Vol. 2, Chap. 9 (by R.C. Hansen), (Peter Peregrinus Ltd., London, 1982).

[6] S. Zionts and J. Wallenius, "An interactive programming method for solving the multiple criteria problem", Management Science, Vol. 22, No. 6, pp. 652-663, Feb. 1976.

[7] R.H. Bartels, A.R. Conn and J.W. Sinclair, "Minimisation techniques for piecewise differentiable functions - the ℓ_1 solution to an overdetermined linear system", SIAM Journal of Numerical Analysis, Vol. 15, pp. 224-241, 1978.

[8] A.R. Conn and T. Pietrzykowski, "A penalty-function method converging directly to a constrained optimum", SIAM Journal of Numerical Analysis, Vol. 14, pp. 348-375, 1977.

[9] Numerical Algoirthms Group (NAG), Mathematical Software Library (FORTRAN Routine E02GBF), Oxfordshire, England.

[10] Numerical Algorithms Group (NAG), Mathematical Software Library (FORTRAN Routine F04JGF), Oxfordshire, England.

[11] I. Barrodale and C. Philipps, "Solution of an overdetermined system of linear equations in the Chebyshev norm", ACM Trans. Math. Software, Vol. 1, No. 3, pp. 240-270, Sept. 1975.

[12] Numerical Algorithms Group (NAG), Mathematical Software Library (FORTRAN Routine E02GCF), Oxfordshire, England.

CHAPTER 9

GENERAL CONCLUSIONS

A number of problems associated with the synthesis of monopulse antenna arrays have been dealt with. The concept of array synthesis by correct space factor zero placement has been reinforced. The information presented permits the synthesis of high performance monopulse arrays. The original contributions to array theory which have been presented in this thesis are:

(a) The development of the Zolotarev polynomial synthesis technique for difference patterns. This method can be used for the exact determination of the optimum excitations and space factor zeros for a pattern with maximum normalised boresight slope and minimum beamwidth, for a given maximum sidelobe level.

(b) The formulation of a systematic direct method for synthesising discrete arrays with difference patterns of specified maximum sidelobe level and arbitrary sidelobe envelope taper. The Zolotarev space factor zeros serve as the starting point for this direct synthesis procedure.

(c) The development of a direct discrete array synthesis technique for sum patterns with arbitrary sidelobe envelope taper. This is a generalisation of the Villeneuve distribution.

(d) The application of constrained numerical optimisation to the simultaneous synthesis of sum and difference patterns subject to given feed network constraints.

In addition a number of results which could not be located in the open literature, have been presented. These include,

(a) Explicit expressions for certain performance indices of symmetrically and anti-symmetrically excited linear arrays, and the formulation of the problem for such arrays in a unified manner which connects the approximation and optimisation theory approaches to array synthesis.

(b) Information on the discrete difference distributions required to provide (without pattern constraints) either maximum possible directivity D_d^{max}, or maximum possible normalised boresight slope K_o, and their comparison to the continuous distribution case. (These results also provide the standards against which to measure array performance and are not readily available elsewhere).

The above contributions must now be placed in the context of the overall monopulse array synthesis problem. Such a design problem is a multi-objective one where, depending on the specific application, certain performance indices may be more important than others.

Consider first the situation in which the sum mode performance must take preference over the difference, as has often been the case in the past. If sum mode directivity is to be maximised at all costs, then a uniform set of excitations should be used. Usually the sidelobe levels for this distribution are too high. The alternative, for the narrowest beamwidth obtainable under a given maximum sidelobe specification, is the Dolph-Chebyshev distribution developed in 1946. For a slightly increased directivity, with the farther-out sidelobes tapering off from the first one which is at the specified maximum level, the Villeneuve distribution can be used. This was first published by Villeneuve in 1984, and uses as its starting point the zeros of an associated Dolph-Chebyshev space factor.

In the ever-increasing number of cases where not only the allowed level of the maximum (first) sidelobe level but also the more remote sidelobe levels or simply the sidelobe envelope taper, is a specification, the generalised Villeneuve distribution developed in Chapter 7 of this thesis can be applied. Further reasons for using this distribution are given in that chapter.

Should the difference performance take preference over the sum, a different path has to be followed. If difference directivity is to be maximised at all costs, the methods developed in Section 4.1.2 can be used. On the other hand, the methods presented in Section 4.1.3 are applicable if the maximum possible normalised boresight slope is desired irrespective of the sidelobe levels obtruded. In the majority of designs though, sidelobe levels are important. The synthesis of difference distributions providing optimum slope and beamwidth characteristics subject to a maximum allowable sidelobe level constraint is possible via the Zolotarev polynomial procedure developed for the first time in Chapters 4 and 5 of this thesis. This is the difference mode analogue of the Dolph-Chebyshev distribution. For a number of useful cases the required element excitations can be obtained directly from the tables published in Appendix II. Alternatively the modified Zolotarev distributions with arbitrary sidelobe envelope tapers can be applied. The details of the latter approach are worked out in Chapter 6 and its significant advantages indicated. This technique utilises the Zolotarev zeros as a point of departure.

If there are no restrictions on the complexity of the array feed network to be used, then the sum and difference synthesis can be considered separately, as outlined above, and independent networks used to set up the desired excitation sets for each mode of operation. Should this not be the case, the methods of simultaneous synthesis which are the subject of Chapter 8, can be followed. These provide the array designer with interactive procedures for obtaining good compromises between sum and difference performance, given the feed network constraints.

For some time now a set of exact synthesis techniques for monopulse arrays of discrete elements, as complete as that which exists for continuous line-sources, has not been available. With the suite of new techniques presented in Chapters 4 to 7 this is no longer the case. These not only complete an aspect important in antenna theory, but, together with the expressions for computing array performance indices given in Chapter 2, and the numerical simultaneous synthesis procedures developed in Chapter 8, have been implemented as a set of computer codes which form a very useful computer-aided design tool at the synthesis stage of monopulse antenna development.

APPENDIX I

APPROXIMATION AND OPTIMISATION

1 INTRODUCTION

The mathematical theories of approximation and optimisation are both well-established in the literature. However, a summary of some pertinent concepts is given here in the interests of completeness.

2 THE CONCEPT OF A NORM

Essential to approximation and optimisation is the concept of a norm. The definition of a norm, which has to satisfy a number of properties to be valid [1, p. 1], is a measure of the "closeness" of two functions or vectors. In any situation there may be many possible definitions for a norm. However, there are a number of standard types which have been adopted (each for some good reason) and which need to be discussed.

Consider two functions $f(x)$ and $g(x)$ defined over the interval $[a,b]$. Let the residual $r(x) = f(x) - g(x)$, and let $\|r(x)\|$ denote the norm of $r(x)$. Then the following norms can be defined:

The least p-th norm (ℓ_p norm),

$$\|r(x)\| = \left[\int_a^b |r(x)|^p \right]^{\frac{1}{p}}$$

Its application in the microwave circuit optimisation context is described by Bandler [2].

If $p = 2$, the above becomes what is known as the least squares norm (ℓ_2 norm).

If $p = 1$, $\|r(x)\|$ is called the ℓ_1 norm.

If $p \to \infty$, the above becomes

$$\|r(x)\| = \max_{a \leq x \leq b} |r(x)|$$

which is referred to as the maximum, uniform, ℓ_∞ or Chebyshev norm. The single vertical lines denote the usual modulus operation.

The ℓ_∞ norm thus measures the maximum deviation that occurs between the two functions $f(x)$ and $g(x)$. On the other hand, ℓ_2 estimates the total deviation over the whole interval. A small value of $\|r(x)\|_2$ does not guarantee that the deviation is not very large at certain isolated points. As p increases, ℓ_p approaches the Chebyshev norm more closely. The particular norm to be used depends on the application.

Although the above definitions have been given for the space of continuous functions of a single variable, they can of course be generalised to cases for which there are many independent variables. Such norms may also be defined for n-dimensional vector spaces and matrices.

Consider an n-dimensional vector space with elements (column vectors) denoted by $\vec{X}$ or $[X]$, with

$$[X] = [x_1 \; x_2 \; \cdots \; x_n]^T$$

where the transpose is used simply for economy of space.

Functions of the form $F(\vec{X})$ can be defined on this vector space. Vector norms may then be defined as follows [7].

Let $\vec{X}$ and $\vec{Y}$ be elements of the vector space, and define the residual vector $\vec{R} = \vec{X} - \vec{Y}$, so that

$$\vec{R} = [r_1 \quad r_2 \cdots r_n]^T$$

where $r_i = x_i - y_i$.

The norms measuring the "closeness" of the vector $\vec{X}$ and $\vec{Y}$ are then

(a) $$\|\vec{R}\|_p = \left[\sum_{i=1}^{n} |r_i|^p \right]^{\frac{1}{p}}$$

(b) $$\|\vec{R}\|_2 = \left[\sum_{i=1}^{n} |r_i|^2 \right]^{\frac{1}{2}}$$

(c) $$\|\vec{R}\|_1 = \sum_{i=1}^{n} |r_i|$$

(d) $$\|\vec{R}\|_\infty = \max_{0 \leq i \leq n} |r_i|$$

3 APPROXIMATION THEORY

The subject of approximate representation of functions in terms of polynomials derives from the work of the Russian mathematician Chebyshev (1821-1894) and his pupils Korkine, Zolotarev and Markoff. Since that time it has become the independent discipline of "approximation theory" [1,3] or "the constructive theory of functions" [4]. The result has been the derivation of many different special types of polynomials with properties of tremendous significance in the solution of engineering problems. The modern theory is no longer limited to the consideration of only polynomials as the approximating functions.

The fundamental theorem of algebra [4, p. 9] proves that every polynomial has a zero. It then follows that

(i) A polynomial $p_n(x)$ of degree n has at most n zeros.

(ii) A polynomial $p_n(x)$ of degree n is determined uniquely by its value at n+1 distinct points, $x_0, x_1, x_2, \cdots x_n$.

Two further theorems which will be quoted without proof are those due to Weierstrass and Borel respectively [5, p. 18]:

(i) If f(x) is a function defined on $x \in [a,b]$, then given $\varepsilon > 0$, there is a polynomial $p_n(x)$ such that $|p_n(x) - f(x)| \leq \varepsilon$ for $x \in [a,b]$.

(ii) If n is a given integer, there is a unique polynomial $p_n(x)$ of degree n or less such that

$$\|p_n(x) - f(x)\|_\infty \leq \|q_n(x) - f(x)\|_\infty$$

for every polynomial $q_n(x)$ of degree n or less.

The existence of a best (in the ℓ_∞ norm sense) approximating polynomial having been established, it is natural to ask how to find this $p_n(x)$ in any given case. There is unfortunately no known closed form procedure which, for general $f(x)$ and interval $[a,b]$, can be used to find the best approximaing polynomial $p_n(x)$ in a finite number of steps.

The best approximating polynomial $p_n(x)$ is that which minimises the maximum norm (and thus the maximum value of the difference $|p_n(x) - f(x)|$). It is therefore referred to as the minimax problem.

A particular but important case, that for which $f(x) = 0$ and $[a,b] = [-1,1]$, is dealt with in a theorem due to Chebyshev [5, p. 28]. It proves that for this special case the best approximating polynomial is the Chebyshev polynomial $T_n(x)$. The use of this polynomial is central to the synthesis of optimum sum patterns of linear arrays, and is described in Section 3.2.2. A second particular case for which analytical solutions have been obtained is that of the Zolotarev polynomial function, which forms the basis of the synthesis procedure developed in Chapter 4.

Numerical methods exist for finding $p_n(x)$ for arbitrary $f(x)$ if the minimax condition is imposed at only a finite number of points at a time. The earliest approaches were the Remez exchange algorithms, details of which are given by Jones [5, p. 19] and Rivlin [1, p. 136]. Such exchange algorithms have largely been superseded by reformulation of the minimax problem as a linear programming one. The latter technique is mentioned later in this appendix. A Remez exchange algorithm application to the difference pattern problem is referenced in Section 3.3.3.

4 OPTIMISATION THEORY

Optimisation and approximation theory are intimately related. The subject of optimisation covers a wider range of problems and approaches, however, and could be considered to contain that of approximation entirely. This is not usually done though, and this practice has been adhered to in this summary.

In Chapter 8 consistent use is made of optimisation algorithms. Wherever possible the advice of Gill, et. al. [7] has been followed. They correctly maintain that because of the steady progress in optimisation methods, anyone who wishes to solve an applied optimisation problem should not start from scratch and devise his own optimisation method or write his own implementation, but should formulate the problem at hand in such a way that selected routines from high-quality mathematical software libraries can be used. However, optimisation codes cannot be used effectively if a "black-box" approach is adopted. An understanding of the essence of a particular technique used is necessary in order to apply and adapt existing software properly. This and a knowledge of a broad classification of optimisation problems in order of increasing complexity is also useful to prevent the use of a method that is of a more general nature than is in fact necessary, since increased complexity also means decreased reliability (relatively speaking) and longer execution times [7. Chap. 8).

The literature on optimisation is voluminous indeed. The sources used for the applications in Chapter 8 were the texts by Gill, et. al. [7], Walsh [8] and Noble [9], the papers by Conn, et. al.. [10,11] and Barrodale et. al. [12,13], and the NAG library of mathematical software [16].

The optimisation problem is one of minimising or maximising a given function, $F(\bar{x})$, where $\bar{X} = [x_1 \; x_2 \; \cdots \; x_n]^T$. $F(\bar{X})$ is called the objective function and the column vector $\bar{X}$ represents a set of independent parameters (variables) of which F is a function. For most physical problems such minimisation (maximisation) must be done subject to a set of constraints imposed on $\bar{X}$, usually for reasons of a practical nature [14,15]. The existence or absence of such constraints determines whether a problem is of the constrained or unconstrained type. The methods used in Section 4.1 are of the unconstrained variety. A flow chart giving an overall arrangement, in order of increasing complexity, of the subject of optimisation from a user's point of view is shown in Fig. 1. It should be pointed out that this is not a standard classification, but rather one based on the experience of the present author in applying optimisation theory to array synthesis.

Problems of the type (1) and (2) are called Linear Programming problems, while (3) and (4) are Quadratic Programming problems. Many algorithms exist for solving such problems, most of them based on what is known as the simplex method, or variations thereof [7,8]. For the linear and quadratic programming problems formulated in Chapter 8 use has been made of the routine E04NAF available from the Numerical Algorithms Group (NAG) library of mathematical software [16]. For the linear programming problem the objective function is of the form $F(\bar{X}) = \bar{C}^T\bar{X}$, where $\bar{C}^T$ is a constant vector, equal to $\nabla F(\bar{X})$, the gradient of $F(\bar{X})$. The gradient of any function $F(\bar{X})$ is of course defined as,

$$\nabla F(\bar{X}) = \begin{bmatrix} \partial F/\partial x_1 \\ \partial F/\partial x_2 \\ \vdots \\ \partial F/\partial x_n \end{bmatrix}$$

The Hessian matrix of a function $F(\bar{X})$, denoted by [G] say, is defined as [7],

$$[G] \triangleq \begin{bmatrix} \partial^2 F/\partial x_1^2 & \cdots & \partial^2 F/\partial x_1 \partial x_n \\ \vdots & & \vdots \\ \partial^2 F/\partial x_n \partial x_1 & \cdots & \partial^2 F/\partial x_n \end{bmatrix}$$

If the Hessian matrix of F is constant, then F is a quadratic function which can be written in the form (quadratic programming problem),

$$F(\bar{X}) = \frac{1}{2} \bar{X}^T [G] \bar{X} + \bar{C}^T \bar{X}$$

Specification of the (constant) quantities [G] and $\bar{C}$ completely defines $F(\bar{X})$.

Problems of the type (5) occur in Section 4.1 and have been solved numerically using the NAG routine E04JAF, which is based on what are referred to as quasi-Newton methods [7, pp. 116-127].

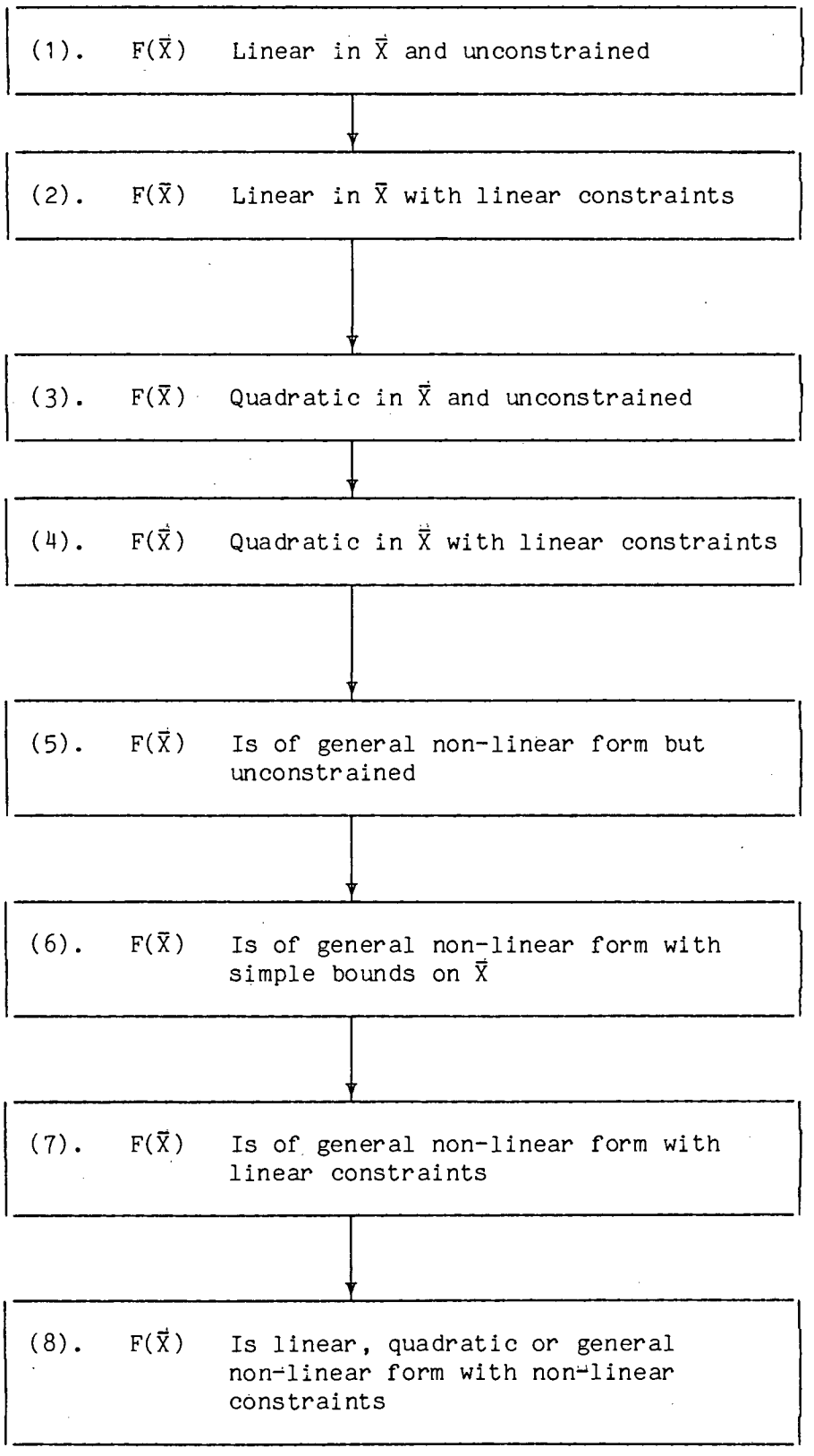

FIGURE 1 : Flowchart of optimisation problems in order of increasing complexity.

5 REFERENCES

[1] T.J. Rivlin, An Introduction to the Approximation of Functions, (Dover Publ. Inc. 1969).

[2] J.W. Bandler, "Optimisation methods for computer-aided design", IEEE Trans. Microwave Theory Tech., Vol. MTT-17, No. 8, pp. 533-552, Aug. 1969.

[3] G. Meinardus, Approximation of Functions : Theory and Numerical Methods, (Springer-Verlag, 1967).

[4] J. Todd, Introduction to the Constructive Theory of Functions, (Academic Press, 1963).

[5] D.S. Jones, Methods in Electromagnetic Wave Propagation, (Oxford University Press, 1979).

[6] L. Fox and I.B. Parker, Chebyshev Polynomials in Numerical Analysis, (Oxford University Press, 1968).

[7] P.E. Gill, W. Murray and M.H. Wright, Practical Optimisation, (Academic Press, 1981).

[8] G.R. Walsh, Methods of Optimisation, (John Wiley and Sons, 1975).

[9] B. Noble, Applied Linear Algebra, (Prentice Hall Inc., 1969).

[10] A.R. Conn and T Pietrzykowski, "A penalty function method converging directly to a constrained optimum", SIAM Journal of Numerical Analysis, Vol. 14, pp. 348-375, 1977.

[11] R.H. Bartels, A.R. Conn and J.W. Sinclair, "Minimisation techniques for piecewise differentiable functions - the ℓ_1 solution to an overdetermined linear system", SIAM Journal of Numerical Analysis, Vol. 15, pp. 224-241, 1978.

[12] I. Barrodale and C. Phillips, "Solution of an overdetermined system of linear equations in the Chebyshev norm", ACM Trans. Math. Software, Vol. 1, No. 3, pp. 264-270, Sept. 1975.

[13] F.D.K. Roberts and I. Barrodale, "An algorithm for discrete Chebyshev linear approximation with linear constraints", Int. J. Num. Meth. Eng., Vol. 15, pp. 797-807, 1980.

[14] G.A. Deschamps and H.S. Cabayan, "Antenna synthesis and solution of inverse problems by regularisation methods", IEEE Trans. Antennas Prop., Vol. AP-20, No. 3, pp. 268-274, May 1972.

[15] D.K. Cheng, "Optimisation techniques for antenna arrays", Proc. IEEE, Vol. 59, No. 12, pp. 1664-1674, Dec. 1971.

[16] Numerical Algorithms Group (NAG), Mathematical Software Library, Oxfordshire, England.

APPENDIX II

TABLES OF DESIGN DATA FOR ZOLOTAREV POLYNOMIAL ARRAYS

TABLE II.1 : Jacobi modulus (k) values for various numbers of elements (2N) and sidelobe ratios (SLR).

SLR \ 2N	10	20	30	40	50	60
15 dB	0.998745828908	0.9985867774745	0.9985589883166	0.9985495421102	0.9985452430448	0.9985429332424
20 dB	0.9996757515225	0.9996208784026	0.9996122308734	0.9996093496527	0.9996080480023	0.9996073511207
25 dB	0.9999156095527	0.9998953160856	0.9998898518608	0.9998880307364	0.9998872079156	0.9998867673677
30 dB	0.9999770191198	0.9999710417524	0.9999701140527	0.9999696784784	0.9999694480226	0.9999693246752
35 dB	0.9999939866708	0.9999919161819	0.9999914923241	0.9999913516146	0.999991288133	0.9999912541684
40 dB	0.9999982703182	0.999996637147	0.9999974904427	0.9999974418081	0.9999974198777	0.9999974081473
50 dB	0.9999998714254	0.9999998067784	0.9999997935154	0.9999997864033	0.9999997831988	0.9999997814853
60 dB	0.9999999911282	0.999999829653	0.999999981613	0.9999999811682	0.9999999809682	0.9999999808614

TABLE II.2 : Sidelobe parameter ζ for various numbers of elements (2N) and sidelobe ratios (SLR).

SLR \ 2N	10	20	30	40	50	60
15 dB	2.90164	2.84979	2.84133	2.83849	2.83721	2.83652
20 dB	3.48912	3.42122	3.41143	3.40821	3.40677	3.40600
25 dB	4.07371	3.98012	3.95802	3.95090	3.94772	3.94603
30 dB	4.63863	4.53823	4.52453	4.51825	4.51496	4.51321
35 dB	5.22089	5.09238	5.07019	5.06306	5.05989	5.05820
40 dB	5.76203	5.62656	5.60040	5.59207	5.58836	5.58639
50 dB	6.89084	6.71394	6.68511	6.67041	6.66394	6.66052
60 dB	8.05199	7.76867	7.73549	7.72511	7.72052	7.71809

TABLES II.3 - II.10

Element Excitations For The Case $d \geq 0.5\ \lambda$

For a Range of Array Sizes (2N) and Sidelobe Ratios (SLR)

TABLE II.3

SIDELOBE RATIO 15 dB						
2N	10	20	30	40	50	60
a_1	0.286771	0.088911	0.042033	0.024339	0.015841	0.011122
a_2	0.763587	0.259548	0.124625	0.072544	0.047328	0.033271
a_3	0.993677	0.409407	0.202862	0.119340	0.078231	0.055137
a_4	0.934697	0.527139	0.274071	0.163828	0.108171	0.076534
a_5	1.000000	0.604817	0.335906	0.205169	0.136787	0.097282
a_6		0.638685	0.386457	0.242609	0.163737	0.117209
a_7		0.629395	0.424331	0.275490	0.188708	0.136150
a_8		0.581715	0.448708	0.303274	0.211421	0.153955
a_9		0.503762	0.459362	0.325551	0.231629	0.170484
a_{10}		1.000000	0.456656	0.342048	0.249132	0.185613
a_{11}			0.441502	0.352636	0.263768	0.199232
a_{12}			0.415299	0.357326	0.275422	0.211249
a_{13}			0.379841	0.356271	0.284028	0.221589
a_{14}			0.337212	0.349753	0.289564	0.230197
a_{15}			1.000000	0.338172	0.292055	0.237035
a_{16}				0.322036	0.291573	0.242084
a_{17}				0.301939	0.288230	0.245344
a_{18}				0.278546	0.282182	0.246835
a_{19}				0.252566	0.273617	0.246593
a_{20}				1.000000	0.262758	0.244673
a_{21}					0.249855	0.241145
a_{22}					0.235180	0.236094
a_{23}					0.219022	0.229620
a_{24}					0.201682	0.221835
a_{25}					1.000000	0.212860
a_{26}						0.202828
a_{27}						0.191876
a_{28}						0.180149
a_{29}						0.167794
a_{30}						1.000000

TABLE II.4

SIDELOBE RATIO 20 dB						
2N	10	20	30	40	50	60
a_1	0.313412	0.154498	0.085569	0.050670	0.033413	0.023662
a_2	0.812779	0.448090	0.252986	0.150784	0.099727	0.070734
a_3	1.000000	0.697575	0.409466	0.247267	0.164513	0.117058
a_4	0.855364	0.880222	0.548441	0.337828	0.226789	0.162147
a_5	0.649432	0.982183	0.664376	0.420377	0.285626	0.205530
a_6		1.000000	0.753082	0.493083	0.340165	0.246765
a_7		0.940499	0.811927	0.554436	0.389638	0.285437
a_8		0.819163	0.839951	0.603290	0.433382	0.321170
a_9		0.657312	0.837860	0.638897	0.470850	0.353630
a_{10}		0.894156	0.807917	0.660916	0.501623	0.382529
a_{11}			0.753730	0.669421	0.525416	0.407628
a_{12}			0.679962	0.664880	0.542080	0.428742
a_{13}			0.591983	0.648131	0.551606	0.445742
a_{14}			0.495494	0.620337	0.554118	0.458553
a_{15}			1.000000	0.582934	0.549869	0.467156
a_{16}				0.537572	0.539230	0.471589
a_{17}				0.486048	0.522684	0.471941
a_{18}				0.430233	0.500804	0.468354
a_{19}				0.372009	0.474244	0.461018
a_{20}				1.000000	0.443718	0.450165
a_{21}					0.409985	0.436067
a_{22}					0.373828	0.419029
a_{23}					0.336036	0.399386
a_{24}					0.297388	0.377495
a_{25}					1.000000	0.353727
a_{26}						0.328466
a_{27}						0.302097
a_{28}						0.275005
a_{29}						0.247565
a_{30}						1.000000

TABLE II.5

SIDELOBE RATIO 25 dB						
2N	10	20	30	40	50	60
a_1	0.339635	0.168346	0.110710	0.082520	0.065381	0.046697
a_2	0.858518	0.485100	0.326403	0.245187	0.194947	0.139501
a_3	1.000000	0.745324	0.525330	0.400826	0.320960	0.230547
a_4	0.778931	0.921637	0.697654	0.545067	0.441149	0.318698
a_5	0.451870	1.000000	0.835431	0.673992	0.553396	0.402866
a_6		0.981285	0.933134	0.784289	0.655779	0.482035
a_7		0.880081	0.987975	0.873373	0.746625	0.555275
a_8		0.721111	1.000000	0.939477	0.824550	0.621758
a_9		0.534100	0.971956	0.981695	0.888485	0.680774
a_{10}		0.536199	0.908946	1.000000	0.937698	0.731739
a_{11}			0.817912	0.995212	0.971812	0.774204
a_{12}			0.706999	0.968930	0.990796	0.807863
a_{13}			0.584861	0.923438	0.994964	0.832551
a_{14}			0.459970	0.861576	0.984953	0.848251
a_{15}			0.683816	0.786594	0.961698	0.855082
a_{16}				0.701998	0.926395	0.853304
a_{17}				0.611383	0.880460	0.843299
a_{18}				0.518280	0.825484	0.825568
a_{19}				0.426007	0.763183	0.800717
a_{20}				0.842952	0.695347	0.769440
a_{21}					0.623784	0.732506
a_{22}					0.550277	0.690740
a_{23}					0.476533	0.645009
a_{24}					0.404138	0.596201
a_{25}					1.000000	0.545208
a_{26}						0.492912
a_{27}						0.440164
a_{28}						0.387773
a_{29}						0.336492
a_{30}						1.000000

TABLE II.6

SIDELOBE RATIO 30 dB						
2N	10	20	30	40	50	60
a_1	0.365699	0.180205	0.119517	0.089238	0.070972	0.058999
a_2	0.902867	0.515913	0.351337	0.264711	0.211399	0.176126
a_3	-1.000000	0.782293	0.562134	0.431320	0.347316	0.290654
a_4	0.714435	0.947927	0.739882	0.583624	0.475871	0.400911
a_5	0.335589	1.000000	0.875325	0.716857	0.594431	0.505316
a_6		0.945505	0.962682	0.827142	0.700663	0.602406
a_7		0.808179	1.000000	0.911661	0.792599	0.690873
a_8		0.622164	0.989136	0.968752	0.868692	0.769581
a_9		0.424087	0.935380	0.997959	0.927849	0.837597
a_{10}		0.329244	0.846766	1.000000	0.969459	0.894199
a_{11}			0.733176	0.976690	0.993394	0.938890
a_{12}			0.605313	0.930796	1.000000	0.971405
a_{13}			0.473685	0.865852	0.990071	0.991711
a_{14}			0.347695	0.785942	0.964806	1.000000
a_{15}			0.394442	0.695464	0.925754	0.996678
a_{16}				0.598892	0.874755	0.982352
a_{17}				0.500542	0.813864	0.957809
a_{18}				0.404374	0.745277	0.923993
a_{19}				0.313812	0.671253	0.881979
a_{20}				0.472085	0.594041	0.832944
a_{21}					0.515804	0.778135
a_{22}					0.438560	0.718843
a_{23}					0.364118	0.656369
a_{24}					0.294042	0.591994
a_{25}					0.552337	0.526954
a_{26}						0.462412
a_{27}						0.399438
a_{28}						0.338990
a_{29}						0.281896
a_{30}						0.635467

TABLE II.7

SIDELOBE RATIO 35 dB						
2N	10	20	30	40	50	60
a_1	0.392702	0.192715	0.127198	0.094930	0.075728	0.062991
a_2	0.947744	0.548216	0.372861	0.281151	0.225337	0.187910
a_3	1.000000	0.820554	0.593184	0.456650	0.369465	0.309666
a_4	0.657489	0.974602	0.774034	0.614936	0.504674	0.426235
a_5	0.258062	1.000000	0.905069	0.750449	0.627833	0.535718
a_6		0.911427	0.980616	0.858853	0.736226	0.636387
a_7		0.742801	1.000000	0.937235	0.827644	0.726721
a_8		0.537397	0.967322	0.984224	0.900443	0.805446
a_9		0.336909	0.890722	1.000000	0.953597	0.871555
a_{10}		0.209751	0.781249	0.986217	0.986706	0.924332
a_{11}			0.651497	0.945833	1.000000	0.963359
a_{12}			0.514182	0.882870	0.994297	0.988521
a_{13}			0.380840	0.802119	0.970957	1.000000
a_{14}			0.260797	0.708817	0.931805	0.998258
a_{15}			0.235806	0.608312	0.879044	0.984021
a_{16}				0.505749	0.815154	0.958246
a_{17}				0.405789	0.742788	0.922091
a_{18}				0.312387	0.664664	0.876879
a_{19}				0.228629	0.583459	0.824053
a_{20}				0.273308	0.501714	0.765135
a_{21}					0.421752	0.701686
a_{22}					0.345602	0.635262
a_{23}					0.274951	0.567374
a_{24}					0.211107	0.499453
a_{25}					0.314613	0.432815
a_{26}						0.368638
a_{27}						0.307937
a_{28}						0.251551
a_{29}						0.200134
a_{30}						0.357628

TABLE II.8

SIDELOBE RATIO 40 dB						
2N	10	20	30	40	50	60
a_1	0.417487	0.205279	0.135117	0.100615	0.080144	0.066594
a_2	0.988039	0.580418	0.394990	0.297527	0.238241	0.198524
a_3	1.000000	0.858099	0.624931	0.481756	0.389853	0.326710
a_4	0.612497	1.000000	0.808659	0.645721	0.530943	0.448772
a_5	0.209022	0.999331	0.934884	0.783081	0.657886	0.562496
a_6		0.879553	0.998333	0.889102	0.767607	0.665892
a_7		0.685015	1.000000	0.960897	0.857694	0.757250
a_8		0.467050	0.946607	0.997534	0.926472	0.835178
a_9		0.270179	0.849393	1.000000	0.973053	0.898634
a_{10}		0.139485	0.722438	0.971044	0.997339	0.946948
a_{11}			0.580780	0.914889	1.000000	0.979831
a_{12}			0.438606	0.836871	0.982408	0.997366
a_{13}			0.307744	0.743012	0.946551	1.000000
a_{14}			0.196654	0.639583	0.894920	0.988513
a_{15}			0.146191	0.532672	0.830377	0.963986
a_{16}				0.427814	0.756013	0.927753
a_{17}				0.329683	0.675009	0.881357
a_{18}				0.241884	0.590498	0.826492
a_{19}				0.166842	0.505434	0.764948
a_{20}				0.163486	0.442485	0.698551
a_{21}					0.343947	0.629116
a_{22}					0.271678	0.558385
a_{23}					0.207062	0.487990
a_{24}					0.150999	0.419407
a_{25}					0.184205	0.353927
a_{26}						0.292630
a_{27}						0.236371
a_{28}						0.185774
a_{29}						0.141234
a_{30}						0.206433

TABLE II.9

SIDELOBE RATIO 50 dB						
2N	10	20	30	40	50	60
a_1	0.437956	0.221055	0.147512	0.110462	0.088236	0.073437
a_2	1.000000	0.617556	0.428836	0.325624	0.261772	0.218618
a_3	-0.938196	0.890985	0.670935	0.523946	0.426643	0.358781
a_4	0.505867	1.000000	0.853582	0.695635	0.577545	0.490768
a_5	0.137377	0.948520	0.964380	0.832907	0.709852	0.611699
a_6		0.779155	1.000000	0.930519	0.819827	0.719065
a_7		0.554790	0.965968	0.986062	0.904784	0.810802
a_8		0.336446	0.875129	1.000000	0.963184	0.885356
a_9		0.165974	0.745125	0.975461	0.994663	0.941719
a_{10}		0.062106	0.595403	0.917806	1.000000	0.979449
a_{11}			0.444305	0.834036	0.981016	0.998661
a_{12}			0.306720	0.732100	0.940425	1.000000
a_{13}			0.192622	0.620178	0.881639	0.984600
a_{14}			0.106642	0.506016	0.808551	0.954015
a_{15}			0.056262	0.396360	0.725301	0.910146
a_{16}				0.296552	0.636042	0.855154
a_{17}				0.210299	0.544736	0.791366
a_{18}				0.139620	0.454962	0.721185
a_{19}				0.084963	0.369772	0.646997
a_{20}				0.058742	0.291595	0.571089
a_{21}					0.222179	0.495575
a_{22}					0.162587	0.422334
a_{23}					0.113230	0.352964
a_{24}					0.073940	0.288750
a_{25}					0.063470	0.230647
a_{26}						0.179283
a_{27}						0.134971
a_{28}						0.097732
a_{29}						0.067335
a_{30}						0.069152

TABLE II.10

SIDELOBE RATIO 60 dB						
2N	10	20	30	40	50	60
a_1	0.451343	0.236727	0.160088	0.119601	0.095390	0.079455
a_2	1.000000	0.654020	0.462948	0.351497	0.282443	0.236211
a_3	0.880774	0.922515	0.716649	0.562140	0.458530	0.386595
a_4	0.427974	1.000000	0.897156	0.739508	0.617050	0.526645
a_5	0.098065	0.903892	0.991695	0.874542	0.752416	0.652816
a_6		0.696728	1.000000	0.961849	0.860351	0.762111
a_7		0.456855	0.933232	1.000000	0.938091	0.852196
a_8		0.248876	0.810954	0.991403	0.984490	0.921469
a_9		0.106199	0.656933	0.941800	1.000000	0.969103
a_{10}		0.030795	0.494730	0.859444	0.986558	0.995049
a_{11}			0.343988	0.754103	0.947375	1.000000
a_{12}			0.218058	0.635989	0.886652	0.985328
a_{13}			0.123237	0.514769	0.809257	0.952986
a_{14}			0.059473	0.398739	0.720373	0.905397
a_{15}			0.023790	0.294264	0.625160	0.845317
a_{16}				0.205493	0.528450	0.775699
a_{17}				0.134370	0.434491	0.699554
a_{18}				0.080874	0.346760	0.619821
a_{19}				0.043442	0.267856	0.539250
a_{20}				0.022556	0.199458	0.460302
a_{21}					0.142362	0.385076
a_{22}					0.096575	0.315258
a_{23}					0.061450	0.252095
a_{24}					0.035852	0.196396
a_{25}					0.023011	0.148551
a_{26}						0.108576
a_{27}						0.076163
a_{28}						0.050745
a_{29}						0.031567
a_{30}						0.024181

TABLES II.11 - II.18

Performances Indices For Array Excitations Given In Preceding Tables,

For The Specific Case Of $d = 0.5\ \lambda$

TABLE II.11

SIDELOBE RATIO 15 dB				d = 0.5 λ		
2N	10	20	30	40	50	60
K	0.966008	1.305248	1.535339	1.705893	1.839143	1.946896
K_r	0.9572	0.9617	0.9392	0.9113	0.8831	0.8563
D_d^m	6.0690	11.4282	15.8951	19.6573	22.8664	25.6352
η_d	0.9379	0.8897	0.8261	0.7666	0.7136	0.6667
η_{ds}	0.6069	0.5714	0.5298	0.4914	0.4573	0.4273

TABLE II.12

SIDELOBE RATIO 20 dB				d = 0.5 λ		
2N	10	20	30	40	50	60
K	0.901639	1.246686	1.507992	1.719668	1.898368	2.053214
K_r	0.8934	0.9186	0.9224	0.9186	0.9116	0.9030
D_d^m	5.9065	11.8124	17.4211	22.7165	27.7172	32.4448
η_d	0.9128	0.9196	0.9054	0.8859	0.8650	0.8439
η_{ds}	0.5907	0.5906	0.5807	0.5679	0.5543	0.5407

TABLE II.13

SIDELOBE RATIO 25 dB				d = 0.5 λ		
2N	10	20	30	40	50	60
K	0.839346	1.160484	1.417219	1.631804	1.818415	1.984772
K_r	0.8317	0.8551	0.8669	0.8717	0.8732	0.8729
D_d^m	5.6239	11.4099	17.1698	22.8330	28.3938	33.8522
η_d	0.8691	0.8883	0.8924	0.8905	0.8861	0.8805
η_{ds}	0.5624	0.5705	0.5723	0.5708	0.5679	0.5642

TABLE II.14

SIDELOBE RATIO 30 dB				d = 0.5 λ		
2N	10	20	30	40	50	60
K	0.788534	1.078081	1.315812	1.518541	1.697187	1.858222
K_r	0.7813	0.7943	0.8049	0.8112	0.8150	0.8173
D_d^m	5.3644	10.8469	16.3906	21.9305	27.4489	32.9405
η_d	0.8290	0.8444	0.8519	0.8553	0.8566	0.8568
η_{ds}	0.5364	0.5423	0.5464	0.5483	0.5490	0.5490

TABLE II.15

SIDELOBE RATIO 35 dB				d = 0.5 λ		
2N	10	20	30	40	50	60
K	0.745736	1.007017	1.227817	1.417024	1.584486	1.736057
K_r	0.7389	0.7420	0.7511	0.7570	0.7609	0.7635
D_d^m	5.1377	10.3148	15.5966	20.8957	26.1963	31.4932
η_d	0.7939	0.8030	0.8106	0.8149	0.8175	0.8191
η_{ds}	0.5138	0.5157	0.5199	0.5224	0.5239	0.5249

TABLE II.16

SIDELOBE RATIO 40 dB				d = 0.5 λ		
2N	10	20	30	40	50	60
K	0.713184	0.948482	1.153562	1.330411	1.487399	1.629760
K_r	0.7067	0.6989	0.7056	0.7107	0.7142	0.7168
D_d^m	4.9628	9.8629	14.8940	19.9529	25.0214	30.0933
η_d	0.7669	0.7678	0.7741	0.7782	0.7808	0.7827
η_{ds}	0.4963	0.4931	0.4965	0.4988	0.5004	0.5016

TABLE II.17

SIDELOBE RATIO 50 dB				d = 0.5 λ		
2N	10	20	30	40	50	60
K	0.661928	0.853326	1.030735	1.186612	1.325605	1.451948
K_r	0.6559	0.6287	0.6305	0.6339	0.6365	0.6386
D_d^m	4.6853	9.1155	13.7037	18.3394	22.9900	27.6478
η_d	0.7240	0.7097	0.7122	0.7152	0.7175	0.7191
η_{ds}	0.4685	0.4558	0.4568	0.4585	0.4598	0.4608

TABLE II.18

SIDELOBE RATIO 60 dB				d = 0.5 λ		
2N	10	20	30	40	50	60
K	0.625489	0.783315	0.939229	1.077816	1.202291	1.315836
K_r	0.6198	0.5772	0.5745	0.5758	0.5773	0.5787
D_d^m	4.4866	8.5580	12.8019	17.0955	21.4094	25.7335
η_d	0.6933	0.6663	0.6654	0.6667	0.6681	0.6693
η_{ds}	0.4487	0.4279	0.4267	0.4274	0.4282	0.4289

TABLES II.19 - II.26

X=axis Roots Of The Zolotarev Polynomials Associated With Arrays Of The Element Numbers And Sidelobe Ratios Indicated.

(Relevant To Arrays Of Any Spacing d).

TABLE II.19

SIDELOBE RATIO 15 dB						
2N	10	20	30	40	50	60
1	.4944800926	.2463541538	.1627843452	.1213931307	.0967451514	.0804039363
2	.6970807298	.3628911917	.2415411506	.1805661204	.1440633759	.1198009606
3	.8830839856	.4982936582	.3360051735	.2522785749	.2016752270	.1678870871
4	.9866127824	.6281019285	.4314946800	.3259812230	.2613213951	.2178648531
5		.7442488985	.5239625069	.3990304843	.3210374668	.2681666524
6		.8420474143	.6113508074	.4702361629	.3800108077	.3181801680
7		.9181786480	.6922167287	.5388303366	.4377574656	.3675639179
8		.9702486146	.7654016869	.6042147132	.4939194394	.4160783502
9		.9966778595	.8299299665	.6658795253	.5481987087	.4635306008
10			.8849743441	.7233730517	.6003316878	.5097528621
11			.9298450035	.7762892329	.6500781940	.5545928312
12			.9639872764	.8242626517	.6972163882	.5979091426
13			.9869826548	.8669667796	.7415404318	.6395690803
14			.9985506928	.9041137363	.7828594716	.6794474185
15				.9354547442	.8209973051	.7174258543
16				.9607808644	.8557924051	.7533927654
17				.9799237926	.8870981292	.7872431530
18				.9927565919	.9147830203	.8188786893
19				.9991942885	.9387311408	.8482078250
20					.9588424055	.8751459287
21					.9750328926	.8996154411
22					.9872351172	.9215460327
23					.9953982596	.9408747572
24					.9994902224	.9575461959
25						.9715125893
26						.9827339538
27						.9911781803
28						.9968211153
29						.9996484893
x_1	0.025352	0.012197	0.008012	0.005963	0.004748	0.003944
x_2	0.224677	0.108808	0.071555	0.053274	0.042426	0.035246
x_3	0.451854	0.223703	0.147661	0.110076	0.087712	0.072890

TABLE II.20

SIDELOBE RATIO 20 dB						
2N	10	20	30	40	50	60
1	.5431199278	.2747749877	.1821041180	.1359401984	.1083896089	.0901044132
2	.7189117002	.3794276750	.2532151728	.1894661520	.1512274910	.1257869097
3	.8902481172	.5083864898	.3436572136	.2582461387	.2065274887	.1719631350
4	.9873797052	.6344626127	.4368849312	.3303278271	.2649075452	.2209005414
5		.7481768749	.5278919540	.4023475213	.3238278706	.2705527342
6		.8443034137	.6142465768	.4728333703	.3822505866	.3201199105
7		.9192923247	.6943386168	.5408904605	.4395899772	.3691758218
8		.9706439302	.7669252774	.6058557979	.4954360119	.4174375219
9		.9967211473	.8309847346	.6671835166	.5494614857	.4646877574
10			.8856629880	.7244003484	.6013852578	.5107440076
11			.9302540587	.7770867010	.6509560019	.5554445928
12			.9641933355	.8248683233	.6979445002	.5986419055
13			.9870562394	.8674127501	.7421398615	.6401989264
14			.9985588369	.9044280276	.7833476787	.6799873761
15				.9356625469	.8213891953	.7178867331
16				.9609053934	.8561010168	.7537837311
17				.9799868977	.8873351181	.7875721329
18				.9927792837	.9149590087	.8191526650
19				.9991967962	.9388559754	.8484330478
20					.9589253508	.8753280813
21					.9750827799	.8997597601
22					.9872604624	.9216574035
23					.9954073586	.9409577882
24					.9994893502	.9576052777
25						.9715519421
26						.9827576666
27						.9911903590
28						.9968254624
29						.9996471033
x_1	0.015073	0.007299	0.004794	0.003567	0.002840	0.002359
x_2	0.238121	0.116232	0.076555	0.057027	0.045426	0.037744
x_3	0.509431	0.256236	0.169659	0.126611	0.100936	0.083902

TABLE II.21

SIDELOBE RATIO 25 dB						
2N	10	20	30	40	50	60
1	.5898249379	.3031687017	.2012057273	.1502753452	.1198475054	.0996419899
2	.7417466907	.3973484794	.2657198915	.1989640255	.1588601665	.1321587391
3	.8979460071	.5196151476	.3520678485	.2647798736	.2118309199	.1764140795
4	.9882103918	.6416079749	.4428663351	.3351321449	.2688643651	.2242468697
5		.7526090452	.5322716839	.4060300373	.3269202478	.2731945426
6		.8468549071	.6174818882	.4757236240	.3847386627	.3222726516
7		.9205534996	.6967126762	.5431863095	.4416285477	.3709672810
8		.9710873178	.7686314785	.6076863457	.4971246760	.4189494921
9		.9967702184	.8321666331	.6686389644	.5508684418	.4659758149
10			.8864349500	.7255474712	.6025596471	.5118477711
11			.9307127336	.7779774742	.6519347961	.5563934498
12			.9644244334	.8255450211	.6987565786	.5994584040
13			.9871387751	.8679111084	.7428085458	.6409008840
14			.9985679722	.9047792862	.7838923719	.6805892462
15				.9358948153	.8218264793	.7184005201
16				.9610445944	.8564454083	.7542196224
17				.9800574415	.8875996029	.7879389454
18				.9928044950	.9151554276	.8194581682
19				.9991995996	.9389968589	.8486842019
20					.9590179330	.8755312156
21					.9751384650	.8999207090
22					.9872887537	.9217816115
23					.9954175155	.9410534053
24					.9994904772	.9576711728
25						.9715958338
26						.9827841147
27						.9912036988
28						.9968302845
29						.9996476400
x_1	0.008841	0.004344	0.002882	0.002152	0.001716	0.001426
x_2	0.250097	0.123059	0.081101	0.060428	0.048140	0.040000
x_3	0.562629	0.287565	0.190634	0.142326	0.113488	0.094346

TABLE II.22

SIDELOBE RATIO 30 dB						
2N	10	20	30	40	50	60
1	.6324280169	.3316462128	.2213073559	.1655481953	.1321121425	.1098766467
2	.7640600559	.4165476079	.2797698516	.2097652214	.1675796819	.1394555327
3	.9056754317	.5319732476	.3617737212	.2724104313	.2180523637	.1816479420
4	.9890517852	.6495573790	.4498434087	.3408032654	.2735558453	.2282239181
5		.7575651850	.5374068203	.4103993081	.3306055882	.2763503600
6		.8497157773	.6212859192	.4791625592	.3877121796	.3248514803
7		.9219697458	.6995087851	.5459226574	.4440690117	.3731169765
8		.9715880623	.7706431756	.6098705260	.4991484903	.4207658193
9		.9968253897	.8335611576	.6703768888	.5525559159	.4675243313
10			.8873462388	.7269179607	.6039689471	.5131754476
11			.9312543750	.7790421111	.6531098439	.5575352525
12			.9646973945	.8263540322	.6997317763	.6004412323
13			.9872362755	.8685070391	.7436117321	.6417460370
14			.9985787645	.9051993860	.7845467454	.6813140289
15				.9361726389	.8223518907	.7190193237
16				.9612111123	.8568592536	.7547446719
17				.9801418344	.8879174557	.7883808301
18				.9928347742	.9153914973	.8198262259
19				.9992061734	.9391627787	.8489868024
20					.9591292162	.8757759736
21					.9752054003	.9001146465
22					.9873227618	.9219312834
23					.9954297248	.9411619847
24					.9994958143	.9577505815
25						.9716487278
26						.9828159879
27						.9912199140
28						.9968361109
29						.9996482868
x_1	0.005219	0.002555	0.001679	0.001252	0.000998	0.000829
x_2	0.260364	0.129437	0.085549	0.063794	0.050838	0.042250
x_3	0.609996	0.318267	0.212204	0.158689	0.126620	0.105300

TABLE II.23

SIDELOBE RATIO 35 dB						
2N	10	20	30	40	50	60
1	.6732459895	.3597614865	.2407922702	.1803969463	.1440411785	.1198435002
2	.7866626594	.4365419639	.2941322803	.2208182030	.1765226290	.1469483738
3	.9137172059	.5451906356	.3719617396	.2804279451	.2246038942	.1871660868
4	.9899353051	.6581587581	.4572523545	.3468312049	.2785535640	.2324656026
5		.7629583711	.5428912276	.4150702189	.3345540659	.2797355094
6		.8528384917	.6253617023	.4828507200	.3909082441	.3276265948
7		.9235183002	.7025104572	.5488630664	.4466972779	.3754348370
8		.9721361114	.7728054641	.6122205874	.5013308396	.4227267474
9		.9968857987	.8350613260	.6722484368	.5543771821	.4691976052
10			.8883271245	.7283947384	.6054909427	.5146109978
11			.9318376114	.7801898354	.6543794451	.5587704049
12			.9649913947	.8272264749	.7007858161	.6015047913
13			.9873413080	.8691498578	.7444800891	.6426608643
14			.9985903914	.9056526263	.7852543649	.6820987335
15				.9364724226	.8229201500	.7196894041
16				.9613908114	.8573069083	.7553133098
17				.9802329144	.8882613126	.7888594545
18				.9928673940	.9156469021	.8202249231
19				.9992106684	.9393439776	.8493146192
20					.9592496287	.8760411451
21					.9752778297	.9003247705
22					.9873595992	.9220934545
23					.9954429370	.9412829009
24					.9994932980	.9578366276
25						.9717060443
26						.9828505267
27						.9912374856
28						.9968424248
29						.9996514030
x_1	0.003003	0.001493	0.000987	0.000736	0.000587	0.000488
x_2	0.269709	0.135361	0.089598	0.066859	0.053300	0.044304
x_3	0.654649	0.348112	0.232791	0.176124	0.139196	0.115804

TABLE II.24

SIDELOBE RATIO 40 dB						
2N	10	20	30	40	50	60
1	.7081754044	.3865358530	.2597383153	.1948325604	.1556916961	.1295819130
2	.8068817402	.4564090690	.3086932091	.2320628739	.1856274035	.1545799246
3	.9210930122	.5586576088	.3825485882	.2887873797	.2314396173	.1929258328
4	.9907532078	.6670272017	.4650421083	.3531900133	.2838291996	.2369448505
5		.7685526524	.5486924402	.4200272725	.3387472537	.2833317930
6		.8560883999	.6296877179	.4867782693	.3943140443	.3305849144
7		.9251329855	.7057031109	.5520009644	.4495039606	.3779109573
8		.9727081653	.7751084569	.6147319726	.5036645863	.4248244894
9		.9969488835	.8366605746	.6742503700	.5563266717	.4709893512
10			.8893734502	.7299754730	.6071212170	.5161492549
11			.9324600272	.7814189640	.6557400632	.5600946075
12			.9653052353	.8281611434	.7019158560	.6026454751
13			.9874534484	.8698387172	.7454113354	.6436423292
14			.9986028063	.9061384320	.7860134100	.6829407994
15				.9367937971	.8235298199	.7204086053
16				.9615834753	.8577872559	.7559237273
17				.9803305737	.8886303256	.7893733105
18				.9929025047	.9159210180	.8206530136
19				.9992104554	.9395384658	.8496666345
20					.9593788799	.8763259117
21					.9753555792	.9005504353
22					.9873990671	.9222676287
23					.9954571203	.9414127718
24					.9994948719	.9579290493
25						.9717676094
26						.9828876265
27						.9912563603
28						.9968492070
29						.9996546785
x_1	0.001785	0.000883	0.00585	0.000436	0.000348	0.000289
x_2	0.277378	0.140719	0.093330	0.069693	0.055577	0.046205
x_3	0.692432	0.376230	0.252599	0.189424	0.151350	0.125960

TABLE II.25

SIDELOBE RATIO 50 dB						
2N	10	20	30	40	50	60
1	.7716448891	.4395793961	.2982654005	.2243869725	.1795141074	.1495140925
2	.8454922438	.4977262129	.3397644630	.2561405067	.2051553589	.1709630666
3	.9356551937	.5876470903	.4059265422	.3073065286	.2466068503	.2057166696
4	.9923900282	.6864675848	.4825580320	.3675330645	.2957469719	.2470719768
5		.7809357353	.5618660869	.4313186778	.3483128442	.2915424039
6		.8633218353	.6395681053	.4957762040	.4021281431	.3373778202
7		.9287383351	.7130211407	.5592158059	.4559667438	.3836171647
8		.9739877572	.7803996481	.6205201253	.5090512699	.4296703344
9		.9970901077	.8403407323	.6788719996	.5608339342	.4751352548
10			.8917838716	.7336290561	.6108949795	.5197129094
11			.9338949706	.7842623446	.6588924339	.5631651204
12			.9660291434	.8303247462	.7045357806	.6052922628
13			.9877121936	.8714340960	.7475715006	.6459208865
14			.9986314558	.9072639633	.7877748522	.6848965544
15				.9375385775	.8249450826	.7220795641
16				.9620300635	.8589026056	.7573423330
17				.9805569776	.8894873392	.7905677772
18				.9929836360	.9165577444	.8216483018
19				.9992194559	.9399902903	.8504851781
20					.9596791805	.8769881660
21					.9755362804	.9010752983
22					.9874908646	.9226727678
23					.9954900795	.9417148814
24					.9994985292	.9581440560
25						.9719108390
26						.9829739413
27						.9913002746
28						.9968649869
29						.9996514922
x_1	0.000594	0.000297	0.000197	0.000147	0.000118	0.000098
x_2	0.290658	0.150673	0.100423	0.075093	0.059922	0.049835
x_3	0.760336	0.431346	0.292456	0.219920	0.175943	0.146530

TABLE II.26

SIDELOBE RATIO 60 dB						
2N	10	20	30	40	50	60
1	.8244456411	.4886813327	.3349917537	.2530892907	.2029552205	.1691958217
2	.8792505737	.5378099495	.3707898785	.2806857421	.2252479684	.1879034976
3	.9488962741	.6169062331	.4302034213	.3269374400	.2628332247	.2194680022
4	.9939046608	.7065528128	.5011763301	.3830945570	.3087961552	.2582147975
5		.7939013164	.5760591720	.4437356297	.3589285730	.3006988941
6		.8709548351	.6503004469	.5057525153	.4108714530	.3450155809
7		.9325604350	.7210116337	.5672573004	.4632362118	.3900669322
8		.9753478212	.7861970190	.6269942984	.5151318578	.4351671169
9		.9972403912	.8443824639	.6840541656	.5659345020	.4798498287
10			.8944354481	.7377330549	.6151732168	.5237727325
11			.9354752645	.7874604483	.6624710280	.5666678924
12			.9668269863	.8327606607	.7075129910	.6083147967
13			.9879975768	.8732316082	.7500282072	.6485250250
14			.9986630533	.9085328166	.7897793543	.6871332032
15				.9383785549	.8265564374	.7239915014
16				.9625338932	.8601729980	.7589662065
17				.9808124578	.8904637966	.7919355509
18				.9930751785	.9172833984	.8227883228
19				.9992339880	.9405053230	.8514229742
20					.9600215465	.8777470527
21					.9757422232	.9016768449
22					.9875955427	.9231371618
23					.9955276654	.9420612157
24					.9995027000	.9583905592
25						.9720750624
26						.9830729133
27						.9913506306
28						.9968830952
29						.9996535010
x_1	0.000188	0.000102	0.000067	0.000050	0.000040	0.000033
x_2	0.301159	0.159259	0.106691	0.079958	0.063870	0.053148
x_3	0.816273	0.481903	0.330108	0.249338	0.199890	0.166660

TABLES II.27 - II.34

Tables Of Space Factor Zeros For Zolotarev Polynomial Arrays

With $d \geq 0.5\ \lambda$, For the Range of Sidelobe Ratios

And Array Sizes Indicated

TABLE II.27

SIDELOBE RATIO 15 dB						
2N	10	20	30	40	50	60
ψ_1	1.03447315	0.49783332	0.32702397	0.24338654	0.19379341	0.16098164
ψ_2	1.54263569	0.74273744	0.48790742	0.36312400	0.28913281	0.24017879
ψ_3	2.16478947	1.04325915	0.68534449	0.51006854	0.40613598	0.33737188
ψ_4	2.81396854	1.35822306	0.89229796	0.66409892	0.52878182	0.43925247
ψ_5		1.67881913	1.10299314	0.82091852	0.65364947	0.54297894
ψ_6		2.00213550	1.31553282	0.97911670	0.77961596	0.64761854
ψ_7		2.32691654	1.52911225	1.13809605	0.90620587	0.75277642
ψ_8		2.65251113	1.74333053	1.29755994	1.03318333	0.85825671
ψ_9		2.97852256	1.95796426	1.45734418	1.16041791	0.96395115
ψ_{10}			2.17287782	1.61735028	1.28783156	1.06979500
ψ_{11}			2.38798275	1.77751541	1.41537467	1.17574714
ψ_{12}			2.60321749	1.93779741	1.54301413	1.28178018
ψ_{13}			2.81853618	2.09816676	1.67072698	1.38787515
ψ_{14}			3.03390208	2.25860201	1.79849675	1.49401850
ψ_{15}				2.41908696	1.92631126	1.60020027
ψ_{16}				2.57960896	2.05416131	1.70641297
ψ_{17}				2.74015777	2.18203974	1.81265082
ψ_{18}				2.90072473	2.30994088	1.91890934
ψ_{19}				3.06130219	2.43786013	2.02518492
ψ_{20}					2.56579366	2.13147465
ψ_{21}					2.69373823	2.23777615
ψ_{22}					2.82169101	2.34408742
ψ_{23}					2.94964945	2.45040677
ψ_{24}					3.07772899	2.55673274
ψ_{25}						2.66306405
ψ_{26}						2.76939956
ψ_{27}						2.87573824
ψ_{28}						2.98207913
ψ_{29}						3.08856200

TABLE II.28

SIDELOBE RATIO 20 dB						
2N	10	20	30	40	50	60
ψ_1	1.14829677	0.55671134	0.36625185	0.27272481	0.21720594	0.18045356
ψ_2	1.60447075	0.77835527	0.51200460	0.38123684	0.30361985	0.25224200
ψ_3	2.19577924	1.06662007	0.70161707	0.52241263	0.41604919	0.34564429
ψ_4	2.82351178	1.37462616	0.90426540	0.67330175	0.53621608	0.44547545
ψ_5		1.69062012	1.11223316	0.82815927	0.65954515	0.54793426
ψ_6		2.01052781	1.32286168	0.98500708	0.78446123	0.65171211
ψ_7		2.33255724	1.53500091	1.14299088	0.91028425	0.75624408
ψ_8		2.65578746	1.74807216	1.30168225	1.0366734	0.86124713
ψ_9		2.97958904	1.96175103	1.46084259	1.1634391	0.96656390
ψ_{10}			2.17583982	1.62032830	1.29046761	1.07209992
ψ_{11}			2.39020930	1.78004751	1.41768624	1.17779504
ψ_{12}			2.60476929	1.93993847	1.54504653	1.28360913
ψ_{13}			2.81945255	2.09995789	1.67251479	1.38951437
ψ_{14}			3.03420515	2.26007424	1.80006682	1.49549083
ψ_{15}				2.42026374	1.92768475	1.60152388
ψ_{16}				2.58050779	2.05535502	1.70760249
ψ_{17}				2.74079130	2.18306710	1.81371819
ψ_{18}				2.90110277	2.31081266	1.91986434
ψ_{19}				3.06142726	2.43858490	2.02603564
ψ_{20}					2.56637820	2.13222782
ψ_{21}					2.69418777	2.23843736
ψ_{22}					2.82200943	2.34466130
ψ_{23}					2.94983945	2.45089715
ψ_{24}					3.07767438	2.55714277
ψ_{25}						2.66339627
ψ_{26}						2.76965596
ψ_{27}						2.87592208
ψ_{28}						2.98218829
ψ_{29}						3.08845755

TABLE II.29

SIDELOBE RATIO 25 dB						
2N	10	20	30	40	50	60
ψ_1	1.26168407	0.61603219	0.40517733	0.30169354	0.24027255	0.19961522
ψ_2	1.67134195	0.81725124	0.53790116	0.40060139	0.31907210	0.26509301
ψ_3	2.23016003	1.09280090	0.71955897	0.53595128	0.42689603	0.35468439
ψ_4	2.83417961	1.39318558	0.91758619	0.68349096	0.54442757	0.45234031
ψ_5		1.70403091	1.12256338	0.83621135	0.66608582	0.55342469
ψ_6		2.02008672	1.33107468	0.99157305	0.78984934	0.65625849
ψ_7		2.33899023	1.54160928	1.14845489	0.91482602	0.76010081
ψ_8		2.65948818	1.75339809	1.30628812	1.04056361	0.86457615
ψ_9		2.98080654	1.96600697	1.46475382	1.16680887	0.96947431
ψ_{10}			2.17917018	1.62365921	1.29340904	1.07466859
ψ_{11}			2.39271344	1.78288057	1.42026644	1.18007804
ψ_{12}			2.60651488	1.94233458	1.54731568	1.28564857
ψ_{13}			2.82048347	2.10196273	1.67451123	1.39134258
ψ_{14}			3.03454613	2.26172236	1.80182039	1.49713316
ψ_{15}				2.42158125	1.92921893	1.60300050
ψ_{16}				2.58151418	2.05668852	1.70892966
ψ_{17}				2.74150068	2.18421487	1.81490916
ψ_{18}				2.90152348	2.31178666	1.92093000
ψ_{19}				3.06156730	2.43940371	2.02698500
ψ_{20}					2.56703133	2.13306836
ψ_{21}					2.69469007	2.23917528
ψ_{22}					2.82236524	2.34530178
ψ_{23}					2.95005177	2.45146228
ψ_{24}					3.07774496	2.55760042
ψ_{25}						2.66376707
ψ_{26}						2.76994216
ψ_{27}						2.87612359
ψ_{28}						2.98230947
ψ_{29}						3.08849797

TABLE II.30

SIDELOBE RATIO 30 dB						
2N	10	20	30	40	50	60
ψ_1	1.36936736	0.67609602	0.44630972	0.33262770	0.26499899	0.22019788
ψ_2	1.7391662	0.85928893	0.56710875	0.42266966	0.33674823	0.27982310
ψ_3	2.2659402	1.1218584	0.74033956	0.55179464	0.43963673	0.36532402
ψ_4	2.8453731	1.41400427	0.93317999	0.69554236	0.55417591	0.46050613
ψ_5		1.7191499	1.13471826	0.84578380	0.67389034	0.55998899
ψ_6		2.0308919	1.34076542	0.99940072	0.79629667	0.66170937
ψ_7		2.34627283	1.54941977	1.15497991	0.92026986	0.76473270
ψ_8		2.66370140	1.75969961	1.31179441	1.04523163	0.86857868
ψ_9		2.98218647	1.97104612	1.46943318	1.17085541	0.97297620
ψ_{10}			2.18311534	1.62764638	1.29694315	1.07776095
ψ_{11}			2.39568085	1.78627312	1.42336777	1.18282760
ψ_{12}			2.60858386	1.94520472	1.55004395	1.28810552
ψ_{13}			2.82170555	2.10436472	1.67691218	1.39354559
ψ_{14}			3.03495036	2.26369728	1.80392963	1.49911256
ψ_{15}				2.42316019	1.93106456	1.60478044
ψ_{16}				2.58272038	2.05829290	1.71052964
ψ_{17}				2.74235096	2.18559591	1.81634509
ψ_{18}				2.90202973	2.31295871	1.92221495
ψ_{19}				3.06189665	2.44036920	2.02812979
ψ_{20}					2.56781735	2.13408197
ψ_{21}					2.69529459	2.24006520
ψ_{22}					2.82279347	2.34607422
ψ_{23}					2.95030730	2.45210456
ψ_{24}					3.07808026	2.55815238
ψ_{25}						2.66421431
ψ_{26}						2.77028734
ψ_{27}						2.87636875
ψ_{28}						2.98245601
ψ_{29}						3.08854672

TABLE II.31

SIDELOBE RATIO 35 dB						
2N	10	20	30	40	50	60
ψ_1	1.47717996	0.73602450	0.48636411	0.36278000	0.28908795	0.24026449
ψ_2	1.81076920	0.90350292	0.59709502	0.44530660	0.35490495	0.29496488
ψ_3	2.30467953	1.15323300	0.76224301	0.56847982	0.45307305	0.37655290
ψ_4	2.85759795	1.43674107	0.94980638	0.70838095	0.56457547	0.46922393
ψ_5		1.73575437	1.14775207	0.85603996	0.68226397	0.56703721
ψ_6		2.04279461	1.35118993	1.00781430	0.80323629	0.66758085
ψ_7		2.35430874	1.55783784	1.16200703	0.92614086	0.76973177
ψ_8		2.66835480	1.76649974	1.31773195	1.05027235	0.87290403
ψ_9		2.98371120	1.97648849	1.47448341	1.17522887	0.97676388
ψ_{10}			2.18737860	1.63195223	1.30076519	1.08110780
ψ_{11}			2.39888877	1.78993846	1.42672333	1.18580481
ψ_{12}			2.61082113	1.94830668	1.55299690	1.29076685
ψ_{13}			2.82302724	2.10696137	1.67951155	1.39593251
ψ_{14}			3.03538757	2.26583267	1.80621366	1.50125766
ψ_{15}				2.42486768	1.93306347	1.60670972
ψ_{16}				2.58402491	2.06003076	1.71226411
ψ_{17}				2.74327063	2.18709201	1.81790189
ψ_{18}				2.90257631	2.31422851	1.92360820
ψ_{19}				3.06212263	2.44142507	2.02937117
ψ_{20}					2.56866903	2.13518118
ψ_{21}					2.69594964	2.24103032
ψ_{22}					2.82325797	2.34691196
ψ_{23}					2.95058420	2.45282049
ψ_{24}					3.07792195	2.55875105
ψ_{25}						2.66469940
ψ_{26}						2.77066175
ψ_{27}						2.87663467
ψ_{28}						2.98261496
ψ_{29}						3.08878226

TABLE II.32

SIDELOBE RATIO 40 dB						
2N	10	20	30	40	50	60
ψ_1	1.57382113	0.79374506	0.52550241	0.39217347	0.31265529	0.25989465
ψ_2	1.87770822	0.94791040	0.62763767	0.46839583	0.37342064	0.31040450
ψ_3	2.34175711	1.18553280	0.78510626	0.58592002	0.46711443	0.38828625
ψ_4	2.86940039	1.46042293	0.96736435	0.72195737	0.57557038	0.47843987
ψ_5		1.75315166	1.16159882	0.86695074	0.69117022	0.57453298
ψ_6		2.05530619	1.36230232	1.01679550	0.81064259	0.67384653
ψ_7		2.36277147	1.56683007	1.16952405	0.93241991	0.77507776
ψ_8		2.67326040	1.77377346	1.32409220	1.05567093	0.87753600
ψ_9		2.98531932	1.98231517	1.47989832	1.17991732	0.98082395
ψ_{10}			2.19194575	1.63657212	1.30486532	1.08469782
ψ_{11}			2.40232682	1.79387309	1.43032487	1.18899999
ψ_{12}			2.61321958	1.95163777	1.55616754	1.29362413
ψ_{13}			2.82444441	2.10975060	1.68230337	1.39849596
ψ_{14}			3.03585641	2.26812691	1.80866737	1.50356195
ψ_{15}				2.42670247	1.93521128	1.60878257
ψ_{16}				2.58542686	2.06189834	1.71412795
ψ_{17}				2.74425906	2.18869997	1.81957503
ψ_{18}				2.90316602	2.31559339	1.92510572
ψ_{19}				3.06211191	2.44256007	2.03070556
ψ_{20}					2.56958460	2.13636284
ψ_{21}					2.69665386	2.24206790
ψ_{22}					2.82375639	2.34781265
ψ_{23}					2.95088191	2.45359024
ψ_{24}					3.07802092	2.55939475
ψ_{25}						2.66522099
ψ_{26}						2.77106434
ψ_{27}						2.87692060
ψ_{28}						2.98278587
ψ_{29}						3.08903096

TABLE II.33

SIDELOBE RATIO 50 dB						
2N	10	20	30	40	50	60
ψ_1	1.76284639	0.91026069	0.60574963	0.45262784	0.36098502	0.30015364
ψ_2	2.01497264	1.04195043	0.69333290	0.51805477	0.41324487	0.34361408
ψ_3	2.42022207	1.25629552	0.83598485	0.62472259	0.49835480	0.41439196
ψ_4	2.89469764	1.51324004	1.00714590	0.75271007	0.60047475	0.49931476
ψ_5		1.79232505	1.19327981	0.89190778	0.71154126	0.59167778
ψ_6		2.08363094	1.38787261	1.03745676	0.82768004	0.68826001
ψ_7		2.38199013	1.58759541	1.18687914	0.94691629	0.78741991
ψ_8		2.68442043	1.79060942	1.33881158	1.06816439	0.88825532
ψ_9		2.98898060	1.99582301	1.49245058	1.19078542	0.99023547
ψ_{10}			2.20254514	1.64729409	1.31438106	1.09302975
ψ_{11}			2.41031180	1.80301257	1.43869089	1.19642218
ψ_{12}			2.61879284	1.9593803	1.56353759	1.30026595
ψ_{13}			2.82773849	2.1162368	1.68879627	1.40445791
ψ_{14}			3.03694633	2.2734640	1.81437627	1.50892343
ψ_{15}				2.4309720	1.94021006	1.61360719
ψ_{16}				2.5886898	2.06624607	1.71846726
ψ_{17}				2.7465599	2.19244409	1.82347123
ψ_{18}				2.9045342	2.31877201	1.92859360
ψ_{19}				3.0625662	2.44520369	2.03381400
ψ_{20}					2.57171735	2.13911584
ψ_{21}					2.6982948	2.24448547
ψ_{22}					2.8249186	2.34991145
ψ_{23}					2.9515755	2.45538405
ψ_{24}					3.0782515	2.56089490
ψ_{25}						2.66643663
ψ_{26}						2.77200267
ψ_{27}						2.87758706
ψ_{28}						2.98318425
ψ_{29}						3.08878901

TABLE II.34

SIDELOBE RATIO 60 dB						
2N	10	20	30	40	50	60
ψ_1	1.93844393	1.02115536	0.68319295	0.51174436	0.40875002	0.34002733
ψ_2	2.14857334	1.13567445	0.75971876	0.56901699	0.45439507	0.37805437
ψ_3	2.49943988	1.32961142	0.88943620	0.66612220	0.53191500	0.44253828
ψ_4	2.92065752	1.56923008	1.04991523	0.78628824	0.62785414	0.52234775
ψ_5		1.83439707	1.22779865	0.91952577	0.73423944	0.61085075
ψ_6		2.11428444	1.41595972	1.06050808	0.84681943	0.70451077
ψ_7		2.40288288	1.61052232	1.20634328	0.96328673	0.80140856
ψ_8		2.69658354	1.80926149	1.35537780	1.08232296	0.90044776
ψ_9		2.99297558	2.01082288	1.50661247	1.20313259	1.00096707
ψ_{10}			2.21433436	1.65941238	1.32521131	1.10254755
ψ_{11}			2.41920308	1.81335575	1.44822537	1.20491224
ψ_{12}			2.62500336	1.96815117	1.57194559	1.30787124
ψ_{13}			2.83141193	2.12359002	1.69620945	1.41129023
ψ_{14}			3.03816172	2.27951793	1.82089839	1.51507156
ψ_{15}				2.43581692	1.94592374	1.61914254
ψ_{16}				2.59239378	2.07121757	1.72344790
ψ_{17}				2.74917228	2.19672673	1.82794481
ψ_{18}				2.90608760	2.32240875	1.93259950
ψ_{19}				3.06330550	2.44822893	2.03738492
ψ_{20}					2.57415835	2.14227906
ψ_{21}					2.70017231	2.24726374
ψ_{22}					2.82624919	2.35232371
ψ_{23}					2.95236956	2.45744602
ψ_{24}					3.07851548	2.56261946
ψ_{25}						2.66783422
ψ_{26}						2.77308151
ψ_{27}						2.87835334
ψ_{28}						2.98364265
ψ_{29}						3.08894142